ISBN 978-82-326-4188-8 (printed version)
ISBN 978-82-326-4189-5 (electronic version)
ISSN 1503-8181

Doctoral theses at NTNU, 2019:296

Shamim Haider

A Semi-Industrial Scale Process To Produce Carbon Membranes For Gas Separation

NTNU
Norwegian University of
Science and Technology
Faculty of Natural Sciences and Technology
Department of Chemical Engineering

NTNU
Norwegian University of
Science and Technology

Doctoral theses at NTNU, 2019:296

NTNU

NTNU
Norwegian University of
Science and Technology

Shamim Haider

A Semi-Industrial Scale Process To Produce Carbon Membranes For Gas Separation

Thesis for the degree of Philosophiae Doctor

Trondheim, October 2019

Norwegian University of Science and Technology
Faculty of Natural Sciences and Technology
Department of Chemical Engineering

NTNU
Norwegian University of
Science and Technology

NTNU
Norwegian University of Science and Technology

Thesis for the degree of Philosophiae Doctor

Faculty of Natural Sciences and Technology
Department of Chemical Engineering

ISBN 978-82-326-4188-8 (printed version)
ISBN 978-82-326-4189-5 (electronic version)
ISSN 1503-8181

Doctoral theses at NTNU, 2019:296

Printed by Skipnes Kommunikasjon as

Preface

This thesis is submitted as a partial fulfillment of the requirements for the PhD-degree at the Norwegian University of Science and Technology (NTNU) and consists of eight papers. The work presented in this thesis was carried out at the membrane production facility "Membranes for Advanced Clean Technologies" (MemfoACT), Heimdal, and Department of Chemical Engineering, NTNU Trondheim, during 2010-2016. MemfoACT AS was the first company world-wide to bring regenerated cellulose-based carbon hollow fiber membranes (self-supported) out of the lab and to the reported technology readiness level (TRL-6). This work is relevant for research covering aspects like, carbon membrane production process, module construction, process simulations, vehicle fuel, air separation, and durability of carbon membranes.

I completed my Bachelors degree in Chemical Engineering from University of Engineering and Technology, Lahore, in September 2007. Thereafter, I joined NTNU for my Masters degree in Chemical Engineering. After completion of my master thesis at NTNU, I was employed by MemfoACT AS in Trondheim in August 2010. While working at MemfoACT, I was in charge of HYSYS simulations and heavily involved in production of carbon hollow fiber membranes. However, I was also briefly involved in module construction process, gas permeation testing, and durability testing of the prepared carbon membranes. Moreover, I was following the carbon membrane-based biogas upgrading plant at GlØR IKS, a biogas production plant at Lillehammer.

Abstract

The utilization of carbon membranes (CM) in pilot scale and industrial scale is still unavailable due to expensive precursor materials and a complex multi-step membrane preparation process with several variables to deal with. The optimization of these variables is essential to gain a competent carbon membrane with high performance and good mechanical properties. Previous work has demonstrated that a low-cost precursor, such as cellulose acetate, can be used to prepare CM with high gas separation performance at lab-scale. However, the focus of this work was to develop and optimize a pilot scale process to produce high performance carbon membranes from cellulose acetate and construct semi-industrial scale modules (0.2-2 m^2) for CO_2-CH_4 and O_2-N_2 separation.

A pilot scale facility with annual production capacity of 700 m^2 CM was developed and the production process was optimized. A dope solution of cellulose acetate (CA)/Polyvinylpyrrolidone (PVP)/N-methyl-2-pyrrolidone (NMP) and bore fluid of NMP/H_2O were used in 460 spinning-sessions of the fibers using a well-known dry/wet spinning process. The spinning parameters, such as dope and bore fluid composition, extrusion rate, spinneret dimensions, air gap (25 mm), coagulation temperature (23 °C), take up rate (14 m/minute), and solvent exchange methods (water wash and glycerol treatment) to preserve the pores from collapsing were optimized to achieve maximum yield (based on length, quantity of good fibers, mechanical properties of CM, and separation properties of resulting CM). Direct carbonization of cellulose acetate hollow fibers (CAHF) will result in discontinuous carbon (more like a powder) since the intermediate product levoglucosane is not formed during carbonization, hence CAHF must be deacetylated. Optimized deacetylation of spun-CAHF was achieved by using 90 vol% 0.075 M NaOH aqueous solution diluted with 10 vol% Isopropanol for 2.5 hours at ambient temperature. Deacetylated cellulose fibers (CHF) dried at room temperature and controlled air circulation under RH 80% → ambient overnight gave maximum yield for both dried CHF as well as CM.

Simultaneous carbonization of thousands of fibers in a horizontal furnace may result in fused fibers if the carbonization residuals (tars) are not removed fast enough. Quartz tubes and perforated stainless steel (SS) flat grids were initially used as fiber carriers to carbonize up to 4000 (160 cm long) fibers in a single batch. It was found that number of fused fibers (sticking together due to residual products) could be significantly reduced by replacing the quartz tubes with perforated grids. It was further found that improved purge gas flow distribution in the

furnace with perforated grids and a 4-6 degree tilt angle in furnace position permitted the residuals to flow downward into the tar collection chamber.

Pilot scale module construction process for high pressure and elevated temperature applications was investigated and is explained in the current work. The prepared modules were tested to separate CO_2 at high pressure (2-70 bar feed vs 0.05-1 bar permeate pressure) and elevated temperature (23-120 °C). Gas permeation results indicated that carbon membranes are hardly affected by high pressure, but a significant drop in CO_2 permeability (up to 40%) was observed at elevated temperature (120 °C) compared to the value at 23 °C. The gas permeation properties of carbon membranes were enhanced (modified) by changing the pore geometry using: oxidation, chemical vapor deposition (CVD) and reduction processes. Maximum CO_2 permeance value for a modified carbon hollow fiber module was recorded to be up to 50,000 times higher and CO_2/N_2 selectivity 40 times higher as compared to prior to modification.

A pilot-scale separation plant based on these carbon hollow fiber membranes for upgrading of biogas to vehicle fuel quality was constructed and operated at the biogas plant, GlØR IKS, Lillehammer Norway. Vehicle fuel quality was successfully achieved in a single stage separation process. The fuel quality was as according to Swedish legislation as this is setting the standard.

To understand membrane lifetime and durability of CHF under harsh conditions, CHF were exposed to biogas for almost one year with a H_2S content extending from 0-2400 ppm. Gas permeation tests for the single gases, N_2, CO_2, CH_4, and O_2 were analyzed periodically at the membrane production facility. CHF storage methods under miscellaneous dry environments like air, vacuum, CO_2, etc. were studied. The air flow through the bore side of the CHF under controlled conditions had a regenerative effect on the membrane permeability, and the membrane performance was quite steady until after 150 days under controlled laboratory environment.

Some experiments were performed to explore the potential of regenerated cellulose-based carbon membranes with respect to air separation. It was observed that O_2 permeability increased exponentially with increase in operating temperature without significant loss in the O_2/N_2 selectivity. The O_2 permeability of 10 Barrer with O_2/N_2 selectivity of 19 was achieved at 68 °C. Chemisorption of oxygen on the active sites of carbon limits the use of carbon membranes in air separation application. A novel online electrical regeneration method was applied to prevent the active sites at the carbon surface to be reacting with O_2 while the membrane was in operation. This method reduced the aging effect, and the membrane showed a relative stable performance with only 20% loss in O_2 permeability and 28% increase in O_2/N_2

selectivity, over the period of 135 days while using various feeds containing H_2S, n-Hexane and CO_2-CH_4 gas.

Aspen HYSYS® interfaced with ChemBrane (in-house developed model) was used to perform the simulations for carbon membranes in applications of biogas upgrading to vehicle fuel, natural gas sweetening, and air separation market. The simulation results were used to estimate the total capital investment, production cost, and net present values of different carbon membrane-based separation plants. The cost evaluation and sensitivity analysis showed that carbon membranes have a nice potential to compete with commercially available polymeric membranes (polyimide and cellulose acetate) in biogas and natural gas applications. However, to be fully competitive with cryogenic distillation and PSA in air separation market, the membrane cost needs to be reduced and the mechanical strength of CM must be increased to maximize the lifetime of the carbon membrane.

Acknowledgements

The material of this thesis is the result of almost six years of interactions with advisors, coworkers, friends and family and everyone deserving a lot of gratitude.

First and foremost, I credit my professor May-Britt Hägg, for giving me opportunity to work with carbon membranes at NTNU and MemfoACT AS. Her visionary approach to research and patient support of my work with seemingly trivial issues has been a major driving force during these years. Thank you so much May-Britt, for your backing and supervision.

I consider myself really lucky to have had two excellent co-workers and supervisor at the same time at MemfoACT AS- Dr. Arne Lindbråthen and Dr. Jon Arvid Lie, who have helped me at important junctures of the thesis. Dr. Lindbråthen and me shared the same office at MemfoACT AS for almost 4 years. Scientific discussions and what to do next have been the hot topics with him. What I really like about his scientific persona is to use simple yet novel methods to carry out converging research. And even during his busy workdays, his response time to oral questions, emails and texts is very fast. Although residing far from Trondheim, Dr. Lie had been really helpful in all aspects of this work. He has always supported the course of the work with valuable research inputs. Arne and Jon, thank you so much for supervising me all these years! You guys have inspired me in so many ways. All my mentors deserve special thanks for showing inter-human values and constructive fellowship, which I believe is both the objective and medium for our research. Their constructive suggestions, generous facilitation and guidance throughout my work inspired me to be a better person with a positive attitude in future.

I would also like to thank my colleagues at MemfoACT AS: Gøril, Inge, Håvard, Petter, Ingrid, Jon Anders, Thorbjørn, Susanne, membrane group (MEMFO) at NTNU, and colleagues at OT Membranes AS: Camilla, Oddbjørn and Maria for their support and collective efforts for making the work environment an exciting place to work.

I am also grateful to all my friends in Trondheim who have helped me in one way or the other. Some of them have supported me throughout the PhD work, while some have shared precious moments over dinners, lunches or during social get-togethers, whereas some have spent nights discussing and debating on topics ranging from religion to history to astronomy to life. Khalid, Irfan, Saeed, Javaid, Majid, Ali, Saad, Adeel, Usman, Saddam, Hassan, Ali Abid, Nabeel, Shahbaz, Ameen, Urooj, Sulalit are few of them who need special mention. Naveed, Shahla baji and Asma baji have actually functioned as family in Trondheim.

In private life, it also turned out quite well. Trondheim saw me passing from being a bachelor to a married man and to a proud father to two lovely kids: Huda and Haadi. I am very thankful to my dear wife, Zubaida Waheed Butt, who has always encouraged and supported me both on my life and scientific research. Zubaida, thank you for showing interest in my work and I appreciate your spirit of inquiry. Zubaida, Huda, and Haadi have been immensely helpful in bearing with my workaholic hours trying to finish my part time PhD with the job. I owe limitless thanks to my parents for allowing me to pursue higher studies miles away from home. Their lifelong efforts to create those facilitating circumstances that paved the challenging phases of my educational career. I would like to thank my entire family back in Pakistan for their support.

And this work wouldn't have seen the light of the day without the blessings from the Almighty, Who knows what is in the heart of every human being! All praise to Him.

Trondheim, August 2018
Shamim Haider

List of Publications

Paper I

S. Haider, J.A. Lie, A. Lindbråthen, M.-B. Hägg, **Pilot – Scale production of carbon hollow fiber membranes from regenerated cellulose precursor: Part I- Optimal conditions for precursor preparation,** *Membranes Journal 8 (2018) 105.*

Paper II

S. Haider, J.A. Lie, A. Lindbråthen, M.-B. Hägg, **Pilot – Scale production of carbon hollow fiber membranes from regenerated cellulose precursor: Part II- Carbonization procedure,** *Membranes Journal 8 (2018) 105.*

Paper III

S. Haider, A. Lindbråthen, J.A. Lie, M.-B. Hägg, **Regenerated cellulose-based carbon membranes for CO_2 separation; Durability and aging under miscellaneous environments,** *Journal of Industrial & Engineering Chemistry 70 (2019) 363-371.*

Paper IV

S. Haider, A. Lindbråthen, J.A. Lie, I.C.T. Andersen, M.-B. Hägg, **CO_2 separation with carbon membranes in high pressure and elevated temperature applications**, *Separation and Purification Technology 190 (2018) 177-189.*

Paper V

S. Haider, A. Lindbråthen, J.A. Lie, P. Vattekar Carstensen, T. Johannessen, M.-B. Hägg, **Vehicle fuel from biogas with carbon membranes; a comparison between simulation predictions and actual field demonstration**, *Green Energy & Environment (2018) 1-11.*

Paper VI

S. Haider, A. Lindbråthen, M.-B. Hägg, **Techno-economical evaluation of membrane based biogas upgrading system: A comparison between polymeric membrane and carbon membrane technology**, *Green Energy & Environment 1(3) (2016) 222-234.*

Paper VII

S. Haider, A. Lindbråthen, J. Arvid Lie, M.-B. Hägg, **Carbon membranes for oxygen enriched air –Part I: Synthesis, performance and preventive regeneration**, *Separation and Purification Technology 204 (2018) 290-297.*

Paper VIII

S. Haider, A. Lindbråthen, J. Arvid Lie, M.-B. Hägg, **Carbon membranes for oxygen enriched air –Part II: Techno-economic analysis**, *Separation and Purification Technology 205 (2018) 251-262.*

Additional Publications

Paper IX

S. Haider, M. Saeed, A. Lindbråthen, M.-B. Hägg, **Techno-economic evaluation of helium recovery from natural gas; A comparison between inorganic and polymeric membrane technology,** *Journal of Membrane Science & Research 5(2019) 126-136*

Outline of thesis

This thesis consists of two parts and the first part includes 9 chapters. However, the second part contains appendices that comprises of some supporting information and publications. The short description of each chapter is as follows:

Part I:

Chapter 1: is a brief introduction to the research objective and the company (MemfoACT AS).

Chapter 2: gives a short theoretical background of gas separation membranes and principal markets of these membranes.

Chapter 3: provides brief background information about the carbon molecular sieve membrane (CMSM), preparation of CMSM, module construction, transport mechanisms, durability and aging, regeneration, and potential applications of carbon membranes.

Chapter 4: describes the details about equipment's, methods, and procedures used in this work for different processes involved in preparation of pilot scale carbon membrane modules. This chapter is further divided into six sections. First two sections describe the preparation of precursor hollow fibers and carbonization procedure of thousands of fibers to produce carbon membranes. The results of these sections are presented and discussed in paper I and II. Section-III-V explains the detailed procedures of pilot scale module construction, gas permeation testing, and pore size adjustment of prepared membranes. The results of these sections are discussed in paper IV. Last section of this chapter presents the durability testing, aging phenomenon in CMSM, and regeneration methods to regain the lost performance during aging. The results of this section are discussed in paper III & VII.

Chapter 5: describes about carbon membrane-based biogas upgrading plant which was designed, constructed, and operated by MemfoACT AS. The biogas upgrading process and results of the pilot plant are discussed in detail in paper V & VI.

Chapter 6: discusses the HYSYS simulation and cost estimation methods that were used to estimate the capital investment and production cost of a carbon membrane-based biogas upgrading system and air separation system. The details of simulations results and cost estimation are discussed in paper VI & VIII

Chapter 7: Summarizes and discuss the main findings from the eight submitted papers as part of this thesis. This chapter has been divided into three sub-parts. The first part discusses the results of membrane synthesis and durabilty-aging of prepared membranes under miscellaneous evironments (Paper I-III). Second part discusses the pilot scale module

construction, CVD, regeneration of membranes, and applications of preparaed CHFM (Paper IV, V, and VII). The third part of this chapter discusses the findings from HYSYS simulations when interfaced with Chembrane to evaluate optimal membrane area and energy requirement for different applications of CHFM (Paper VI & VIII).

Chapter 8: is conclusions from this research work

Chapter 9: based on experience obtained from pilot scale production of carbon membranes, the chapter discusses the suggestions for future work towards commercialization.

Part II:

- Appendix A: List of all the equipment's and suppliers that were used at MemfoACT facility
- Appendix B: Cross section of cellulose acetate (CA) and carbon fibers while using different compositions of precursor solution
- Appendix C: Production cost of carbon membranes at lab, pilot, and industrial scale
- Appendix D: Photos of different equipment's and their components
- Appendix E: Paper I- Pilot – Scale production of carbon hollow fiber membranes from regenerated cellulose precursor: Optimal conditions for precursor preparation
- Appendix F: Paper II- Pilot – Scale production of carbon hollow fiber membranes from regenerated cellulose precursor: Carbonization procedure
- Appendix G: Paper III- Regenerated cellulose-based carbon membranes for CO_2 separation; Durability and aging under miscellaneous environments
- Appendix H: Paper IV- CO_2 separation with carbon membranes in high pressure and elevated temperature applications
- Appendix I: Paper V- Vehicle fuel from biogas with carbon membranes; a comparison between simulation predictions and actual field demonstration
- Appendix J: Paper VI- Techno-economical evaluation of membrane based biogas upgrading system: A comparison between polymeric membrane and carbon membrane technology
- Appendix K: Paper VII- Carbon membranes for oxygen enriched air –Part I: Synthesis, performance and preventive regeneration
- Appendix L: Paper VIII- Carbon membranes for oxygen enriched air –Part II: Techno-economic analysis

Table of Contents

Nomenclature

Symbol	Explanation	Unit/value
Latin characters		
A	Membrane area; constant of polymer-penetrant system	m^2; -
a	constant	-
B	Constant of polymer-penetrant system	-
b	Langmuir affinity parameter; constant	bar^{-1}; -
c	concentration of component i; constant	mol m^{-3}; -
D	diffusion coefficient	$m^2\ s^{-1}$
d	kinetic diameter; d-spacing	nm; Å
E	activation energy	kJ mol^{-1}
e	electron charge; width	1.602×10^{-19} C; m
f	fugacity	Bar
h	Planck constant	6.626×10^{-34} J s
J	flux	mol $m^{-2}\ s^{-1}$
K	Boltzmann constant	1.381×10^{-23} J K^{-1}
k	kinetic rate constant	s^{-1}
L	average micropore width; Length of material	Å
l	effective membrane thickness	µm
M	molecular weight	g mol^{-1}
m	mass	G
N	Knudsen number	-
n	shape factor	-
P; P/ℓ	Permeability; Permeance	Barrer*; [m^3(STP) m^{-2} h^{-1} bar^{-1}]
p	pressure	Bar
q	adsorption amount; flow rate	g g^{-1}; kmol h^{-1}
R	molar gas constant	8.314 J K^{-1} mol^{-1}
S	entropy; solubility	J K^{-1}; m^3(STP) m^{-3} bar^{-1}
T	temperature; mass flow rate	°C; tons day^{-1}
t	time	s or h
V	volume	m^3
w	micropore volume	$cm^3\ g^{-1}$

x	mole composition	
y	mole composition	-

Greek Characters

Δ	delta (finite difference)	-
φ	Volume fraction; pressure ratio	-
α	selectivity	-
ε	microporosity; Lennard-Jones well depth	; J
θ	diffraction angle; stage-cut	; %
λ	mean free path	m
ρ	density	g cm^{-3}
τ	tortuosity	-

Subscripts

A	component A
p	permeate stream
f	feed stream
B	component B
a	activation
d	diffusion; dispersed phase
K	Knudsen
MS	molecular sieve
c	continuous phase
e	effective
exp.	experimental
h, l	high, low pressure side
i, j	component i, j
l	distance in the transport direction
r	retentate stream

Abbreviations

CA	cellulose acetate
CAHF	cellulose acetate hollow fibers
CHF	cellulose hollow fiber

CM	carbon membranes
CHFM	carbon hollow fiber membrane
CMSM	carbon molecular sieve membranes
CMC	carbon membrane cost
CC	compressor cost (installed)
VC	vacuum pump cost (installed)
PC	production cost
MRC	membrane replacement cost
EC	electricity cost
CRC	capital recovery cost
LC	labor cost
TLC	total labor cost
VP	vacuum on permeate
FC	feed compression approach
	combined feed compression and vacuum on permeate
FC-VP	side
CVD	chemical vapor deposition
NMP	N-methyl-2-pyrrolidone
PVP	Polyvinylpyrrolidone
DMSO	Dimethyl sulfoxide
RT	room temperature
OD	outer diameter
ID	inner diameter
TEG	triethyleglycol
SBG	Synthetic biogas
WCG	Worst case gas
RBG	Real biogas field exposure
ABS	Acrylonitrile Butadiene Styrene
PER	preventive electrical regeneration
RM	reference module
DC	direct current
DP	dew point
GA	gas analyzer

TS	temperature swing
RH	relative humidity
MMS	multi-module system
PMC	Polymeric membrane cost
CBGC	High pressure compressor cost
FC	Fixed cost
BPC	Base plant cost
PC	Project Contingency
TFI	Total facility investment
SC	Start-up cost
TPI	total plant investment
LTI	Local taxes and insurance
LOC	Labor overhead cost
UC	Utility cost
EPO2	equivalent pure oxygen
TCI	total capital investment

The units used to describe gas permeability (the transport coefficient) in membranes can be a controversial subject, with some preferring SI units to the traditional units. However, Barrer, which is traditional, is convenient because the range of permeability in carbon membranes is usually between 1 and 2000 Barrer. This is compared to 2.735×10^{-14} to 5.472×10^{-11} $m^3(STP)\cdot m/m^2\cdot Pa\cdot h$ for the same range in SI units or even 2.735×10^{-9} to 5.472×10^{-6} $m^3(STP)\cdot m/m^2\cdot bar\cdot h$ for the more common metric units. Furthermore, Barrer is in common use in the literature, including by the Editor-in-chief of the Journal of Membrane Science, WJ Koros, and so it is easier to compare experimental data by reporting in Barrer. The situation is different in simulations. Here, the inputs to the software are permeances (permeability normalised by thickness) and it was more convenient to report them with the units $mol/m^2\cdot kPa.h$ or $m^3(STP)/m^2\cdot bar\cdot h$. Conversions are provided where clarity is required.

Conversions:

From	**To**	**Conversion factor**
Barrer	$cm^3(STP)\ cm\ cm^{-2}\ s^{-1}\ cm\ Hg^{-1}$	1×10^{-10}
	$m^3(STP)\ m\ m^{-2}\ bar^{-1}\ h^{-1}$	2.736×10^{-9}
	$mol\ m\ m^{-2}\ bar^{-1}\ h^{-1}$	1.217×10^{-7}
$m^3(STP)\ m^{-2}\ bar^{-1}\ h^{-1}$	$mol\ m^{-2}\ kPa^{-1}\ h^{-1}$	4.45×10^{-1}
	$mol\ m^{-2}\ bar^{-1}\ h^{-1}$	44.50
$cm^3(STP)\ cm^{-2}\ s^{-1}\ cm\ Hg^{-1}$	$mol\ m^{-2}$ kPa-1 h^{-1}	1.217×10^{3}

Part I

1. Introduction

1.1. Background

The development of effective separation and purification technologies that are robust and have much smaller energy requirements are undeniably needed to pause the growing demand of energy [1, 2]. The challenge of developing efficient separation technologies for capture or removal of carbon dioxide (CO_2) from other gases is significant for several reasons: Firstly due to its involvement in climate change, then CO_2 is an impurity in natural gas, biogas, syngas (the main source of hydrogen in refineries) and many other gas streams [3].

Conventional methods for CO_2 separation are based on reversible absorption, such as amine scrubbing, but these processes are energy intensive and pose environmental concerns [4]. Membrane processes have been considered as suitable processes for gas separation due to their simple operation, relatively low cost, compact design and high efficiency [5]. Polymeric membranes have been commercially produced for gas separation processes since 1980s [6]. However, plasticization, poor chemical durability, and insufficient thermal resistance of polymeric material, have restricted their applications and led the researchers to explore new robust and competent novel materials.

Among many other new membrane materials, carbon is one class of material that can provide attractive solutions to the above-mentioned problems of polymeric materials. Carbon membranes (CM) are usually prepared by carbonization of the precursor membranes at high temperature (550 – 850 °C) under vacuum or in an inert environment (Ar, He or N_2). Gas permeation properties of CM are affected by the type of precursor chosen and carbonization conditions. The concept of carbon membrane is well known and tested out. Ash et al. [7, 8] compressed nonporous graphite carbon into a plug and called it carbon membrane in early seventies. The practical usefulness of carbon membrane was however realized in the beginning of eighties for the first time by the work of Koresh and Soffer [9] who carbonized many thermosetting polymers to produce carbon molecular sieve membranes (CMSM). The separation properties of prepared carbon membranes depend largely on the type of their polymeric precursor. Several polymers have been extensively studied to produce carbon membranes, which includes polyimides, polyetherimide, phenolic resin, cellulose, among others. Nevertheless, most of the polymeric precursors used to produce carbon membranes are expensive, environmentally non-degradable, and most of them are exclusively obtained only at laboratory scale [10-19].

Although there is an increasing interest academically in CMSM research activities, there has been limited commercial success reported. Carbon Membranes Ltd. (Israel) proved that carbon hollow fiber modules could be produced on pilot scale using a complex multistep production method [20]. Their membranes showed potential for some separations, such as SF_6 recovery in dielectric environments, but the business unfortunately had to close down [21].

Regenerated cellulose based carbon hollow fiber membranes (CHFM), exhibiting excellent permeation properties, were developed by Department of Chemical Engineering at NTNU [22]. Membranes for Advanced Clean Technologies (MemfoACT AS), was a spin-off company established in 2008 to commercialize these membranes. A pilot scale facility was set up in Trondheim, Norway to produce CHFM from regenerated cellulose precursor with annual production capacity of 700 m^2 of carbon membranes.

The produced CHFM were installed on a pilot-scale plant (designed and built by MemfoACT AS) for upgrading 60 Nm^3/hr of raw biogas to vehicle fuel at the biogas field, GlØR IKS, Lillehammer, Norway. MemfoACT AS was the first company world-wide to bring regenerated cellulose-based (self-supported) carbon hollow fiber membranes out of the lab and to the reported technology readiness level (TRL-6). However, the company had to close down in 2015 – due to lack of investors, but all the valuable experience with respect to scaling up from lab to commercial modules within the field of hollow fiber carbon membranes, should be shared with fellow researchers, as is the motivation for this doctoral thesis as stated below.

1.2. Motivation and research Objectives

The motivation of writing this thesis is to document a comprehensive summary of the production process of carbon hollow fiber membranes on pilot scale, and to review and discuss for publication results from this development which was done at MemfoACT AS and NTNU. This information is judged to be remarkably helpful for further development in the field of carbon membranes.

The objectives for this development were to use a relatively low cost, easily commercially available, and environmentally friendly precursor to:

- *produce carbon hollow fiber membranes at semi-industrial scale*
- *develop industrial module design for high pressure and elevated temperature applications*
- *design the process, construct, and deliver the plants for CO_2-CH_4 and O_2-N_2 separation processes*

In this PhD work the above-mentioned development is documented and results discussed. Also, the engineering behind the scale-up process of MemfoACT AS facility and the performance of the produced carbon membranes in different gas separation applications, e.g. CO_2-CH_4 (in natural gas and biogas) and O_2-N_2 (for O_2 enriched air) are presented. Based on gained experience from this semi-industrial scale production of carbon membranes, this work also discusses the current drawbacks (high costs, aging issues, and mechanical brittleness) of carbon membranes and proposes a few recommendations for future research. In this thesis, the focus is on carbon membranes from regenerated cellulose precursor at semi-industrial scale facility. However, other materials may also be used as precursors for membranes, and references are provided, wherever required, for the other materials.

1.3. Main contribution of the author

The author of this thesis was heavily involved in all production steps of carbon hollow fiber membranes along with Dr. Jon Arvid Lie - (dope formation, spinning of cellulose acetate fibers, pre-treatment processes, deacetylation, drying of cellulose fibers, and carbonization). The author was also briefly involved in module construction process, gas permeation testing, and durability testing of the prepared carbon membranes under the supervision of Dr. Arne Lindbråthen. All HYSYS simulations were performed by the author. Moreover, he was also following the carbon membrane-based biogas upgrading plant at GlØR IKS, a biogas production plant at Lillehammer.

1.3.1. Contribution to the papers

Paper I- *Pilot – Scale production of carbon hollow fiber membranes from regenerated cellulose precursor: Part I- Optimal conditions for precursor preparation*

The paper is written by Shamim Haider. The spinning of hollow fibers was performed by Shamim Haider and John Anders Hamnes under the supervision of Dr. Jon Arvid Lie. Pre-treatment, deacetylation, and drying of hollow fibers was done by Shamim Haider. The rest of the authors were involved in the project and contributed to the manuscript structuring and revisions.

Paper II- *Pilot – Scale production of carbon hollow fiber membranes from regenerated cellulose precursor: Part II- Carbonization procedure*

The paper is written by Shamim Haider. The carbonization was performed by Dr. Jon Arvid Lie and Shamim Haider. The rest of the authors were involved in the project and contributed to the manuscript structuring and revisions.

Paper III- *Regenerated cellulose-based carbon membranes for CO_2 separation; Durability and aging under miscellaneous environments*

The paper is written by Shamim Haider. The experiments were performed by Dr. Arne Lindbråthen, Dr. Jon Arvid Lie, Shamim Haider, Cathrine Hval Carlsen, and Ingerid Caroline Tvenning Andersen. The rest of the authors were involved in the project and contributed to the manuscript structuring and revisions.

Paper IV- *CO_2 separation with carbon membranes in high pressure and elevated temperature applications*

The paper is written by Shamim Haider. The experiments were performed by Dr. Arne Lindbråthen, Shamim Haider, Dr. Jon Arvid Lie and Ingerid Caroline Tvenning Andersen. The rest of the authors were involved in the project and contributed to the manuscript structuring and revisions.

Paper V- *Vehicle fuel from biogas with carbon membranes; a comparison between simulation predictions and actual field demonstration*

The paper is written by Shamim Haider. The experiments were performed by Arne Lindbråthen, Jon Arvid Lie, Petter Vattekar Carstensen, Thorbjørn Johannessen, and Shamim Haider. The rest of the authors were involved in the project and contributed to the manuscript structuring and revisions.

Paper VI- *Techno-economical evaluation of membrane based biogas upgrading system: A comparison between polymeric membrane and carbon membrane technology*

Shamim Haider performed the simulations and wrote the paper. The rest of the authors contributed to the manuscript structuring and revisions.

Paper VII- *Carbon membranes for oxygen enriched air –Part I: Synthesis, performance and preventive regeneration*

The paper is written by Shamim Haider; The experiments were performed by Dr. Arne Lindbråthen, Dr. Jon Arvid Lie, and Shamim Haider. The rest of the authors were involved in the project and contributed to the manuscript structuring and revisions.

Paper VIII- *Carbon membranes for oxygen enriched air –Part II: Techno-economic analysis*

Shamim Haider performed the simulations and wrote the paper. The rest of the authors contributed to the manuscript structuring and revisions.

2. Theoretical background

This chapter provides a short introduction of the gas separation membranes and principal markets of these membranes.

2.1. Gas separation membranes

Membrane is a perm selective barrier which separates two phases and restricts transport of various molecules in a selective manner. Various mechanisms that cause this separation include: solution/diffusion, Knudsen diffusion, capillary condensation, and molecular sieving. Membrane materials can be organic (polymeric) or inorganic (carbon, zeolite, ceramic, glass or metallic) [23]. A simple flow diagram of a membrane process is shown in figure 2.1.

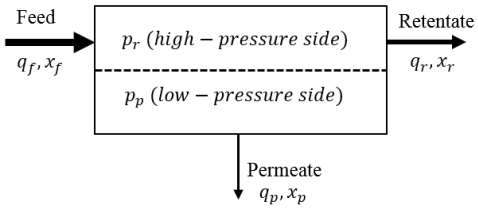

Figure 2.1: A simple flow diagram of a membrane process, with symbols for the equations [see list of symbols]

The key characteristic of membranes that determines the mechanism for transporting permeate molecules is whether the membranes are classified as either porous or dense (membrane with no detectable pores) [24]. As stated, carbon membranes are in the group of inorganic porous membranes and may have varying pore size. For porous membranes, the pore size distribution determines the size of particles (molecules at the smallest scale) that can pass through the membrane, as shown in table 2.1 [25].

Table 2.1: Porous membrane classification

Process classification	**Pore size range**	**Filtration classification**
Macroporous	> 50 nm (500 Å)	Microfiltration
Mesoporous	2-50 nm (20-500 Å)	Ultrafiltration
Microporous	1-2 nm (10-20 Å)	Nanofiltration
Nanoporous	< 1 nm (10 Å)	Molecular sieving

A simplified representation of porosity in a solid is shown in figure 2.2. The diagram and following description is taken from Rouquerol et al. (1994) [26].

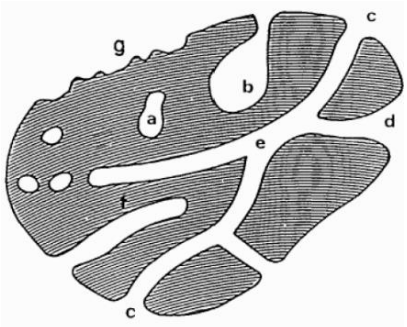

Figure 2.2: Schematic cross-section of a porous solid [26]

The first category of pores is those totally isolated from their neighbors, as in region (a), which are closed pores. Pores which have a continuous channel of communication with the external surface of the body, like (b), (c), (d), (e) and (f), are open pores. Some may be open at one end only, like (b) and (f); they are then described as blind pores. Others may be open at two ends (through pores), like around (e). These pores are responsible for gas permeation in carbon membranes. Pores may also be classified according to their shape: they may be cylindrical (either open (c) or blind (f)), bottle shaped (b), funnel shaped (d) or slit-shaped. Related to, but different from porosity is the roughness of the external surface, represented around (g).

2.2. Basic principles of membrane gas separation

One of the first milestones in the history of membrane formation was done by Fick in 1855, making symmetric (homogenous structure throughout the membrane) nitrocellulose films. This work resulted in the formulation of the well-known Fick's (equation 2.1) first law giving the flux J of a component A through a plane perpendicular to the direction of diffusion:

$$J_A = -D_A \frac{dc_A}{dx_A} \tag{2.1}$$

Where D_A is the diffusivity of the component A and $^{dc_A}/_{dx_A}$ is the driving force. Symmetric membranes suffered from low flux, but Loeb et al. [27] managed to produce *asymmetric* (gradual change in structure throughout the membrane) cellulose acetate membranes to be used for reverse osmosis in 1963. Those membranes had a reasonable flux because of thin, separating top-layer. Since then lots of membrane materials have been developed for a variety of separations.

In membrane processes, the driving force across the membrane could be, a partial pressure difference chemical potential difference, or an electrical potential difference. The permeability *P* of a gas through the membrane is a thickness and driving force normalized flux. The driving force in gas permeation is the partial pressure difference of the permeating component, therefore, the permeability [24], P_A, of a component A is given as the product of its diffusivity, D_A [m^2/s], and its solubility coefficient, S_A [m^3(STP)/(m^3(mat.) bar].

$$P_A = D_A S_A \tag{2.2}$$

Permeability is often given in the unit Barrer. Conversion factor between Barrer and other units is given in list of symbols.
The solubility, c_A [m^3(STP)/m^3(mat.)], of a gas A in a material can be described by Henry's law,

$$c_A = S_A p_A \tag{2.3}$$

Where p_A is the external gas pressure [Pa]. With reference to Fick's law (equation 2.1) the flux of component A may be calculated by inserting equation 2.2 and 2.3 and integrating. Hence, with partial pressure p_{fA} on the feed side (figure 2.1), with penetrant concentration in the membrane material c_{fA}, and partial pressure of permeate side p_{pA}, with concentration c_{pA}. Substitution of equation 2.3 into 2.1 and integration along the membrane thickness ℓ gives equation 2.4.

$$J_A \equiv \frac{q_p x_{pA}}{A} = \frac{D_A S_A}{\ell}\left(p_{fA} - p_{pA}\right) = \frac{P_A}{\ell}\left(p_f x_{fA} - p_p x_{pA}\right) \tag{2.4}$$

Where q_p is the permeate flow rate [m^3(STP)/h], x_p is the permeate mole fraction and A is the membrane area [m^2]. Hence, the flux of a component through a membrane is proportional to the trans-membrane partial pressure difference, and inversely proportional to the membrane thickness. The factor P/ℓ is called permeance, and is a practical property to use, because the lowest possible thickness differs from material to material. An optimized permeance will thus give an indication of the potential of the membrane to be used in a scaled-up process. Permeance should be used for asymmetric or composite membranes, while permeability (an

intrinsic material property) should only be used for isotropic structures, or when the thickness of separating membrane layer is known.

The ideal separation factor (also referred as perm-selectivity), α is the ratio of the permeability of component A to that of component B where a perfect vacuum exists at the downstream membrane face.

$$\alpha_{A/B} = \frac{P_A}{P_B} \tag{2.5}$$

For a gas mixture (binary mixtures only), the separation factor is the ratio of the compositions, x, of components A and B in the permeate relative to the composition ratio of these components in the retentate:

$$\alpha_{A/B} = \frac{x_{pA}/x_{pB}}{x_{rA}/x_{rB}} \tag{2.6}$$

2.3. Principal markets of gas separation membranes

In 1980, Permea (now a division of Air Products) launched its hydrogen-separating Prism membrane. This was the first large industrial application of gas separation membranes. Since then, membrane-based gas separation has grown into a $150 million/year business, and substantial growth in the near future is likely [6]. A list of principal gas separation applications and the approximate market size of each application is given in table 2.2.

Although numerous new polymer materials have been reported in the past few years and many have significantly higher separation performance than those in table 2.2. Yet, only eight or nine polymer materials are in use so far to make at least 90% of the total installed gas separation membrane base. Thus, it is surprising that, so few materials are actually used to make industrial membranes. However, permeability and selectivity are only two of the criteria that must be met to produce a useful membrane; other criteria include the ability to form stable, thin, low-cost membranes that can be packaged into high-surface-area modules (m^2/m^3).

Table 2.2: Principal Gas Separation Markets, Producers, and Membrane systems [5]

Company	Principal markets/estimated annual sales	Principal membrane material used	Module type
Large gas companies			
Permea (Air Products)	nitrogen/air ($75 million/year) hydrogen separation ($ 25 million/year)	Polysulfone	hollow fiber
Medal (Air Liquide)		Polyimide/polyaramide	hollow fiber
IMS (Praxair)		polyimide	hollow fiber
Generon (MG)		tetrabromo polycarbonate	hollow fiber
Mostly natural gas			
W.R. Grace	separations, CO_2/CH_4 ($30 million/year)	cellulose acetate	Spiral-wound
Separex (UOP)		cellulose acetate	spiral-wound
Cynara (Natco)		cellulose acetate	hollow fiber
Vapor/gas separation			
Aquilo	air dehydration ($20 million/year	polyphenylene oxide	
Parker-Hannifin		polyimide	hollow fiber
GKSS Licensees			plate-and-frame
ABB/MTR		Perflouro polymers, silicon rubber	spiral-wound

In 1991 Robeson [28] established upper bounds in the selectivity-permeability plots of several gas-pairs by compiling experimental data for many polymeric materials. Although the boundary lines have shifted in the desirable direction after nearly 20 years' research efforts, the achievements have not yet been truly spectacular. Attention of membrane research community was then later also focused on inorganic and mixed matrix materials, such as silica, zeolite and carbon, which exhibited molecular sieving properties. Remarkable improvements have been made in terms of the selectivity-permeability plot but the exploitation of these materials for the practical application remains underachieved primarily due to their poor processability for scaling up. Currently, 26 companies are manufacturing inorganic membranes and most of them were introduced to the market over the last 5 or 10 years. List and details of these membrane manufacturing companies can be found in the reference [29]. The Robeson plot was revised again in 2008 [30]. Figure 2.3 presents the prior upper bound (1991) and revisited upper bound (2008) for separation of gas pair O_2/N_2.

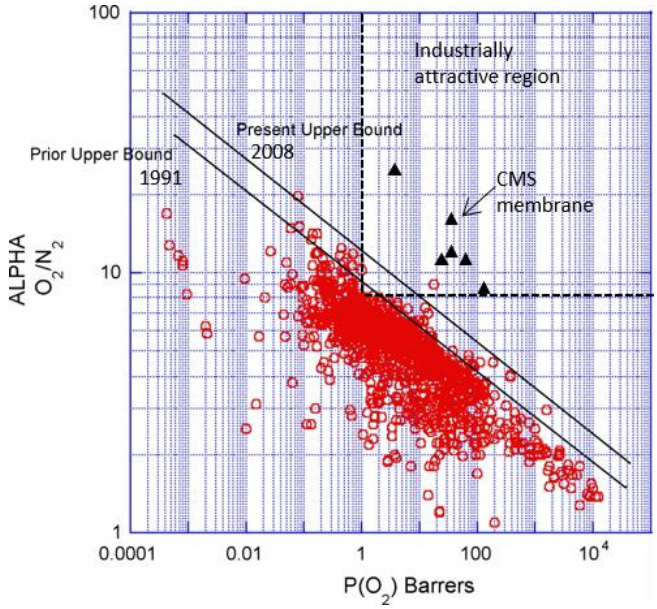

Figure 2.3: Robeson upper bound for gas pair O_2/N_2 (comparing separation performance of dense polymer membranes [30] with carbon membranes [31-35]). Data for CMSM and industrial applicability region [32] was added to the original Robeson plot. However, data for mixed matrix membranes and surface modified membranes can be found in [36].

3. Carbon molecular sieve membranes

Carbon molecular sieve membranes (CMSM) are the focus of the work presented in this thesis. CMSM have been studied in more than three decades as a promising candidate for energy-efficient gas separation. Strong interests have been in the preparation of CMSM for gas mixture separation such as CO_2-N_2, O_2-N_2, and CO_2-CH_4. These membranes can be divided into two categories: unsupported/self-supported (flat film, hollow fiber, and capillary tube configurations) and supported (flat film and tube configuration). Self-supported carbon hollow fiber membrane is the focus in this work however, detailed description of other configurations can be found in [29].

The focus of this chapter is to introduce background information about preparation of carbon membranes (CM), transport mechanisms in CM, aging and regeneration of CM, and potential applications of CM. A short overview of MemfoACT AS company is also provided in the last section of this chapter.

3.1. Structure and preparation of carbon molecular sieve

Bisco and Warren [37] introduced the concept of turbostratic order for graphitic carbons. The carbon consists of turbostratic groups, where each group has several graphite layers stacked together roughly parallel and equidistant, but with each group having a random orientation as shown in figure 3.1. Packing imperfection between the stacked layers contains slit-like pores which give rise to the molecular sieving structure and have a bimodal pore size distribution. The edges of adjacent stacked layers are believed to make the slit-like ultra-micropores (≤0.7nm), while micropores (0.7-2nm) are formed between the planes due to the random orientation of the adjacent carbon sheets [6]. The gases may diffuse through the pores, or they may adsorb on the walls and travel through the pores by a mechanism known as surface flow [38]. The bigger, more strongly adsorbed molecules may also block the pores of smaller molecules in a phenomenon known as competitive adsorption or selective surface flow. This results in reverse selectivity; the smaller components are retained.

CMSM are prepared by the thermal decomposition, in a controlled chemical environment, of organic compounds that do not melt or soften during carbonization [38-40]. Precursors include thermosetting resin, graphite, coal, pitch and plants and synthetic polymers [41]. Synthetic polymers include polyimide and derivatives, polyacrylonitrile, phenolic resin, polyfurfuryl alcohol, polyvinylidene chloride – acrylate terpolymer and phenol formaldehyde [42].

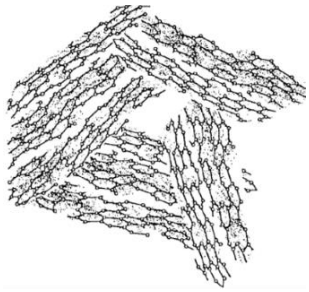

Figure 3.1: Structure of turbostratic graphite [37]

A block diagram for the pilot-scale production of CHFM from cellulose acetate is presented in Figure 3.2. Also, Figure 3.3 presents the comparison between CHFM and polymeric hollow fiber membrane.

Geiszler and Koros [43] reported that an inert gas (Ar, He or N_2) atmosphere resulted in more open, but less selective CMSM matrix compared to vacuum carbonization. They explained this with acceleration in the carbonization process due to increased gas phase heat and mass transfer. By increasing the final temperature in polyimide carbonization from 550 °C to 800 °C (in vacuum or He gas), the authors observed that a decrease in permeance while selectivity increased. Precursors for CMSM include thermosetting resin, graphite, coal, pitch, plants and synthetic polymers [41].

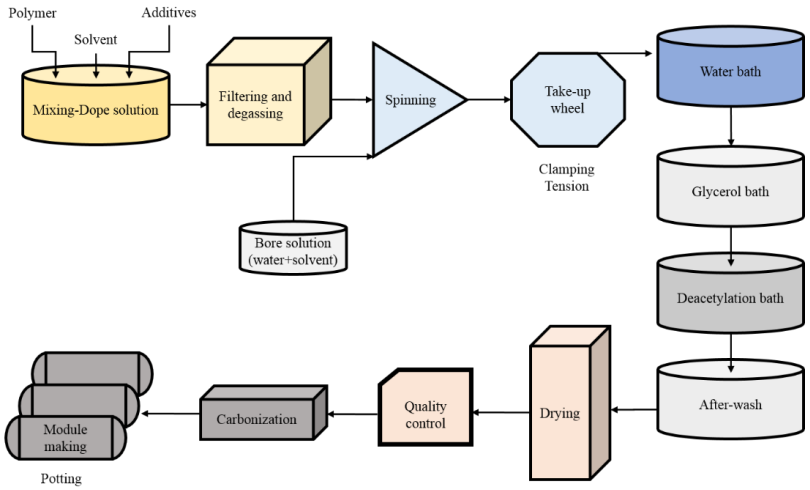

Figure 3.2: Block diagram for the pilot-scale production process of CM from CAHF

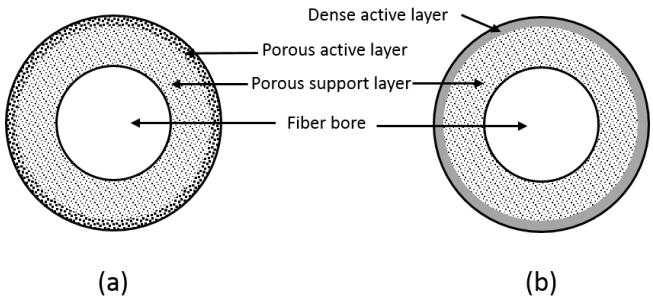

Figure 3.3: Comparison of (a) carbon hollow fiber membrane with (b) polymeric hollow fiber membrane [41]

Koresh and Soffer [40] summarized the benefits of CMSM compared to polymeric membranes:

- CMSM have a different permeation mechanism and may produce far superior permeability-selectivity combinations than any known polymer membrane.
- Different pyrolysis conditions can be used to tailor the micropore structure for different separation purposes, starting from the same precursor.
- They are far more stable at high temperatures than polymers and may be suited to high-temperature applications as shown in table 3.1.
- They are more stable in the presence of organic vapors at high temperatures, organic solvents and non-oxidizing acid or base environments.
- They are mechanically stronger and can withstand higher pressure differences for a given wall thickness.

Table 3.1: Thermal stability of carbon membranes in the presence of various gases [40]

Gas	**He**	**H_2**	**CH_4**	**CO_2**	**O_2**
Temp. °C	700	> 500	500	400	< 200

The disadvantages mentioned were:

- Carbon membranes are more brittle and may require special handling.
- Strongly adsorbing organic vapors may block the pore system, requiring a pre-purifier.

However, this may be avoided by operating at higher temperatures.

The focus of this thesis is the semi-industrial scale production of carbon hollow fiber membranes from regenerated cellulose. Flat sheet carbon membranes derived from cellulose have been investigated by Lie [22] at the Norwegian University of Science and Technology primarily for use in biogas upgrading application. Whereas, carbon hollow fiber membranes

derived from regenerated cellulose have been investigated on laboratory-scale by He [44] in the same university for use in CO_2 separation applications.

3.2. Carbon membrane module construction

MemfoACT AS developed a pilot-scale CHFM module design for high pressure and elevated temperature applications. Membrane module construction is, however, seldom referred in open literature as details on this will typically be confidential information for a company producing membrane modules. To date, only tubular and hollow fiber lab-scale modules have been reported for carbon membranes. The potentially industrial use of these membranes was reported by two companies; Carbon Membranes Ltd. (Israel) in the late nineties, and later Blue Membranes GmbH (Germany). Carbon Membranes Ltd. Produced hollow fibers on pilot scale and demonstrated successful operation in various applications, while Blue Membranes developed a new concept based on honeycomb membrane module configuration (HM) [45] for their carbon membranes. None of these companies succeeded in taking their carbon membranes all the way to the market. Saufi S. M. et al. [41] reported that all system designs for module must consider the factors of production cost, maintenance, and efficiency. A typical lab-scale CHFM module is shown in figure 3.4 (Swagelok tubing was used in this study, but any tubing within a given wall thickness and roundness can be used).

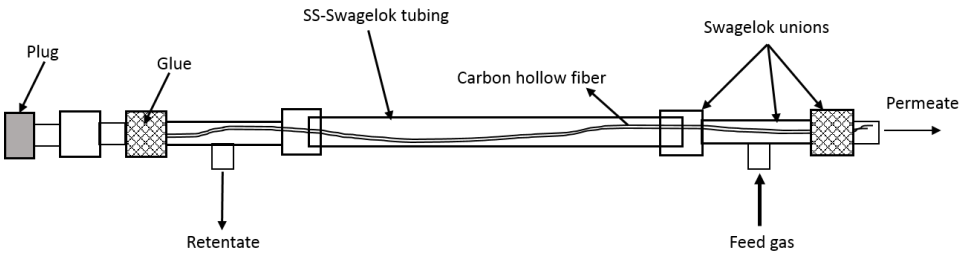

Figure 3.4: A schematic of lab-scale CHFM module

3.3. Post treatment of carbon membranes

Upon pyrolysis polymeric membranes are transformed into carbon membranes with varying degrees of porosity, structure and separation properties that depend to an extent on the pyrolysis conditions. In some cases, it is found to be advantageous that the pore dimension and its distribution in a carbon membrane are finely adjusted by a simple thermochemical treatment to meet different separation needs and objectives [46]. The increase in performance

(permeability and selectivity of a preferred gas) of the membrane cuts the capital cost, as less area is required to treat the same volume of gas. Numerous methods are being used to enhance the performance of carbon membranes and most of them involve changing precursor, precursor geometry, and pyrolysis conditions. Variations in these factors offer desirable carbon membrane morphology and tailored microstructure resulting in desired permeation properties [11, 38, 47-53].

Typically, when a membrane is exposed to an oxidizing atmosphere after the pyrolysis step, the ensuing oxidation increases the average pore size [29, 54-56]. The oxidation of carbon membranes can be performed using pure oxygen, oxygen admixed with other gases, air, or other oxidizing agents such as steam, carbon dioxide, nitrogen oxides and chlorine oxides or solutions of oxidizing agents such as nitric acid, mixtures of nitric and sulfuric acids, chromic acid and peroxide solutions at elevated temperatures [56]. The selectivity of a carbon membrane may be increased through the introduction of organic species into the pore system of the carbon membrane and their pyrolytic decomposition (i.e. chemical vapor deposition, CVD) [55-58]. Generally, to manufacture carbon molecular sieves, the inherent pore structure of the carbonaceous precursor is initially tailored into a suitable pore size range by controlling the thermal pretreatment, followed by a final adjustment of the pore structures by CVD [59].

3.4. Gas transport through carbon membranes

The ability of a porous carbon to separate gases depends on the pore size (distribution) of the membrane, the physicochemical properties of the gases and surface properties of the pore. The pore size of a carbon membrane for gas separation is usually within the range of 3.5 – 10 Å, depending on the conditions of preparation of the membrane during the carbonization or the post-treatment (post oxidation or chemical vapor deposition) [11, 39, 43, 60].

The transport mechanism is basically one of the three mechanisms listed below [61-64].

1) *Classical or activated Knudsen diffusion*; the square root of the inverse ratio of the molecular weights gives the separation factor for classical Knudsen as shown in table 3.2.
2) *Selective surface diffusion*; governed by a selective adsorption of the larger non-ideal components on the pore surface, hence retaining the smaller components from permeation.
3) *Molecular sieving (configurational diffusion)*; separation according to molecular size and shape. All three transport mechanisms are shown in figure 3.5.

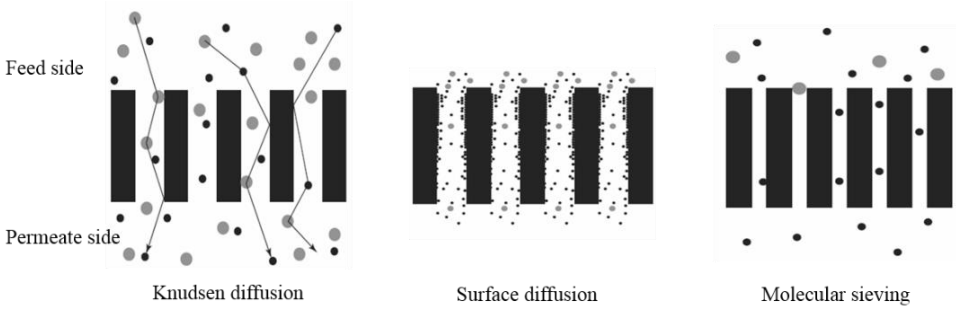

Figure 3.5: Transport mechanisms, depending on the pore size, penetrant and process conditions [65]

Table 1.2: Porous membrane selectivity under Knudsen flow

Gas components	**Molecular weight ratio**	**Knudsen flux ratio**
CO_2/H_2	21.83	1/4.67
CO_2/CH_4	2.75	1/1.66
CO_2/N_2	1.57	1/1.25
O_2/N_2	1.14	1/1.07

Knudsen diffusion will dominate for the largest pores, and molecular sieving for the smallest ones. However, different mechanisms may occur simultaneously.
The general equation for all types of diffusion (from equation 2.1) is:

$$D = g_d \lambda u . exp\left(\frac{-E_a}{RT}\right) \tag{3.1}$$

Where g_d is the probability of doing a jump in the right direction, i.e. from the high-pressure side towards the low-pressure side, with jump length λ and velocity u. The exponent expresses the probability that a molecule has sufficient energy to overcome an energy barrier E_a [66].

3.4.1. Knudsen diffusion

If the mean free path is very much larger than the membrane pore radius, gas molecules will collide more frequently with the pore walls than they will with other gas molecules. This situation is termed free molecule flow, or Knudsen flow. It may be difficult to know exactly when transport due to Knudsen diffusion is taking place. One way to approach this problem is to calculate the Knudsen number, N_{Kn}, for the system, which is λ/d_p, where λ is the mean free

path and dp is the pore size. This means that the mean free path for the molecule, which is temperature dependent, first must be calculated, and then Knudsen number (N_{Kn}) checked. If $N_{Kn} \geq 10$, the separation can be assumed to take place according to Knudsen diffusion [67]. The classical Knudsen diffusivity D_K of a component is independent of pressure, and can be calculated from equation 3.2:

$$D_K = \frac{d_p}{3} u = \frac{d_p}{3} \sqrt{\frac{8RT}{\pi M}} = 48.5 \, . d_p \sqrt{\frac{T}{M}} \tag{3.2}$$

Where d_p is the average pore diameter (nm), u is average molecular velocity (m/s), M is molecular weight (g/mol) and T is the temperature (K) . The flux can then be calculated according to:

$$J_K = \frac{D_K \, . \Delta p}{RT\ell} \tag{3.3}$$

Here ℓ is the effective membrane thickness.

For Knudsen diffusion to take place, the lower limit for pore diameter has usually been set to dp > 20 Å [62, 67]. Gilron and Soffer [63] have however discussed thoroughly how Knudsen diffusion may contribute to transport in smaller pores, and from a model considering pore structure, shown that contributions to transport may come from both activated transport and classical Knudsen diffusion through one specific microporous membrane. Lindbråthen [68] Showed that permeation of He through a modified glass membrane (dp ~ 1nm) was best described with activated Knudsen diffusion, and not classical, judged from the temperature dependence. Other permanent gases, like H_2, N_2 and O_2, also seemed to follow an activated Knudsen diffusion through a membrane with porosity ε and tortuosity τ (ratio of the mean path length of a penetrant crossing the membrane, and the nominal membrane thickness ℓ) is given by equation 3.4:

$$\left(\frac{P}{\ell}\right)_{Ka} = \frac{4\varepsilon d_p}{3\tau\ell\sqrt{2\pi}} \sqrt{\frac{8}{\pi MRT}} \exp\left(\frac{-E_a}{RT}\right) \tag{3.4}$$

3.4.2. Selective surface flow (SSF)

The driving force for separation according to a surface selective flow is basically the difference in the concentration of the adsorbed phase of the diffusing components. This means that a large driving force can be attained even with a small partial pressure difference for the permeating component. The larger molecules (more condensable, e.g. hydrocarbon) in a gas mixture will be selectively adsorbed, hence the smaller molecules will be retained due to reduced pore size. The pore size region where selective surface flow is expected to take place is about 5 Å < dp < 10 Å; or up to 3 × (diameter of molecule) [62]. The transport of gas molecules through a carbon membrane can also be described by Fick's first law as given in equation 2.1 and activated diffusion was described by an Arrhenius type of equation:

$$D_a = D_0 \,.\exp\left(\frac{-E_d}{RT}\right) \tag{3.5}$$

Here E_d is the activation energy for diffusion. Now if Henry's law is assumed to apply, the integrated flux equation is written as:

$$J_s = \frac{\Delta p}{RT\ell} D_0 \; exp\left\{\frac{-\left(E_{a,s} - E_{ads}\right)}{RT}\right\} = \frac{\Delta p}{RT\ell} D_0 \,.\exp\left(\frac{-\Delta E_s}{RT}\right) \tag{3.6}$$

Here D_0 is a temperature-dependent pre-exponential factor. ΔE_s, the difference in transport activation energy and adsorption energy may be positive or negative. When $\Delta E_s < 0$, transport due to SSF increase with decreasing temperature; with $\Delta E_s > 0$, it decreases. In simple words; adsorption and hence selectivity increase with decreasing temperature [66].

3.4.3. Molecular sieving

Molecular sieving, also referred to as configurational diffusion, is the dominating transport mechanism in most carbon membrane applications.

This has also given the name to these membranes; carbon molecular sieve membranes. The pore size is usually within the range of 3-5 Å. The dimensions of a molecule are usually described either with the Lennard-Jones radii or the Van der Waal radii. The sorption selectivity has little influence on the separation when molecular sieving is considered. Equation 3.6 is still

valid for the activated transport, but now attention should be drawn to pre -exponential term, D_0 [69].

$$D_0 = e\lambda^2 \frac{kT}{h}\, exp\left(\frac{S_{a,d}}{R}\right) \tag{3.7}$$

Where e is the natural logarithmic base number(~ 2.72), λ is the jump length, k and h are Boltzmann's and Planck's constants, respectively, and $S_{a,d}$ is the activation entropy for diffusion. This means that change in entropy will give a significant contribution to increase in selectivity when molecular sieving is considered. Singh and Koros [70] have discussed it thoroughly. Flux may be described as:

$$J_s = \frac{\Delta p}{RT\ell} D_0\, exp\left(\frac{-E_{a,MS}}{RT}\right) \tag{3.8}$$

Here $E_{a,MS}$ is the activation energy for diffusion in the molecular sieving regime for CMSM. Nguyen et al. [71] reported that the CMSM presents reasonable sieving effect for gas molecules with different kinetic diameters, which suggests that the CMSM is predominantly microporous with no major contribution from Knudsen diffusion or viscous flow in its overall mass transfer.

3.4.4. Separation properties in single gas vs. mixed gas

As opposed to most polymers, carbon membranes may give higher selectivity in mixed gas tests than in single gas tests. The main reasons for this are that i) carbon shows a very small degree of freedom of swelling (e.g. in CO_2) and that ii) the most permeable molecules hinder some of the least permeable molecules from entering the pore network. However, the selectivity obtained from mixed gas tests may also be less than from single gas test, if the most permeable component partly entrains the other component.

3.4.5. System operating conditions

Gas separation performance for a given membrane system is mainly dependent on membrane permeability and selectivity. However, the operating conditions for a specific process can also affect the membrane separation performance. One of the most important parameters is the pressure ratio across the membrane, which is the ratio between the pressure on the feed side and on the permeate side.

The component i can only transport through the membrane when the partial pressure in the feed side (p_F) is higher than the pressure in the permeate side (p_p):

$$\chi_{i,F} p_F > y_{i,p} p_p \quad \text{or} \quad \frac{y_{i,p}}{\chi_{i,F}} < \frac{p_F}{p_p} = \phi \tag{3.9}$$

Equation 3.9 indicates that the enrichment of component i can never exceed the pressure ratio, regardless of the membrane selectivity [65]. The relationship between pressure ratio and the membrane selectivity can be derived from the Equation 2.4, 2.6, and 3.9 [65, 72].

$$y_{i,p} = \frac{\phi}{2}\left[\chi_{i,F} + \frac{1}{\phi} + \frac{1}{\alpha - 1} + \sqrt{\left(\chi_{i,F} + \frac{1}{\phi} + \frac{1}{\alpha - 1}\right)^2 - 4\frac{\alpha \chi_{i,F}}{(\alpha - 1)\phi}}\right] \tag{3.10}$$

If the membrane selectivity (α) is much larger than the pressure ratio (ϕ), that is, $\alpha \gg \phi$, thus the equation 3.10 can be simplified as

$$y_{i,p} = \chi_{i,F}\, \phi \tag{3.11}$$

This is generally called the pressure-ratio-limited region, and the membrane separation performance is mainly controlled by the pressure ratio across the membrane while the selectivity has only minor effect.

However, if the membrane selectivity is much smaller that the pressure ratio ($\alpha \ll \phi$), the equation 3.10 becomes,

$$y_{i,p} = \frac{\alpha \chi_{i,F}}{1 - \chi_{i,F}\,(1 - \alpha)} \tag{3.12}$$

This is called the membrane selectivity-limited region, and the membrane separation performance is mainly controlled by the membrane selectivity and pressure ratio has minor effects in this region. In between, both the pressure ratio and the membrane selectivity will influence the membrane performance.

An example for the dependence of the permeate concentration vs. the pressure ratio and selectivity was reported by [72] as shown in figure 3.6 and 3.7. The pressure ratio is very

important for gas separation processes in industrial scale due to the practical limitation of the pressure ratio. Achieving the high-pressure ratios by compressing the feed side to high pressure or drawing a high vacuum on the permeate side will significantly increase the energy cost. Therefore, the practical pressure ratios are typically in the range 5-20 [65].

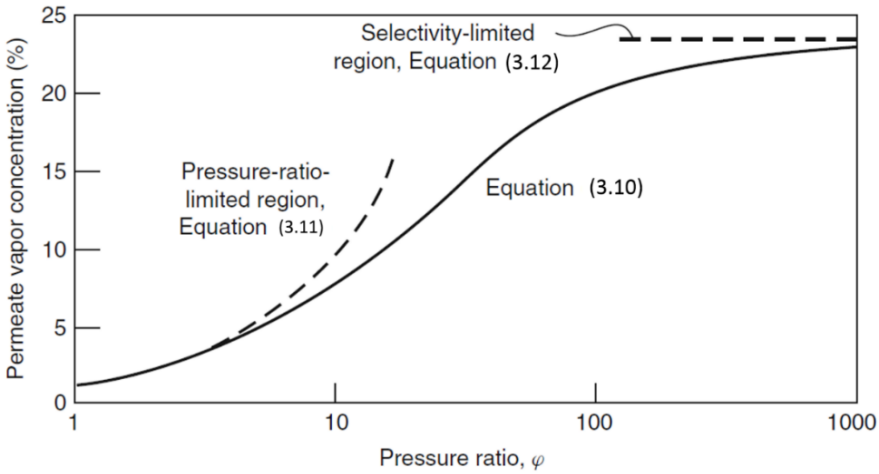

Figure 3.6: The dependence of the permeate vapor concentration on the pressure ratio at a vapor/nitrogen selectivity of 30 and a feed vapor concentration of 1%. Below the pressure ratio of about 10, the separation is controlled by the pressure ratio across the membrane. Above the pressure ratio of 100, the separation is controlled by membrane selectivity [72]

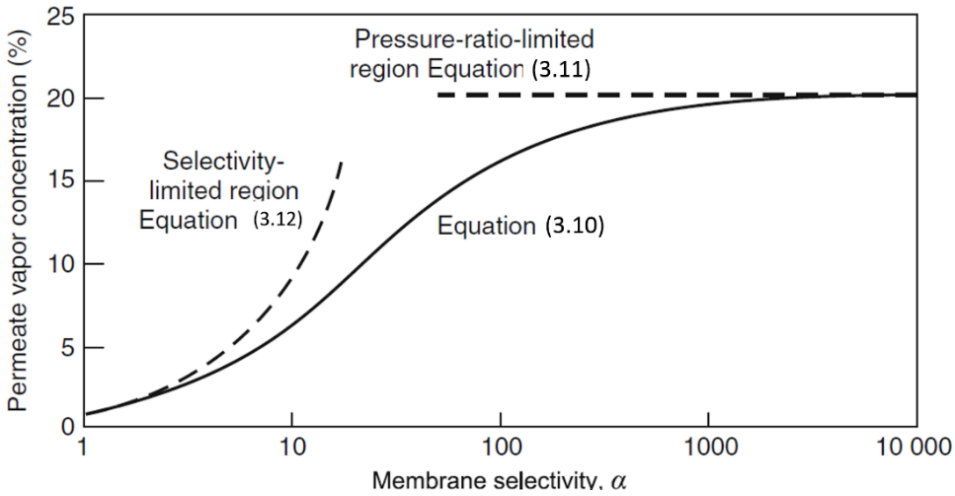

Figure 3.7: The dependence of the permeate vapor concentration on selectivity at a pressure ratio of 20 and a feed vapor concentration of 1%. Below the membrane selectivity of about 10, the separation is controlled by the membrane selectivity. Above the membrane selectivity of 100, the separation is controlled by the pressure ratio across the membrane [72]

3.5. Durability and aging of carbon membranes

Carbon membranes are known to age, and extended exposure to various molecules such as H_2O and O_2 change the effective pore size by physical or chemical sorption, hence modifying the performance of the membrane. The vulnerability of CMSM to water is a complex phenomenon. Carbon surfaces are basically hydrophobic; however, the microporous walls of the carbon membrane will quickly become partially covered with an oxygen containing functional group which hence results in the membrane having a hydrophilic character. Therefore, once the first layer of water molecules is adsorbed, adsorbate-absorbate interactions promote further adsorption of more water through hydrogen bonds [73, 74]. This results in a reduction in capacity of the membrane, and hence is a serious problem for the industrial application of carbon membranes as most feed streams contain some humidity. Jones et al. [75] reported that performance losses were minimum for carbon membranes prepared at 550 °C as compared to the one pyrolyzed at 500 °C when tested in the range of 23-85% humidity. Xu et al. [76] have recently reported the importance of physical aging showing that physical aging appears to be the leading source for rapid changes of transport properties at the early stage after the membrane fabrication. It may happen due to shrinkage of pores over time to achieve a thermodynamically stable state. Wenz et al. [77] has recently reported the postsynthetic modification method to suppress the physical aging by tuning the pores of carbon membranes. Chemical sorption involves chemical bonds, usually C-O bonds, and the bonding forces here are stronger than van der Waals forces (physical bonding), making removal of these components more complex and energy demanding [78, 79].

3.5.1. Regeneration of carbon membranes

Although CM have reported better performance compared to polymeric membranes, the operational stability and aging are the important issues to be considered for the implementation of these carbon membranes. CM usually age very rapidly due to physical aging (pore shrinkage to achieve a thermodynamically stable structure and or physical adsorption of gas molecules) and or chemical aging (chemical bonding, usually C=O bonds) [76-79]. This aging effect may seriously reduce the permeability of a membrane and hence it is still a major problem for the industrial application of CM in air separation where the membrane is exposed to O_2 all the time.

Several techniques have been reported to achieve a stable performance of CM under oxygen environment. Menendez et al. [78] used *thermal regeneration* and found that thermal treatment

of membranes at 120 °C in a vacuum could remove oxygen-containing surface groups from activated carbons. However, the regenerative effect is very brief because it leaves a surface with reactive carbon sites that can re-adsorb oxygen very quickly even at room temperature. *Chemical regeneration* requires an addition of a chemical (gas) to restore the membrane performance. Jones and Koros [80] tested purging of propylene at about 10 bar to restore the membrane performance, however, the permeance of O_2 was not successfully recovered.

Lie et al. [19] studied *electrothermal regeneration* to enhance the permeation of CO_2 in iron-doped flat-sheet CM. They applied a direct current of 30 mA (17.5V) on the iron-doped CM and studied the effect of pulsating electrothermal regeneration (i.e. electric current set to "on" and "off" periodically). After electrothermal regeneration, the CO_2 permeability was 65% higher compared to initial value because the sorption of gases in carbon matrix was reduced, while diffusivity was increased to a considerable extent. Nevertheless, the membrane without any regeneration showed 60% loss in permeance of CO_2.

The electrical resistance R (Ω) can be evaluated from media resistivity and its dimensions [81] as shown in equation 3.13.

$$R = \frac{\rho L}{e\ell} \qquad 3.13$$

Where ρ is electrical resistivity of the material (Ωm), L is the length of material (m), e is the width (m) and ℓ is the thickness (m). Resistivity is defined as resistance times cross sectional area for the current flow, divided by the resistor length [64].

3.6. Potential applications of Carbon membranes

There are several potential applications of the CM in gas separation which may include: biogas upgrading, natural gas sweetening, CO_2 capture from flue gas, air separation, elevated temperature applications (hydrocarbon dehydrogenation and steam methane reforming). Carbon membranes are also promising candidate for the separation of light alkenes/alkanes especially for propene/propane separation, and also showed a good performance for the 1,3-butadiene/n-butane separation [82]. Carbon molecula sieve membranes have high He permeance along with significant He/N_2 and He/CH_4 selectivities [83-86]. Carbon membrane development for air separation and CO_2/CH_4 separation (biogas upgrading to vehicle fuel and natural gas sweetening) is closest to market level and is the focus of this thesis. Therefore, only

these two applications will be discussed here however, more information about other applications can be found in the references [29, 44, 87, 88].

3.6.1. Membranes for CO_2-CH_4 separation

In case of CO_2-CH_4 separation, there are two potential markets for carbon membrane; biogas upgrading to vehicle fuel and natural gas sweetening. Biogas upgrading to vehicle fuel/natural gas is an emerging market. However, natural gas sweetening is a billion-dollar industry. In recent times, biogas has become a valuable renewable energy source and is considered a strategy for greenhouse gas reduction. Renewable technologies are making relatively fast progress and expected to increase significantly (30-80%) in 2100 [2, 89]. The major components of biogas are CH_4 and CO_2 with traces of H_2S, some other gases and vapors [90, 91]. A study on different utilizations of biogas reports that biogas upgrading to fuel quality gives the highest portion of exportable energy with a medium range (10%) energy demand [92]. In the aforesaid statement, upgrading was done with membrane process. A detailed description about biogas composition, pre-treatment process, and upgrading process is discussed in chapter 5 of this thesis.

Natural gas sweetening is a huge market for CO_2-CH_4 separation process. The purification process of natural gas by removal of CO_2 (natural gas sweetening) is in principal the same separation process as for upgrading of biogas. However, in this case, the feed is present at much higher pressure (50-70 bar) which is also favorable for separation with carbon membranes as they can be operated at high pressure. The demand for natural gas has increased by around 2.7% per year over the last decade with a total consumption of 3.54 trillion cubic meters (125 trillion standard cubic feet) in 2016 [1], and this consumption drives a worldwide market of over $5 billion per year for new natural gas separation equipments. Currently, membrane processes have < 5% of this market, almost all of which is applied toward the removal of CO_2. The market for gas separation membranes is expected to grow from US$ 150 million in 2002 to around US$ 750 million in 2020 [6, 93, 94].

Conventional methods for CO_2 separation are based on reversible absorption, such as amine scrubbing, but these processes are energy intensive and pose environmental concerns. Amine absorption is considered the most mature technique to separate out CO_2, but the limitation of regular maintenance and continuous operator care hinder the use of amine absorber-strippers at remote locations [4].

Membrane could be a potential candidate for this application. Various membranes for CO_2/CH_4 separation are available. Based on the materials of the membranes, three major categories exist,

e.g. polymeric membranes, inorganic membranes and mixed matrix membranes. However, membrane processes have < 5% of the natural gas sweetening market, as this technology is still facing challenges to overcome the plasticization and degradation of the membrane (caused by H_2O, CO_2, C_{4+} hydrocarbons and aromatic compounds). There is a further limitation of low selectivity and flux of currently available polymeric membranes that bounds its application to only process small/medium gas flows (< 50,000Nm^3/h) [23, 65]. Insufficient thermal and chemical stability of polymeric membranes limits the regeneration/cleaning of these membranes which is essential when impurities like mist of higher hydrocarbons and fine particles deposit on the membrane surface.

Inorganic membranes are useful for CO_2 separation under severe conditions (high temperature and pressure) when organic based membranes are not functional. Porous inorganic membranes such as zeolites, which contain sub-nanometer pores, are favorable for CO_2 separation and removal from CH_4 because of their chemical resistance to CO_2 induced plasticization and superior selectivity to polymeric membranes [64, 95, 96]. Other porous inorganic membranes such as silica and carbonized membranes are also available for CO_2/CH_4 separation. Both membranes normally separate CO_2 from other gases including CH_4 by molecular sieving principles e.g. silica has sub nanometer sized pores which would pass different gases according to their sizes [97]. Robeson [28] made a literature data collection of the gas permeability and selectivity of different polymers and found a trad-off relationship for gas pairs. The empirical upper bound relationship for membrane separation of gases initially published in 1991 was reviewed with the numerous data available in 2008 [30]. This plot for CO_2/CH_4 pair is shown in figure 3.8 (a) and (b).

A lot of researchers have been conducting Simulations and modelling of multi stage membrane systems to evaluate and optimize membrane systems for CO_2 capture [98-105]. Baker et al. [5] have provided a guideline for conducting simulations on commercially available membranes, which also shows the comparison between membrane system and amine absorption process. Baker suggested that membrane technology is viable in small (less than 6000 Nm^3/h) and medium scale (6000–50,000 Nm^3/h) processes.

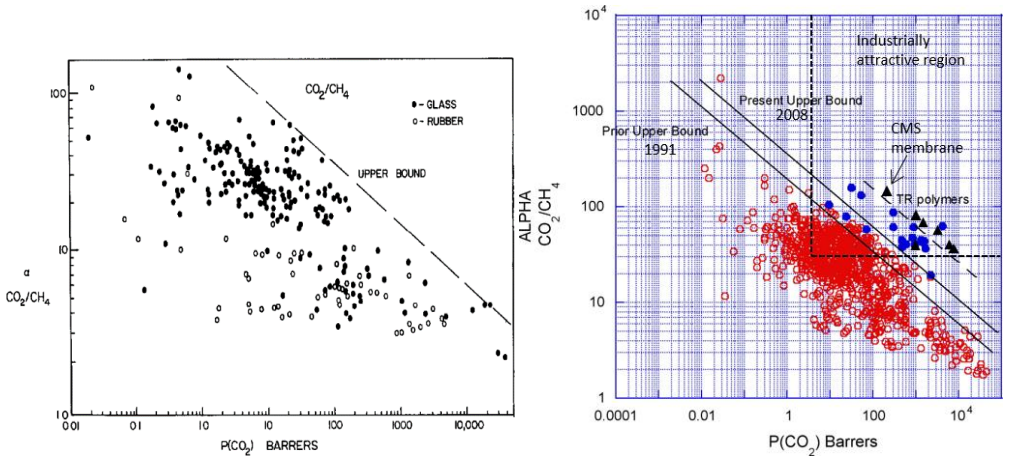

(a) (b)

Figure 3.8: Robeson upper bound for gas pair of CO_2/CH_4; (a) Upper bound-1991 [28] (b) revisited upper bound-2008 (comparing separation performance of dense polymer membranes(red dots), thermally rearranged (TR) polymer membranes (blue dots) [30], and carbon membranes from different precursors (black triangles) [19, 31, 106-108]. Data for CMSM and industrial applicability was added to original Robeson plot.

3.6.2. Membranes for air separation

The O_2/N_2 separation remains the most studied gas pair with more data existing in the literature than any of the other pairs. The principal market for both nitrogen and oxygen demands 99% or higher purity. A single stage process with commercially available membranes can accomplish 99% nitrogen at an overall recovery of 50% [6]. High purity oxygen is difficult using only membranes because of the high content of nitrogen present (79%) in the air, resulting in oxygen enriched permeate (30-60% O_2 in permeate), rather than pure oxygen (relatively low driving force over the membrane) [6, 109]. The pressure differential across the membrane can be generated either by pulling a vacuum on permeate side or using a compressor on the feed side. Compression of the feed is not an economically viable option as only a small part of the feed permeates through the membrane. However, using a vacuum could be a suitable option if a membrane with high O_2 flux of is available. If not, then larger membrane area is required and it will require when vacuum is used instead of feed pressure for any membrane material.

In polymeric membranes, the gas molecules dissolve into the membrane, then subsequently diffuse across the membrane thickness, and desorb on the other side (solution-diffusion mechanism) [23]. Polymeric materials may have high permeability for O_2, but rather low O_2/N_2

selectivity (usual range 2-8), and the maximum permeate purity achievable for O_2 with polymeric membranes seems to be 30-60% [5, 6, 110-114].

The difference in molecular size of O_2 (kinetic diameter: 3.46 Å) and N_2 (kinetic diameter: 3.64 Å) is very small [115], and separation of such small difference in size could be much easier if the membrane pore walls were rigid and the space available for permeation fixed. This mechanism is known as molecular sieving [12, 116-118]. In molecular sieving, the available pore size is below the kinetic diameter of one of the gas components in the feed. This increases selectivity by reducing the rotational degrees of freedom of nitrogen versus oxygen in the diffusion (kinetic) transition state. In this regard, inorganic membranes with molecular sieving effect resulting in higher performance compared to polymeric materials can be potential candidates. The Robeson plot from 1991 and revised upper bound for O_2/N_2 pair are shown in figure 3.9 (a) and (b). In these figures, polymeric membranes lie below Upper bound and hence, are not commercially viable solution for separation of O_2 from air.

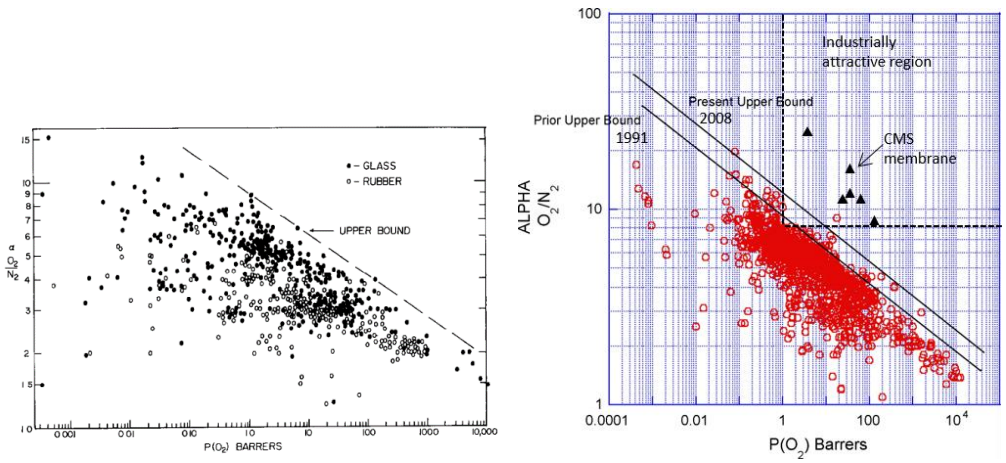

(a) (b)

Figure 3.9: Robeson upper bound for gas pair of O_2/N_2; (a) Upper bound-1991 [28] (b) revised upper bound-2008 [30]

As stated earlier, high purity oxygen is difficult using membranes because of the high content of nitrogen in the air, (79%) and the relative low selectivity of O_2/N_2 resulting in oxygen enriched air (OEA) in permeate, rather than pure oxygen. Based on the performance of commercially available polymeric membranes, the separation process is competitive only for medium O_2 purity (25-40%) and small-scale plants (10-25 tons/day) [111, 119]. Oxygen enriched air is already used for numerous chemical processes (Claus process, the Fluid

Catalytic Cracking technology, the oxidation of *p*-xylene to give terephthalic acid) combustion processes (natural gas furnaces, coal gasification), medical purposes, and has more recently also attracted attention for hybrid carbon capture process [120].

Carbon is a class of material that can offer improved performance due to molecular sieving effect. In addition, carbon membranes (CM) offer superior thermal resistance and chemical stability in corrosive environments [42]. Many prior studies have reported higher selectivity and permeability of CM compared to polymeric membranes for air separation [9, 19, 52, 121, 122].

In 1991, Bhide and Stern calculated the membrane performance required to produce OEA at a cost competitive to cryogenically produced oxygen at $40-60/ton of equivalent pure oxygen (EPO_2) [119]. They showed that none of the today's polymers can reach the $40-60/ton EPO_2 target. To reduce the capital and production cost (PC) of the membrane-based process, both selectivity and permeability must be improved. Higher O_2/N_2 selectivity is required to reach the high purity of O_2 with a lower driving force (partial pressure ratio) hence, the operating cost will be reduced. A higher O_2 permeability will cut the required membrane area for the separation, therefore, low capital investment is needed. Much academic research is focusing on producing highly selective membranes, but if the membranes then have too low permeabilities they are most likely not an optimum choice for the application in focus.

3.7. MemfoACT AS production facility

The intention of this section is to give a brief introduction of MemfoACT AS and her pioneers. MemfoACT AS was a spin-off established in August 2008 as a joint venture between Norwegian University of Science and Technology (NTNU) and the entrepreneurs' professor May-Britt Hägg, Dr. Jon Arvid Lie and Dr. Arne Lindbråthen. The goal was to produce and commercialize the carbon membranes, and further optimize the product for the biogas market, more specifically for the upgrading of biogas to fuel quality. The production at MemfoACT AS was based on patented carbon membrane technology [22, 123]. Spinning of Cellulose acetate hollow fibers, post treatment, carbonization, module construction, pore tailoring, and permeation testing were done in production facility at Trondheim. Total capacity of production plant was 700 m^2/year (250 modules).

The core business of the company was to commercially produce and deliver high performance carbon hollow fiber membrane modules-based gas separation systems in different applications; CO_2/CH_4, H_2/CH_4, O_2/N_2. The focus, in initial stage, was CO_2/CH_4 separation in biogas upgrading and natural gas, and then gradually expand the business for other markets. As the

removal of CO_2 is the only membrane-based natural gas separation process currently practiced on a large scale (more than 200 plants have been installed), membranes are increasingly being selected for new projects, especially for large flow, medium to high CO_2 concentration and remote-location applications. Table 3.3 shows a comparison between different methods for CO_2 separation with capital and operating cost issues.

In figure 3.10 (a) and (b), the separation powers for polymers are compared to the MemfoACT Carbon membrane, indicating favorable properties for carbon membranes produced by MemfoACT AS.

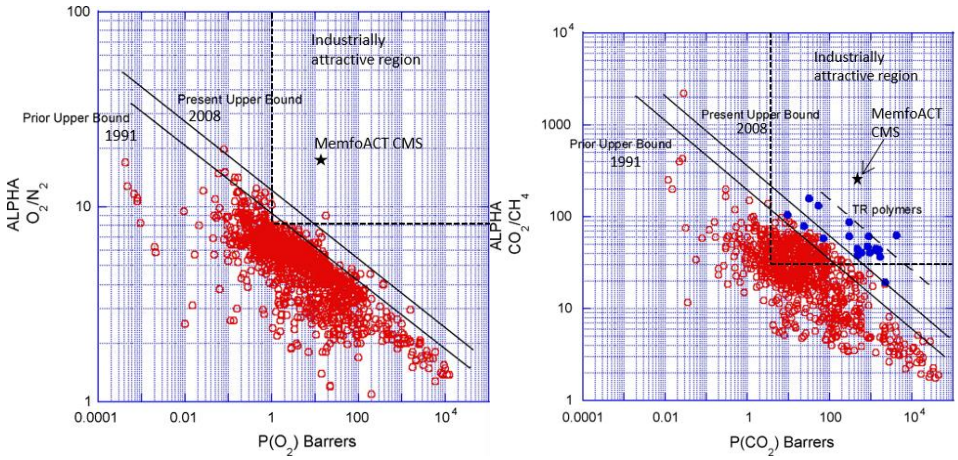

(a) (b)

Figure 3.10: Position of CHFM in Robeson upper bound (2008) for O_2/N_2 gas pair (left side); for CO_2/CH_4 pair (right side). CHFM produced by MemfoACT

Carbon membrane technology is relatively new technology, and still in developing phase. However, pilot scale production and testing of carbon membranes for CO_2 separation applications helped to understand few aspects related to capital cost, operating cost, and issues during operation. Table 3.3 shows the comparison of carbon membrane technology with amine based and polymeric membrane-based technologies for CO_2 separation process. Due to high performance, CM have less operating cost, energy cost, and maintenance cost compared to conventional technologies. In addition, the impact on environment is also low.

Table 3.3: CO_2 separation with capital and operating cost issues while using different technologies (adopted from [65])

Cost related issues	**Separation technologies**		
	Amines	Polymeric Membranes	Carbon Membranes
Operating cost issues			
User Comfort Lever	Very familiar	Early market footprint	New technology
Hydrocarbon Losses	Very low	Losses depend upon conditions	Low
Meets Low CO_2 spec.	Yes (ppm levels)	No (< 2% is challenging)	Yes, but less than amines
Meets Low H_2S spec.	Yes (< 4 ppm)	Sometimes	Sometimes [Pilot verification]
Energy Consumption	Moderate to high	Moderate due to compression	Low
Operating Cost	Moderate	Low	Very low
Maintenance Cost	Low to moderate	Moderate due to compression	Low
Ease of Operation	Relatively complex	Relatively simple	Simple
Environmental Impact	Moderate	Low	Low
Dehydration	Product gas saturated	Product gas dehydrated	Required dewpoint not determined [pilot testing]
Capital Cost Issues			
Delivery Time	Long for large systems	Modular construction is faster	Fast, easy set-up
On-Site Installation time	Long	Short for skid-mounted	Short, skid-mounted
Pretreatment Costs	Low	Low to moderate	Low to moderate
Recycle Compression	Not used	Use depends upon conditions	Not needed

4. Production of pilot scale modules - Methodology

This chapter describes the materials, equipment, and procedures used at MemfoACT AS production facility to produce CHFM and pilot scale modules. The procedure for pore tailoring of CMSM through chemical vapor deposition (CVD), aging of CMSM under miscellaneous environments, and regeneration of CM are also explained.

4.1. Materials

4.1.1. Materials used in spinning and pre-treatment processes

- Cellulose acetate (CA, MW 100,000) with an average acetyl content of 39.8% was purchased from Chiron (ACROS Organics Belgium).
- N-methyl-2-pyrrolidone (NMP: purity > 99.5%) was purchased from Merck (Norway).
- The additive polymer Polyvinylpyrrolidone (PVP: MW 10,000) was purchased from Sigma Aldrich (Norway).
- Water was used for coagulation and after wash process.
- Dimethyl sulfoxide (DMSO > 99%), Isopropanol, NaOH (> 99%), and Glycerol (> 98%) were purchased from VWR (Norway).

All materials were used directly for production without further treatment.
Materials and equipment for carbonization process are discussed in detail in the section 4.3.

4.1.2. Materials for gas permeation testing

- Single gas CO_2 (99.999%) and N_2 (99.999%) were supplied by YARA Praxair.
- Experiments with single gas CH_4 and mixed gas 40% CO_2 and 60% CH_4 were performed at NTNU. These gases were delivered by AGA.

List of various equipment's used in spinning and carbonization procedures and the vendors are shown in table A.1 of appendix A.

4.2. Procedures for spinning and pre-treatment processes

This section describes the procedures for spinning of precursor hollow fibers and pre-treatment process. The results for the spinning and pretreatment processes are presented and discussed in paper-I (Pilot – Scale production of carbon hollow fiber membranes from regenerated cellulose precursor: Part I- Optimal conditions for precursor preparation).

4.2.1. Spinning of CA hollow fibers

The dope solution was prepared in a 50L stainless steel mixing tank by adding 22.5 wt% of cellulose acetate (CA) and 5 wt% of PVP in dry state first and then 72.5 wt% of NMP solvent at room temperature (20-25 °C) was added before start stirring. After mechanical stirring for at least 72 hours to ensure homogeneity of the dope solution, it was subsequently left to rest for 24 hours to remove air bubbles before filtration process was started. The spinning rig had a bore tank too, but to ensure mixing, the bore solution was premixed outside, and then collected in the bore tank reservoir. The bore solution was made by adding solvent (NMP or DMSO) and water in the desired ratio.

A well-known dry/wet phase separation spinning process was used to spin the CA hollow fibers [124, 125]. The dope solution and bore fluid were extruded through a tube-in-orifice jet type of spinneret to form a nascent hollow fiber. The extrusion rate of dope and bore fluid was controlled by two separate gear pumps, respectively. Spinnerets with three different sets of inner and outer dimensions (photos and range are shown in figure 4.1) were used to spin the hollow fibers.

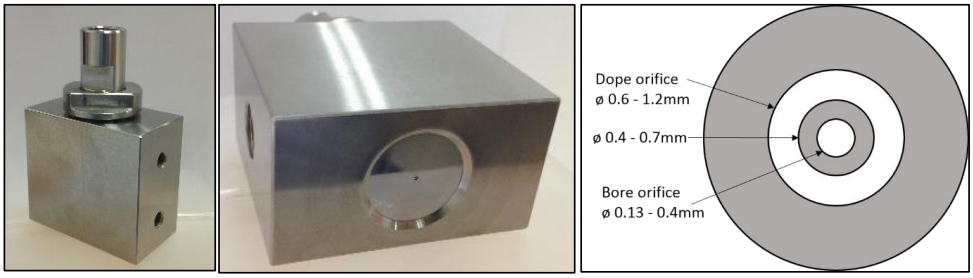

Figure 4.1: Spinneret photos (left) and range (right) of different dimensions used for spinning of CAHF

For each spinning-session, a continuous fiber length of (at least) 2.4 km was spun and rolled up in three layers on a collecting wheel. The fiber was cut into 1200 fibers of 2 m length for each fiber. Altogether, more than 460 spinning-sessions of CA hollow fibers were spun with 50 batches of dope mixture, of which at least 100 sessions were spun by varying spinning conditions, e.g. spinneret dimension, air gap, extrusion rate, coagulation bath temperature, take up speed and different fiber collection methods to optimize the pilot scale production of CA hollow fibers. A schematic diagram of hollow fiber spinning process is presented in figure 4.2. After optimizing the spinning process, the parameters were kept constant for rest of the sessions and these parameters are shown in table 4.1.

The partly coagulated fibers from coagulation bath were guided by a wheel from the bottom of the coagulation bath to the godet-bath where some residence time (1-2 minutes) was provided for solvent exchange/water wash before they were rolled up on a collection wheel.

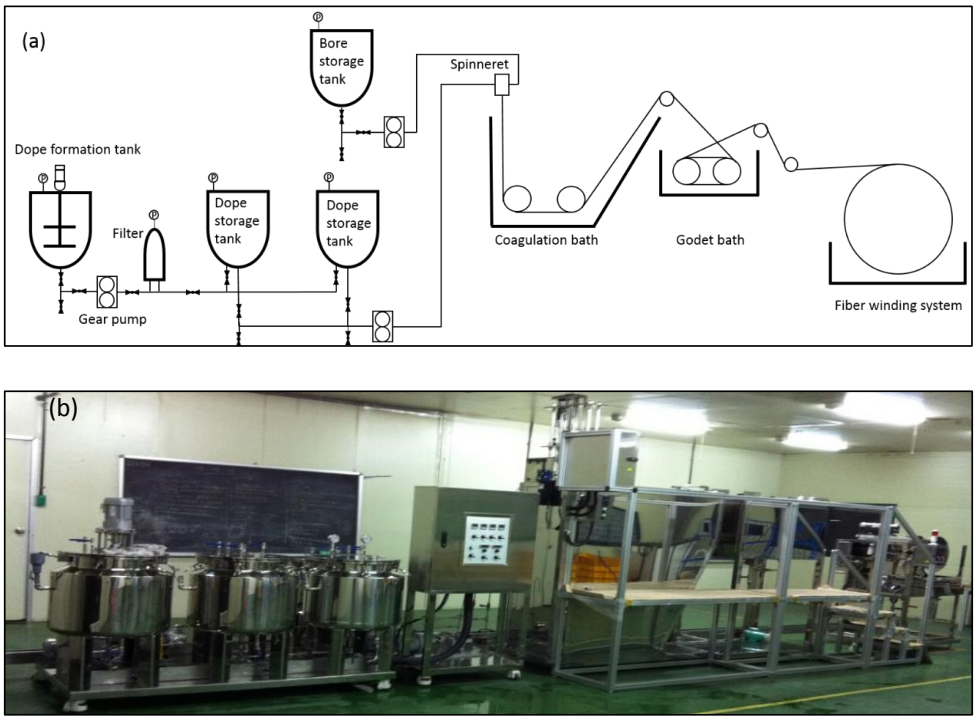

Figure 4.2: (a) Schematic diagram of hollow fiber spinning process (b) Photograph

Table 4.1: Optimized parameters for spinning, pre-treatment and carbonization processes

Parameter	values	units
Dope solution		
Composition	22.5 CA / 5 PVP/ 72.5 NMP	wt%
flow rate	0.4	l/hr
Temperature	RT (20-23)	°C
Bore fluid		
Composition	30/35 H_2O - 65/70 NMP	vol%
flow rate	0.2	l/hr
Temperature	RT (20-23)	°C
Other parameters		
Air gap	25	mm
Coagulation medium / T	H_2O / RT (20-23)	°C
*Godet bath temperature	25-40	°C
Collection wheel	10	°C
Take up speed	14	m/minute
Post-treatment		
Water wash	10 °C	24 hr
Glycerol wash	7.5 vol% in water (20 °C)	24 hr
Deacetylation	0.075 M NaOH (aqueous sol.) diluted with 10 vol% IP	2.5 hr
After wash	7.5 wt% glucose (20 °C)	30 minutes
Drying	T: 40-45 °C, RH: 90% → ambient	16 hr
Carbonization		
Temperature	650 °C, 2 hr soak	
Medium	N_2, CO_2	0.7-1.9 l/minute

**a rinsing bath for solvent exchange after coagulation bath*

4.2.1.1. Squared collection wheel

Figure 4.3 presents the collection methods of CA hollow fibers. Four specially made stands "fiber carrier" (also shown in the figure 4.3) were connected on a rotating shaft of the rig in such way that fibers were kept straight on each fiber carrier along the length and a sharp bending radius (avoiding the kink) was provided on the edges of the carrier. A fiber guiding device moved the fiber position along the fiber carrier, and a sensor was installed to control the

fiber tension. In order to promote the solvent exchange, a water bath with the continuous flow was present in such way that each fiber carrier got immersed in it while rotating on the shaft. After completion of the spinning process, clamps were applied on both sides of the fiber carrier and fibers were cut with a sharp knife to separate the wheel into 4 individual carriers (Nicknamed “Guitars”).

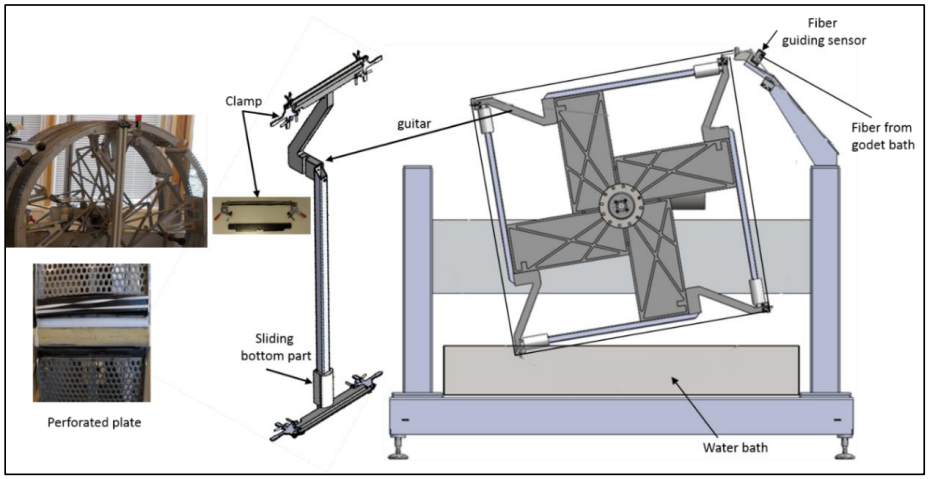

Figure 4.3: Collection wheel: Four fiber carriers attached to a rotating shaft (right side), perforated plate photos (left side)

These fiber carriers applied some tension on the fibers, but they were designed to allow some contraction of the fibers to occur. Clamping was adjusted in such way that bore side of the fiber was open to exchange the solvent efficiently during water wash. Allowing some of the solvent exchange in a water bath, the wheel was left rotating for 2 hours after clamping and cutting the fibers. Then fiber carriers were removed from the stand and placed in horizontal position (such that all fibers are dipped in the solvent but not touching the bottom of the washing bath) in a water bath overnight. A continuous flow (1.5 l/minute) of fresh water was supplied to remove the solvent from the bath.

4.2.1.2. Circular wheel with perforated collecting plate

There is a trade-off between how long the fiber stays on the wheel (aging by bore solution) and production efficiency, and this may determine the diameter of the collection wheel, the number of fiber layers or the take-up speed. The easy escape of water is favorable as it results in suppression of macrovoids formation in CA matrix. To enhance the efficiency of solvent

exchange process during spinning, two perforated circular plates with the same width (25 cm) as the fiber carriers were used to collect the fibers. Each plate was making half of the wheel's circumference and after spinning was completed, the fibers were transferred to two fiber carriers (2 m long each). Figure 4.3 shows the photo of such plates. A halfpipe made of ABS tubing (32 mm OD) was attached to the gap between the plates by 2 elastic bands (GUMA 120x8 mm). Foam was pre-fixed (glued in the halfpipe to conduct water). The halfpipe was placed at a level which prevents sharp bending of the collected fibers. A polycarbonate plate and an elastic band were used to make a loose clamp on the edges of each wheel half to ease the fiber endings and allow bore solution to exchange with water as shown in Figure 4.3 (left hand side). The other half of the ABS pipe made in a similar way was placed on top of the fibers. Fibers were water-washed for 30 minutes in this way before clamping and moving them on the carriers. After clamping fibers on the carriers, they were placed in a horizontal bath for further water wash overnight to promote the removal of the bore solvent.

After water wash, the CA hollow fibers were soaked horizontally in glycerol solution (7.5% aqueous solution) overnight to remove the residual NMP in the fibers, and to prevent the bore side from collapsing.

4.2.2. Deacetylation

The CAHF were then deacetylated with 90 vol% 0.075 M NaOH (Water) solution diluted with 10 vol% 2-propanol (isopropanol, IP) at ambient temperature for 2.5 hours. Different concentrations of NaOH and dilutions of IP were investigated, but it was observed that optimized degree of deacetylation of fibers was obtained by above mentioned composition. To improve mass transfer and homogeneous treatment of all fibers, liquid circulation via pumping and shaking of the bath and/or the fiber carriers was applied. It was experienced that fibers not allowed to shrink during deacetylation could not give CO_2/N_2 selectivity more than 50 (CO_2 permeability over 100 Barrer), however, fibers allowed to move along fiber carrier length and shrink (Typically, 1-3%, during the deacetylation process) improved the permeation properties of the final carbon membrane. Therefore, fibers had no restriction to move along the carrier during deacetylation. Two stirrers were used on both ends of the carriers and circulation pump was also installed to circulate the solution in cross-pattern (suction on one corner of the bath and distribution on diagonally opposite corner) to avoid any stagnant regions for the solution in the bath. During deacetylation process, the fibers contact between with each other or the bottom of the bath should be minimized as it can inhibit the reaction and partial deacetylation may result. This can ultimately destroy the whole fiber quality by making that part brittle after

drying and potentially burn off during carbonization. Shaking was applied to improve on this situation.

Direct drying of deacetylated fibers caused the curliness and highest shrinkage (difference in length of fiber when treating with the additive solution and fiber length after drying) of hollow fiber membranes resulting in dense membranes with very low CO_2 permeability. It was found that cellulose fibers immersed in 7.5% glucose (aqueous) solution gives straight fibers with good mechanical properties after drying. Therefore, deacetylated fibers were then immersed in an aqueous solution (T: 20 °C) of 7.5 wt% glucose for 30 minutes and the lock on the bottom was engaged. For drying, the fiber carriers were placed vertically inside the drying cabinet and the lock on the bottom end of the carrier was removed, allowing for shrinking of the fibers. A custom-made comb with 10 mm spacing between each tooth was used to further separate the sticky fibers (glucose effect) into equal groups. The purpose of using a comb was to achieve as close as possible an equal number of fibers in each strand, as the number of fibers in each bundle would determine the drying speed of that bundle. The effect of strand (number of fibers in the bundle) size on shrinkage of dried fiber was also studied. An extra load (averaged to 2.5 g per fiber) was added to the bottom end of the carrier. This acts as a counter force to the shrinking of the fiber clusters and assists in obtaining straighter fibers. This extra load had a significant effect on the permeation properties of carbonized fibers, hence, was optimized in ordered to get straight enough fibers with good enough mechanical and acceptable permeation properties after carbonization. Fibers were dried overnight at room temperature (20-25 °C) in a controlled humidity chamber. Figure 4.4 shows photos of fibers in various production states: (a) fiber carriers during deacetylation, (b) fiber carriers inside drying cabinet, (c) hanging dry fibers and fibers ready for carbonization (d) comb to separate the fibers in equal bundles during drying.

A systematic investigation of the influences of drying parameters such as humidity, extra load on the fibers, drying temperature was performed to obtain the straight cellulose fibers with high yield and good mechanical properties. Tensile strength and elongation at break of the fibers were also measured after different production steps (spinning, water wash, deacetylation, and drying).

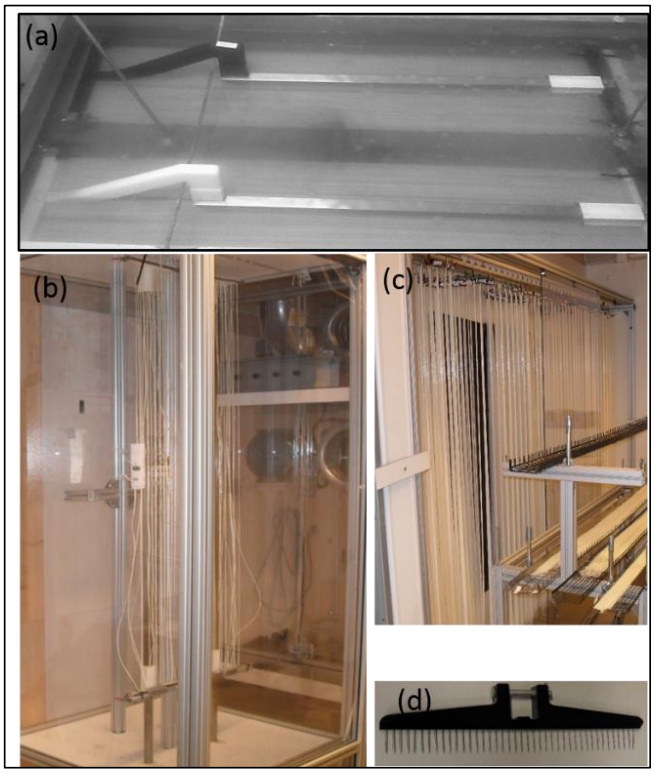

Figure 4.4: (a) Fibers lying in the deacetylation bath (b) Fibers inside drying cabinet (c) hanging bundles of dry fibers and trolley with steel trays containing dry fibers (c) Comb to split the fibers in equal bundles before drying

4.3. Carbonization procedure

This section describes the carbonization procedure. The results for the carbonization procedure are presented and discussed in paper-II (Pilot – Scale production of carbon hollow fiber membranes from regenerated cellulose precursor: Part II- Carbonization procedure).

4.3.1. Description of the furnace

The furnace used in this work was specially made (Model: Carbolite special HZS 12/150/2400, bought from VWR International AS) with three independently controlled heating zones. A custom-built stand under the furnace was used to adjust the height and tilt accordingly. The height of the furnace could be adjusted independently on each end. A quartz tube with outer diameter (OD) of 150 mm, 5 mm wall thickness and 3000 mm in length and seven smaller quartz tubes with 34 mm OD, 2 mm wall thickness and 2700 mm in length were purchased from Chemi-Teknik AS, Norway. One end of the bigger tube was sealed with gasket and stainless-steel flange. Whereas, the other end was used for loading/unloading of the small

quartz tubes and gas inlet/outlet connections. Glass wool (can withstand 800 °C) was used for insulation purpose and was provided by Rockwool Colnite AS, Norway.

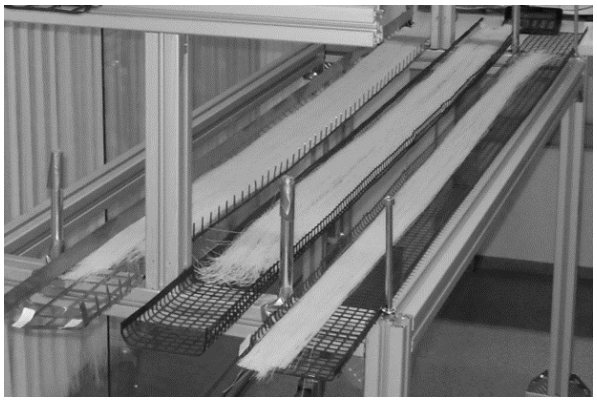

Figure 4.5: Perforated plates with square openings (10 by 10 mm) and (20 by 20 mm)

Two types of 2 m long perforated plates (purchased from Nisjemetall AS, Norway) with square openings (10 X 10 mm and 20 X 20 mm) and width of 120 mm were also used to carry carbonize the hollow fibers during carbonization process. Figure 4.5 shows the photograph of the perforated plates loaded with fibers which are ready for carbonization.

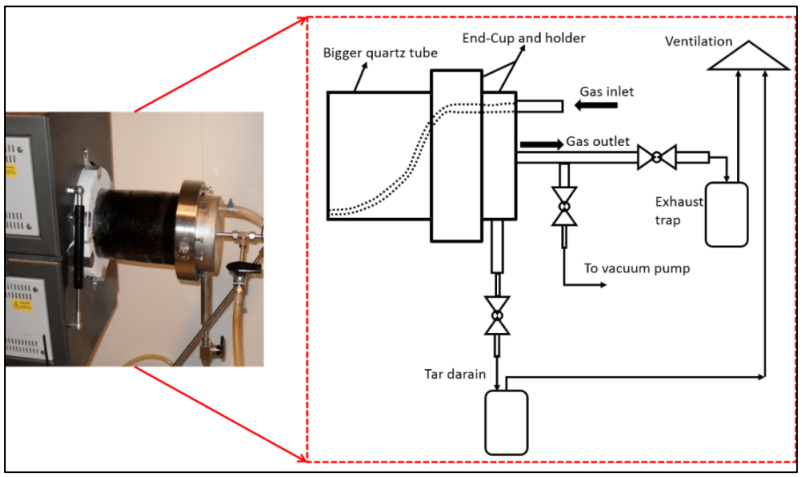

Figure 4.6: A photograph (on left) and a schematic diagram (on right) of End-cup and holder on the fiber loading-end of the furnace tube

A complete drawing of the gas inlet, gas outlet, and tar drain system from furnace is presented in Figure 4.6 along with photograph of the furnace. Gas flow controllers were bought from Aalborg, USA.

4.3.2. Loading the furnace

The angle between support/level and furnace/tube was set to 6 degrees by raising the closed end of the furnace to enhance the flow of residue downward. 1-7 quartz tubes were filled with 500-1000 fibers in each tube. A thread with loose knot around the fibers was used to pull the fibers inside the quartz tubes. This thread was removed after fibers are inserted in the tube. An insulation plate was cut OD 120 mm and holes were made according to the template (honey comb arrangement) as shown in Figure 4.7 (number of tubes loaded, 30 mm hole diameter), a 32 mm OD hole for tar drain tube, and a 3/8" OD sweep gas tube. Insulation plate along with quartz tubes were pushed inside the bigger/furnace tuber into the heating zone of the furnace (46-48 cm from the edge of the furnace tube).

In case of using the perforated plate/grid, the grid was filled with 1600-4000 fibers. The fibers were distributed as equal as possible on the grid, so that the layer thickness across the width of the grid become as uniform as possible.

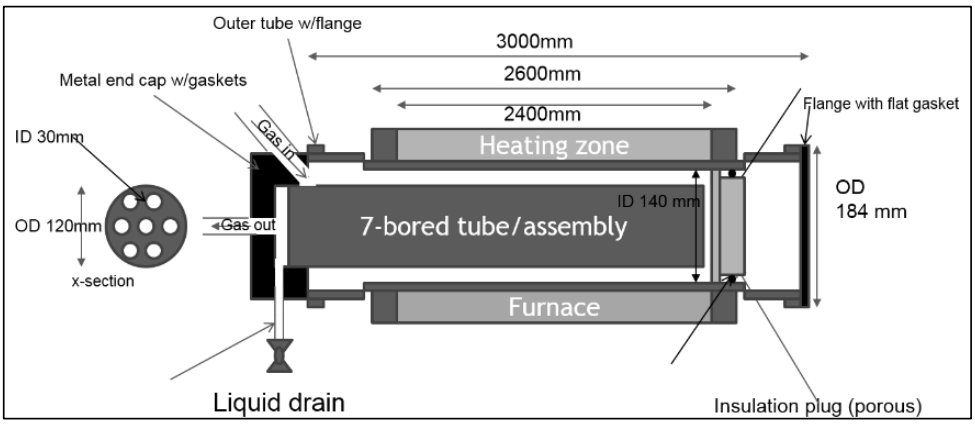

Figure 4.7: Drawing of furnace, bigger quartz tube, smaller quartz tube assembly

4.3.3. Carbonization

After evacuating the air out of the system ($p < 10$ mbar), N_2 or CO_2 flow of 0.8 l/minute was supplied through a gas flow controller. The flow was gradually increased to 1.9 l/minute to fill the oven. As soon as the pressure inside the furnace tube reached just above the atmospheric

pressure (1.1-1.2 atm), the valve to the exhaust trap and the valve to the tar trap was slowly opened. H_2O/NMP in volume ratio of 4/1 was used as exhaust trap on the outlet of the furnace. For tar absorption, 10% triethyleglycol (TEG) in water was used and outlet from both exhaust trap and tar trap was then connected to the ventilation. Gas flow was varied for a few batches to optimize according to the fiber holders (no. of quartz tubes or SS-grid), but it was always kept in the superficial velocity range of 1-10 cm/minute [43].

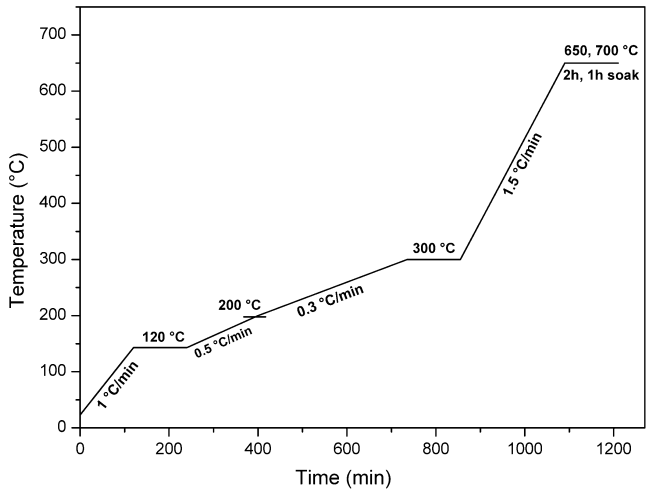

Figure 4.8: Carbonization protocol used by MemfoACT AS

The carbonization protocol (as illustrated in Figure 4.8) was then started. The weight loss of precursor during the carbonization process using Thermogravimetric analysis (TGA) can be found in reference [44, 64]. The heating rate, final soak time, and final temperature were tuned to achieve best combination of selectivity. At the end of the protocol the system was left to cool naturally, and gas continued to flow at the original flow rate. When the furnace temperature was 70 °C or below, the gas flow was stopped and both traps (exhaust and tar) were disconnected. Because the cooling of the furnace may create slight vacuum inside, the liquid in the exhaust trap is thus hindered to flow into the furnace tubes or tar trap. Quartz tubes/grids were pulled out of the furnace tube and fibers were stored on a clean surface (a plain paper). Then fibers were left to degas overnight before they were further processed. Stainless-steel grid did not need any washing after carbonization as there were no residue stuck on them, however the quartz tube needed washing after each carbonization.

4.4. Construction of high-pressure CHF module

This section explains the procedure to construct pilot scale module of carbon hollow fibers. The results of this section are presented and discussed in paper-IV (CO_2 separation with carbon membranes in high pressure and elevated temperature applications).

This section provides details on module construction, choice of epoxy, repair of broken fibers inside a module, and finally gas separation testing which is the ultimate quality control. The procedure for construction of lab-scale modules can be found in the references [44, 64].

4.4.1. Potting/Sealing

Membrane modules were constructed using up to 3000 good quality carbon hollow fibers with outer diameter between 0.15 and 0.25 mm. The length of the finished module was 800 mm. The good quality fibers were defined as the fibers which are not curly, brittle, and/or collapsed on any part along the length of the fibers. Manually sorted good quality fibers were bundled loosely with wool thread so that fibers are held together while inserting in the stainless-steel tube as shown in figure 4.9(a). The fiber bundle was carefully pulled through the tube and a thread was tied onto the section of the bundle facing up. Then a piece of duct tape was placed on the bottom side as shown in fig. 4.9(b). The module side with dead end fibers (figure 4.9(b)) was first exposed to extra fast curing adhesive (Loctite 9455) for fiber ends clogging, so that the sealing glue (Loctite 9483) was not sucked into the fibers via capillary action. The module was fixed vertically in a clamp and glued by filling adhesive in the right amount to achieve a hermetic sealing. A period of 24 hrs was required for the glue to fully cure at room temperature. However, after sufficient curing the module can be turned upside down and glued on the other side of the module. A plastic cup with the same diameter as the steel tube was used to prepare a glue plug with a significant length of fibers suspended within the plug. Loctite 9483 was filled through the holes in the smart plug until glue reached the gas holes. Figure 4.9(d) presents the specially designed smart plug used on “open endings” side of the fibers and a glue plug with fiber endings (white dots) is shown on the top.

When sealing is cured after 24 hours at room temperature, hack saw, chisel together with rubber hammer was used to open the fiber endings on the top side of the module. After opening all fibers, modules were tested for any leakage.

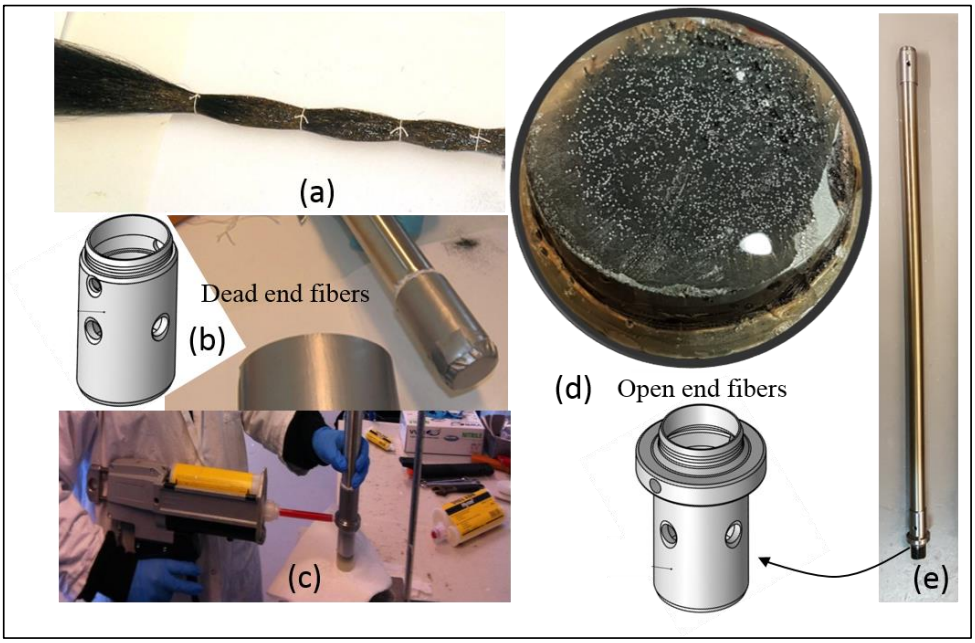

Figure 4.9: CHF module construction process, (a) CHF loosely bundled with thread, (b) smart plug and dead-end potting, (c) filling glue on top end of the fibers (d) Open end fibers and smart plug (e) Module ready for testing broken or damaged fibers

4.4.2. Selective clogging

It is not attainable, at least currently to prevent some broken or damaged fibers to remain in the fiber bundle when the membrane package in figure 4.9(a) is produced. This leads to a bundle consisting of three principal fiber types (good fibers, broken fibers, and surface damaged fibers) randomly distributed. It has been investigated, the possibility of using what is known as selective clogging of faulty fibers. The idea of this process is reported elsewhere [126], however, the procedure was developed at MemfoACT. The outline of this process is indicated in figure 4.10.

The membrane package is partly mounted into a pressure vessel in such a manner that the fiber end is exposed to the surroundings. By applying vacuum to the outer surface of the fiber, the lift flow force in the failed fiber types can easily be estimated using the Hagen Poiseuille equation (equation 4.1) if surface effects are ignored. However, the inner fiber diameter is only 0.19 mm (190 µm) so the capillary forces can most likely not be ignored, and the capillary rise (or lowering) is estimated via the Pascal equation (equation 4.2), which requires knowledge about both surface tension of glue on carbon (our carbon consists of randomly oriented graphene sheets).

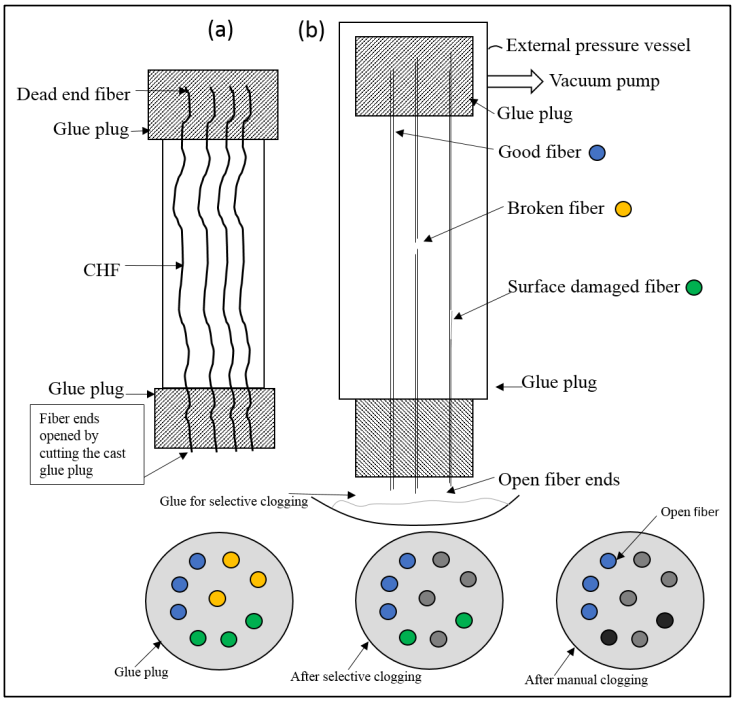

Figure 4.10: (a) Membrane Package, (b) Selective clogging of failed fibers in membrane package

$$\frac{dx}{dt} = \Delta P \frac{r^2}{8\eta x}\phi, \quad x = \sqrt{\Delta P \frac{r^2 \cdot t}{8\eta}} \tag{4.1}$$

Where x is the penetration height, ΔP is the pressure difference (~1 bar), r is the internal radius of the fiber (95 µm), t is the time the pressure works (approximated as the pot life of the glue) and η is the viscosity of the liquid mixed glue.

$$x = \frac{2g \cdot \cos\theta}{r \cdot \rho \cdot \gamma} \tag{4.2}$$

Where γ is the surface tension of glue on carbon, θ is contact angle between glue and carbon, ρ is density of glue, g is the acceleration of gravity.

In figure 4.10, the fibers marked as blue are good fibers, yellow are broken fibers, green color represents the surface damaged fibers, and grey color is showing clogged fibers after selective clogging process. Loctite 9492 and 9484 was used for selective clogging. As shown in figure

4.10(b), the membrane module was clamped in upside down position. The glue was mixed in a pot and kept under the module in such a way that the fiber endings from the glue plug of the module are dipped in it. Now apply the vacuum for 1-2 minutes so that the required penetration is achieved and let it cure. Then cut the glue plug up to 3-5 cm in length depending upon the glue type. The glue types used here have the penetration rise in this range for the good fibers. Now all the broken fibers are clogged because these fibers have maximum penetration rise. It is difficult to estimate the exact penetration rise for the surface damaged fibers. In practice, only 30-40% surface damaged fibers were clogged by selective clogging process. Therefore, manual clogging was done to identify and block the remaining damaged fibers. For the manual clogging, the module was clamped facing open fibers endings in upward direction. Slight over pressure than atmospheric pressure was applied instead of vacuum. Then soap or thin layer of liquid water was poured on the glue plug to identify the fibers with fastest flow (making the bubbles faster). Using magnifying glass, the fibers with fastest gas flow were marked with a colored marker. Now wipe the liquid and apply the vacuum again before using some instant glue (Loctite 3090 here) on marked fibers. In case of manual clogging (dark grey fibers), more than one fiber (including good fibers) is blocked while clogging the one defective fiber as fibers are packed closely together. Therefore, this process reduces the membrane effective area to a much larger extent.

Several glue types were tested for selective clogging application by studying both self-penetration of glue and forced penetration (under vacuum). It was determined that the requirements for a suitable glue that could be used for selective clogging are as follows in prioritized order:

1. The glue must have an overall forced penetration height of about 10 cm,
2. The capillary rise alone should not be more than 1 cm.
3. The glue must cure into a solid plug inside the fibers (not form a gel, or plastic/ rubber)
4. Preferably cure within an hour (at least enough to be removed from the vacuum)
5. For analytical purposes, it is an advantage that the glue has a color other than clear or black.

4.5. Gas permeation testing

This section describes the procedure for gas permeation testing of prepared modules. The results from gas permeation testing are presented and discussed in paper-IV (CO_2 separation

with carbon membranes in high pressure and elevated temperature applications) and paper-VII (Carbon membranes for oxygen enriched air – Part I: Synthesis, performance, and preventive regeneration)

For the permeation experiments discussed here, CHF modules were tested in a pilot scale permeation system with shell side feed configuration. The system was constructed for single gas tests (CO_2, N_2, O_2). The mass transport properties of CHF were measured with the single pure gases CO_2 and N_2 at different feed pressure and experiments were carried out with no sweep on the permeate side at MemfoACT facility (set-up shown in figure 4.12). Due to fire hazard limitations, CH_4 was not tested at the membrane production facility. However, single gas CH_4 and mixed gas (40% CO_2 in CH_4) experiments were performed at NTNU (set-up is described in [44]).

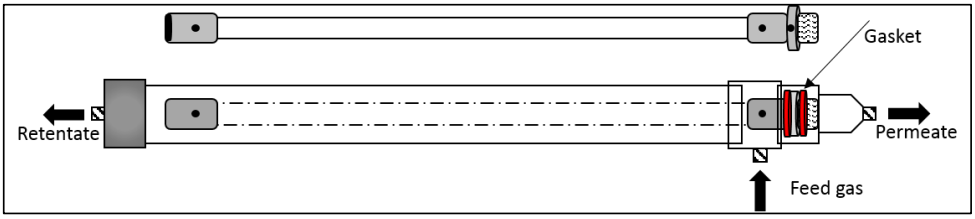

Figure 4.11: Membrane module in high pressure vessel for permeation testing

The performance of the membrane was evaluated by measuring the gas permeance in [m^3(STP)/ (m^2·h·bar)] and selectivities (α) using equations 4.3 and 4.4. A high-pressure vessel (schematic) used for permeation tests is shown in figure 4.11. The tests were run from several hours to several days, to ensure that the transient phase of diffusion was passed, and dp/dt tends to a constant. The gas permeance, P/ℓ [m^3(STP)/ (m^2·h·bar)] was evaluated using the equation 4.3.

$$P/\ell = \frac{9.824.\mathrm{V}\cdot(dp/dt)}{\Delta P \cdot A \cdot T_{exp}} \tag{4.3}$$

Here, V is the permeate side volume (cm^3) that can be measured with a pre-calibrated permeation cell reported elsewhere [64, 127]. However, the permeate side volume for this study was estimated by the tube length and cylinder volume on the permeate side. *dp/dt* and A are the collection volume pressure increase rate (mbar/s) and total active area of membrane (cm^2)

respectively, ΔP (bar) the pressure head and T_{exp} (K) is the temperature for experiment. The ideal selectivity was defined as the ratio of the pure gas permeances as shown in equation 4.4.

$$\propto_{A/B} = \frac{P_A}{P_B} \tag{4.4}$$

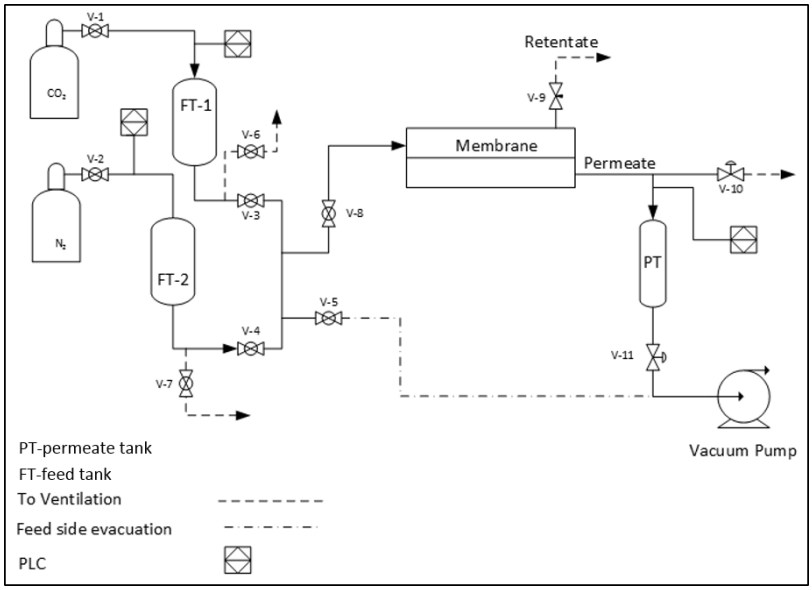

Figure 4.12: A schematic diagram for gas permeation set-up (MemfoACT AS)

4.6. Pore size adjustment

The prepared CHF modules after permeation tests were modified through CVD process to enhance the membrane performance (results are presented and discussed in paper-IV; CO_2 separation with carbon membranes in high pressure and elevated temperature applications). For this purpose, modules were installed in a custom designed rig to allow the potting material (temperature limitations) to remain outside the heated area, with integrated external cooling of the potting during the process. The figure 4.13 illustrates the steps followed in this work, as also explained in the patent held by Soffer et al. [126].

The virgin carbon will most likely have too narrow pores to yield a feasible permeability, and the whole membrane wall thickness is expected to contribute to mass transfer resistance. Thus, the overall permeance of the carbon is infeasible low for practical usage. Due to the narrow pores, the selectivity is expected to be high (i.e. the selectivity of CO_2 over methane is normally more than 100).

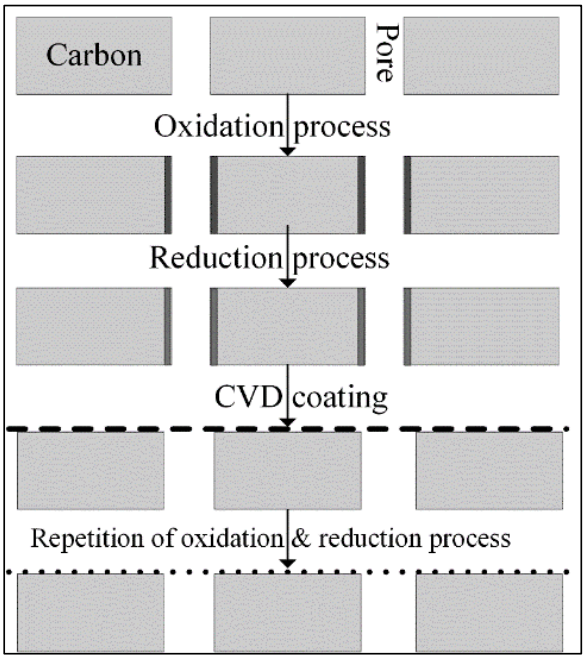

Figure 4.13: Steps followed for pore tailoring of CHF

A mild oxidation in synthetic air at about 300 °C for a defined time will cause the pores to widen. The internal pore surface of the carbon is now obviously in a highly-activated condition and will most likely exhibit a rapid clogging if exposed to water or any other hydrogen bonding molecules. (The carbon in this condition is surface wise like a process aged carbon. Hence, this and the following steps might also be modified to be a regeneration technique for the degenerated modules. The process is normally referred to as thermal regeneration.)

The surface is deactivated using hydrogen at ca 500 °C, which will widen the pores slightly more. The permeance of the carbon is now significantly increased (normally, several orders of magnitude higher) and the selectivity is now expected to approach unity.

Chemical vapor deposition (CVD) using propene for a short time will cause a new layer of carbon to be generated on all accessible surfaces. The thickness of this layer is a strong function of reaction time and hence a thin layer of new virgin carbon with calculable thickness is achieved. This will lead to a decrease in flux and an increase in selectivity. Subsequent post oxidation and reduction may be needed to achieve the desired transport properties for the membrane module.

4.6.1. Procedure for pore tailoring process

Figure 4.14 presents the set-up (and a photograph) used for post oxidation-reduction and CVD process. The module was connected within the furnace, in a way that the sealing glue is kept outside the oven as shown in figure 4.14.

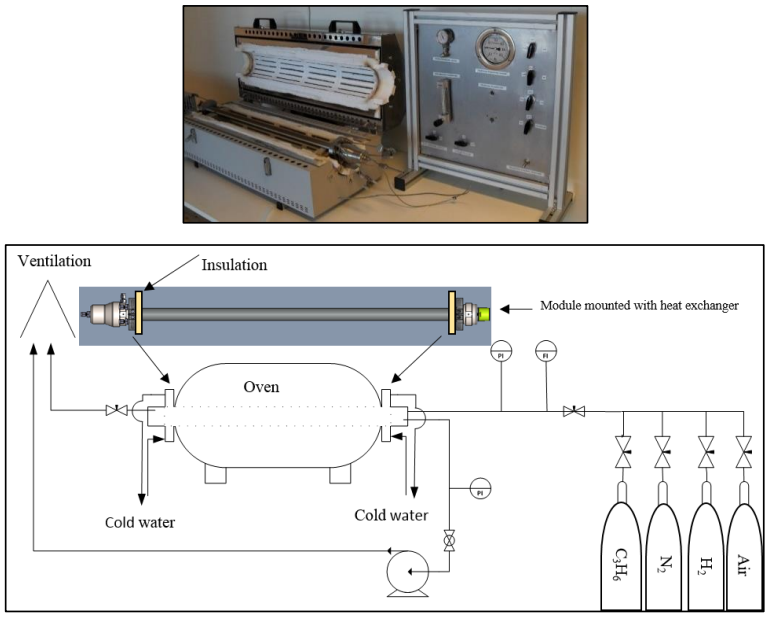

Figure 4.14: Post oxidation and CVD process (a photograph of the setup on top)

Glue cannot withstand temperature above 150 °C, therefore it was kept cold by chilled water. An insulation between furnace and heat exchanger was also applied. Then module and lines connected to the module were evacuated using vacuum pump down to 50 mbar. To start first post-oxidation, the gas (synthetic air) bottle was opened and pressure/flow values were adjusted per protocol (e.g. 1 bar and 10 ml/minute). The oven was programmed for the protocol (e.g. 4 °C/minute to 300 °C, dwell 180 minutes, cooling) and turned on. When the temperature in the cooling sequence is below 100 °C, the vacuum pump was switched off and the gas supply was stopped. Now 2nd heating sequence was started using N_2 atmosphere using same protocol until it reached 500 °C, then switched the gas to H_2 for first post-reduction process and kept for 30 minutes. After post-reduction, CVD was started using propene gas and then the cooling process was initiated swapping again to N_2 until the temperature goes down to 300 °C for the 2nd post-oxidation process. The module can be removed from the oven when the temperature is below 40 °C.

4.7. Aging of carbon membranes

To understand the life time and effect of miscellaneous environments on performance of carbon membranes, some aging and durability tests were performed. The results from durability and aging are presented and discussed in paper-III (CO_2 separation with carbon membranes; Durability and aging under miscellaneous environments).

4.7.1. Effect of storage environment

The carbon fibers were stored in different environments before they were mounted in a module to study the aging under different environments.

4.7.1.1. Storage in air (ambient temperature)

Different air environments were tested at ambient temperature (21±2 °C):

- Stored in open air inside lab
- Rolled in plain paper lying on open shelf
- Rolled in plain paper lying inside cabinet (dark place; a chemical storage cabinet with dimension as; H: 1990 x W: 1000 x B: 435 mm)
- Rolled in aluminum foil lying on open shelf
- Rolled in aluminum foil inside cabinet (dark place)
- Rolled in tightly packed aluminum foil lying on open shelf
- Rolled in tightly packed aluminum foil lying under dark fume hood
- Rolled in plain paper lying under dark fume hood

4.7.1.2. Storage under vacuum (ambient temperature)

- Stored under vacuum lying inside ABS tube
- Stored in vacuum bag in dark place inside cabinet
- Stored in vacuum bag under the light

4.7.1.3. Storage under CO_2 atmosphere (ambient temperature)

- Stored under CO_2 lying inside ABS tube

4.7.2. Aging when exposed to real biogas

Carbon hollow fiber modules were installed and exposed to biogas on three different fields in Norway to study the aging while membrane is in operation. In total 31 modules of the area

ranging from 0.5-2 m^2 of each module were installed on Field-1 biogas plant for a period ranging from 25 to 212 days to separate biomethane from raw biogas mixture. Gas permeation measurements were performed with pure gas (CO_2 and N_2) at MemfoACT AS production facility, using 5 bar feed pressure against vacuum on permeate side in ambient temperature. These permeation tests on the membrane module were conducted before and after the module was exposed to biogas field, and the results were analyzed to evaluate the aging effect of real biogas on CHF. Moisture and H_2S were removed before the biogas was in contact with CHF, so the maximum concentration of H_2S exposed to the membranes was below 5 ppm. Figure 4.15 shows the process diagram of Field-1 and Field-2. Field-3 was similar but had no H_2S removal system. Table 4.2 shows the biogas source, H_2S loading in biogas and the concentration going to the membrane.

Table 4.2: Biogas source and H_2S loadings in different fields (biogas contained 0-0.5% O_2 and 0-3% N_2)

Biogas field	Biogas source	H_2S loading (ppm)	Membrane exposure (ppm)
F1	Food waste	150-1000	< 5
F2	Food waste, fish oil	0-2000	< 5
F3	Sewage, municipal waste	150-2400	150-2400

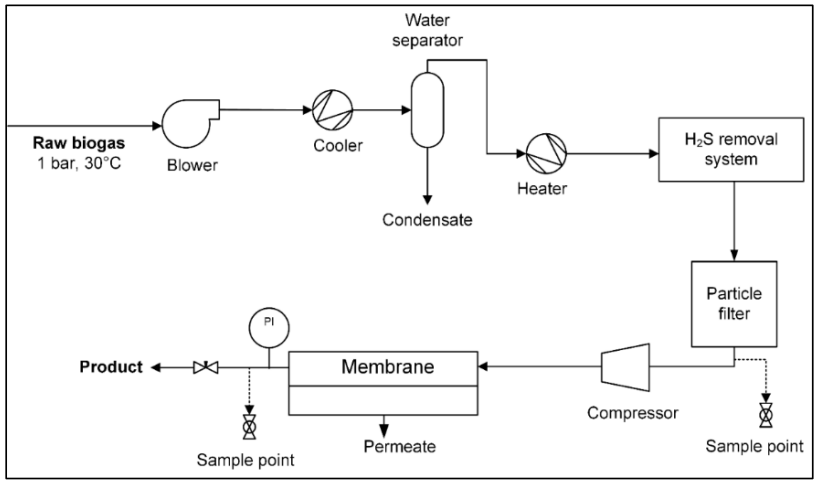

Figure 4.15: Biogas exposure process using CHF membrane at Field-1, 2 and 3. (Field-3 did not have H_2S removal system)

4.8. Regeneration of carbon membranes

Some regeneration experiments were also performed to attempt to regain the lost performance of carbon membranes. To enhance the aging effect on CM, these membranes were exposed to a biogas containing three different concentrations of H_2S as shown in table 4.3. The results of membrane regeneration process are presented and discussed in paper-VII (Carbon membranes for oxygen enriched air – Part I: Synthesis, performance, and preventive regeneration).

Table 4.3: Different gas mixtures used to enhance the aging effect on CM

Gas mixture name	Gas composition
Synthetic biogas (SBG)	40 ppm H_2S in a CO_2-CH_4 mixture
Worst case gas (WCG)	1% H_2S and 0.1% n-Hexane in artificial biogas mixture
Real biogas field exposure (RBG)	250 ppm H_2S in biogas (source: microbial digestion of slurry from waste water)
Air exposure during the storage period	Ambient air with average relative humidity 40%

4.8.1. Thermal and chemical regeneration

Adsorption is an exothermic phenomenon; and as a consequence the desorption is an endothermic phenomenon and energy must be supplied to desorb the adsorbents [64]. A membrane module with stainless steel housing was prepared using two carbon hollow fibers (0.0004 m^2 effective area) in the module. Single gas experiments for pure O_2 and N_2 were performed at 30 °C (2 bar feed pressure and vacuum on permeate side) to measure the reference permeability values. After determining the initial permeability values, both sides (shell and bore) of the membranes were exposed to WCG for 24 hours. The permeability of pure gases was measured again to examine the possible aging effects in the membrane.

The membranes were regenerated chemically using propylene. The CM were flushed with propylene gas for 24 hours and the single gas permeation tests were performed systematically after the exposure to detect any change in membrane performance. After single gas tests, thermal regeneration was applied by heating the membrane module. The module was heated up to 80 °C and kept at this temperature for 24 hours to desorb the adsorbed gas molecules in the pore structure of the membrane. Then final gas permeation tests were performed at 30 °C to see the effect of thermal regeneration. The procedure for thermal and chemical regeneration is explained in detail elsewhere [64].

4.8.2. Electrical regeneration

Two new membrane modules with Acrylonitrile Butadiene Styrene (ABS) housing were prepared containing two carbon hollow fibers (0.0004 m^2 effective area, OD: 198µm, ℓ: 31µm) in each module. A conductive glue (Eccobond 56C) was applied between carbon hollow fibers and Swagelok® fittings on each end of the module. The electric power source was connected (Alligator clips) to the external of the Swagelok ® fitting containing conductive glue on both sides of one module as shown in figure 4.16. However, the second module (reference module) was not connected to electric current. The conductive glue was not gas tight enough at high pressure, therefore, another set of Swagelok® unions were connected to a non-conductive glue on the outer section of the module. Teflon tubing was used for feed, retentate and permeate flows. Single pure gases were tested to determine the initial permeability values of the membranes.

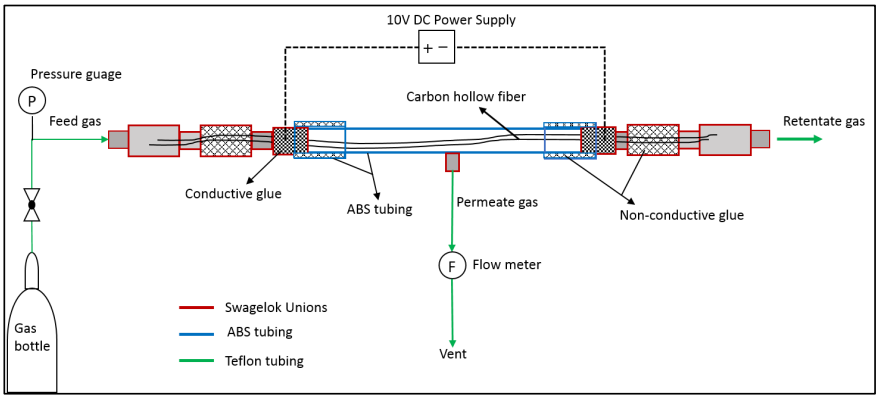

Figure 4.16: Experimental setup for electrical regeneration of carbon hollow fiber membrane module

Both modules with CM were exposed on both sides (shell and bore side) to WCG for four days. Then "preventive electrical regeneration" (PER) was performed on one module and the second module was used as reference (RM) module (no electrical treatment). The term "Preventive electrical regeneration" (PER) is used for the electric regeneration in this study. PER means a continuous supply of electrical potential during membrane operation to prohibit the molecules adsorbing on the membrane surface. PER was conducted using a direct current (DC) power source and an applied voltage of 10 V which corresponds to about 45-55 µA measured amperage on carbon fibers. The current was continuously applied during the whole exposure.

Table 4.4: Electrical regeneration of CM and exposure to different gases (reported in consecutive days from left to right)

Single gas tests	**WCG**	**Single gas**	**WCG**	**Single gas**	**RBG**	**SBG**
PER module	4 days, 10V	no voltage	14 days, 10V	no voltage	14 days, no voltage	no voltage
RM module	4 days, no voltage	no voltage	14 days, no voltage	no voltage	14 days, no voltage	no voltage

Table 4.4 shows the steps followed during electrical regeneration of the CM. As shown, single gas tests were performed for both the PER module (which is going to be regenerated electrically and current is on during the exposure with WCG) and reference module (RM). Then both modules were exposed to WCG for four days, with PER under 10V and RM without any current. After four days voltage supply was turned off on PER module, and both modules were tested for single gases. After the single gas tests, both modules were exposed again to WCG for 14 days keeping voltage supply "on" for PER module, and then tested again for single gases afterward.

The CM modules were then installed at a real biogas plant for 14 days and exposed to the real biogas containing 250 ppm H_2S. The modules were disconnected from the biogas plant and reconnected to the synthetic biogas in the laboratory for several days. The membrane modules were then tested for single gases again to check if a stable performance had been achieved after the preventive electrical regeneration.

The electrical resistance of the carbon fibers was measured by a handheld Ohm meter to calculate the specific conductivity of the membranes. Carbon fibers obtained at different soak temperatures (550 °C. 650 °C, 750 °C) were used to measure the electric conductivity.

5. Pilot plant for biogas upgrading to vehicle fuel

As described in introduction chapter that carbon membrane modules prepared at MemfoACT AS facility were used to upgrade the biogas to vehicle fuel. A biogas upgrading system including pre-treatment process was designed, commissioned, and operated by MemfoACT AS to treat up to 60 Nm^3/hour. of raw biogas. This chapter describes the equipment and process that was installed and operated at Glør IKS for upgrading of biogas to vehicle fuel. The results from pilot-scale plant are presented and discussed in paper-V (Vehicle fuel from biogas with carbon membranes; a comparison between simulation predictions and actual field demonstration).

5.1. Equipment

The list of equipment used to construct the biogas upgrading pilot plant is shown in table 5.1.

Table 5.1: List of equipment for carbon membrane-based biogas upgrading unit

Equipment	Supplier	Description
Membrane system/	Air Products Norway	
Odorant for GLØR	InterGas AS	
Biogas analyzers	Pronova GmbH	
Compressors	SAFE srl	
Instrumentation and automation	Siemens	
Process equipments	Somas AS	
Connections, tubing	Tess	
Isolation, steel plates	Trøndelag Isolering	
Tubing, parts and valves	Swagelok	
Dedicated product gas analyzer	Simtronics ASA	GD 10P
Handheld gas analyzer	Geotechnical instruments	GA 2000
Online gas analyzer	Pronova	SSM 6000C
Temperature transmitter	Officina Orobiche	TT-Classe A
Dew point transmitter	Michell Instruments	DP-001
Pressure transmitter	Emerson	3051S

5.2. Biogas composition and vehicle fuel quality

The raw biogas feed originates from microbial anaerobic digestion of food waste. Raw biogas composition is shown in table 5.2. Untreated biogas was fed to a biological H_2S scrubber, and a slip stream of the treated biogas was fed to the membrane pilot plant.

Table 5.2: Composition of raw biogas obtained from anaerobic digestion of food waste

Component	Food waste (mole%)
Methane (CH_4)	64 ± 3%
Carbon dioxide (CO_2)	30 - 35%
Nitrogen (N_2)	< 1%
Oxygen (O_2)	ca. 0%
Hydrogen sulfide(H_2S)	1000 ppm (average)
Water (H_2O), 35 °C	saturated

For the biogas to be used as vehicle fuel, it must meet certain quality requirements/standards. Norway does not have its own fuel quality legislation yet; therefore, Swedish standards were used to acquire vehicle fuel with carbon membrane separation process as both countries have an alike climate. The requirements for clean biogas used as vehicle fuel according to Swedish standards is shown in table 5.3. According to the legislation, an odorant must be added into flammable gas to ensure that the gas can be smelled below 20% of the lower explosion limit (LEL). Tetrahydrothiophene was used as an odorant to the upgraded biogas in this study.

Table 5.3: The requirement for vehicle fuel quality; Swedish legislation [128, 129]

Components	Standard
CH_4 (vol%)	96-98
H_2O (mg/Nm^3)	< 32
Dew point (°C)	-60 °C at 250 bar(g)
$CO_2 + O_2 + N_2$ (Vol %)	< 4
O_2 (vol%)	< 1
H_2S (ppm)	< 23

5.3. Carbon membrane-based pilot plant

This section describes the pre-treatment and biogas upgrading processes.

5.3.1. Biogas upgrading Process

In principal, the raw biogas is compressed, bulk water is removed by means of a chiller (dew point: 4 °C at 1 bar), gas is reheated and then led through the membrane system. Carbon membranes are more selective for CO_2 relative to CH_4, therefore, in the biogas upgrading process CO_2 from the feed biogas passes through the membrane (low pressure side/permeate) and CH_4 remains on the high-pressure side (retentate). Hence, the retentate is the desired product. The ratio of permeate flow rate and feed flow rate is defined stage cut (q_p/q_f).

Biomethane purity in the retentate stream depends on (1) CO_2/CH_4 selectivity, (2) pressure ratio on both sides of the membrane and (3) stage cut. H_2S and water need to be removed from the biogas stream prior to the membrane and this is done in pre-treatment section as shown in figure 5.1. Pre-treatment is a vital part of the process to meet the fuel standards and enhance the life time of the upgrading plant together with membranes.

The process flowsheet of the upgrading process with essential components is shown in figure 5.1. The plant was designed to process up to 60 Nm^3/hr of raw biogas at feed pressure up to 21 bar and vacuum on permeate side. The raw biogas was available at 1.06 bar and a blower was used to increase the pressure up to 1.3 bar. An activated charcoal system was used to remove most of the H_2S and bring it down to 5 ppm in the biogas stream. To ensure the compressor safety, in form of scale formation or deposition of charcoal inside the compressor, a filter was present after H_2S removal system to remove the entrained particulates of activated charcoal. Then the water knockout through temperature swing (TS) at 4 °C and 1 bar was introduced just before the feed to the compressor to reduce the water level in the feed gas.

In the case of carbon membranes, less than 40% relative humidity (RH) is satisfactory [13, 78] as the performance of carbon membrane deteriorates at higher RH, so (partly)drying is needed. However, as a precaution, a heater was introduced just before membrane unit. The compressor was “oil -free” but in case of any leakage from lubrication side, it may deposit on the membrane surface and thus have a deleterious effect on the membrane performance, therefore several oil filters were used downstream to remove oil from the compressed feed gas. The compressed biogas then entered a cylindrical multi-module (shown in figure 5.2) containing 24 medium sized carbon hollow fiber modules (≈ 0.5-2 m^2 each). A single stage separation configuration was successfully tested to obtain 96% CH_4 and a significant amount of data was collected. The membrane feed gas temperature was regulated by an electric heater, and the pressure was controlled by a modulating valve (v-4 in figure 5.1, a globe valve with Kvs 2.5, supplied by Samson). The membrane pressure, temperature, flow of the two outlet streams, permeate and retentate, were monitored with different instruments. To accomplish the dew point: -60 at 250 barg in the final product, a zeolite-H_2O absorbing column was installed followed by a particle filter prior to the high-pressure compressor. The purpose of particle filter was to retain potential zeolite particles from entering the high-pressure compressor. High-pressure compression up to 250 bar and odor addition was performed before storage of the vehicle fuel.

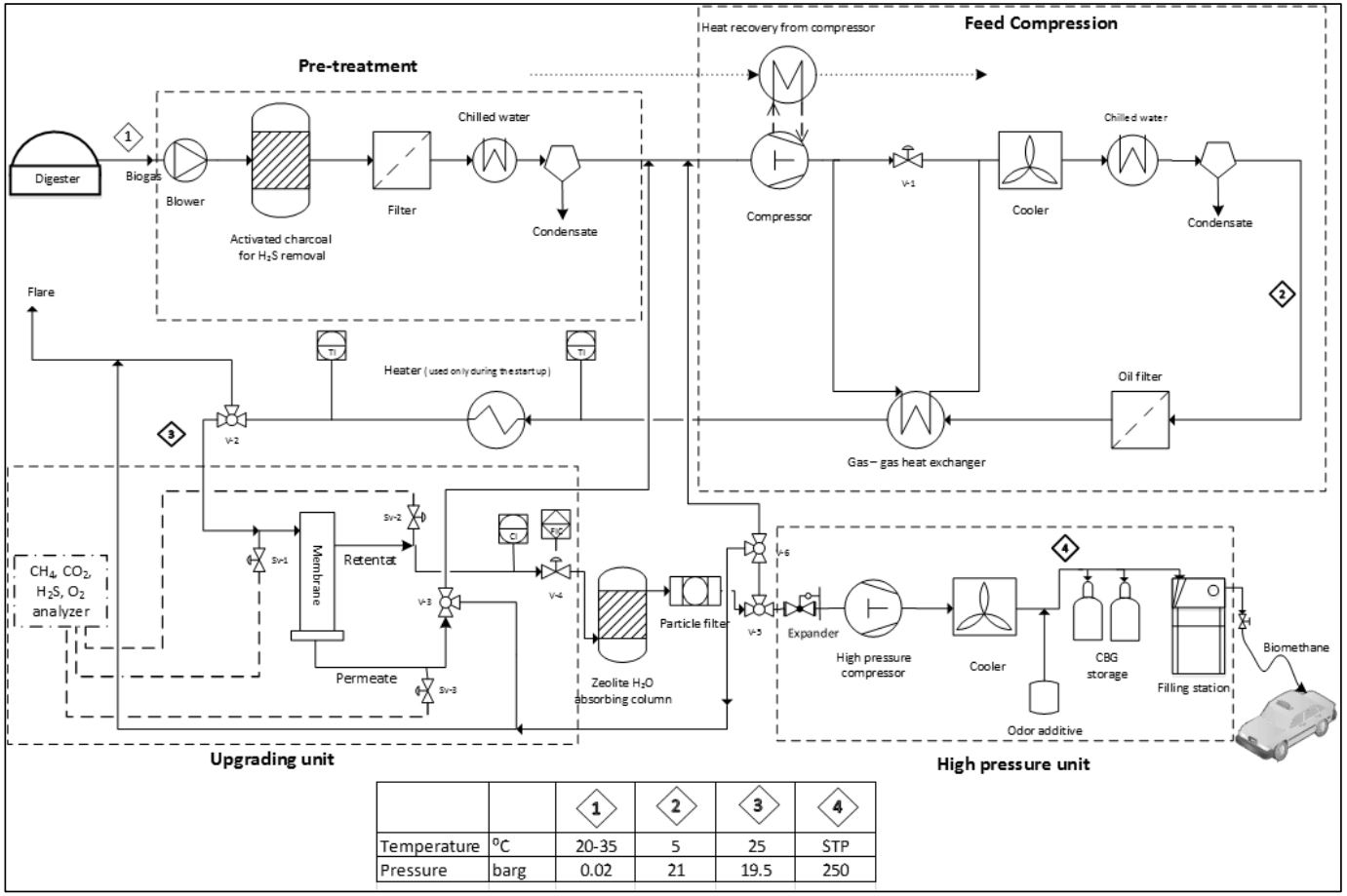

		1	2	3	4
Temperature	°C	20-35	5	25	STP
Pressure	barg	0.02	21	19.5	250

Figure 5.1: *Process flowsheet of biogas upgrading pilot plant based on carbon hollow fiber membrane*

5.3.2. Multi-module system assemblage

A multi-module system (MMS) was comprised of up to 24 medium sized modules, of which, each module was made up of up to 2000 carbon hollow fibers, which were tested for strength in bundles with effective area ranging from 0.5-2 m^2. Feed is on the shell side of the module (outer membrane surface) and permeate flows internally (bore side) along the fibers. The structural strength, low fouling tendency, membrane replacement, and ease to clean the MMS were important considerations for its application in a biogas upgrading plant. The MMS size was 0.324 m in diameter and 1 m in active length and consisting of three parts: (1) the vertical tank having both feed, retentate connecting ports and three legs with screws to secure it to the skid. (2) Middle part to insert the medium sized modules and, consisting of two round plates with holes according to the outer diameter of the medium sized modules. One partition plate on the top to separate the permeate section from feed section and 2nd partition plate between feed and retentate also helping to hold the modules firmly and avoid bumping into each other. (3) The lid on the top with permeate connection. The arrangement of the medium sized modules inside the MMS is shown in figure 5.2(C). After the assembly and before fitting the lid, each of the medium sized module was tested again for any leakage (fiber breakage) using air pressure and soap water.

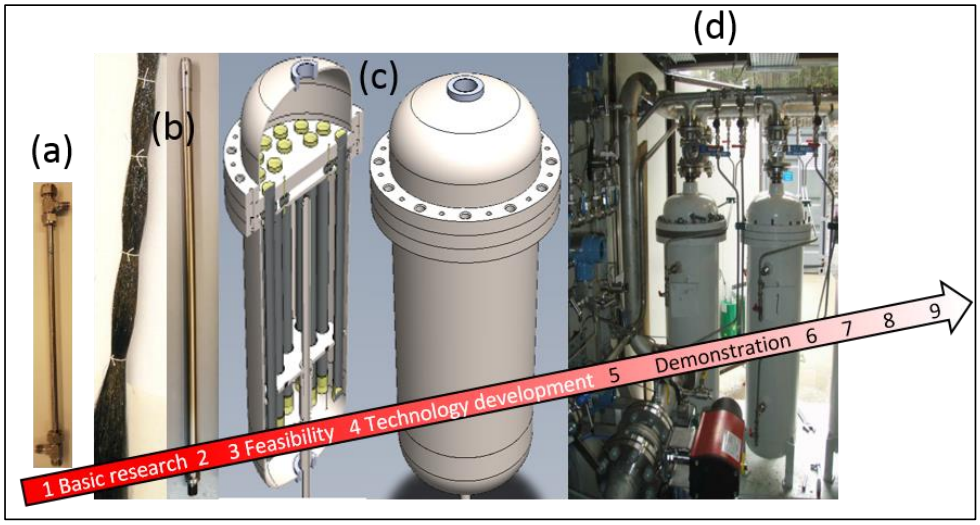

Figure 5.2: Technology readiness level according to the EU commission/Up-Scaling from lab to pilot-scale; (a) lab scale module, (b) medium sized module, (c) Multimodule, (d) Membrane Pilot plamt

6. Process simulation and cost estimation

The permeation properties of carbon membranes prepared at MemfoACT AS were almost similar or even higher in some batches as compared to lab-scale process. These data were used to simulate the required membrane area and compression energy for biogas upgrading system described in chapter 5. A lot of simulations were performed to explore different membrane configurations; single stage, two stage, three stage, with recycle and without recycle. The information obtained from simulations were used to estimate the total capital investment and running cost of carbon membrane-based systems. This chapter describes the procedures, parameters, and different assumptions that were used to perform the simulations and cost evaluation of carbon membrane-based separation processes. The results from simulations and cost estimation are presented and discussed in paper-VI (Techno-economical evaluation of membrane based biogas upgrading system: A comparison between polymeric membrane and carbon membrane technology**)** and paper-VIII (Carbon membranes for oxygen enriched air – Part II: Techno-economic analysis)

6.1. Background on membrane model and process simulation

Memfo group at the Chemical engineering department at NTNU has developed a membrane simulation model (Chembrane), which can easily be interfaced into Aspen HYSYS. Chembrane is essentially a mass transfer equations solver that can be applied for co-current, counter current, and a perfectly-mixed flow configuration. The thermodynamic fluid package applying sour Peng-Robinson equation of state was used. For a shell fed module, based on MemfoACT AS module design [108], the counter-current configuration explains real behavior of gas flow as the best. Therefore, counter-current configuration was used in the current study. However, other configurations and details of the model can be found elsewhere [130].

6.2. Simulation and cost estimation for biogas upgrading process

6.2.1. Membrane Configurations

Membrane plants may vary with respect to operational units, their arrangement and applied process conditions. Therefore, three different cases were evaluated for CO_2-CH_4 separation process to investigate different scenarios. The gas permeation properties of CO_2 and CH_4 used in these simulations were experimental data.

Single stage membrane system: A membrane system using only one stage to separate biogas for required methane recovery and purity was simulated. Figure 6.1 is showing a single stage membrane-based separation process.

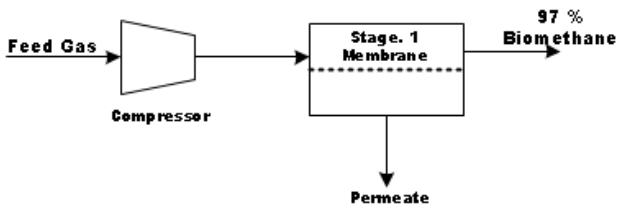

Figure 6.1: Single stage membrane system

Two-stage membrane system: To maximize the recovery of biomethane from biogas, a two-stage system was simulated using different (carbon and polymeric) types of membranes. Retentate from second stage mix with feed in the form of recycle stream prior to the compressor for better CH_4 recovery (Figure 6.2). There is no compression between the stages and the pressure of permeate 1 is adjusted with flow valve at Retentate 2. The pressure at permeate 1 was kept a constant value for the specific feed pressure, obtained with formula as shown in equation 6.1. The basis of the formula is to maximize the pressure ratio (hence maximum perm purity) on both stages simultaneously by setting the interstage retentate. It was observed that intermediate pressure value acquired, gave optimized membrane area for required purity and recovery of CH_4.

$$P_{interstage}=\sqrt{(P_{feed}\,P_{permeate2})} \tag{6.1}$$

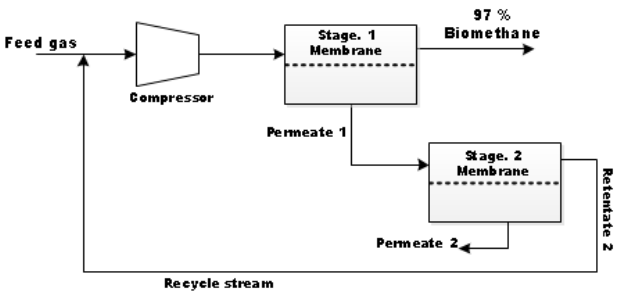

Figure 6.2: Two stage membrane system

Three-stage membrane system: Three-stage membrane system can give better separation and reduce energy demand [131]. A three-stage configuration is shown in Figure 6.3. Evonik Fibers Gmbh has applied for a patent of this configuration, and according to the patent, no one but Evonik can use a membrane with a CO_2/CH_4 selectivity of 30 or higher on the first stage [132]. Considering this patent accepted, the energy demand of the process will increase by 0.027 kWh/Nm^3 for the other membrane providers. The three-stage system is simulated and economically evaluated by using polyimide membranes.

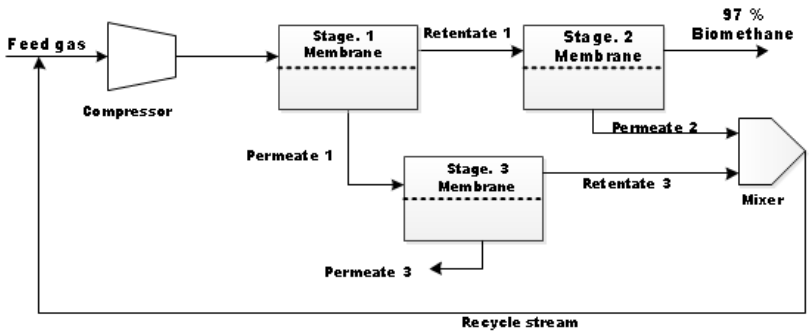

Figure 6.3: Three stage membrane system

6.2.2. Cost estimation

Accurate economic assessment of any plant depends on the available design detail, the method of analysis used for calculation and the accuracy of the available cost data. Therefore, the economic calculation may differ from each other considerably and justified by the data available.

An economic evaluation was performed to assess the different membranes and their configurations, by taking capital cost, operating cost, pre-treatment cost and high-pressure compression cost into account. A high recovery of biomethane is achieved, resulting a very small fraction of CH_4 permeating through membrane together with CO_2. Therefore, CO_2 obtained on permeate side is 99% pure which could be used for other applications. The price for the CO_2 is not considered in this economical assessment. Table 6.1 is showing process parameters for economic assessment of biogas upgrading plant.

Table 6.1: Process parameters for economic assessment of biogas upgrading plant [133, 134] ($ used in this work is US$)

Total plant investment (TPI)	
Polymeric membrane cost (PMC)	$\$20/m^2$
Carbon membrane cost (CMC_o)	$\$100/m^2$
Installed compressors cost (CC)	$\$ 8700 \times (HP/\eta)^{0.82}$
High pressure compressor cost (CBGC)	$C_{comp,ins} = 912 \cdot (Wcomp)^{0.9315} \cdot f_m \cdot f_i \cdot f_{inst}$ [135]
Fixed cost (FC)	$PMC/CMC_o + CC + {}^1VP + CBGC$
Base plant cost (BPC)	1.12 x FC
Project Contingency (PC)	0.2 x BPC
Total facility investment (TFI)	BPC + PC
Start-up cost (SC)	0.10 x VOM
TPI	TFI + SC
Annual variable operating and maintenance cost (VOM)	
Contract and material maintenance cost (CMC)	0.05 x TFI
Local taxes and insurance (LTI)	0.015 x TFI
Direct labor DL, cost based on 8hr/day	$ 15/hr
Labor overhead cost (LOC)	1.15 x DL
Utility cost (UC) ($/kWh)	0.07/kWh
VOM	CMC + LTI + DL + LOC + MRC + UC
Other assumptions	
Membrane life for polyimide (t)	7.5 years
Membrane life for carbon (t)	5 years
Biomethane sales price ($)	$\$0.8/Nm^3$
Nominal interest rate (%)	6%
Depreciation (t)	15 years
LCC/LCI factor (Ordinary annuity factor)	9.7122
Plant availability (%)	96%
CO_2/CH_4 in feed (%)	40/60

[1] *Vacuum pump*

6.3. Simulation and cost estimation for air separation process

The gas permeation properties of O_2 and N_2 used in these simulations were both experimental and predictive data. The experimental data were obtained at different temperatures, 5 bar feed pressure and vacuum (10 mbar) on low pressure side as listed in table 6.2. CM have superior thermal resistance compared to polymeric membranes and can be operated at elevated temperatures. The reported membranes showed exponential increase in O_2 permeability with increasing temperature and according to Arrhenius model (extrapolation of experimental data as in table 6.2), the separation process at elevated temperature between 190-205 °C using reported CM may achieve high O_2 permeability without sacrificing the selectivity. Another solution may be to achieve high permeability by adding some nano particles to the precursor [34]. Three permeability values; 100, 200, and 300 Barrer with constant O_2/N_2 selectivity of 18 were also considered to investigate the effect on production cost of EPO_2 and total capital investment of the plant.

Table 6.2: Experimental data for simulations

Temperature (°C)	O_2 Permeability (Barrer)	Selectivity O_2/N_2
20	2.98	18
35	4.58	18
45	5.88	19
50	6.41	19
68	9.93	18

(1 Barrer =2.736E−09 m^3(STP)m/(m^2 bar h))

The ratio between feed side pressure and permeate side pressure ($\Psi = P_{permeate} / P_{feed}$) is a key operating parameter that effects both separation performance and energy requirement [23]. To achieve required pressure ratio in this case, three different compression approaches as shown in figure 6.4 (a), (b), (c) were used to simulate the required energy and membrane area:

- *Feed compression (FC)*; a feed compressor was used to compress the air to 10 bar.
- *Vacuum pump on permeate side (VP);* No compression of the feed air, a vacuum pump was used to create 10 mbar on permeate side of the membrane.
- *Combination of Feed compression and permeate vacuum (FC-VP)*; In this case, feed air was compressed to 10 bar, and vacuum (10 mbar) was used on permeate side of the membrane.

Process simulations and economical assessment were done for a CM unit which would increase O_2 concentration (based on permeation values) in air from 21 mole% to between 50-78 mole% in a single stage separation process (no recycle).

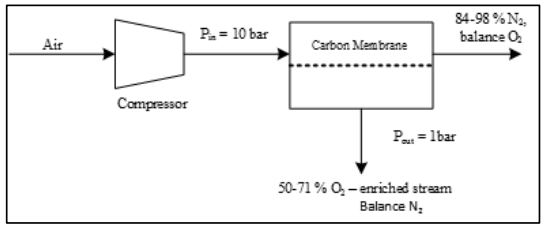

(a)

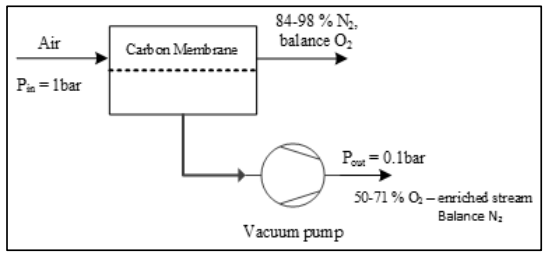

(b)

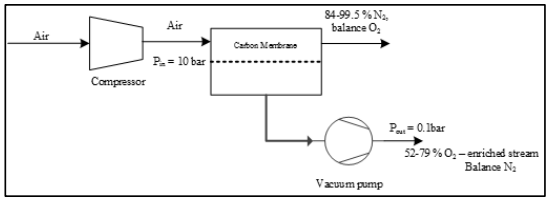

(c)

Figure 6.4: Single stage process configuration, (a) FC approach, (b) VP approach, (c) FC-VP approach

6.3.1. Equivalent pure oxygen, EPO_2

The base for the O_2 production was taken to be 1 ton of equivalent pure oxygen (EPO_2) per day, and EPO_2 is the amount of pure oxygen that would be mixed with air to make a mixture of oxygen-enriched air (E moles) of a specified O_2 concentration. The molar flow rates of EPO_2 and oxygen-enriched air (*E*) can be related by the simple equation shown in equation 6.2 [4].

$$\frac{EPO_2}{E} = \frac{y_{O_2} - 0.21}{0.79} \tag{6.2}$$

Here y_{O_2} is the oxygen mole fraction in enriched air.

In terms of weight, the flow rates (tons/day) of equivalent pure O_2 ($TEPO_2$) and of oxygen-enriched air (*TE*) are related as shown in equation 6.3.

$$\frac{TEPO_2}{TE} = \frac{y_{O_2} - 0.21}{(0.0989\, y_{O_2} + 0.692)} \tag{6.3}$$

6.3.2. Cost estimation

The assumptions and parameters used in this economic assessment are shown in Table 6.3. The first-time installation of membrane modules was included in the TCI. However, membrane replacement cost (MRC) was added in PC as a variable cost which is proportional to plant's operation rate. MRC was calculated based on daily usage (1 ton/day production of EPO_2) via dividing the total membrane area cost by total plant life (10 years) and then multiplied by plant availability (90%). The membrane operation does not need continuous labor inspection. Therefore, labor cost (LC) has been estimated as 8 hr/day per 25 tons per day of EPO_2. This cost analysis considers a CM price of \$ 100/m^2, a depreciation rate of 10% for the plant which includes compressor, vacuum pump, valves, and piping (except membrane), and a return on investment of 12%/year. The assumptions made in this economic analysis involves many adjustable variables, therefore a sensitivity analysis was also performed to determine the cost of EPO_2 which involves variation in CM module cost, membrane life time, and operating temperature which is directly related to membrane permeability.

Table 6.3: Economic parameters used to calculate TCI and PC per ton of EPO_2 [110, 119]

Total capital investment (TCI)	
CM module cost: CMC	$\$100/m^2$
Installed compressor cost: CC	$\$ 8,700 \times ([a]HP)^{0.82}$
Installed vacuum pump cost: VC	$\$32,500 \times ([a]HP/10)^{0.5}$
Production cost (PC)	
Membrane replacement cost: MRC	at $\$100/m^2$
Electricity cost: EC	\$0.05/kWh
Capital recovery cost: CRC	0.25 x (TCI)
Labor cost: LC	\$15/hour
Production cost: PC	MRC + EC + CRC + LC
Other assumptions	
Membrane life time	5 years
Annual depreciation	10% over 10 years
Annual Return on capital investment	12%
Plant availability	90% (329 days/year)

[a]*HP is the installed horse power for the installed compressor*

7. Results and Discussion

This chapter summarizes and discusses the main findings from the eight submitted papers as part of this thesis. The chapter has been divided into three sub-parts. The first part describes the process, synthesis, procedures to develop carbon hollow fiber membranes, durabilty, and aging of prepared membranes under miscellaneous environments. Second part discusses the pilot scale module construction, CVD, regeneration of membranes, and applications of preparaed CHFM. The third part of these papers presents the findings from HYSYS simulations when interfaced with Chembrane to evaluate optimal membrane area and energy requirement for different applications of CHFM.

The sequence in which papers will be discussed is presented in figure 7.1. Three different colors indicate the main focus of each paper – synthesis (blue), applications (red), and simulations (green). The degree of the filled color represents the relative composition of the paper with respect to these parameters.

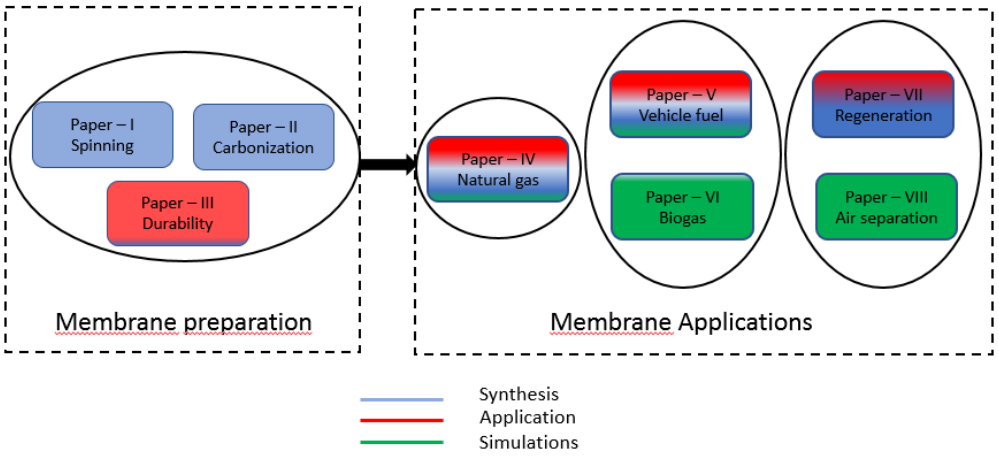

Figure 7.1: Flowline of thesis papers showing research work carried out related to carbon hollow fiber membranes at MemfoACT AS

7.1. CHFM preparation and aging

In this subsection, the main results from papers I-III will be discussed. The main focus is on preparation of CHFM (paper I and II), followed by aging and durability of CHFM under miscellaneous evironemnts (paper III).

7.1.1. *Paper – I: Pilot – Scale production of carbon hollow fiber membranes from regenerated cellulose precursor: Part I- Optimal conditions for precursor preparation (Membranes Journal 8(2018) 105)*

The main aim of this paper was to explain the procedures for preparation of the precursor hollow fibers for carbon membranes on a pilot scale plant. A dope solution consisting of cellulose acetate (CA), NMP, and PVP was prepared to spin the hollow fibers. Altogether, more than 460 spinning-sessions of CA hollow fibers were spun with 50 batches of dope mixture, of which at least 100 sessions were spun by varying spinning conditions, e.g. spinneret dimension, air gap, extrusion rate, coagulation bath temperature, take up speed and different fiber collection methods to optimize the pilot scale production of CA hollow fibers. Direct carbonization of CA will result in discontinuous carbon (more like a powder) hence, CA must be deacetylated after the spinning process prior to carbonization. Furthermore, drying of deacetylated fibers is another crucial step while preparing the cellulose hollow fibers from CA. The rate of drying, temperature, and humidity need to be optimized to achieve the carbon fibers with acceptable mechanical and gas peremation properties.

First, CA hollow fibers were spun using a dry/wet spinning method. Water was used to wash out the bore liquid from spun fibers. The collection of spun fibers is the critical step and need to be optimized for desired permeation properties of resulting carbon fibers. Intially, a squared wheel (nick named “guitar”) was used to collect and wash the fibers. But it was observed that a circular wheel with perforated collecting plates instead of guitars was more efficient during collection of fibers and water wash processes. After water wash process, adsorption of 10% glycerol (aqueous solution) into the pores of the hollow fibers over night prior to deacetylation improved both the gas peremeation properties and mechanical properties of the carbon fibers.

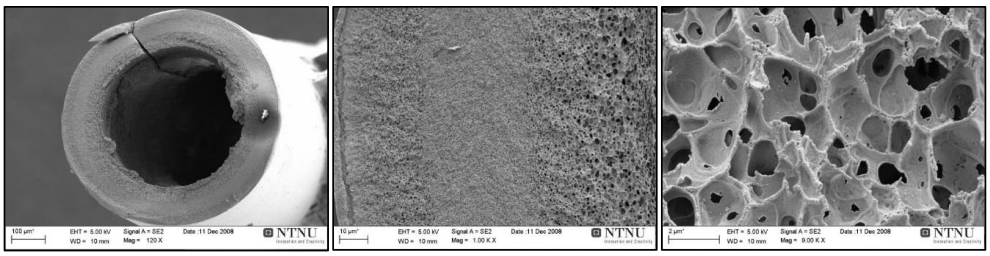

Figure 7.2: (a) CAHF cross-section-72.5% NMP in dope solution (b) Wall magnified (c) wall inner edge magnified

Glycerol treatment is important to prevent the largest pores from collapsing and to prevent the bore of the fiber from collapsing. The SEM images of NMP/H_2O (bore solvent) based CA

hollow fibers can be seen in Figure 7.2. The coagulation bath temperature of 25 °C resulted in the fiber wall more prorous on the bore side. Pure water in the bore coagulant results in a thick and dense inner wall, which is not desired as the feed is introduced at the shell side of the fibers and the inner structure is only acting as a support. Membranes spun with bore solution containing 65 and 70% of NMP showed CO_2 permeability of 256 Barrer and 144 Barrer with CO_2/CH_4 selectivity of 156 and 172 respectively (Figure can be found in Appendix E). Bore solution containing up to 70% NMP have successfully been used, resulting in a porous lumen structure of the fiber, which is desired to minimize the gas transport resistance.

The CAHF were then deacetylated with 90 vol% 0.075 M NaOH (Water) solution diluted with 10 vol% 2-propanol (isopropanol, IP) at ambient temperature. It was concluded that optimal duration for deacetylation process is 2.5 hours. The optimum was based on the appearance (e.g. degree of curling), the mechanical properties of the resulting carbon fibers and their weight loss. The SEM images of deacetylated hollow fiber are shown in figure 7.3. Deacetylation in water medimum would result in only on the surface of the fiber and not the bulk of the fiber, however, isopropanol was taken as reaction medium which successfully deacetylated the both surface and bulk of the fiber. This is probably due to swelling of CA in the presence of alcohol. Other alcohols may also be used, if they are suitable solvents for the base, as well as mixtures of alcohols and water.

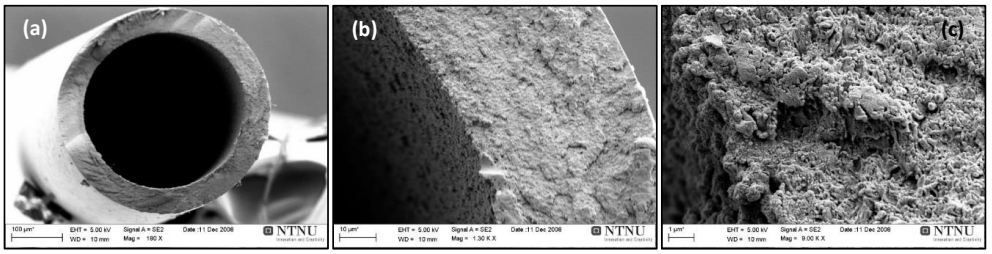

Figure 7.3: (a) Regenerated CHF after deacetylation of CA/cross section (b) wall magnified (c) wall inner edge magnified

These hollow fibers with optimized deacetylation gave stronger carbon fibers (loop with diameter: 8 mm) and permeation properties above Robeson upper bound 2008. Longer than 2.5 hours deacetylation time resulted in decreased CO_2 permeability after carbonization. Fibers deacetylated for short time than 2.5 hours gave brittle and curly fibers after both deacetylation (yield after drying < 50% of good fibers) and carbonization. It could be that fiber surface is fully deacetylated, however, non/partially deacetylated inner part of the fiber may cause different drying rates on both surfaces which ultimately would result in curly or brittle fibers.

In order to achieve high yield after deacetylation, an optimal drying procedure was established. It was concluded that rate of drying and relative humidity (% RH) play a key role to produce high yield of dry fibers. To achieve high yield, the fibers should be straight and mechanically strong. Figure 7.4 (left side) presents the effect of RH on straigtness and usefulness of the dried fibers. The straightness was graded a visual level range from 1-10, where 10 was very straight fiber and 1 very curly fiber. The fibers dried at RH over 50% at ambient temperature were straight and a high yield was obtained. It was observed that slow drying overnight with RH changing from 90 to ambient maximized the yield of the dried cellulose fibers. Figure 7.4 (right side) presents the yield of 460 spinning sessions of cellulose fibers dried using the drying protocol developed by MemfoACT AS.

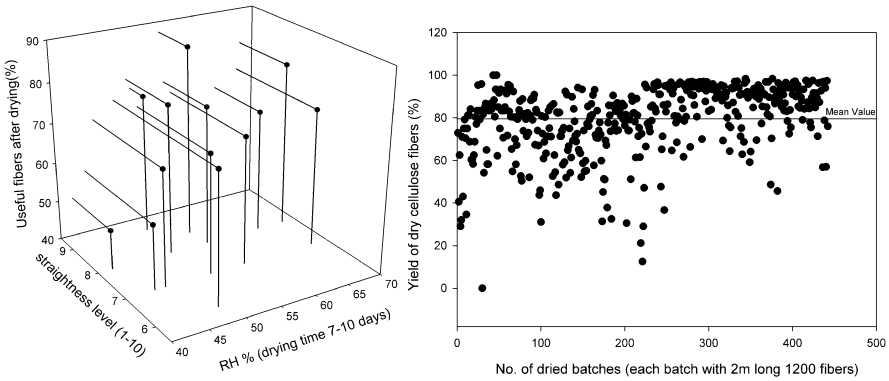

Figure 7.4: Effect of humidity on fiber quality (figure on left), and yield of 460 spinning sessions (figure on right)

The effect of %RH on gas permeation properties of carbon hollow fibers can be seen in figure 7.5. It was observed that fibers dried in RH: 65 →35% when drying overnight at ambient temperature (23 °C) produced lowest number of carbon fibers. However, the gas permeation properties of these fibers were better compared to the fibers dried in RH: 55 →35%. Maximum number of good fibers possessing both high gas permeation properties and mechanical properties were obtained at RH: 85 →35%. These results indicate that slow drying of fibers at high RH humidity prevents the pore structure of dried cellulose fibers. It could be because along the cellulose fiber, water exists in two states: as bonded water (strong hydrogen bonds with cellulose molecules) and as free water (sorrounded by the bonded water and no contact with the cellulose molecules) [136]. In the natural drying at lower RH: 55 →35%, the water evaporated quite fast and the water-cellulose bonds were strong enough to pull the cellulose

structure in a region with more dense/collapsed structure. However, in slow drying at higher RH: 85 →35%, it could be that the hydrogen bonds of water-cellulose pulled the cellulose structure closer and closer until new hydrogen bonds between cellulose chains were formed, and keeping the pores structure stable as the free water evaporated gradually.

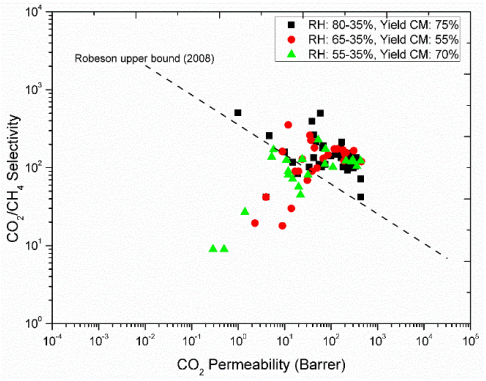

Figure 7.5: Gas permeation properties of carbon hollow fibers from regenerated cellulose precursor (RH: 80-35%; Black squares, RH: 65-35%; Red circles, RH: 55-35; green triangles)

7.1.2. Paper – II: Pilot – Scale production of carbon hollow fiber membranes from regenerated cellulose precursor: Part II- Carbonization procedure (Membranes Journal 8(2018) 105)

The simultaneous carbonization of thousands of precursor fibers in a horizontal furnace may result in fused fibers if the carbonization residuals (tars) are not removed fast enough. Paper-II describes the custom-made furnace and procedure to carbonize up to 4000 fibers in a single batch. It was found that optimized purge gas flow rate and a small degree angle in the furnace position may enhance the yield of high quality carbon fibers up to 97% by removing the by-products. A smaller and more compact microporous structure with smooth surface was obtained after carbonization of deacetylated fibers as shown in figure 7.6. Average diameter of carbon fibers was 210 µm with wall thickness of 23 µm. Carbonization is a critical step and varying carbonization conditions would result in dissimilar carbon matrix for each carbonized batch of hollow fibers.

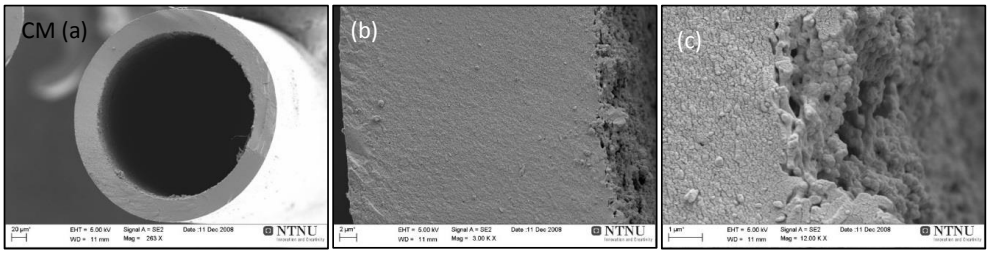

Figure 7.6: SEM images of carbon hollow fiber membrane, (a) cross section, (b) wall magnified (c) inner edge of the wall magnified

The regenerated cellulose fibers were carbonized in a horizontally oriented 3-zone furnace. Quartz tubes and perforated stainless steel (SS) flat grids were initially used to carbonize up to 4000 (160 cm long) fibers in a single batch. It was concluded that number of fused fibers (sticking together due to residual products) could be reduced significantly by replacing the quartz tubes with perforated grids. It was further observed that improved purge gas flow distribution in the furnace with perforated grids and a 4-6-degree angle in furnace position permitted the residuals to flow downward into the tar collection chamber. Carbonization under an inert atmosphere, which is more realistic in an industrial process, was successfully performed. The final temperature (thermal soak) was maintained for 2 hours in each protocol, to reduce the number of dangling bonds in the carbon. This may reduce the aging (irreversible sorption) behavior when gas permeation testing is carried out. In total, 390 spun- batches of fibers were carbonized. Usually each perforated SS-grid contained 2000-4000 individual fibers and these fibers comprised 4-6 spun-batches of vertically dried regenerated cellulose fibers. Gas permeation properties were investigated for the produced carbon fibers.

Figure 7.7 summarizes the results of 390 spun-batches, carbonized both in the quartz tubes and on the SS-grid. As can be seen in figure 7.7, on average 40% of the total carbonized fibers, fibers in the quartz tubes, were fused and unusable. Although some batches exceeded to even 60% fused fibers. The brittle fibers obtained from the same batches were in the range from 0-30%. The percentage of curly and collapsed fibers (not shown here) was between 0-5%. Hence the "survival rate" of these batches was very low (< 10%). It was assumed (i.e. % of good fibers) that honey comb arrangement of quartz tubes might create more uniform conditions in cross-section within each bundle, but it was observed that the unequal flow rate of gas was distributed in each bundle/tube.

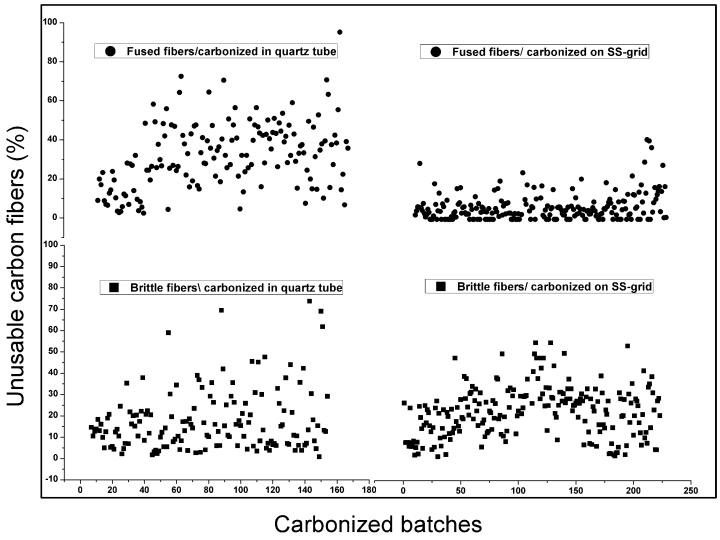

Figure 7.7: Fused and brittle fibers after carbonization, results with quartz tube (left), results with SS-grid (right)

Therefore, most of the residual produced during carbonization stayed inside the bundle resulting in fused and brittle fibers. Using an angle on furnace (4-6 degrees by raising the closed end of the furnace to enhance the flow of residue downward) improved the rate of survival but still could not produce successful fibers consistently. Residual amount was also different in all batches depending on the changed parameters during precursor preparation or number of fibers in each carbonization batch. It could be noted that the survived fibers were always on the top of the bundle and those in bottom part was fused.

The number of fused fibers were significantly reduced when carbonized on the perforated SS-grids as shown in the figure 7.7. Usually each perforated SS-grid contained 2000-4000 individual fibers and these fibers included 4-6 spun-batches of vertically dried regenerated cellulose fibers. Initially all fibers on the grid were placed in same direction (top side during drying) for all batches. After several carbonizations, it was observed that the fibers fused more only on one side of the bundle (top side). Hence the dried batches were arranged on SS-grid in an alternating order (top of one batch in one direction neighboring with bottom of the other batch and so on). It improved the number of survival fibers but there were still some fused fibers in each bundle. Then a perforated grid with bigger openings (20 X 20 mm) was used which increased and results were almost similar as with previous grid (10 X 10 mm). It was observed that fibers on the bottom of the bundle touching to the grid and specifically sections of the fibers in contact with SS-grid were sometimes fused and got stuck with the grid. That

portion of the fibers became brittle and pulling it away from bundle (separating the fibers) would break the fibers. Although numerous batches had zero fused fibers, but it was still challenging to keep the consistent production rate. While gas distribution was improved by use of grids, there were still some sections where pressure drop was higher (fibers not equally dispersed on grid) and gas was not able to isolate the fiber-tar-fiber and fiber-tar-grid connections.

The carbonized hollow fibers should be sufficiently strong, flexible, straight, and uniform to produce bigger commercially modules with high packing density. The challenge during carbonization is the fiber brittleness. As shown in figure 7.7, both carbonization methods (fibers inside quartz tube and on SS-grid) had almost similar number of brittle fibers. These fibers could not be looped into 10 mm diameter before they broke - this was used as the definition of brittleness in this study. There might be two possible reasons for the brittle carbon fibers: (1) varying properties of the precursor in each batch, e.g. partial deacetylation, fast drying at lower relative humidity (40-30%), etc. (2) surface of carbon is not fully free from low-molecular products (tar). In future research, a continuously rotating perforated tube (SS or glass) is suggested for the carbonization of big batches. This would help to distribute the gas equally in a more efficient way, remove the residual tar, and avoid the continuous contact of fibers with tube and each other. Furthermore, a model to estimate the gas flow pattern inside carbonization chamber would be very helpful to manipulate the gas distribution inside the chamber for a homogenous flow.

The separation properties of the resulting membrane will be determined by the pore structure formed during carbonization. It was observed that high temperature (700 °C) carbonization resulted in dense membrane with decreased CO_2 permeability (up to 20 Barrer) and high CO_2/CH_4 selectivity (above 200). Whereas, 650 °C final temperature improved the permeation properties of the resulting carbon membranes by sacrificing some of the selectivity. It could be that high temperature caused the carbon structure collapse (sinters) and the pore size was decreased. However, at 650 °C the carbon structure was stiff enough to keep the high porosity (high micropore volume) with effective pore size. It is important to note that a high carbon yield is not wanted when making carbon membranes. Most important is high micropore volume and effective pore size with a distribution as narrow as possible. However, the resulting carbon should not contain any macrovoids or fractures and be a continuous matrix.

Figure 7.8 presents the permeation results of the carbon hollow fiber membrane prepared from regenerated cellulose hollow fibers. As shown in figure 7.8, some batches were carbonized under CO_2 atmosphere. Despite good permeation properties, the resulting fibers possessed very

weak mechanical properties. Fibers carbonized under vacuum had lower CO_2 permeability and selectivity values than when prepared in CO_2 or N_2 atmosphere. The membranes prepared in N_2 atmosphere exhibited high performance (as shown in figure 7.8) and good mechanical properties. Therefore, rest of the batches were exposed to N_2 atmosphere during carbonization.

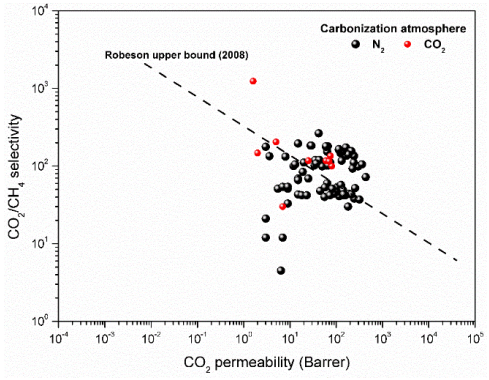

Figure 7.8: Separation performance of carbon hollow fiber membrane when carbonized under N_2 and CO_2 atmosphere (Final temperature: 650 °C) (1 Barrer =2.736E−09 m^3(STP)m/m^2 bar h)

Geiszler and Koros [43] reported that an inert gas atmosphere resulted in more open, but less selective CMSM matrix compared to vacuum carbonization. They explained this with acceleration in the carbonization process due to increased gas phase heat and mass transfer. The same authors also observed that CO_2 purge produced a highly porous, nonselective membrane by oxidizing the carbon, and ten times reduction in purge gas flow rate caused a decrease in the permeate flux which was presumably by the deposition of tar (carbon) either on the membrane surface or in the pores. Based on our own observations where carbonization in CO_2 atmosphere with previously mentioned flow rates looked promising, reasonable permeability and selectivity was achieved, the yield of produced carbon fibers was significantly reduced due to weak mechanical properties.

As already stated, N_2 atmosphere was chosen to be used for rest of the batches. The optimized flow rate of purge gas yielded mechanically strong fibers with acceptable gas permeation properties. CM produced on pilot-scale plant showed equal or higher performance as compared to laboratory scale carbon membranes in CO_2-CH_4 separation. The performance of carbon membranes was enhanced further by chemical vapor deposition (CVD) process.

7.1.3. *Paper – III: CO_2 separation with carbon membranes; Durability and aging under miscellaneous environments (Journal of Industrial & Engineering Chemistry 70(2019) 363-371)*

To exploit the aging phenomenon in carbon membranes, this paper discusses the effect of miscellaneous environments when fibers were in storage (static aging) or in operation. The difficulty in carrying out any type of aging experiment on bundles of these CHF in a module is that the membranes cannot be tested immediately after carbonization, as the time required to prepare the modules is a minimum of 6 hours. The epoxy resin requires this duration of time to set. Placing the module directly in the gas testing unit under vacuum, would cause distortion of the epoxy resin, break the seal and hence the gas would permeate through the fibers as well as the module resulting in an inaccurate evaluation of permeability.

To understand the aging, dry storage environments like air, vacuum, CO_2, etc. were studied. In order to study the durability and aging during operation, CHF were exposed to biogas for almost one year with H_2S content extending from 0-2400 ppm, and gas permeation tests for single gases, N_2, CO_2, CH_4, and O_2 were analysed periodically at the membrane production facility.

Effect of dynamic aging, defined as "aging under controlled environment and continuous gas flow (air in this study) through the membrane" was studied. Following a period of 27 days, permeation tests were conducted on a membrane module as a function of dynamic aging. The pump was then disconnected from the module at the feed end and the module was exposed to the atmosphere, undergoing a period of static aging (ambient temperature). A vacuum remained on the permeate side of the module, to prevent the adsorption of air on the remainder of the gas unit. Thus, this combination of dynamic and static aging was termed "intermediate aging".

The aging effect on the CO_2 permeability of carbon membrane stored under different conditions is shown in figure 7.9. Figure 7.9(a) presents the four sets of CHFM which are rolled in plain paper and then stored at different conditions. The decline in CO_2 permeability is fastest for the fibers lying on an open shelf, whereas slowest in the fibers stored inside the cabinet, which decelerated the chemisorption phenomena by reducing the O_2 supply inside the cabinet. Apparently, membrane performance losses here are due to chemisorption of O_2, rather than other contaminants.

Figure 7.9(b) shows the CO_2 permeability loss over time for CHFM rolled inside aluminum foil and stored under different conditions. Low temperature (4 °C) was not helpful in preventing or slowing the performance loss of the membranes. Not surprisingly, the identical effect as figure 7.9(a) was observed for the CHF rolled in aluminum foil and stored inside the cabinet.

In all cases, membrane performance becomes constant after all active sites on the carbon had reacted or stabilized by the formation of oxygen surface groups.

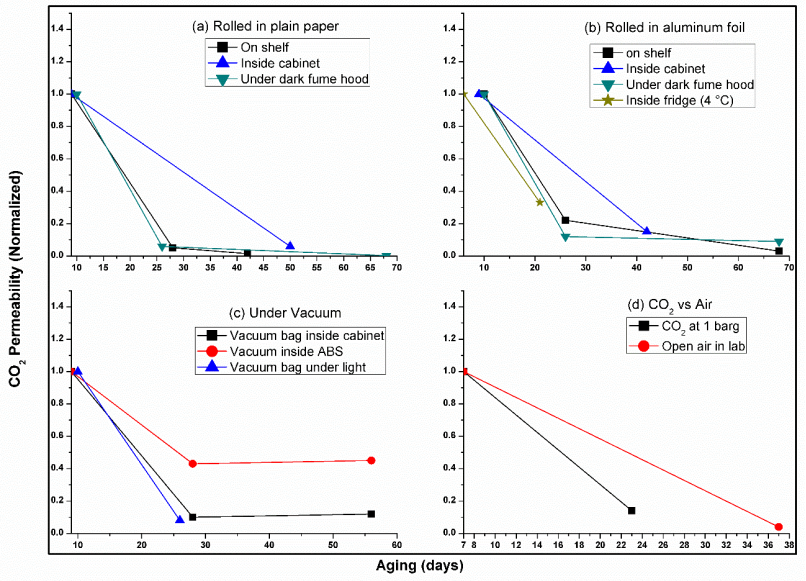

Figure 7.9: Storage of CHFM under different environments

The storage of CHF under vacuum was helpful in keeping the membrane performance to some extent. Figure 7.9(c) illustrates the change in CO_2 permeability when CHF were stored under vacuum in different conditions. Fibers stored inside an ABS tube under vacuum slowed down the aging effect until first 28 days and then performance remained constant for next 32 days. First permeation test was performed 10 days after the carbonization and then fibers were stored under vacuum, which explains that some reactive sites of carbon surface had formed oxygen surface groups during first 10 days reducing CO_2 permeability from 74 to 33 Barrer, however applying vacuum helped in slowing down and further preventing chemisorption of O_2, when stored inside ABS tube. CHF stored in vacuum bag was not effective to prevent the aging and that was due to small leakages present in vacuum bags. Figure 7.9(d) shows the aging comparison for CHF stored under CO_2 atmosphere and in open air. It was observed that fibers stored under CO_2 environment lost the performance faster than fibers stored under open air inside the lab.

Dynamic aging had a promising regenerative effect on the membranes to recover some permeability. The fibers which underwent dynamic aging were not susceptible to static aging

anymore. They showed the same performance even after 128 days when stored in the laboratory environment.

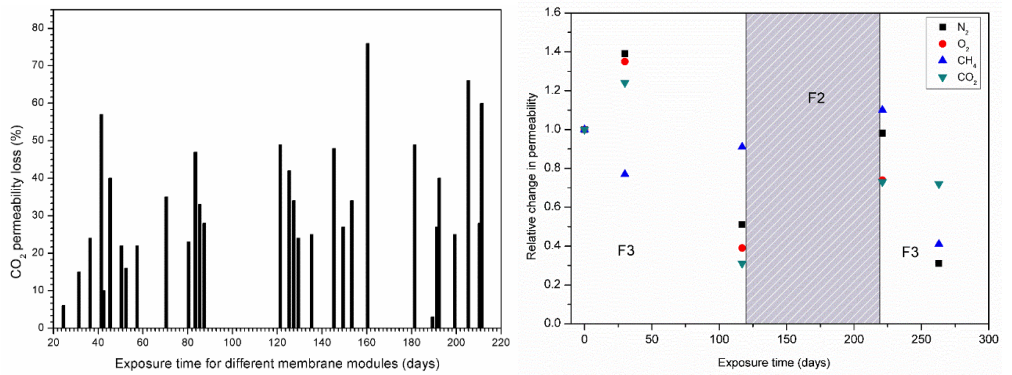

Figure 7.10: CO_2 permeability drop at Field-1 (figure on left); Relative change in permeability of N_2, CO_2, O_2, and CH_4 after exposed to Field-2 and Field-3 (figure on right)

In total, 31 modules of area 0.5-2 m^2 for each module were used to separate biogas in actual biogas field for days ranging from 25-212. Most of these modules lost 40% CO_2 permeability within a few days after installation and were stable afterwards. It explains that after oxygen adsorption (whether during module preparation or in a later stage) CHF start stabilizing without further loss in performance. CHF were mechanically stable at 20 bar in real industrial conditions. Figure 7.10 (left side) is presenting the loss in CO_2 permeability as a function of exposure time for 31 modules.

Further real gas exposure was performed in two biogas fields by exposing CHF to the H_2S in the sequence high-low-high concentrations. Membranes installed at high H_2S (150-2400 ppm) concentration lost CO_2 permeability by up to 65% in 125 days, and 55% of this lost permeability was regenerated by exposing membrane to a biogas field with low H_2S (< 5 ppm) concentration for 100 days. When this membrane was installed again on high concentration field, the CO_2 permeability was stable for the next 50 days. Relative change in permeability of O_2, N_2, CH_4, and CO_2 after exposure at Field-2 and Field-3 is shown in figure 7.10 (right side).

7.2. Carbon membrane applications

In this section, the main results from papers IV, V, and VII will be discussed. Paper-IV focuses on pilot scale module construction, CVD, high pressure and elevated temperature testing, and simulations for natural gas application of carbon membranes. Paper-V is about the process design, simulations for a pilot scale biogas upgrading plant, construction and demonstration of

carbon membrane-based pilot plant for biogas upgrading to vehicle fuel. However, Paper-VII discusses the carbon membrane application in air separation market. This paper also describes a novel online electrical regeneration method to regain the lost membrane efficiency due to continuous oxygen exposure.

7.2.1. Paper – IV: CO_2 separation with carbon membranes in high pressure and elevated temperature applications (Separation and Purification Technology 190 (2018) 177-189)

In this paper, procedures for pilot scale module construction, selective clogging, and CVD processes were explained in detail. Simulations were performed for a two stage process with recycle stream to achieve optimal membrane area and energy requirement for maximum recovery of CH_4 in natural gas application. Thermal expansion experiment was filmed during the entire heating and cooling cycle and snapshots indicated that fibers are intact and stable up to 374 °C. Above this temperature, change is probably due to oxidation.

To enhance membrane permeation properties, the pore structure was tailored by means of an oxidation and reduction process followed by chemical vapor deposition with propene and named as "modified carbon hollow fibers (MCHF)". Permeation properties using shell-side feed configuration of 70 modules (0.2-2 m^2) for both CHF and modified carbon hollow fibers (MCHF) were investigated for single gases performed (using standard pressure-rise set up [137]), N_2 and CO_2 at high pressure (2-70 bar feed vs 0.05-1 bar permeate pressure) and temperature from 25-120 °C. Maximum CO_2 permeance value for a MCHF module was recorded 50,000 times higher compared to prior modification, and CO_2/N_2 selectivity was improved 41 times. Results indicated that carbon membranes are hardly effected by high pressure, but significant drop in CO_2 permeability was observed at elevated temperature.

A membrane module consisting of two MCHF was used for high pressure experiments to understand the behavior of pure gas CO_2 and N_2 permeation (fluxes, pure gases) at seven different pressure set points for shell-feed configuration as shown in figure 7.11 (left). In this study, all experiments were done at 1 bar pressure on the permeate side.

Permeabilities of N_2 and CO_2 changed, but the effect was much smaller, and it explains that the dominant mechanism here is molecular sieving, which is not being affected by pressure for pure gases. It was found that the carbon membrane is not swollen by high partial pressures of CO_2. Fibers were fed to shell side, however, pressures higher than 70 bar were not tested at our facility due to HSE (health and safety executive) limitations.

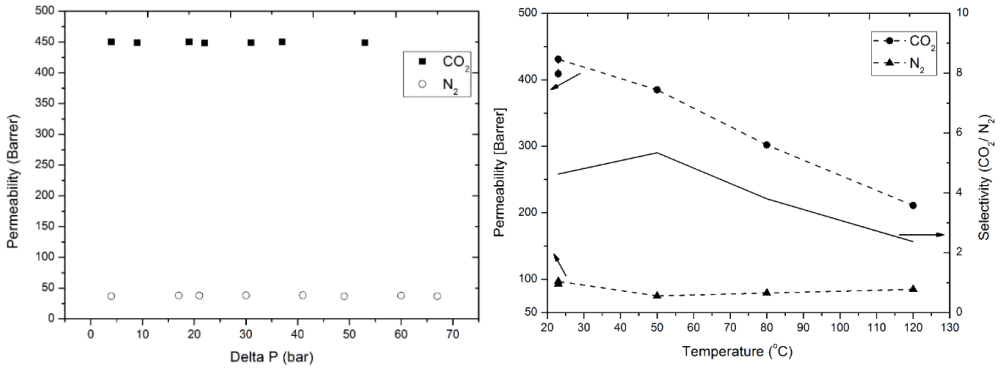

Figure 7.11: CO_2 and N_2 permeability at elevated pressure (T:23 °C) [Left]; Effect of temperature (P: 5 bar) [right]

In the later stage, dynamic mechanical properties of MCHF were measured and then burst pressure was calculated by Barlow`s formula. The fibers were kept bore side fed at 60 bar (10% CO_2 in N_2) for 1 hour. It was observed that fibers are quite stable when fed through bore side as well.

To investigate the temperature dependence of mass transport through the MCHF, pure gas CO_2 and N_2 has been studied between 23 and 120 °C as shown in figure 7.11 (right). The extensive temperature span showed that CO_2 and N_2 have different transport behavior with the temperature elevation. For inert gases, the separation can be done at temperatures up to the carbonization temperature (~500-800 °C). If the operational temperature is limited by the sealing material, this may be overcome by installing heat exchangers at the module ends. As shown in figure 7.11, CO_2 permeability declined significantly almost 50% in a linear fashion when the temperature was increasing. Fuertes et al. [14] suggested that the CO_2 permeability decline at high temperature and low pressure is a result of a compensation between increasing mobility and decreasing adsorption. In contrast, the effect of temperature on N_2 permeability was very low and above 45 °C, the N_2 permeability was almost constant.

A total of 70 CHF modules of effective area range 0.2-2 m^2 for each module, were modified to study the effect of pore tailoring process and separation performance of CHF and MCHF. The results are shown in figure 7.12. Single gas N_2 and CO_2 permeation tests were before and after modification at 23 °C, 5 bar feed (shell-side configuration) pressure and vacuum on permeate side. Permeation results indicated that overall performance of all modules was improved after physicochemical treatment of the membrane surface, and performance for most of the MCHF was above the Robeson's upper bound 2008 as shown in figure 7.12 [30]. In a few modules, selectivity was reduced after surface treatment and the reason may be that the chemical vapor

deposition process did not create a sufficient layer on all the fibers, or that the oxidation-reduction process opened the pores too wide before or after the CVD process. The modules referred in figure 7.12 contained fibers between 200-2000. Numerical values of CO_2/CH_4 selectivity, CO_2 permeabilities, membrane area for CHF and MCHF are shown in table 7.1.

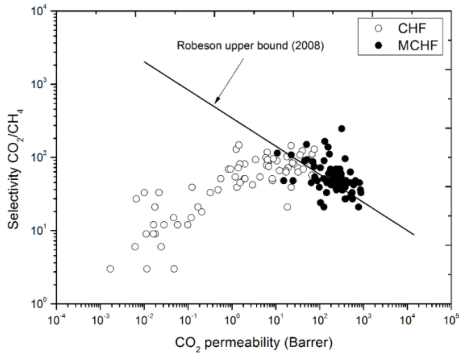

Figure 7.12: Separation performance of CHF and MCHF

Table 7.1: Separation performance of CHF and MCHF

		CHF		MCHF	
No.	Area m^2	Selectivity CO_2/CH_4	CO_2 Permeability Barrer	Selectivity CO_2/CH_4	CO_2 Permeability Barrer
1	1.0	21	1.75E-02	60	1.60E+02
2	0.8	33	2.18E-02	48	2.46E+01
3	0.7	12	2.81E-02	24	1.05E+02
4	0.8	12	1.63E-02	39	9.82E+01
5	1.0	18	2.05E-01	45	6.47E+01
6	0.9	9	1.11E-02	69	1.76E+02
7	1.0	3	4.80E-02	72	1.04E+02
8	0.7	6	2.43E-02	54	3.10E+02
9	1.0	15	4.68E-02	138	1.55E+02
10	0.8	27	6.59E-03	60	3.08E+02
11	1.1	9	1.78E-02	45	1.78E+02
12	0.7	3	1.15E-02	69	2.52E+02
13	0.8	9	1.61E-02	51	1.23E+02
14	1.0	3	1.69E-03	57	2.62E+02
15	1.0	12	5.76E-02	42	5.96E+02
16	0.9	6	6.20E-03	246	3.18E+02
17	1.1	51	5.57E-01	48	3.39E+02
18	1.0	12	9.88E-02	165	1.31E+02
19	1.3	15	1.18E-01	21	1.25E+02
20	1.1	21	1.68E-01	42	2.93E+02
21	1.1	51	1.92E+00	45	2.45E+02
22	1.0	51	1.97E+00	42	1.80E+02

23	1.5	72	3.14E+01	36	2.42E+02
24	1.4	90	7.09E+00	39	2.90E+02
25	1.5	39	1.24E-01	48	8.76E+01
26	1.4	33	3.19E-01	39	2.35E+02
27	1.5	54	1.19E+00	48	2.40E+02
28	1.4	72	1.90E+01	42	2.52E+02
29	1.4	81	2.59E+01	39	3.80E+02
30	1.6	48	8.39E+00	36	3.23E+02
31	1.7	69	8.27E-01	36	3.34E+02
32	1.7	36	4.83E-01	57	2.80E+02
33	1.9	66	1.69E+01	45	2.94E+02
34	1.6	84	2.41E+01	27	3.87E+02
35	1.1	39	1.30E+00	45	3.06E+02
36	1.5	87	6.62E+00	54	7.70E+01
37	1.5	63	3.25E+01	27	3.81E+02
38	1.7	54	4.37E+00	60	1.89E+02
39	1.6	63	1.70E+01	48	2.77E+02
40	1.7	66	1.22E+01	21	7.71E+02
41	1.4	90	5.45E+01	30	5.16E+02
42	1.5	69	4.22E+01	27	5.60E+02
43	1.4	129	1.25E+00	45	1.46E+02
44	0.3	117	6.36E+00	33	1.44E+02
45	0.3	123	4.04E+01	36	8.55E+02
46	0.3	111	6.76E+01	33	8.76E+02
47	0.2	78	6.09E+00	33	5.51E+02
48	0.2	144	2.23E+01	48	4.02E+02
49	0.2	39	2.25E+01	45	5.20E+02
50	0.2	42	2.94E+00	96	3.82E+02
51	0.2	69	9.22E-01	69	2.88E+02
52	0.2	102	2.08E+01	48	1.53E+02
53	0.2	51	8.30E+00	93	5.16E+01
54	0.3	99	5.89E+00	108	2.25E+01
55	0.3	93	3.46E+00	150	5.03E+01
56	0.3	108	3.56E+01	45	4.54E+02
57	0.3	129	7.56E+01	48	6.55E+02
58	0.2	90	1.06E+01	69	2.32E+02
59	0.3	102	1.79E+01	45	8.05E+02
60	0.2	75	6.82E+00	63	5.04E+02
61	0.2	81	1.96E+00	111	1.68E+02
62	0.2	81	1.52E+00	66	1.85E+02
63	0.3	93	6.49E+00	51	2.03E+02
64	0.1	147	1.44E+00	114	1.08E+01
65	0.3	72	1.39E+00	90	1.26E+02
66	0.3	96	8.83E+00	48	2.99E+02
67	0.9	45	1.53E+00	90	4.57E+01
68	1.0	21	1.84E+01	75	7.52E+01
69	0.9	57	6.65E+01	87	7.02E+01
70	1.1	33	1.00E-02	48	1.51E+01

Selection of a separation process is entirely based on economic considerations. Costs must be calculated for every specific separation problem in details and it cannot be considered very general. In paper-IV, the effect of CO_2 contents in feed for a fixed product purity (98% CH_4) and loss (2.5% CH_4) using membranes with different efficiencies was also simulated and hence the subsequent effect on total cost in form of membrane area and compression duty was evaluated. A short capital cost comparison among MCHF, polyimide and CA membranes, which include the capital cost of the membrane and installed compressor for required duty was investigaed.

The modified carbon membranes offer high efficiency in a single stage process reducing methane losses, footprint, and energy consumption as shown in figure 7.13 (Gas permeation properties used in the simulations are, *CO_2: 318 Barrer, CH_4: 1.3 Barrer, (1 Barrer =2.736E−09 m^3(STP)m/(m_2 bar h)))*. Results indicate that CH_4 recovery of 99.2% can be achieved in a single stage with MCHF membrane system when 5% CO_2 is present in the feed gas. Required membrane area is almost constant from 20% and higher contents of CO_2 in natural gas which indicates that area is fully optimized towards the desired purity and recovery of methane. However, two stage process with recycle was required to achieve desired purity and recovery while using polyimide or CA membrane.

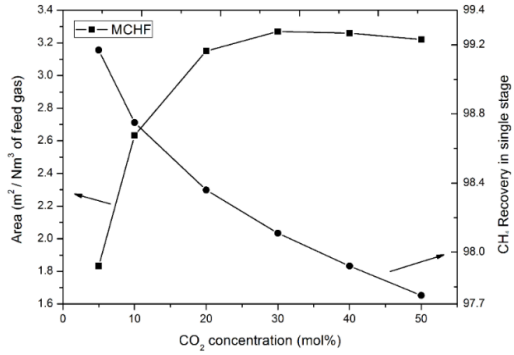

Figure 7.13: Required membrane area and CH_4 recovery in a single stage MCHF system

For the natural gas facility, in the case of single stage separation, the largest cost item is the membrane and associated housing for high pressure, because there is not any compression cost associated with natural gas feed, which is already at high pressure. But in the case of two stage membrane system, the need for compression of recycle stream adds up the cost as shown in figure 7.14.

Due to the limitation caused by plasticization, CA membranes were simulated for maximum 30% CO_2 contents in feed at 50 bar, whereas maximum 50% CO_2 was considered for other

membranes [138]. From the results, for the natural gas stream, increasing the membrane performance (both permeability and selectivity) reduces the process complexity by achieving the goal in a single stage and hence reduces the total cost. Although MCHF membrane price is higher than polyimide and CA membranes, still the separation process with MCHF is economical and offers small foot prints owing to only single stage requirement. Carbon hollow fiber membranes are still in the development phase, and the membrane price will most likely be reduced by further optimization of the carbon membrane production and modification process in the future.

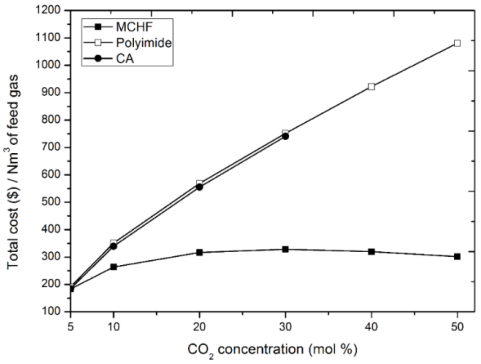

Figure 7.14: Total cost per Nm^3 of feed for CA and polyimide two-stage membrane process and MCHF single stage process

A schematic plot (adopted from Baker and Lokhandwala [4]) illustrating the effect of gas flow rate and CO_2 composition on the choice of the separation process is shown in figure 7.15.

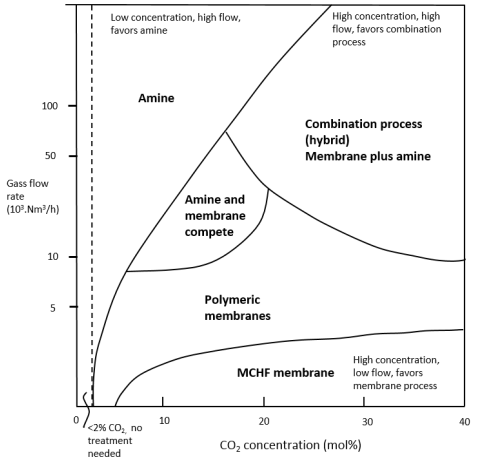

Figure 7.15: MCHF application region in "gas flow rate and CO_2 concentration diagram" adopted from Baker and Lokhandwala [4]

High CO_2 concentration and low flow favour carbon hollow fibers membrane processes. Stand-alone membrane systems are ideal for small distributed fields with small gas flows (< 20 million scfd / < 23,600 Nm^3/h). Membrane area is dictated by the percentage of acid gas removal rather than absolute acid gas removal, and small variations in feed acid gas content hardly change the sales-gas purity. In the case of MCHF, the membrane has high performance which keeps the membrane far into the selectivity driven region and the installed area is not much effected by CO_2 contents in the feed. Simulation data showed that installing a MCHF membrane area for 20% CO_2 contents can work for CO_2 range of 1-50% with less than 1% loss in both purity and recovery. Installing membrane area for equal or below 5% CO_2 contents brings it into the pressure ratio driven region and additional compression cost adds up, (pipeline purity and recovery) if actual CO_2 concentration increases in the line.

7.2.2. Paper – V: Vehicle fuel from biogas with carbon membranes; a comparison between simulation predictions and actual field demonstration (Green Energy & Environment (2018) 1-11)

This paper describes carbon membrane based biogas upgrading process and design of a multimodule membrane system (MMS). The results from biogas upgrading plant are discussed and compared with simulation resutls. The capital cost and running cost of the plant were also compared with simulated values. A pilot-scale separation plant based on carbon hollow fiber membranes for upgrading biogas to vehicle fuel quality was constructed and operated at the biogas plant, belonging to Glør IKS, Lillehammer, Norway by MemfoACT AS. Vehicle fuel quality according to Swedish legislation was successfully achieved in a single stage separation process. The first trial was run relatively quickly, using one MMS comprising of medium sized membrane modules of low permeance, and a feed flow rate of 4 Nm^3/hr was applied. The CO_2/CH_4 selectivity obtained in this run was quite low, and high permeance was recorded compared to the values estimated from individual module testing and MMS results at the production facility. Two reasons were considered: firstly, the trial was run for too short time, and it is unlikely that the permeate stabilizes so quickly, therefore, relatively low selectivity was obtained in the beginning. Stabilizing the permeate concentration for the low permeance modules may take days, due to long residence time on the permeate side of the MMS. Secondly, due to fiber breakage as carbon hollow fibers being self-supported hold relatively poor mechanical stability.

The plant was stopped, and MMS was opened to check the fiber breakage. Each medium-sized module was tested using air pressure and soap water to find the leakage in the modules. Many broken fibers were found which ultimately were manually clogged on site using epoxy "Loctite 3090". It was considered that vibration from compressor could break the fibers as many of the broken fibers were found close to the support legs of MMS where vibration effect was at maximum. Therefore, the membrane skid was dampened down to reduce the vibration amplitude and ultimately the broken fibers during operation.

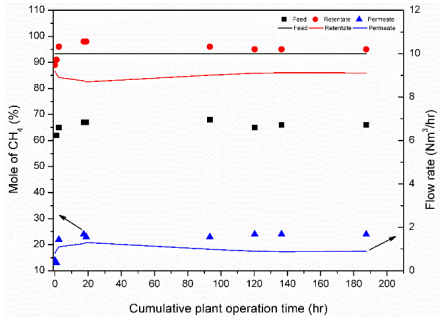

Figure 7.16: Carbon membrane separation process for biogas upgrading; Flow rates as "solid lines" and CH_4 contents as "dots" in the graph

These initial problems of fiber breakage were solved, and in the fourth test the pilot plant was run for eight days at stable conditions and measurements were done periodically both by an online infrared analyzer and a portable analyzer. The plant was working as expected by giving required vehicle fuel quality as shown in figure 7.16. The results in figure 7.16 show that CH_4 concentration in the feed, retentate and permeate streams and flow rate of each stream was almost constant during the cumulative test period of 192 hours. The concentration of CH_4 in the product stream was 96 mol% (CH_4 loss: 2 - 4%) throughout this time, and maximum selectivity for CO_2/CH_4 was measured 130**.** Thus, the feed pressure of 21 bar (against the 0.1 bar in permeate) the required methane purity (96%) and recovery (98%) of the product was achieved in a single stage process (estimated through simulations before installation). As already mentioned, the first three operations were not successful and very low selectivity was achieved due to the fiber breakage problem. This was however resolved, and the plant was working as expected by giving required quality vehicle fuel. The effective membrane area was significantly reduced due to the manual clogging process of broken fibers. The modules with a high number of damaged fibers were later replaced by the good performing modules. After

installation of the good modules, the membrane area that was lost due to clogging was only about 1-2% of the total installed membrane area.

To make an economically viable membrane separation process, both high permeability and high efficiency (selectivity) are needed. The total capital investment was quite close to the projected values based on simulations. The membrane cost was considered \$ 100/m^2 in the simulations based on knowledge from pilot-scale production at MemfoACT AS. The running cost was much lower (0.014 €/Nm^3 of biogas upgraded) than the polymeric membranes (0.05 €/Nm^3) reported in literature. However, the brittleness of hollow fibers remained a challenge and the total cost of the membrane was almost doubled when required membrane area was in operation at the biogas facility. Hence, the total capital investment and production cost increased because of that extra membrane area. The energy consumption by the compressor and vacuum pump, product (methane) purity, and methane recovery were very much comparable with the simulated results.

7.2.3. Paper – VII: Carbon membranes for oxygen enriched air – Part I: Synthesis, performance, and preventive regeneration (Separation and Purification Technology 204 (2018) 290-297)

Chemisorption of oxygen on the active sites of carbon layers limits the use of carbon membranes in air separation application. A novel online electrical regeneration method was successfully applied to prevent the active sites on carbon surface to be reacting with O_2 while the membrane was in operation. The rationale behind the study of preventive electrical regeneration (PER) was to add ohmic heating (Ohm's law) to desorb the molecules and prevent new adsorption. Electric potential is a very strong driving force compared to pressure. It was presumed that while introducing elecric current, the cross coupling of driving force and mass flow would enhance the membrane flux by reducing the adsorption of gas molecules on the pore edges. An online regeneration (DC: 44-55 µA, 10V) was tested to achieve a stable performance of CM in air separation application. In addition, thermal and chemical regeneration methods were also pursued to find an effective, simple, and economical solution to restore the membrane performance. The term "Preventive electrical regeneration" (PER) was used for the electric regeneration in this study. PER means a continuous supply of electrical potential during membrane operation to prohibit the molecules adsorbing on the membrane surface. In order to test the performance of carbon membranes for air separation, the impact of temperature on O_2 and N_2 permeability at constant pressure and feed flow rate is plotted in

figure 7.17. The results reported are from pure gas permeation experiments. He et al. [107] has performed the mixed gas experiments on the same type of CM (same protocol) and results indicated that the membrane performance is same or even higher in some cases for mixed gas as compared to single gas separation. Singh et al. [12] also confirmed that pure gas permeation properties were within 3% of mixed gas permeation properties for the pyrolyzed hollow fibers.

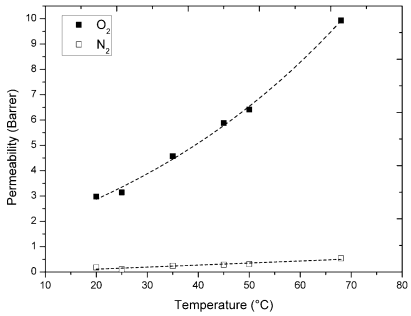

Figure 7.17: Effect of temperature on O_2 and N_2 permeability (P:5 bar)

The trend in figure 7.17 shows that O_2 permeability is increasing exponentially with increase in temperature which is also comparable with an Arrhenius law type effect. The high permeability is a result of high diffusivity and high solubility as well, and the increase in O_2 permeability here indicates a more open molecular matrix aiding O_2 flux. Whereas, change in N_2 permeability is quite modest with an increase in temperature. The carbon matrix is comprised of relatively large pores interconnected by constrictions of negligible thickness that approach the dimensions of diffusing molecules. In this case, penetrant molecules require characteristic activation energies to overcome the resistance at the constrictions. Hence, a small increase in activation energy in form of high temperature increased the activated diffusion of O_2 and N_2. Permeation experiments were performed at 20, 35, 45, 50 and 68 °C in order of increasing temperature.

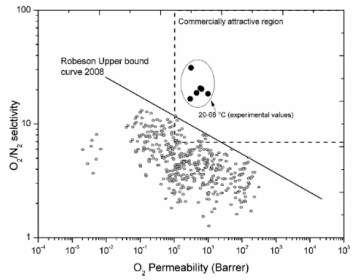

Figure 7.18: O_2 permeability and O_2/N_2 selectivity of CM with respect to Robeson upper bound curve (2008) [30]

Figure 7.18 presents the Robeson upper bound (2008) and as can be seen, the membrane performance for all experiments reported here, are in the commercially attractive region. Chemisorption sorption occurs only on active sites; therefore, it might be that the O_2 had already penetrated the micro and ultra pores of the carbon structure and occupied a large fraction of the active sites and formed covalently bounded O-bridges with the carbon. However, further blockage of pores occurred by physiosorption when H_2S, CO_2 and hexane molecules were present in WCG and adsorbed on the carbon surface. The strong aging may be explained by both a strong physiosorption of bigger molecules on the carbon surface and chemisorption in the matrix.

Flushing the module with propylene for 24 hours could partially (ca. 10%) restore the lost permeability for both O_2 and N_2, but selectivity decreased further. Propylene acted as a cleaning agent by removing adsorbed compounds from carbon surface and the exposure broadened the membrane pores, thus reducing the resistance to the transport of O_2 and N_2. Thermal treatment of the membrane at 80 °C for 24 hours could not regain the lost flux. Instead, the permeability values for both O_2 and N_2 decreased as shown in figure 7.19. It might be that all the reactive sites cleaned by propylene were occupied again by the adsorption O_2 which blocked the pores and ultimately decreased the permeability of both gases. The thermal limitations of the used epoxy in module construction prevented the use of elevated temperature in this study.

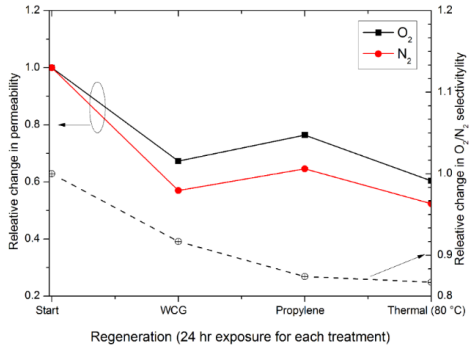

Figure 7.19: Relative change in permeability and selectivity of O_2/N_2 after chemical and thermal treatment

Electrical regeneration with 10V DC yielded a positive effect for the O_2 permeability when applied while membrane was in operation and being exposed to WCG, as shown in figure 7.20 (left).

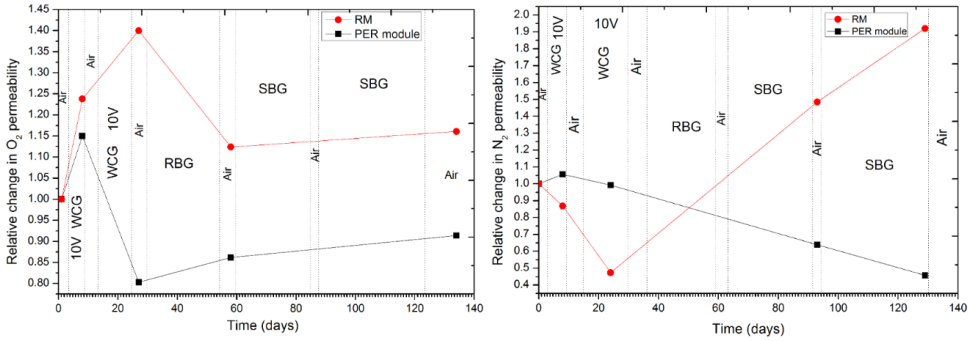

Figure 7.20: Aging of CM under different environments and effect of electrical regeneration on O_2 permeability (left) and N_2 permeability (right)

The O_2 permeability increased by 15% but the effect did not last long. Later, the membrane was stored in air for five days and the membrane lost some of the permeability. After repetition of the electrical regeneration along with WCG exposure did not gain the lost permeability but rather it declined and lost 20% of the initial value after exposed to WCG for 12 days. Almost similar effect was observed for N_2 with 5% increased permeability in the first attempt of electric regeneration, as shown in figure 7.20 (right). The effect of applied current was instantaneous, indicating that electrostatic repulsion was also active. Desorption or an instantaneous change would not result only by Ohmic heating. Therefore, some other factors could also be contributing in the results. One explanation for this opposite behavior of current could be that electro potential driving force and cross coupled mass transfer were influencing the flux through the membranes. Deconvolution of electric field effects and heating effects on permeation is a challenging task. Mixed gas tests with applied current will probably provide more insight to this problem. The N_2 permeability dropped in a continuous way after the first electrical regeneration till the end of the run (130 days) by losing 60% of the initial value.

Although, the lost performance was partially regained for O_2 after 10 days' exposure to RBG and remained steady for next 3 months. But the observed phenomenon is still unclear with respect to how the electric current desorbs the absorbed gases.

Regenerated cellulose-based carbon hollow fiber membranes produced at the pilot-scale plant demonstrated competitive air separation properties. Experimental results showed that elevated temperature operations increase O_2 permeability without significant loss in O_2/N_2 selectivity. The prepared CM had reasonable performance over a time span of about 5 months under harsh environments (air, H_2S, n-Hexane, CO_2, CH_4). Online preventive electrical regeneration (PER) enhanced the O_2 permeability by eliminating the aging effect on the membrane and the O_2/N_2

selectivity was also increased. However, it is important to note that aging behavior of CM may depend on the precursor and the manufacturing conditions used. Carbon membranes with e.g. different structure and surface chemistry will behave differently as also shown by other researchers.

7.3. Simulations and cost estimation

This final subsection culminates in two simulation-based papers, paper-VI and paper-VIII, that consider cost analysis and sensitivity analysis in CO_2-CH_4 and air separation processes while using carbon hollow fiber membranes, respectively. Paper-VI discusses the results from membrane simulations which compare carbon membranes, modified carbon membranes (after CVD), and polyimide membranes in biogas application. Paper-VIII discusses different compression approaches to achieve oxygen enriched air. That paper also describes an efficient way to obtain oxygen enriched air with low capital investment and running cost while using carbon membranes. Single gas properties were used in all simulations.

7.3.1. Paper – VI: Techno-economical evaluation of membrane-based biogas upgrading system; a comparison between polymeric membrane and carbon membrane technology (Green Energy & Environment 1(3) (2016) 222-234)

This simulation investigations were directed towards finding the efficient membrane-based process for biogas upgrading to vehicle fuel. A carbon hollow fiber (CHF) membrane, modified carbon hollow fiber (MCHF) membrane, and a commercially available polymeric membrane (polyimide) were compared through economical assessment. Single, two, and three stage membrane configurations with and without recycle stream were investigated to achieve 97.5% CH_4 purity and 99.5% CH_4 recovery.

Table 7.2: Gas permeation properties used in the simulations

Membrane Type	Permeability, (Barrer)			Single gas selectivity		Reference
	CO_2	CH_4	N_2	CO_2/CH_4	CO_2/N_2	
Polyimide hollow fiber	21.47	0.62	0.69	34	31	[139]
CHF	40	0.45	1.32	90	30	MemfoACT AS
PORCHF	154	0.63	1.9	245	81	MemfoACT AS
Benchmarking Polymeric membrane	102	1.02	3	100	34	See text

[Assumed selectivity wall thickness of polyimide 01 μm and 20 μm for rest of the membranes]
(1 Barrer =2.736E−09 m^3(STP)m/(m^2 bar h))

A benchmarking polymeric membrane was considered for comparison, as a future biogas upgrading membrane with a 1 μm thick selective layer, having a permeability of 100 barrer and a selectivity of 100 for CO_2/CH_4, which is above Robeson upper bond 2008. Gas permeation properties of CHF and PORCHF with other membranes used in the simulation of this work, are shown in table 7.2.

A water-saturated biogas stream of 300 Nm^3/h with 3000 ppm of H_2S was considered as a base-case. Biogas enters into biological H_2S remover for bulk removal down to between 50-100 ppm and passes further through activated charcoal, where H_2S is taken down to below 1 ppm. The refrigeration process followed by zeolite molecular sieve was used to remove water from biogas in order to achieve a dew point of -10°C at 200 bar.

Biogas was compressed to required feed pressure (6, 8, 10 bars) and then filtered to remove dust and oil droplets before entering the membranes. Biogas was fed to the membrane and the resulting biomethane was compressed up to 250 bar before it is stored for further usage as a vehicle fuel.

Simulations results showed that polyimide membrane requires lowest membrane area to achieve desired purity and recovery of CH_4 while using a three stage membrane process at 10 bar feed pressure. However, PORCHF needs lowest energy to achieve the desired results in a two stage process when recycle stream is used.

Operating cost of a biogas upgrading process depends largely on the compressor duty, and the recycle ratio (recycle/feed) higher than 1 can increase this compression energy requirement to a higher level. Results obtained by the simulation of different membranes with two and three stage configurations are plotted in figure 7.21 and figure 7.22. The figure 7.21(A), demonstrates the recycle ratio at 6 bar feed pressure, which is seven for the two-stage polyimide membrane system and it would result in high operating cost; in the form of compression energy and also, a compressor with high capacity is required to treat the total volume of the gas which would increase capital cost as well. Whereas, the recycle ratio is below one (figure 7.21 (A)) for PORCHF membrane system and the compression duty required for this system is one fourth of the amount required for two stage polyimide system as shown in figure 7.22 (A). The efficiency of a membrane system increases with high selectivity as it can be seen from the recycle ratio and specific duty plots. The data showed that PORCHF having highest selectivity gives lowest recycle ratio and the required specific duty values. It was observed that the recycle ratio decreases in CHF and PORCHF membranes unlike polyimide membranes with high CO_2 present in the feed. It is very important to choose an optimal point where capital investment and running cost are low and the system is efficient at the same time.

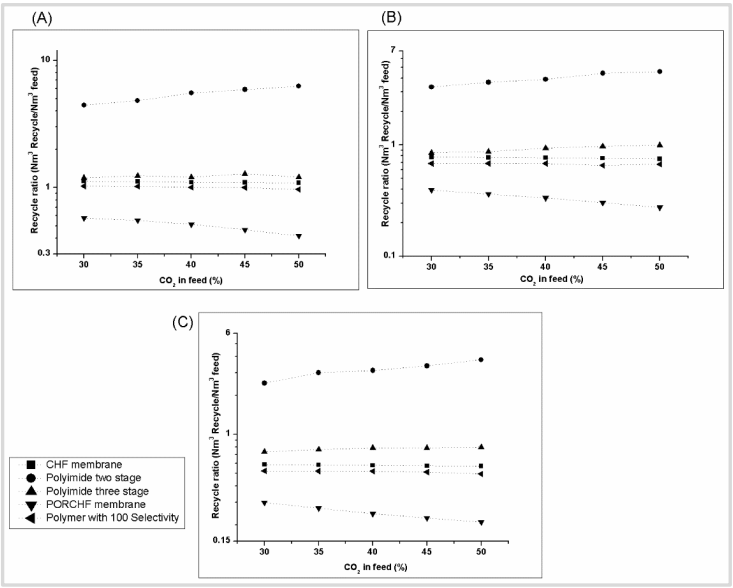

Figure 7.21: Recycle ratio at different CO_2 loadings in feed at 23 ^oC, (A) at 6 bar, (B) at 8 bar, (C) at 10 bar

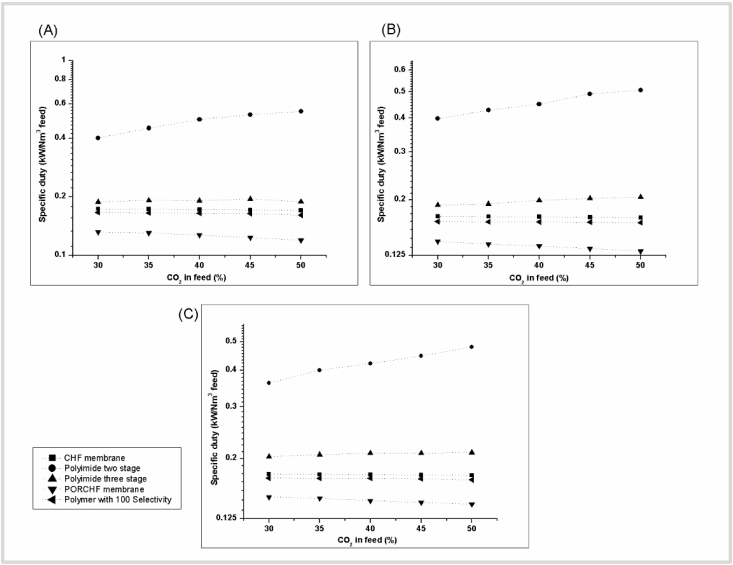

Figure 7.22: Specific Compression duty at different CO_2 loadings in feed at 23 ^oC, (A) at 6 bar, (B) at 8 bar, (C) at 10 bar

The increasing of feed pressure to 8 bar results in lower recycle ratio and energy demand. However, for two stage polyimide membranes, recycle ratio is still quite high especially when 50% CO_2 is present in the feed as shown in figure 7.21 (B). The figure 7.22 (B) indicates that the specific duty required is still four times higher for the polyimide membrane system as

compared to PORCHF system. Plasticization effect inhibits polyimide membrane to go to high pressures [140], so maximum pressure tested for polyimide membrane systems was 10 bar in this section of work, which shows high recycle ratio in two-stage configuration as shown in figure 7.21 (C). The three-stage system with polyimide shows recycle ratio about 1 for 8 bar and 10 bar simulations, and the specific energy demand for three stage polyimide was double as compare to PORCHF membrane system.

A sensitivity analysis showed that assuming an optimized process producing PORCHF at a price of \$ 60/m^2 instead of \$ 100/m^2 and a membrane lifetime of 7.5 years instead of 5 will give NPV for PORCHF of \$ 8.8M while using 50 bar feed pressure in a two-stage membrane system with recycle stream. However, applying 70 bar feed pressure can increase NPV for PORCHF over \$ 9M which is comparable with a three-stage polyimide-based system that is operating at 20 bar feed pressure as shown in figure 7.23.

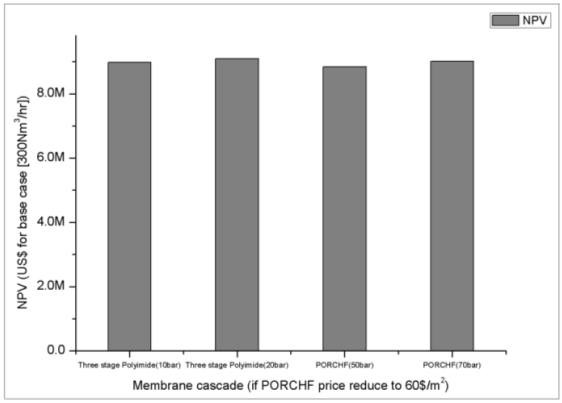

Figure 7.23: NPV comparison of three stage polyimide and PORCHF membrane

7.3.2. Paper – VIII: Carbon membranes for oxygen enriched air –Part II: Techno-economic analysis (Separation and Purification Technology 205 (2018) 251-262)

After getting good results of membrane performance for air separation and online electrical regeneration in paper-VII, this paper-VIII (second part of paper-VII) discusses the optimal conditions to obtain equivalent pure oxygen (EPO_2) at lowest cost. Experimental data and a set of predictive values were simulated to find the most efficient way of achieving EPO_2 in below \$ 100 for small scale plants (1-10 tons/day). Three different approaches with respect to pressure were investigated; (1) feed compression (FC), (2) vacuum on permeate side (VP) and (3) combination of (1) and (2)- (FC-VP). Simulation results indicated that these carbon membranes may produce 78% O_2-enriched permeate stream and at the same time obtain 15% O_2 (hypoxic)

retentate stream in a single-stage process when using combination of feed compression and vacuum on permeate side (FC-VP) as shown in figure 7.24. Although retentate stream usage was not considered in the economic calculations, the retentate stream may be used as hypoxic air (Air containing 15 vol% O_2 is named as hypoxic air, and over the last years use of the hypoxic air has increased in venting system to reduce the fire hazards. Further, in multifunctional buildings, electrical appliance rooms and computer rooms use of hypoxic air have been found to be essential to societal important functions [141].

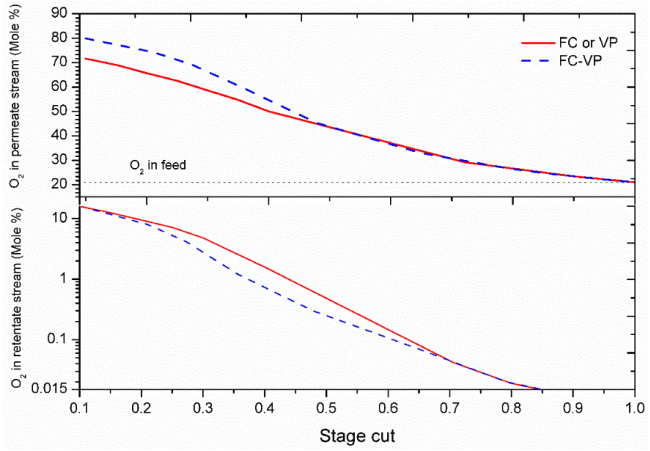

Figure 7.24: Mole-fraction of O_2 in permeate and retentate streams as function of stage cut in a single stage separation process (O_2/N_2 selectivity: 18)

Figure 7.25 presents the energy requirement while using different compression approaches. As can be seen FC and FC-VP approaches offer maximum energy requirement at lowest stage cut. However, the energy demand reduces up to 50% at stage cut of 0.25. The FC-VP approach offers high energy requirement because a direct feed gas (air) compression require a higher energy and in this context, using vacuum pump at the same time will need even more power as shown in figure 7.25. At the contrary, lowest energy requirement of vacuum pumping in VP approach results from the fact that the permeate flow only has to be pumped. The VP approach is an energy efficient process compared to FC, FC-VP, and cryogenic distillation.

The simulation results indicated that although the membrane performance (experimental data) is within the commercially attractive region of Robeson plot as previously shown in figure 7.18, and FC-VP approach has lowest production cost $ 644/ton of EPO_2, the price is nevertheless very high compared to other technologies. Increase in O_2 permeability to some

extent would scale down the effect of membrane price on FC-VP approach since the membrane area is optimized for the required production rate.

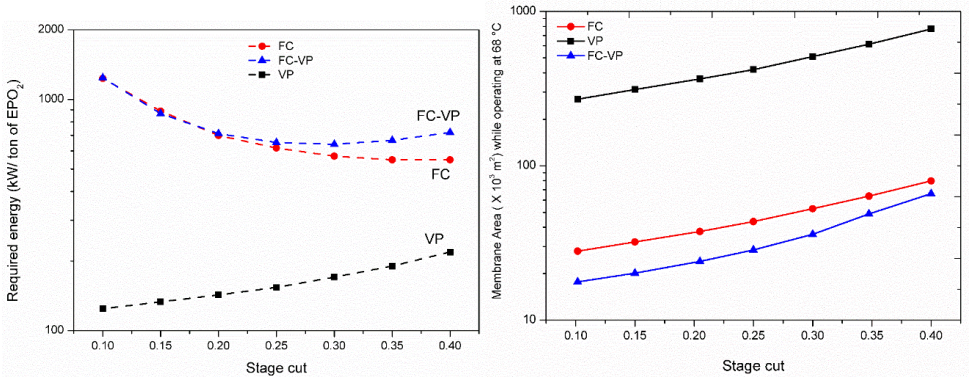

Figure 7.25: Required energy to produce 1 ton of EPO_2 as a function of stage cut while using different compression approaches (Energy for cryogenic unit: 285 kW/ton of 99.6% O_2 [120]), Required membrane area (O_2 permeability: 10 Barrer)

As discussed earlier in Paper-VII, the O_2 permeability and selectivity of O_2/N_2 are very much dependent on operating temperature. Thus, higher temperature offers high O_2 permeability with sufficient O_2/N_2 selectivity to keep the membrane in the commercially attractive region. Operating membrane at 205 °C gives O_2 permeability of 300 Barrer with O_2/N_2 selectivity of 18 in comparison to operation at 190 °C which offers O_2 permeability of 200 Barrer with O_2/N_2 selectivity of 18 (according to Arrhenius model extrapolation of experimental data). Elevated temperature operations are costly, so the extra energy cost adds up to the TCI and PC per ton of EPO_2. The adiabatic heating of the compressor can be utilized to increase the gas temperature for achieving higher flux. Depending on compressor type, the actual compression may heat the gas significantly to increase the temperature to well beyond 100 °C. In addition, the separation operated at elevated temperature may act as regeneration by removing physically adsorbed gases and eliminating the water aging effe on the carbon membranes. However, a good sealing/potting material for module construction is challenging to develop when operating at temperatures higher than 150 °C.

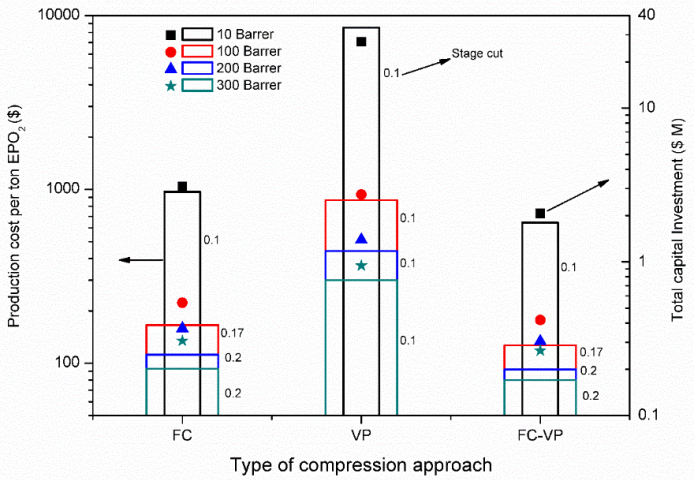

Figure 7.26: Lowest PC and TCI for different compression approaches at optimal stage cut value

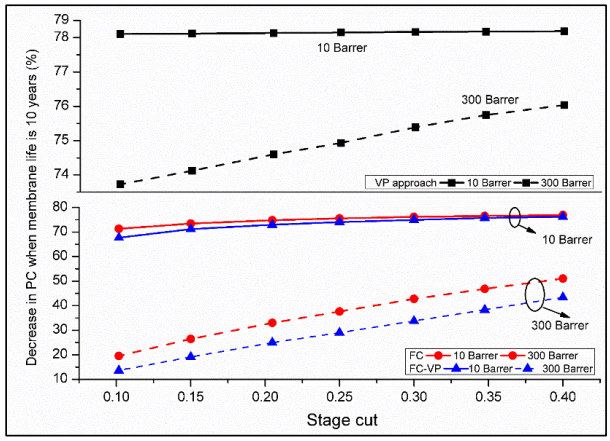

Figure 7.27: Effect of CM life time on PC of EPO_2 for different compression approaches (CM cost: $\$100/m^2$

The plots in figure 7.26 demonstrate the lowest production cost (PC) per ton of EPO_2 (bar chart) and total capital investment (TCI) (scatter plot) for different compression approaches at optimal stage cut and different predicted permeability values. Results show that FC-VP approach is the most efficient approach to produce EPO_2 economically for the CM discussed here. This approach can produce a ton of EPO_2 below $ 100 if the membrane permeability is 200 Barrer and O_2/N_2 selectivity of 18, and this performance can be accomplished either operating the membrane at 190 °C or adding nano particles to the precursor.

Sensitivity Analysis was used to identify components that are most sensitive to achieve economically suitable results. This section presents the results of simulation analysis in which

impact of different variables on TCI and PC per ton of EPO_2 is investigated and discussed. The parameters investigated here are membrane cost, membrane life time, and operating temperature which directly is related to the permeability of the membrane. Figure 7.27 presents the percent decrease in PC/ ton of EPO_2 when CM life time is increased to 10 years. The results show that production cost is significantly affected by the membrane life time while using VP approach. The production cost can be reduced 73-78% by doubling the membrane life and keeping the cost \$100 per m^2. The membrane life is considered 5 years in this study due to the challenges with mechanical properties of carbon membranes. FC and FC-VP approaches are also affected by membrane life, but the effect decreases exponentially with increase in permeability up to 300 Barrer. This effect is almost negligible at 400 Barrer as the membrane area seems fully optimized towards the production rate of EPO_2. However, in case of VP approach, the membrane area optimizes towards the production rate of EPO_2 when O_2 permeability is above 1000 Barrer.

Table 7.3 illustrates the sensitivity of the separation process to the membrane cost, membrane life and operating temperature which is directly related to the permeability of the membrane. VP approach is greatly affected by the membrane cost, for example the PC and TCI for this approach reduces 27 times for permeability of 300 compared to 10 by cutting the membrane cost to half. Similar trend is observed for the PC/ton of EPO_2 when membrane life is 10 years while using VP approach. However, the TCI would remain quite high due to membrane cost of \$ 100/m^2.

That is why even the PC is decreased to \$ 80 / ton EPO_2, but the TCI is about \$ 0.95 million which is not feasible. The sensitivity of FC and FC-VP approaches towards membrane cost is higher between permeability of 10-100 and beyond that the effect is very small (< 10%). If the carbon membrane production process is fully optimized in future and price is reduced to \$ 50 per m^2 then PC per ton of EPO_2 can be cut to \$ 67 which presently is \$ 80 while operating at 300 Barrer.

Even though CM is almost five times more expensive than polymeric membranes, the high performance (selectivity) and tolerance to elevated temperatures CM is a potential candidate in production of OEA and or high purity (99.5%) N_2 in a single stage process. The simulation study indicated that CM process for OEA have the best potential of becoming economically competitive with conventional technologies for small plant capacities (1-10 tons/day) and a high degrees of oxygen enrichment, 50-78 mole% O_2. To be fully competitive with cryogenic distillation and PSA, the membrane cost needs to be reduced and mechanical strength of CM should be increased to maximize the life time of membrane.

Table 7.3: Sensitivity of the process towards membrane life and membrane cost (optimal stage cut for each compression)

Compression approach	Permeability (Barrer)	Membrane life (10 years, cost: $100/m^2)		Membrane Cost ($ 50/m^2)		Stage cut
FC		PC	TCI	PC	TCI	
	10	$ 270	$ 3,000,000	$ 530	$ 1,600,000	0.1
	100	$ 87	$ 540,000	$ 120	$ 380,000	0.15
	200	$ 66	$ 360,000	$ 83	$ 270,000	0.2
	300	$ 63	$ 300,000	$73	$ 240,000	0.2
VP						
	10	$ 1,800	$ 27,000,000	$ 4,200	$ 13,000,000	0.1
	100	$ 200	$ 2,700,000	$ 440	$ 1,300,000	0.1
	200	$ 110	$ 1,300,000	$ 230	$ 710,000	0.1
	300	$ 80	$ 940,000	$ 160	$ 490,000	0.1
FC-VP						
	10	$ 200	$ 2,000,000	$ 370	$ 2,000,000	0.1
	100	$ 77	$ 400,000	$ 95	$ 310,000	0.15
	200	$ 62	$ 300,000	$ 73	$ 240,000	0.2
	300	$ 60	$ 260,000	$ 67	$ 220,000	0.2

(1 Barrer =2.736E−09 m^3(STP)m/(m^2 bar h))

8. Conclusions

This chapter concludes the results obtained from pilot scale production and testing of prepared carbon membranes.

8.1. Precursor preparation

- Asymmetric CA hollow fibers were spun on pilot scale plant using a dry/wet spinning process and the effect of DMSO and NMP as solvents in dope solution was studied. It was found that fibers spun with CA in DMSO contain macrovoids in the wall. However, the fibers spun with CA in NMP gave high quality carbon fibers with promising (above Robeson upper bound 2008) gas permeation properties. The influence of DMSO and NMP as bore solvent on gas permeation properties was also studied. It was found that increase in concentration of DMSO improve the CO_2 permeability in resulting carbon membranes, but maximum value measured was 25 Barrer at 95% DMSO in bore fluid. Whereas membranes spun with bore solution containing 65 and 70% of NMP showed CO_2 permeability of 256 Barrer and 144 Barrer with CO_2/CH_4 selectivity of 156 and 172 respectively.
- Pre-treatment process like water wash for solvent removal was optimized by using perforated plates during spinning (fiber take-up) process.
- Deacetylation of CA hollow fibers is the most critical step in preparation of precursor hollow fibers. Optimized deacetylation of spun-CA hollow fibers (CAHF) was achieved by using 90 vol% 0.075 M NaOH aqueous solution diluted with 10 vol% Isopropanol for 2.5 hours at ambient temperature.
- Drying conditions (temperature, relative humidity, rate of drying, stretch in fiber during drying) were optimized to achieve maximum (> 95%) number of successful good cellulose fibers. Separation performance results showed that RH changing from 80% to 35% at room temperature overnight gave maximum separation (above Robeson upper bound 2008) performance for the subsequent carbon hollow fibers.

8.2. Carbonization

- The carbonization temperature is the important parameter when preparing the carbon membranes for different applications from regenerated cellulose precursor. It was found that 650 °C under N_2 environment is the optimal temperature for CM with good

CO_2-CH_4 separation properties. However, 550 °C under N_2 environment was found to be optimal for prepartion of CM with good air separation properties.

- Number of fused fibers were significantly reduced by tilting the furnace with a 3-6 degree angle and replacing the quartz tubes with perforated trays of stainless steel.
- Brittleness of the fibers remained a problem for all carbonization batches. It was found that partial/non-optimal deacetylation process caused the brittleness of the fibers.
- It was concluded that a relatively low-cost precursor material (regenerated cellulose) can obtain over 90% successful carbon fibers which would then make the pilot production more economically attractive.

8.3. Carbon membrane performance

- Carbon membranes prepared from regenerated cellulose showed high perfromance for CO_2-CH_4 separation. CM can be used for biogas upgrading to vehicle fuel (separating CO_2 from CH_4) and are able to achieve 97% CH_4 purity and 98% CH_4 recovery in a single stage process.
- CM showed stable performance when tested for single gases (CO_2, N_2) at high pressure (70 bar) and 25 °C. However, CO_2 permeability was lost by 50% at 120 °C (5 bar pressure) compared to the value at 25 °C. In contrast, the effect of temperature on N_2 permeability was very low and above 45 °C (5 bar pressure), the N_2 permeability was almost constant.
- CVD process can be used to enhance (by modifying the pore size) the CO_2 permeability a thousand times by keeping the CO_2/CH_4 selectivity same or even higher compared to prior CVD.
- Increasing the operating temperature increases O_2 permeability exponentially without significant loss in O_2/N_2 selectivity. Online preventive electrical regeneration (PER) enhance the O_2 permeability by eliminating the aging effect on the membrane and the O_2/N_2 selectivity was thus also increased.

8.4. Aging and regeneration of carbon membranes

- Membranes stored in lab condition and CO_2 atmosphere lost the CO_2 permeability by more than 80% within the first 30 days. CHF stored in ABS tube under vacuum were stable after losing 65% CO_2 permeability in one month, and fibers lost their permeability very fast when stored in air at low temperature (4 °C).

- Dynamic aging, defined as "aging under controlled environment and continuous gas flow through the membrane", had a promising regenerative effect on the membranes to recover some permeability. The fibers which underwent dynamic aging were not susceptible to static aging anymore, and showed the same performance even after 128 days when stored in the laboratory environment.
- Most of the modules (area of each module: 0.5-2 m^2) installed at biogas plant lost 40% CO_2 permeability within a few days after installation and were stable afterwards. CHF were mechanically stable at 20 bar in real industrial conditions.
- Membranes installed at high H_2S (150-2400 ppm) concentration lost CO_2 permeability by up to 65% in 125 days, and 55% of this lost permeability was regenerated by exposing membrane to a biogas field with low H_2S (< 5 ppm) concentration for 100 days which was stable for the next 50 days at high concentration of H_2S.
- Online electrical regeneration method was effective to keep stable permeabilities of the membrane for different single gas separation experiments; O_2, N_2, CO_2.
- Chemical (propylene) treatment and thermal (80 °C) regeneration methods were not very effective to regain the lost permeabilities of gases when tested for single gases; O_2, N_2, CO_2.

8.5. Simulations and cost estimation

- A single stage process with carbon membranes can upgrade biogas to vehicle fuel with 98% CH_4 recovery. The running cost with carbon membranes is much lower ($ 0.016/Nm^3 of biogas upgraded) than the polymeric membranes ($ 0.06/Nm^3 of biogas upgraded) reported in literature.
- Simulation results indicated that CH_4 recovery of 99.2% can be achieved in a single stage with CM based system when 5% CO_2 is present in the natural gas feed at 70 bar.
- In air separation application, carbon membranes may produce 78% O_2-enriched permeate stream and at the same time obtain 15% O_2 (hypoxic) retentate stream in a single-stage process when using combination of feed compression and vacuum on permeate side.
- To be fully competitive with cryogenic distillation and PSA in air separation market, the membrane cost needs to be reduced and mechanical strength of CM should be increased to maximize the life time of membrane.

9. Challenges and Recommendations for Future work

Carbon membrane technology has been the focus of this research and development. Although CM still require improvement before they can become dominant commercialized membranes, they have a great potential as a replacement for other membranes in the market. This is because they have many useful characteristics and can efficiently separate gas mixtures that have molecules of similar sizes. However, there are only a few manufacturers involved in the production of carbon membranes, and this is because greater costs are involved in producing and making carbon membrane modules. Nevertheless, more research work is needed to produce carbon membranes at a lower price.

This chapter describes the challenges that need consideration when using cellulose acetate to produce carbon hollow fiber membranes. A few recommendations based on pilot scale production experience are also made for future investigative work. It should be noted that these recommendations are more valid when using CA as a precursor for producing carbon membranes. However, using cellulose as a precursor may avoid the pre-treatment steps and the most critical step of deacetylation.

9.1. Spinning

It is best to remove the solvent quickly, to avoid aging of the fiber. Hence, higher temperature in the coagulation bath should be tested.

9.2. Fiber take-up and water wash

There is a trade-off between how long the fiber stays on the wheel and production efficiency (aging by bore solution as the fiber can collapse if bore solution is not washed quickly). This may determine the diameter of the wheel, the number of fiber layers on the wheel, or the take-up speed. Clamping on the fiber ends should be adjusted to see effect of closed vs. open bores (solvent removal), alternatively having clamp in one end only. To remove solvent more efficiently, different methods are thus proposed: heat, air bubbling, pumping and stirring. A handling tube may also improve the mass transfer (described in the section below). The amount of residual solvent in the fiber should be measured analytically to optimize the process operating conditions and determine the trends.

9.3. A handling-tube

To reduce handling of fibers and increase mass transfer for solvent removal, it is might be advantageous to evolve from flat fiber carriers ("guitars" in this study) into a handling tube. From a manufacturing point of view, tube processing is easy to scale up and automate. For improved mass transfer, it is important to have well distributed flow (avoid channeling) and preferably cross-flow instead of parallel flow. To distribute the flow in the tube, there are two potential designs. For the first design, the tube should be vertical with feed at bottom and an exit of the feed at the top on opposite side of the tube. For the second design, the tube should be horizontal with feed through a perforated plate at the bottom and exit on top of other end of the tube. Both processes can be formed in a stationary rig, connected to different fluids. The handling tube does not necessarily have to be a circular cross-section tube; it may also be a rectangular or squared cross-section channel. Any given step should be run at maximum temperature to speed up the mass transfer coefficients. A schematic diagram of such handling tube is shown in figure 9.1.

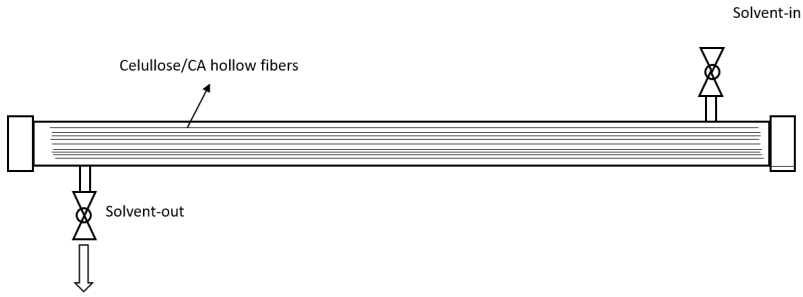

Figure 9.1: A handling tube for solvent exchange process

9.4. Glycerol wash

In this study, fibers were soaked overnight in 7.5% glycerol solution to preserve the bigger pores and bore of the fibers from collapsing. To absorb the desired amount of glycerol more quickly, the same measures as for water wash are proposed should be tested. More experiment should be performed to see if the glycerol is necessary (if water wash is sufficient to remove all solvent then permeation properties may be adjusted in carbonization step). The amount of glycerol adsorbed in the fibers can be determined to help optimization.

9.5. Deacetylation

Currently, deacetylation is the most critical step in preparation of precursor fibers from CA. The rate of deacetylation depends on the diffusion velocity of OH^- ions inside the CA hollow fiber matrix and substitution reaction rate with an acetyl group. Optimal deacetylation is somewhere between partial decetylation and full deacetylation. Due to the high sensitivity of the process, the attempts to lead an optimal deacetylation (instead of full) may deteriorate a uniformity and repeatability in cellulose fibers properties. There are too many parameters starting from non-uniformity of the initial cellulose acetate, external parameters as temperature, mixing conditions etc. which may change from batch to batch or even within the same batch. This uncertainty leads to somewhat uncontrolable final chemical composition. To improve mass transfer and homogenous treatment of all fibers, pumping and shaking/rolling is proposed.

9.6. After wash

Glucose wash was necessary to provide fiber stiffness and minimize curling after drying. The glucose should preferably be avoided due to stickiness. It may be substituted by a surfactant. It is however challenging to find a suitable surfactant. Some candidates are alcohols of different chain lengths and short chain polymers, e.g. PEG, PVP. Alternatively, several washing steps may be used, e.g. pure water, sugar solution, and finally surfactant solution. Another alternative for increasing the stiffness of the fiber is to crosslink the cellulose by a difunctional acid. Then reaction time, concentration of reactants, and temperature should be optimized.

9.7. Drying

Dry fibers give a first insight to how uniformly the fibers are processed (fiber color, length, shape etc.). Curly fibers may be caused by:

- Bending at corners of take-up wheel
- Inconsistent solvent removal (bores opened to different extents)
- Asymmetric cross-section of spun fiber (geometric difference, porosity gradient, PVP gradient)
- Strain in fiber due to loss of mass in deacetylation process
- Non-homogenous/incomplete deacetylation
- Hydrophilic surface (bound water may cause chain to slip)
- Too fast drying (improvements by lower temperature and higher relative humidity)

The following improvements are suggested:

- Determine drying time by weight or dew point measurements
- Controlled air flow, temperature, and RH inside the drying chamber
- The optimum chain mobility before drying should be determined. This may depend on e.g. the amount of glycerol or solvent left in the fiber. It has been observed that fibers dried at RH 20-30% at room temperature were curlier than the fibers dried at RH 80-40%. Controlling humidity seemed to be the most important parameter during drying process.

Each process step should be more accurately determined. This means optimization of concentration, time, temperature, and mechanical properties by making trend curves. Knowing the necessary tension on the fibers is important for fiber properties, and especially if the production line is developed towards continuous line in the future.

9.8. Carbonization

Although the successful fibers were above 95% in some batches, the reproducibility for all batches is challenging. The fibers on the bottom of the bundle were fused and had D-shaped or oval cross-section instead of circular. Brittleness of fibers remained a challenge due to non-homogenous/non-optimal deacetylation of the hollow fibers. Following recommendations are suggested:

- A perforated rotating fiber chamber inside the furnace may reduce the fused fibers by removing the tar with more consistency.
- A vertical furnace should prevent the D-shaped/oval shaped cross-section of the carbon bundle. However, in vertical furnace, challenges may be temperature profile, gas flow (chimney effect) and keeping glass tubes or perforated grids in place.
- Purge gas flow pattern inside the furnace should be determined.
- Factors that may improve the mechanical properties of carbon fibers should be considered, e.g. rough handling during shipping and installation/operation. To some extent one potential cure could be adding HCl gas during carbonization. However, due to toxicity of HCl, this method was never tested at MemfoACT AS facility.
- CA was used in this study because it is soluble in common solvents like NMP (N-methyl-2-pyrrolidone),DMSO (dimethylsulfoxide) and acetone. Some environmentally

friendly solvent should be explored to spin Cellulose directly to avoid the deacetylation step. (I.e. Ionic Liquids).

9.9. Module making

The final carbon fibers should not be perfectly straight, but preferably having waves (i.e. wavelength > 10 cm) to i) improve the flow patterns in the module and ii) to have the ability to handle thermal expansion or shrinkage without breakage. The module efficieny of bigger modules (2000-5000 fibers) can be expected to be up to 95% compared to a small test module of 2-4 fibers. The packing density should be increased. For potting, the following improvements are suggested:

- Heating high viscosity epoxy for better filling between the fibers
- Currently curing time is very long therefore, finding right curing temperature (cross-linking is important to avoid swelling by CO_2)
- Avoid vapor sorption on carbon; quicker cure to reduce exposure time and to lower the sorption ability. However, it is less of a problem if post oxidation and CVD I performed on the module as these processes will burn the adsorbed vapors.

9.10. Multi-module system (MMS) and biogas upgrading experience

Although the carbon membrane pilot plant successfully obtained the vehicle fuel, there are still challenges that need consideration. The manually sorted and randomly packed hollow fibers of carbon membranes had lower mass transfer-coefficients than those for regular dense packings (polymeric hollow fibers). Flow through the randomly packed hollow fiber bundle could be highly non-uniform. Membrane effective area was very much reduced due to selective and manual clogging. Furthermore, regions, where fibers come in close contact, may create sections of high pressure drop. The gas velocity through these regions is much lower than the velocities in the regions where fiber spacing is larger, yielding higher mass transfer coefficient in these regions. On the other hand, in high velocity regions, there are increased chances of fiber breakage if any weak point occurs on the fiber surface. It may result in flow-channels formation and hence, bypassing effect which would result in selectivity loss. The MMS design for 24 medium size modules was not most efficient in this development phase of the operation. It could have been easier with individual module housing instead of MMS housing in order to isolate and treat the modules with bad performance separately. The process of dismantling the

MMS to take out the medium sized module, finding and clogging of the broken fibers, and again assembling the MMS increased the probability of fiber breakage in neighboring modules inside MMS and the entire process was time consuming as well. The shell-side feed configuration might have damaged the fibers due to high pressure feed flow. Bore-side feed configuration might have been more efficient in the MMS system. However, the biggest challenges with bore flow is fiber rupture. It is not easy to do online clogging of the broken fibers, and at least double work is needed for opening the ends and quality assure the modules. The membrane production cost at semi-industrial production plant was about 80 €/m^2, but due to a decrease in membrane effective area, the membrane cost doubled for the biogas pilot plant, which ultimately increased the total capital investment and production cost of the plant. The mentioned problems must be solved before a successful hollow fiber membrane module sees the market.

References

[1] British petroleum, BP Stastical Review of World Energy, 2017. https://www.bp.com/content/dam/bp/en/corporate/pdf/energy-economics/statistical-review-2017/bp-statistical-review-of-world-energy-2017-full-report.pdf. (Accessed: 29.09 2017).

[2] G. Sweeney, Predicted rise in global energy demand, 2013. http://www.zeroemissionsplatform.eu/extranet-library/publication/226-zepop-ed.html. (Accessed 23.05 2018).

[3] P. Nugent, Y. Belmabkhout, S.D. Burd, A.J. Cairns, R. Luebke, K. Forrest, T. Pham, S. Ma, B. Space, L. Wojtas, M. Eddaoudi, M.J. Zaworotko, Porous materials with optimal adsorption thermodynamics and kinetics for CO2 separation, Nature 495 (2013) 80.

[4] R.W. Baker, K. Lokhandwala, Natural gas processing with membranes: An overview, Ind Eng Chem Res 47(7) (2008) 2109-2121.

[5] R. Baker, Future directions of membrane gas-separation technology, Membrane Technology 2001(138) (2001) 5-10.

[6] R.W. Baker, Future Directions of Membrane Gas Separation Technology, Ind Eng Chem Res 41(6) (2002) 1393-1411.

[7] R. Ash, R.W. Baker, R.M. Barrer, Sorption and surface flow in graphitized carbon membranes - I. The steady state, Proceedings of the Royal Society of London. Series A. Mathematical and Physical Sciences 299(1459) (1967) 434-454.

[8] R. Ash, R.M. Barrer, R.T. Lowson, Transport of single gases and of binary gas mixtures in a microporous carbon membrane, Journal of the Chemical Society, Faraday Transactions 1: Physical Chemistry in Condensed Phases 69(0) (1973) 2166-2178.

[9] J.E. Koresh, A. Sofer, Molecular Sieve Carbon Permselective Membrane. Part I. Presentation of a New Device for Gas Mixture Separation, Separation Science and Technology 18(8) (1983) 723-734.

[10] N. Tanihara, H. Shimazaki, Y. Hirayama, S. Nakanishi, T. Yoshinaga, Y. Kusuki, Gas permeation properties of asymmetric carbon hollow fiber membranes prepared from asymmetric polyimide hollow fiber, Journal of Membrane Science 160(2) (1999) 179-186.

[11] A.B. Fuertes, T.A. Centeno, Carbon molecular sieve membranes from polyetherimide, Microporous and Mesoporous Materials 26(1–3) (1998) 23-26.

[12] A. Singh-Ghosal, W.J. Koros, Air separation properties of flat sheet homogeneous pyrolytic carbon membranes, Journal of Membrane Science 174(2) (2000) 177-188.

[13] D.Q. Vu, W.J. Koros, S.J. Miller, High Pressure CO2/CH4 Separation Using Carbon Molecular Sieve Hollow Fiber Membranes, Ind Eng Chem Res 41(3) (2002) 367-380.

[14] A.B. Fuertes, T.A. Centeno, Preparation of supported asymmetric carbon molecular sieve membranes, Journal of Membrane Science 144(1–2) (1998) 105-111.

[15] M.G. Sedigh, L. Xu, T.T. Tsotsis, M. Sahimi, Transport and Morphological Characteristics of Polyetherimide-Based Carbon Molecular Sieve Membranes, Ind Eng Chem Res 38(9) (1999) 3367-3380.

[16] T.A. Centeno, A.B. Fuertes, Carbon molecular sieve membranes derived from a phenolic resin supported on porous ceramic tubes, Separation and Purification Technology 25(1) (2001) 379-384.

[17] A.B. Fuertes, Effect of air oxidation on gas separation properties of adsorption-selective carbon membranes, Carbon 39(5) (2001) 697-706.

[18] T.A. Centeno, J.L. Vilas, A.B. Fuertes, Effects of phenolic resin pyrolysis conditions on carbon membrane performance for gas separation, Journal of Membrane Science 228(1) (2004) 45-54.
[19] J.A. Lie, M.-B. Hägg, Carbon membranes from cellulose: Synthesis, performance and regeneration, Journal of Membrane Science 284(1–2) (2006) 79-86.
[20] A. Soffer, J. Gilron, S. Saguee, R. Hed-Ofek, H. Cohen, Process for the production of hollow carbon fiber membranes, Patents, EP0671202A3, 1999.
[21] O. Karvan, J.R. Johnson, P.J. Williams, W.J. Koros, A Pilot-Scale System for Carbon Molecular Sieve Hollow Fiber Membrane Manufacturing, Chemical Engineering & Technology 36(1) (2013) 53-61.
[22] M.-B.H. Jon Arvid Lie, Carbon Membranes, Patents, US20100162887 A1, 2010.
[23] M. Mulder, Basic Priciples of Membrane Technology, Kluwer Academic Publishers, Netherlands, 1996.
[24] W.J. Koros, Y.H. Ma, T. Shimidzu, Terminology for membranes and membrane processes (IUPAC Recommendations 1996), Pure and Applied Chemistry, 1996, p. 1479.
[25] S.A. Rackley, 8 - Membrane separation systems, Carbon Capture and Storage (Second Edition), Butterworth-Heinemann, Boston, 2017, pp. 187-225.
[26] J. Rouquerol, D. Avnir, C.W. Fairbridge, D.H. Everett, J.M. Haynes, N. Pernicone, J.D.F. Ramsay, K.S.W. Sing, K.K. Unger, Recommendations for the characterization of porous solids (Technical Report), Pure and Applied Chemistry, 1994, p. 1739.
[27] S. Loeb, S. Sourirajan, Sea Water Demineralization by Means of an Osmotic Membrane, Saline Water Conversion—II, AMERICAN CHEMICAL SOCIETY1963, pp. 117-132.
[28] L.M. Robeson, Correlation of separation factor versus permeability for polymeric membranes, Journal of Membrane Science 62(2) (1991) 165-185.
[29] D.R. Ahmad Fauzi Ismail , Takeshi Matsuura, Henry C. Foley, Carbon-based Membranes for Separation Processes, Springer, London, 2011.
[30] L.M. Robeson, The upper bound revisited, Journal of Membrane Science 320(1–2) (2008) 390-400.
[31] M. Yoshimune, I. Fujiwara, K. Haraya, Carbon molecular sieve membranes derived from trimethylsilyl substituted poly(phenylene oxide) for gas separation, Carbon 45(3) (2007) 553-560.
[32] B. Zhang, T. Wang, S. Zhang, J. Qiu, X. Jian, Preparation and characterization of carbon membranes made from poly(phthalazinone ether sulfone ketone), Carbon 44(13) (2006) 2764-2769.
[33] A.C. Lua, J. Su, Effects of carbonisation on pore evolution and gas permeation properties of carbon membranes from Kapton® polyimide, Carbon 44(14) (2006) 2964-2972.
[34] J.A. Lie, M.-B. Hägg, Carbon membranes from cellulose and metal loaded cellulose, Carbon 43(12) (2005) 2600-2607.
[35] J.N. Barsema, J. Balster, V. Jordan, N.F.A. van der Vegt, M. Wessling, Functionalized Carbon Molecular Sieve membranes containing Ag-nanoclusters, Journal of Membrane Science 219(1) (2003) 47-57.
[36] R.S. Murali, T. Sankarshana, S. Sridhar, Air Separation by Polymer-based Membrane Technology, Separation & Purification Reviews 42(2) (2013) 130-186.
[37] J.W. Biscoe, B. E., An X-Ray Study of Carbon Black, Journal of Applied Physics 13(6) (1942) 364-371.
[38] J.E. Koresh, A. Soffer, Mechanism of permeation through molecular-sieve carbon membrane. Part 1.-The effect of adsorption and the dependence on pressure, Journal of

the Chemical Society, Faraday Transactions 1: Physical Chemistry in Condensed Phases 82(7) (1986) 2057-2063.
[39] J. Koresh, A. Soffer, Study of molecular sieve carbons. Part 1.-Pore structure, gradual pore opening and mechanism of molecular sieving, Journal of the Chemical Society, Faraday Transactions 1: Physical Chemistry in Condensed Phases 76(0) (1980) 2457-2471.
[40] J.E. Koresh, A. Soffer, The Carbon Molecular Sieve Membranes. General Properties and the Permeability of CH4/H2 Mixture, Separation Science and Technology 22(2-3) (1987) 973-982.
[41] S.M. Saufi, A.F. Ismail, Fabrication of carbon membranes for gas separation—a review, Carbon 42(2) (2004) 241-259.
[42] W.N.W. Salleh, A.F. Ismail, Carbon membranes for gas separation processes: Recent progress and future perspective, Journal of Membrane Science and Research 1(Issue 1) (2015) 2-15.
[43] V.C. Geiszler, W.J. Koros, Effects of Polyimide Pyrolysis Conditions on Carbon Molecular Sieve Membrane Properties, Ind Eng Chem Res 35(9) (1996) 2999-3003.
[44] X. He, Development of Hollow fiber carbon membranes for CO2 separation, Department of Chemical engineerg, NTNU, Trondheim, 2011.
[45] S. Lagorsse, A. Leite, F.D. Magalhães, N. Bischofberger, J. Rathenow, A. Mendes, Novel carbon molecular sieve honeycomb membrane module: configuration and membrane characterization, Carbon 43(4) (2005) 809-819.
[46] C. Liang, G. Sha, S. Guo, Carbon membrane for gas separation derived from coal tar pitch, Carbon 37(9) (1999) 1391-1397.
[47] K. Briceño, D. Montané, R. Garcia-Valls, A. Iulianelli, A. Basile, Fabrication variables affecting the structure and properties of supported carbon molecular sieve membranes for hydrogen separation, Journal of Membrane Science 415–416 (2012) 288-297.
[48] H.-H. Tseng, K. Shih, P.-T. Shiu, M.-Y. Wey, Influence of support structure on the permeation behavior of polyetherimide-derived carbon molecular sieve composite membrane, Journal of Membrane Science 405–406 (2012) 250-260.
[49] W.N.W. Salleh, A.F. Ismail, Effect of Stabilization Condition on PEI/PVP-Based Carbon Hollow Fiber Membranes Properties, Separation Science and Technology 48(7) (2013) 1030-1039.
[50] A.C. Lua, Y. Shen, Preparation and characterization of polyimide–silica composite membranes and their derived carbon–silica composite membranes for gas separation, Chemical Engineering Journal 220 (2013) 441-451.
[51] M. Teixeira, M. Campo, D.A. Tanaka, M.A. Tanco, C. Magen, A. Mendes, Carbon–Al2O3–Ag composite molecular sieve membranes for gas separation, Chemical Engineering Research and Design 90(12) (2012) 2338-2345.
[52] C.W. Jones, W.J. Koros, Carbon molecular sieve gas separation membranes-I. Preparation and characterization based on polyimide precursors, Carbon 32(8) (1994) 1419-1425.
[53] R. Steiner, Microfiltration and Ultrafiltration - Principles and Applications, Chemie Ingenieur Technik 69(10) (1997) 1479-1479.
[54] E.Schindler, F. Maier, Manufacture of porous carbon membranes, Patents, US4919860A. Akzo NV, 1986.
[55] A. Soffer, M. Azariah, A. Amar, H. Cohen, D. Golub, S. Saguee, H. Tobias, Method of improving the selectivity of carbon membranes by chemical carbon vapor deposition, Rotem Industries Ltd, Patents, US5695818A, 1997.
[56] A. Soffer, J E. Koresh, S. Saggy, Separation device, Patents, US4685940A, 1987.

[57] J.-i. Hayashi, M. Yamamoto, K. Kusakabe, S. Morooka, Simultaneous Improvement of Permeance and Permselectivity of 3,3',4,4'-Biphenyltetracarboxylic Dianhydride-4,4'-Oxydianiline Polyimide Membrane by Carbonization, Ind Eng Chem Res 34(12) (1995) 4364-4370.
[58] A.L. Cabrera, J.E. Zehner, C.G. Coe, T.R. Gaffney, T.S. Farris, J.N. Armor, Preparation of carbon molecular sieves, I. Two-step hydrocarbon deposition with a single hydrocarbon, Carbon 31(6) (1993) 969-976.
[59] S.K. Verma, P.L. Walker, Preparation of carbon molecular sieves by propylene pyrolysis over microporous carbons, Carbon 30(6) (1992) 829-836.
[60] R.F.P.M. Moreira, H.J. José, A.E. Rodrigues, Modification of pore size in activated carbon by polymer deposition and its effects on molecular sieve selectivity, Carbon 39(15) (2001) 2269-2276.
[61] J.M.D. MacElroy, S.P. Friedman, N.A. Seaton, On the origin of transport resistances within carbon molecular sieves, Chemical Engineering Science 54(8) (1999) 1015-1027.
[62] M.B. Rao, S. Sircar, Performance and pore characterization of nanoporous carbon membranes for gas separation, Journal of Membrane Science 110(1) (1996) 109-118.
[63] J. Gilron, A. Soffer, Knudsen diffusion in microporous carbon membranes with molecular sieving character, Journal of Membrane Science 209(2) (2002) 339-352.
[64] J.A. Lie, PhD. Thesis: Synthesis, performance and regeneration of carbon membranes for biogas upgrading – a future energy carrier, Norwegian University of Science and Technology, 2005.
[65] R.W. Baker, Membrane Technology and Applications, Second ed., John Wiley & Sons, Ltd, California, 2004.
[66] A.J. Burggraaf, Single gas permeation of thin zeolite (MFI) membranes: theory and analysis of experimental observations, Journal of Membrane Science 155(1) (1999) 45-65.
[67] C.J. Geankoplis, Transport processes and Unit Operations, Chapter 7, 3rd ed., Prentice-Hall, Eaglewood Cliffs, New jersey, 1993.
[68] A. Lindbråthen, PhD. Thesis: Development and modification of glass memrbranes for aggressive gas separations, Department of Chemical Engineering, Norwegian University of Science and Technology, NTNU, Trondheim, 2005.
[69] M.M. Haring, The Theory of Rate Processes (Glasstone, Samuel; Laidler, Keith J.; Eyring, Henry), Journal of Chemical Education 19(5) (1942) 249.
[70] A. Singh, W.J. Koros, Significance of Entropic Selectivity for Advanced Gas Separation Membranes, Ind Eng Chem Res 35(4) (1996) 1231-1234.
[71] C. Nguyen, D.D. Do, K. Haraya, K. Wang, The structural characterization of carbon molecular sieve membrane (CMSM) via gas adsorption, Journal of Membrane Science 220(1) (2003) 177-182.
[72] D. R. Paul, Y P. Yampolski, Polymeric gas separation membranes, 1st ed, CRC Press, , London, Tokoyo, 1994.
[73] S. Lagorsse, M.C. Campo, F.D. Magalhães, A. Mendes, Water adsorption on carbon molecular sieve membranes: Experimental data and isotherm model, Carbon 43(13) (2005) 2769-2779.
[74] M.C. Campo, S. Lagorsse, F.D. Magalhaes, A. Mendes, Comparative study between a CMS membrane and a CMS adsorbent: Part II. Water vapor adsorption and surface chemistry, J Membrane Sci 346(1) (2010) 26-36.
[75] C.W. Jones, W.J. Koros, Characterization of Ultramicroporous Carbon Membranes with Humidified Feeds, Ind Eng Chem Res 34(1) (1995) 158-163.

[76] L. Xu, M. Rungta, J. Hessler, W. Qiu, M. Brayden, M. Martinez, G. Barbay, W.J. Koros, Physical aging in carbon molecular sieve membranes, Carbon 80 (2014) 155-166.
[77] G.B. Wenz, W.J. Koros, Tuning carbon molecular sieves for natural gas separations: A diamine molecular approach, AIChE Journal 63(2) (2017) 751-760.
[78] I. Menendez, A.B. Fuertes, Aging of carbon membranes under different environments, Carbon 39(5) (2001) 733-740.
[79] S. Lagorsse, F.D. Magalhães, A. Mendes, Aging study of carbon molecular sieve membranes, Journal of Membrane Science 310(1–2) (2008) 494-502.
[80] C.W. Jones, W.J. Koros, Carbon molecular sieve gas separation membranes-II. Regeneration following organic exposure, Carbon 32(8) (1994) 1427-1432.
[81] A. Subrenat, P.L. Cloirec, Adsorption onto Activated Carbon Cloths and Electrothermal Regeneration: Its Potential Industrial Applications, Journal of Environmental Engineering 130(3) (2004) 249-257.
[82] K.-i. Okamoto, S. Kawamura, M. Yoshino, H. Kita, Y. Hirayama, N. Tanihara, Y. Kusuki, Olefin/Paraffin Separation through Carbonized Membranes Derived from an Asymmetric Polyimide Hollow Fiber Membrane, Ind Eng Chem Res 38(11) (1999) 4424-4432.
[83] A.B. Shelekhin, A.G. Dixon, Y.H. Ma, Adsorption, permeation, and diffusion of gases in microporous membranes. II. Permeation of gases in microporous glass membranes, Journal of Membrane Science 75(3) (1992) 233-244.
[84] T.A. Centeno, A.B. Fuertes, Carbon molecular sieve gas separation membranes based on poly(vinylidene chloride-co-vinyl chloride), Carbon 38(7) (2000) 1067-1073.
[85] S.S. Hosseini, T.S. Chung, Carbon membranes from blends of PBI and polyimides for N2/CH4 and CO2/CH4 separation and hydrogen purification, Journal of Membrane Science 328(1) (2009) 174-185.
[86] E.P. Favvas, N.S. Heliopoulos, S.K. Papageorgiou, A.C. Mitropoulos, G.C. Kapantaidakis, N.K. Kanellopoulos, Helium and hydrogen selective carbon hollow fiber membranes: The effect of pyrolysis isothermal time, Separation and Purification Technology 142 (2015) 176-181.
[87] H. Suda, K. Haraya, Alkene/alkane permselectivities of a carbon molecular sieve membrane, Chemical Communications (1) (1997) 93-94.
[88] A.B. Fuertes, T.A. Centeno, Preparation of supported carbon molecular sieve membranes, Carbon 37(4) (1999) 679-684.
[89] A. Demirbas, Global Renewable Energy Projections, Energy Sources, Part B: Economics, Planning, and Policy 4(2) (2009) 212-224.
[90] M. HÅ, Biogas för fordonsdrift - kvalitetsspecifikation, kommunikations forskningsberedningen (KFB4), Stockholm (in Swedish), 1997.
[91] K. Wågdahl, DISTRIBUTION AV BIOGAS I NATURGASNÄTET, ©Svenskt Gastekniskt Center, Sweden, 1999.
[92] R. Rautenbach, K. Welsch, Treatment of landfill gas by gas permeation — pilot plant results and comparison to alternatives, Journal of Membrane Science 87(1) (1994) 107-118.
[93] B. Petroleum, BP Statistical Review of World Energy, 65th Edition (2016). https://www.bp.com/content/dam/bp/pdf/energy-economics/statistical-review2016/bp-statistical-review-of-world-energy-2016-full-report.pdf. (Accessed:29.09.2017)
[94] USA, Annual Energy Outlook with projections to 2040, U.S.Energy Information Administration EIA-038 (2015). https://www.eia.gov/outlooks/aeo/pdf/0383(2015).pdf (Accessed:29.09.2017)
[95] T. Tomita, K. Nakayama, H. Sakai, Gas separation characteristics of DDR type zeolite membrane, Microporous and Mesoporous Materials 68(1) (2004) 71-75.

[96] W. Zhu, P. Hrabanek, L. Gora, F. Kapteijn, J.A. Moulijn, Role of Adsorption in the Permeation of CH4 and CO2 through a Silicalite-1 Membrane, Ind Eng Chem Res 45(2) (2006) 767-776.
[97] R.M. de Vos, H. Verweij, High-selectivity, high-flux silica membranes for gas separation, Science (New York, N.Y.) 279(5357) (1998) 1710-1.
[98] A. Makaruk, M. Miltner, M. Harasek, Membrane biogas upgrading processes for the production of natural gas substitute, Separation and Purification Technology 74(1) (2010) 83-92.
[99] L. Deng, M.-B. Hägg, Techno-economic evaluation of biogas upgrading process using CO2 facilitated transport membrane, International Journal of Greenhouse Gas Control 4(4) (2010) 638-646.
[100] C. Micale, Bio-methane Generation from Biogas Upgrading by Semi-permeable Membranes: An Experimental, Numerical and Economic Analysis, Energy Procedia 82 (2015) 971-977.
[101] J.A. Lie, T. Vassbotn, M.-B. Hägg, D. Grainger, T.-J. Kim, T. Mejdell, Optimization of a membrane process for CO2 capture in the steelmaking industry, International Journal of Greenhouse Gas Control 1(3) (2007) 309-317.
[102] D. Grainger, M.-B. Hägg, Techno-economic evaluation of a PVAm CO2-selective membrane in an IGCC power plant with CO2 capture, Fuel 87(1) (2008) 14-24.
[103] X. He, J. Arvid Lie, E. Sheridan, M.-B. Hägg, CO2 capture by hollow fibre carbon membranes: Experiments and process simulations, Energy Procedia 1(1) (2009) 261-268.
[104] A. Hussain, M.-B. Hägg, A feasibility study of CO2 capture from flue gas by a facilitated transport membrane, Journal of Membrane Science 359(1–2) (2010) 140-148.
[105] B. Belaissaoui, Y. Le Moullec, D. Willson, E. Favre, Hybrid membrane cryogenic process for post-combustion CO2 capture, Journal of Membrane Science 415–416 (2012) 424-434.
[106] P.S. Tin, T.-S. Chung, Y. Liu, R. Wang, Separation of CO2/CH4 through carbon molecular sieve membranes derived from P84 polyimide, Carbon 42(15) (2004) 3123-3131.
[107] X. He, J.A. Lie, E. Sheridan, M.-B. Hägg, Preparation and Characterization of Hollow Fiber Carbon Membranes from Cellulose Acetate Precursors, Ind Eng Chem Res 50(4) (2011) 2080-2087.
[108] S. Haider, A. Lindbråthen, J.A. Lie, I.C.T. Andersen, M.-B. Hägg, CO2 separation with carbon membranes in high pressure and elevated temperature applications, Separation and Purification Technology 190(Supplement C) (2018) 177-189.
[109] R. Prasad, F. Notaro, D.R. Thompson, Evolution of membranes in commercial air separation, Journal of Membrane Science 94(1) (1994) 225-248.
[110] B.D. Bhide, S.A. Stern, A new evaluation of membrane processes for the oxygen-enrichment of air. II. Effects of economic parameters and membrane properties, Journal of Membrane Science 62(1) (1991) 37-58.
[111] S.L. Matson, W.J. Ward, S.G. Kimura, W.R. Browall, Membrane oxygen enrichment, Journal of Membrane Science 29(1) (1986) 79-96.
[112] C.-L. Lee, H.L. Chapman, M.E. Cifuentes, K.M. Lee, L.D. Merrill, K.L. Ulman, K. Venkataraman, Effects of polymer structure on the gas permeability of silicone membranes, Journal of Membrane Science 38(1) (1988) 55-70.
[113] H.M. Ettouney, H.T. El-Dessouky, W. Abou Waar, Separation characteristics of air by polysulfone hollow fiber membranes in series, Journal of Membrane Science 148(1) (1998) 105-117.

[114] K.M.P. Kamps, H.A. Teunis, M. Wessling, C.A. Smolders, Gas transport and sub-Tg relaxations in unmodified and nitrated polyarylethersulfones, Journal of Membrane Science 74(1) (1992) 193-201.
[115] B E. Poling, J M. Prausnitz, J P. O'connell, The properties of Gases and Liquids, 4th ed., McGraw-Hill, United States of America, 1987.
[116] M. Niwa, K. Yamazaki, Y. Murakami, Separation of oxygen and nitrogen due to the controlled pore-opening size of chemically vapor deposited zeolite A, Ind Eng Chem Res 30(1) (1991) 38-42.
[117] M. Acharya, H.C. Foley, Spray-coating of nanoporous carbon membranes for air separation, Journal of Membrane Science 161(1–2) (1999) 1-5.
[118] J. Koresh, A. Soffer, Study of molecular sieve carbons. Part 2.-Estimation of cross-sectional diameters of non-spherical molecules, Journal of the Chemical Society, Faraday Transactions 1: Physical Chemistry in Condensed Phases 76(0) (1980) 2472-2485.
[119] B.D. Bhide, S.A. Stern, A new evaluation of membrane processes for the oxygen-enrichment of air. I. Identification of optimum operating conditions and process configuration, Journal of Membrane Science 62(1) (1991) 13-35.
[120] B. Belaissaoui, Y. Le Moullec, H. Hagi, E. Favre, Energy Efficiency of Oxygen Enriched Air Production Technologies: Cryogeny vs Membranes, Energy Procedia 63 (2014) 497-503.
[121] W. Shusen, Z. Meiyun, W. Zhizhong, Asymmetric molecular sieve carbon membranes, Journal of Membrane Science 109(2) (1996) 267-270.
[122] H. Hatori, Y. Yamada, M. Shiraishi, H. Nakata, S. Yoshitomi, Carbon molecular sieve films from polyimide, Carbon 30(4) (1992) 719-720.
[123] E. Sheridan, T. Borge, J. A. Lie, M.-B Hagg, Carbon Membranes from cellulose esters, MemfoACT AS, Patents, US8394175B2, 2013.
[124] X. Jie, Y. Cao, J.-J. Qin, J. Liu, Q. Yuan, Influence of drying method on morphology and properties of asymmetric cellulose hollow fiber membrane, Journal of Membrane Science 246(2) (2005) 157-165.
[125] J.-J. Qin, Y. Li, L.-S. Lee, H. Lee, Cellulose acetate hollow fiber ultrafiltration membranes made from CA/PVP 360 K/NMP/water, Journal of Membrane Science 218(1) (2003) 173-183.
[126] A. Abraham Soffer, Jack Gilron, Haim Cohen, Separation of Linear from Branched hydrocarbons using a Carbon Membrane, Carbon membranes Ltd, Patents, US5914434, 1999.
[127] W.-H. Lin, R. H. and Chung, T.-S., Gas transport properties of 6FDA-durene/1,4-phenylenediamine (pPDA) copolyimides, J. Polym. Sci. B Polym. Phys. 38 (2000) 2703-2713.
[128] M. Svensson, National Biomethane Standards (Svenskt Gastekniskt Center AB), Swedish gas technology center, 2014.
[129] H.Consult. As, Forprosjekt: Biogassoppgradering; vurdering av ulike teknologier for oppgradering av biogass fra Nye Mjøsanlegget (in Norwegian), Norway, 2013, p. 12 av 47.
[130] D. Grainger, PhD. Thesis, Development of carbon membranes for hydrogen recovery, Department of Chemical Engineering, Norwegian University of Science and Technology, Trondheim, 2007.
[131] S.P. Kaldis, G. Skodras, G.P. Sakellaropoulos, Energy and capital cost analysis of CO2 capture in coal IGCC processes via gas separation membranes, Fuel Processing Technology 85(5) (2004) 337-346.

[132] G.B. Markus Ungerank, M. Priske, H. Roegl, Process for separation of gases, Evonik Fibres Gmbh, Patents, US20130098242A1, 2013.
[133] M.S. Peters, K.D. Timmerhaus, Plant design and economics for chemical engineers, McGraw-Hill, New York, 1991.
[134] W.D. Baasel, Preliminary chemical engineering plant design, Van Nostrand Reinhold, New York, 1990.
[135] A. Lindbråthen, D.R. Grainger, M.B. Hägg, Membranes for Purification of Chlorine in the Chlor-Alkali Industry: A Viable Option, Separation Science and Technology 42(14) (2007) 3049-3070.
[136] M. Hubbe, A. Ayoub, J. Daystar, R. Venditti, J. Pawlak, Enhanced absorbent products incorporating cellulose and its derivatives: A Review, BioResources 8(4) (2013), 6556-6629.
[137] K.C. O'Brien, W.J. Koros, T.A. Barbari, E.S. Sanders, A new technique for the measurement of multicomponent gas transport through polymeric films, Journal of Membrane Science 29(3) (1986) 229-238.
[138] G. Valenti, A. Arcidiacono, J.A. Nieto Ruiz, Assessment of membrane plants for biogas upgrading to biomethane at zero methane emission, Biomass and Bioenergy 85 (2016) 35-47.
[139] F. Falbo, F. Tasselli, A. Brunetti, E. Drioli, G. Barbieri, Polyimide Hollow Fiber Membranes for CO2 Separation from Wet Gas Mixtures, Braz J Chem Eng 31(4) (2014) 1023-1034.
[140] S. Kanehashi, T. Nakagawa, K. Nagai, X. Duthie, S. Kentish, G. Stevens, Effects of carbon dioxide-induced plasticization on the gas transport properties of glassy polyimide membranes, Journal of Membrane Science 298(1–2) (2007) 147-155.
[141] G. Jensen , A. Gussiås, Hypoxic air venting for protection of heritage, Riksantikvaren, Directorate for Cultural Heritage and Crown, 2006.

Part II

Appendix list

- Appendix A: List of all the equipments and suppliers that were used at MemfoACT facility
- Appendix B: Cross section of cellulose acetate (CA) and carbon fibers while using different compositions of precursor solution
- Appendix C: Production cost of carbon membranes at lab, pilot, and industrial scale
- Appendix D: Photos of different equipments and their components
- Appendix E: Paper I- Pilot – Scale production of carbon hollow fiber membranes from regenerated cellulose precursor: Optimal conditions for precursor preparation
- Appendix F: Paper II- Pilot – Scale production of carbon hollow fiber membranes from regenerated cellulose precursor: Carbonization procedure
- Appendix G: Paper III- Regenerated cellulose-based carbon membranes for CO_2 separation; Durability and aging under miscellaneous environments
- Appendix H: Paper IV- CO_2 separation with carbon membranes in high pressure and elevated temperature applications
- Appendix I: Paper V- Vehicle fuel from biogas with carbon membranes; a comparison between simulation predictions and actual field demonstration
- Appendix J: Paper VI- Techno-economical evaluation of membrane based biogas upgrading system: A comparison between polymeric membrane and carbon membrane technology
- Appendix K: Paper VII- Carbon membranes for oxygen enriched air –Part I: Synthesis, performance and preventive regeneration
- Appendix L: Paper VIII- Carbon membranes for oxygen enriched air –Part II: Techno-economic analys

Appendix A

List of all the equipments and suppliers that were used at MemfoACT facility is presented in table A.1.

Table A.1: List of Equipments and suppliers used at MemfoACT facility

Equipment	Supplier	Description
Pilot scale Spinning set-up	PHILOS (Korea)	
Tools, safety equipment	Albert E. Olsen	
Fireproof materials	Borgestad Fabrikker	
Electronics	Elma	
Gas analyzers	ExTeVent AB	
Pumps	Finisterra	
Pumps	Haakon Rygh AS	
Measuring equipment	Flow-Teknikk AS	Gas flow meters
Plastic tubing and accessories	GPA Flowsystem	
Clamps, tubing, connections	Heidenreich	
Glue, grease	Henkel	
Design and production	Inventas	Guitars, modules
Production of equipment	Landteknikk Fabrikk	Collection wheel and baths
Measuring equipment	Leif Kølner	
Automation	Maskon	
Mechanical accessories	Misumi Europa GmbH	
Perforated plates	Nisjemetall	
Chemicals, industrial scale	Norkem	
Measuring equipment	Norsk Analyse	
Steel products	Norsk Stål	
Water cleaning	Norvann	
Production of equipment	PTM Production	
Aluminum profiles and accessories	Rexroth, Bosch Group	
Chemicals	Sigma-Aldrich	
Tubing, connections and valves	Swagelok/Svafas	Permeation rig and testing
Plexiglass, steel plates	Teknolakk	
Tubing	W. Tverdal AS	
Chemicals, lab equipment	VWR	
Gas/equipment/HMS	Yara Praxair	

Appendix B

Cross section of cellulose acetate (CA) and carbon fibers while using different compositions of precursor solution:

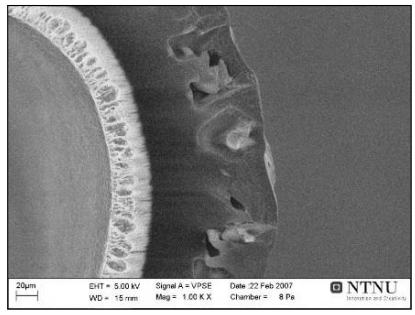

Figure B.1: Cross section of a CA fiber spun from 22.5% CA in NMP. Bore solution 1:1 mixture of NMP: H_2O

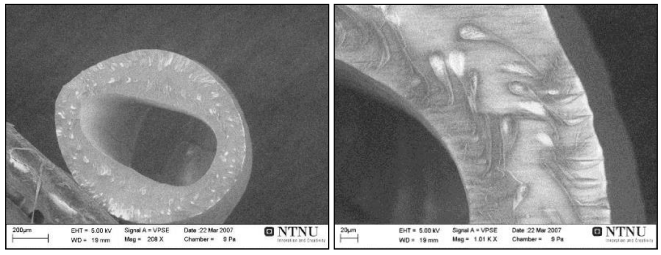

Figure B.2: Cross section of CA fiber containing 630K PVP additive. Dope mixture 22.5%CA, 2.5% 630K PVP and NMP

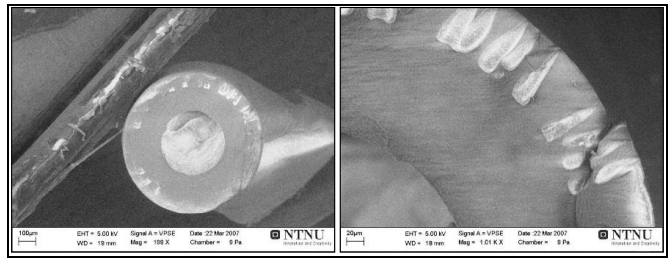

Figure B.3: Cross section of CA fiber containing 10K PVP additive. Dope mixture 22.5%CA, 2.5% 10K PVP and NMP

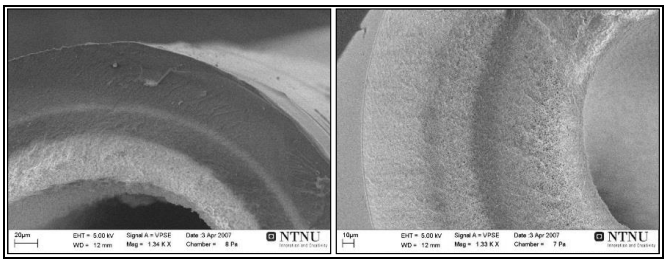

Figure B.4: (left) CA fiber spun at 7ºC and (right) at 50ºC. Dope solution 22.5% CA, 2.5% PVP 10K, 5% H_2O and NMP

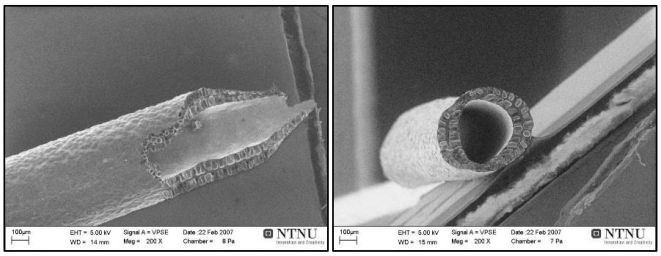

Figure B.5: Carbonized fiber showing large number of macrovoids present. Dope 22,5% CA in NMP

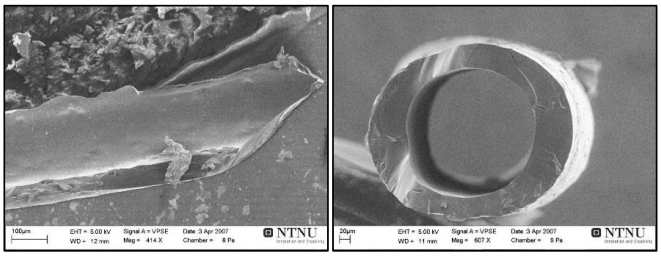

Figure B.6: Carbonized fiber showing no macrovoids present. Dope 22,5% CA, 2,5% PVP 10K in NMP.

Appendix C

Production cost of carbon membranes at lab, pilot, and industrial scale:

Basis = 2.5 m^2 module [M]

Basis module = M (module) = 2.5 m^2 membrane area

Active length of fibers: 1.5 m

Number of fibers in module: 3 000

Electricity pric = 0.09 $/kWh

Table C.1: carbon membrane production scale, automation level, and limiting steps

Production-scale	Automation level	Spinning speed	Production Lines	Trash fibers	Labor cost	Limiting step	Max capacity
		m/min	spinnerets	%	$/hr		M/week
Lab	manual	6	1	50	37	spinning	0.5
Pilot	Semi-automated	50	2	20	25	carbonization	10
Industrial	Fully-automated	500	20	10	28	24/7 production	84

**Costs not included: shipping of chemicals/materials, tap water*

**Pilot scale production: 5 days a week and 8 hrs a day*

**Industrial scale production: 24/7, night factor included (in labor cost)*

Table C.2: Retention time and labor hours for different processes involved in production of CM modules

	Polymer preparation	Spinning	Collation	Pre-treatment	Carbonization	Module making, M
Retention time	[h/Batch]	[h/M]	[h/M]	[h/Batch]	[h/Batch]	[h/M]
Lab	49	50	53	79.16	30	30
Pilot	96	3.75	1.5	23.66	30	25
Industrial	148	0.33	0.1	22.26	30	15
Labor	[h/M]	[h/M]	[h/M]	[h/M]	[h/M]	[h/M]
Lab	7	62	53	62	34	5
Pilot	0.2	4.5	1.5	7.1	0.95	2
Industrial	0.02	0.33	0.1	0.66	0.06	0.2

**M: 2.5 m^2 module*

Table C.3: Production cost for different processes involved in production of CM module

PRODUCTION COST	Polymer prep.	Spinning	Collation	Pre-treat.	Carb.	Module making	TOT. COST/M
Energy	[$/M]	[$/M]	[$/M]	[$/M]	[$/M]	[$/M]	[$/M]
Lab	26	10	0	0.8	5	0	27
Pilot	1	2	0.25	3	3	0	10
Industrial	2	1	0.36	1	3	1	8
Chemicals							
Lab	382	62	0	1003	13	611	2071
Pilot	86	21	0	181	6	152	446
Industrial	28	10	0	42	3	28	111
Man labor							
Lab	257	2273	1332	1662	1247	183	6954
Pilot	5	110	37	174	23	49	398
Industrial	1	9	3	18	2	6	39

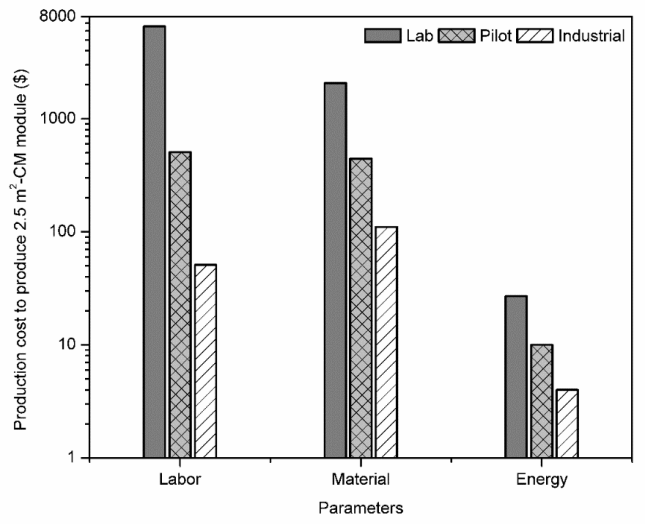

Figure C.1: Labor, material, and energy costs involved in production of CM 2.5 m^2 module

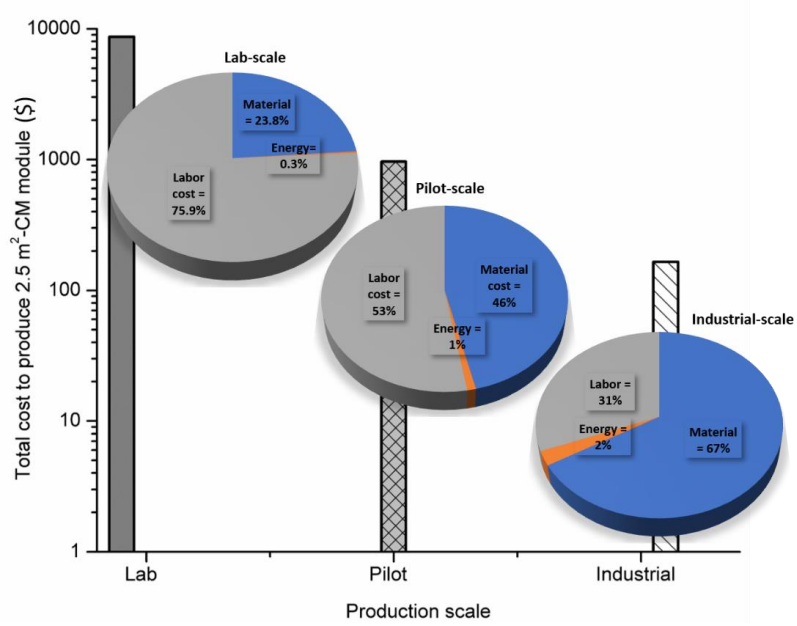

Figure C.2: Total cost to produce 2.5m^2 of CM module on different production scales

Appendix D

Photos of different equipments and their components:

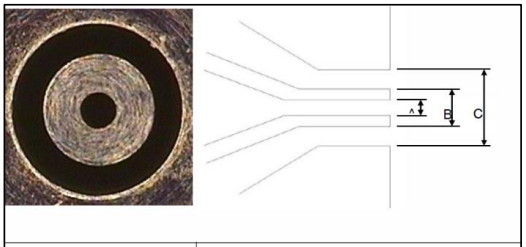

No.	SN-D0015
A (0.13 mm)	0.13 (±0.015)
B (0.40 mm)	0.40 (±0.015)
C (0.60 mm)	0.60 (±0.015)

Figure D.1: One type of spinneret and its dimensions used at MemfoACT AS

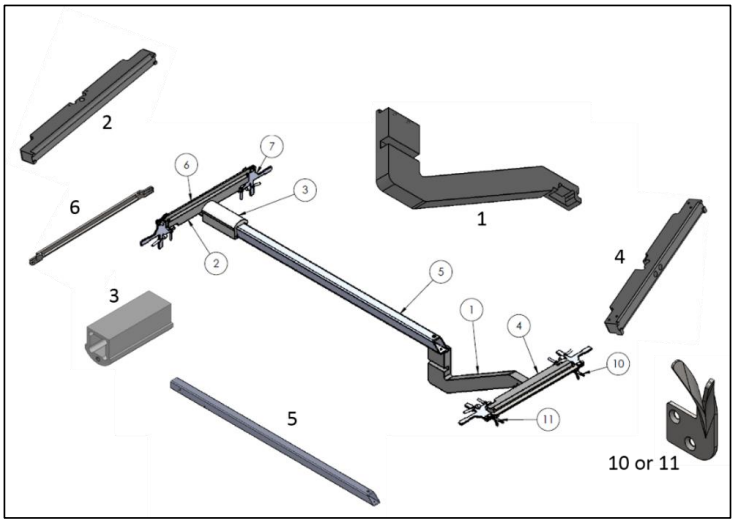

Figure D.2: Fiber carrier "Guitar" and its components

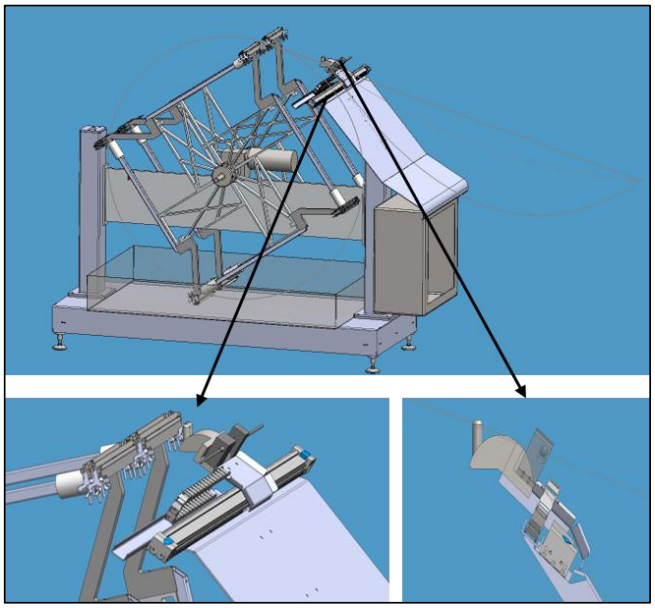

Figure D.3: Fiber collection wheel (top); a mechanical device for fiber sliding over "guitar" (bottom left), and a sensor to control fiber tension (bottom right)

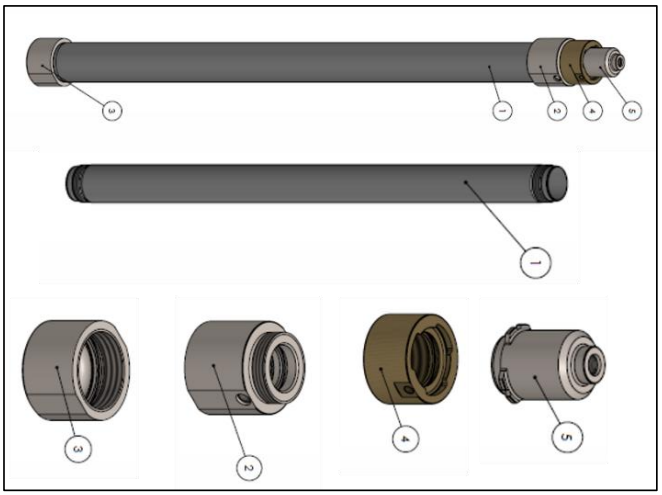

Fiber D.4: A vessel used for gas permeation testing of CM modules

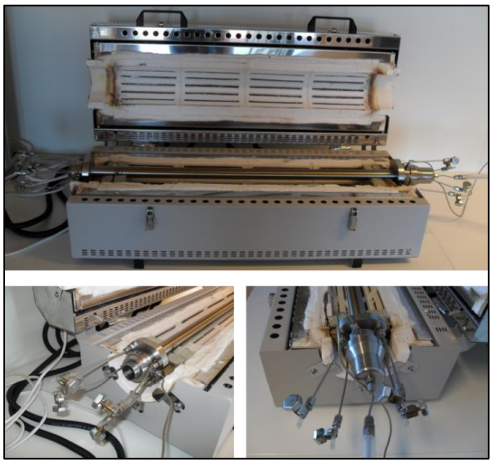

Figure D.5: The apparatus used for CVD process

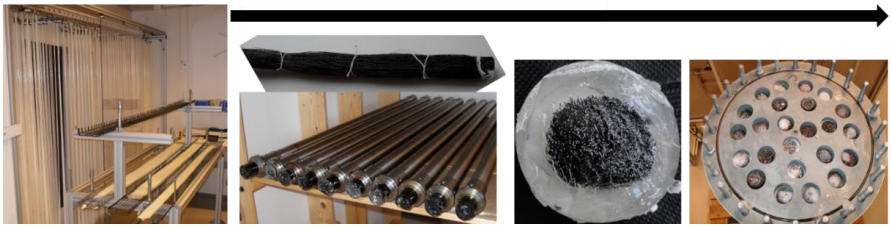

Figure D.6: storage of Cellulose fibers, prepared CM, and a multimodule system (left to right)

Figure D.7: Biogas upgrading plant at Glør IKS, Lillehammer, Norway

Appendix E

Paper I

Pilot – scale production of carbon hollow fiber membranes from regenerated cellulose precursor: Part I- Optimal conditions for precursor preparation

Paper published in Membranes Journal 8(2018) 105

membranes

MDPI

Article

Pilot–Scale Production of Carbon Hollow Fiber Membranes from Regenerated Cellulose Precursor-Part I: Optimal Conditions for Precursor Preparation

Shamim Haider, Jon Arvid Lie, Arne Lindbråthen and May-Britt Hägg *

Department of Chemical Engineering, Norwegian University of Science and Technology (NTNU), 7491 Trondheim, Norway; haider@ntnu.no (S.H.); jonarvidlie@gmail.com (J.A.L.); arne.lindbrathen@ntnu.no (A.L.)

* Correspondence: may-britt.hagg@ntnu.no; Tel.: +47-93080834

Received: 17 September 2018; Accepted: 8 November 2018; Published: 13 November 2018

Abstract: Industrial scale production of carbon membrane is very challenging due to expensive precursor materials and a multi-step process with several variables to deal with. The optimization of these variables is essential to gain a competent carbon membrane (CM) with high performance and good mechanical properties. In this paper, a pilot scale system is reported that was developed to produce CM from regenerated cellulose precursor with the annual production capacity 700 m^2 of CM. The process was optimized to achieve maximum yield (>95%) of high quality precursor fibers and carbonized fibers. A dope solution of cellulose acetate (CA)/Polyvinylpyrrolidone (PVP)/*N*-methyl-2-pyrrolidone (NMP) and bore fluid of NMP/H_2O were used in 460 spinning-sessions of the fibers using a well-known dry/wet spinning process. Optimized deacetylation of spun-CA hollow fibers (CAHF) was achieved by using 90 vol% 0.075 M NaOH aqueous solution diluted with 10 vol% isopropanol for 2.5 h at ambient temperature. Cellulose hollow fibers (CHF) dried at room temperature and under RH (80% $\rightarrow$ ambient) overnight gave maximum yield for both dried CHF, as well as carbon fibers. The gas permeation properties of carbon fibers were also high (CO_2 permeability: 50–450 Barrer (1 Barrer = 2.736×10^{-9} m^3 (STP) m/m^2 bar h), and CO_2/CH_4 selectivity acceptable (50–500).

Keywords: pilot scale process; carbon membrane precursor; dry/wet spinning; deacetylation; regenerated cellulose; drying conditions

1. Introduction

In the 1960s, the term carbon membrane was introduced for the first time for carbon plugs prepared from compressed carbon powders [1,2]. However, the materials reported were too porous to achieve selective membranes. Two decades later Koresh and Soffer [3] reported the concept of pre-shaped polymeric precursor materials for the direct formation of carbon membranes. In 1995, Soffer et al. [4] developed and patented the protocol for carbonization of cellulose precursor. Cellulose is a natural polymer that produced by plants through photosynthesis. It is abundantly available in the world. However, only a limited number of solvents exist to dissolve (strong inter and intra-molecular hydrogen bonding [5]) and treat cellulose in such way that monosaccharides are preserved to form a suitable carbon structure after carbonization [6,7].

Cellulose esters, in particular, cellulose acetate (CA), is relatively inexpensive, easily commercially available, and have been applied successfully for many years, as a membrane material in different applications, such as water treatment, pervaporation, gas separation etc. [8–12]. CA is soluble in common solvents like NMP (*N*-methyl-2-pyrrolidone), DMSO (dimethylsulfoxide) and acetone.

However, direct carbonization of CA will result in discontinuous carbon (more like a powder), since the intermediate product levoglucosane [7] is not formed during carbonization. Hence, CA must be deacetylated after the membrane casting/spinning process to allow the formation of the critical intermediate product of levoglucosane.

Deacetylated cellulose hollow fibers (CHF) from spun-cellulose acetate hollow fibers (CAHF) showed good potential to as a precursor for carbon hollow fiber membrane (CM) with promising permeation properties in gas separation applications when tested on laboratory scale [13–17]. However, the scaling up process and control of spinning parameters for CAHF, post-treatment of the spun fibers, deacetylation to obtain CHF, and drying of regenerated CHF have been challenging processes to obtain the carbon fibers with good mechanical and acceptable permeation properties.

The goal for and novelty of this study was to develop and optimize a pilot-scale production process for the CHF, using a low-priced precursor to generate carbon membranes. The sub-goal for the development of the pilot-scale facility was to achieve CM exhibiting high permeability and selectivity for the CO_2/CH_4 separation for biogas upgrading to vehicle fuel or for natural gas purification (natural gas sweetening). The separation properties of the CM for O_2/N_2 separation were also investigated. The CM from CHF were produced and tested on semi-commercial scale plant by MemfoACT AS (Norway), a company which has now closed down. The plant had a capacity to produce 700 m^2 of carbon hollow fiber membranes per year. The well-known dry/wet spinning method was used to spin the CAHF [18,19] from the dope solution consisting of CA/polyvinylpyrrolidone (PVP)/*N*-methyl-2-pyrrolidone (22.5%/5%/72.5% *w*/*w*/*w*). The spinning parameters, such as dope and bore fluid composition, extrusion rate, spinneret dimensions, air gap, coagulation temperature, take up rate and solvent exchange method, were optimized to achieve maximum yield (based on length, quantity of good fibers, mechanical properties of CHF, and separation properties of resulting CM) of CHF. The CAHF can be deacetylated by exchange of acetyl group with a hydroxyl group using a base catalyst [12]. Various authors have reported the importance of different types of base solutions, concentrations, and the reaction time for deacetylation process [12,20–23]. The deacetylation process is crucial to regenerate CHF with desired structure and properties as a precursor for carbon membrane. However, not much data is available for the pilot-scale deacetylation of CAHF. The deacetylation of CAHF was in our study performed by using NaOH/water/isopropanol solution and different parameters were optimized to enhance the yield of dried precursor CHF. A block diagram for the pilot-scale production of CM from CAHF is shown in Figure 1. As shown in Figure 1, the next challenging step after deacetylation is after-wash/solvent rinsing and drying of the CHF.

The resulting cellulose fibers are more hydrophilic than CAHF and stronger hydrogen bonds are expected between cellulose and water. An efficiently controlled drying process was thus needed to dry these membranes. The natural drying of these membranes at ambient conditions influenced the structure (shrunken, curly, adhered, and/or collapsed fibers) and permeation properties of resulting carbon membranes.

Jie et al. [24] investigated natural drying and solvent exchange drying methods and concluded that ethanol-hexane exchange drying was an appropriate method to produce a membrane with minimum morphology variation. Whereas the natural drying caused the greatest shrinkage of fibers transforming porous membrane into a dense membrane. In this study, various types of additives were tested to explore the appropriate solvent-rinsing process to obtain the maximum yield of CHF after drying and CM after carbonization. The effect of humidity on the drying process, as well as on the permeation properties of resulting carbon membranes were studied, and the process was optimized to obtain both high yield and permeation properties of carbon fibers.

The current research reports the development and optimization of a simple process to scale up the manufacturing of CHF precursor for CM. The information obtained from this research may be used to produce a limited number of CHF (laboratory scale) and several hundred fibers in one cycle (pilot-scale). The reported research discusses the design concept of the process to produce CHF, as well as the performance of resulting carbon hollow fiber membranes at pilot scale.

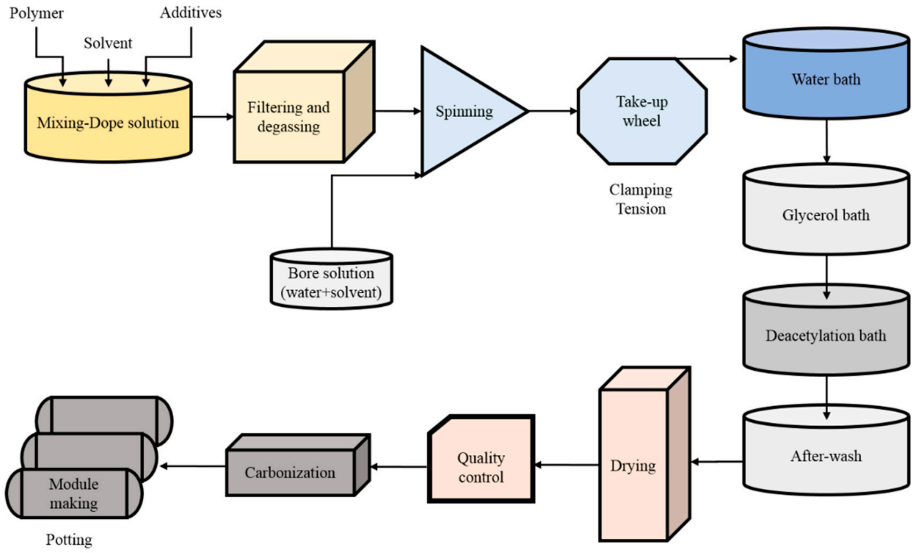

Figure 1. Block diagram for the pilot-scale production process of carbon membrane (CM) from cellulose acetate hollow fibers (CAHF).

2. Materials and Methods

2.1. Materials

Acros Organics (Geel, Belgium) delivered the cellulose acetate (CA:MW 100,000, average acetyl content: 39.8%). *N*-methyl-2-pyrrolidone (NMP:purity > 99.5%) was purchased from Merck, Oslo, Norway. The additive polymer Polyvinylpyrrolidone (PVP:MW 10,000) was purchased from Sigma Aldrich, Oslo, Norway. Ionic exchanged water was used for coagulation and water wash process. Dimethyl sulfoxide (DMSO), Isopropanol, NaOH (>99%), and Glycerol (>98%) were purchased from VWR, Oslo, Norway.

2.2. Dope and Bore Solution Preparation and Filtration

The dope solution (20 kg in each batch) was prepared in a 50 L stainless steel mixing tank by adding 22.5 wt% of cellulose acetate (CA) and 5 wt% of PVP in dry state first and then 72.5 wt% of NMP solvent at room temperature (20–25 °C) was added before start stirring. Some spinning experiments were also performed by using DMSO solvent in the dope solution (replacing the NMP). After mechanical stirring for at least 72 h to ensure homogeneity of the dope solution, it was subsequently left to rest for 24 h to remove air bubbles before filtration process was started. By using 2 bara pressure of N_2 and a gear pump, the dope solution was then forced through polypropylene melt blown filters into a storage tank. Then storage tank was held under a vacuum of −0.6 bara for 30 min to degas the dope solution before the vacuum was released. The dope solution was degassed at 1 atm by resting for at least three days after filtration prior usage. Figure 2 shows the steps followed during the dope formation process.

The bore solution was made in a bottle by adding a solvent (NMP or DMSO) and ionic exchanged water in the desired ratio, and then poured into the bore liquid storage vessel. The bore solution should preferably rest 24 h prior to use. A particle filter was installed in the bore line to avoid any contaminants in the bore solution.

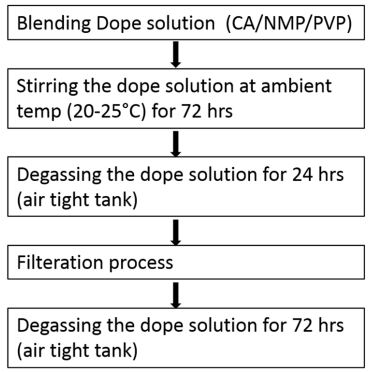

Figure 2. Steps involved in dope formation. CA, cellulose acetate; NMP, *N*-methyl-2-pyrrolidone; PVP, Polyvinylpyrrolidone.

2.3. Spinning of CA Hollow Fibers

A well-known dry/wet phase separation spinning process was used to spin the CA hollow fibers [19,24]. The dope solution and bore fluid were extruded through a tube-in-orifice jet type of spinneret to form a nascent hollow fiber. The extrusion rate of dope and bore fluid was controlled by two separate gear pumps, respectively. Spinnerets with three different sets of inner and outer dimensions (range is shown in Figure 3) were used to spin the hollow fibers. Principal component analysis (PCA) of three different types of spinnerets and resulting fiber yield (CHF and CM) are shown in Figure A1. Principal component analysis (PCA) of three different types of spinnerets and resulting fiber yield of Appendix A. The solvent would then evaporate into a dry environment for a short period (Air gap: 25 mm) before the fiber was immersed in a wet environment (water as external coagulant) in the coagulation bath. For each spinning-session, a continuous fiber length of (at least) 2.4 km was spun and rolled up in three layers on a collecting wheel. The rolled-up fiber was cut into 1200 fibers of 2 m length for each fiber. Altogether, more than 460 spinning-sessions of CA hollow fibers were spun with 50 batches of dope mixture, of which at least 100 sessions were spun by varying spinning conditions, e.g., spinneret dimension, air gap, extrusion rate, coagulation bath temperature, take up speed and different fiber collection methods to optimize the pilot scale production of CA hollow fibers. After optimizing the spinning process, the parameters were kept constant for the rest of the sessions, as shown in Table 1.

The partly coagulated fibers were guided by a wheel from the bottom of the coagulation bath to the godet-bath where some residence time was provided for solvent exchange before they were rolled up on a collection wheel.

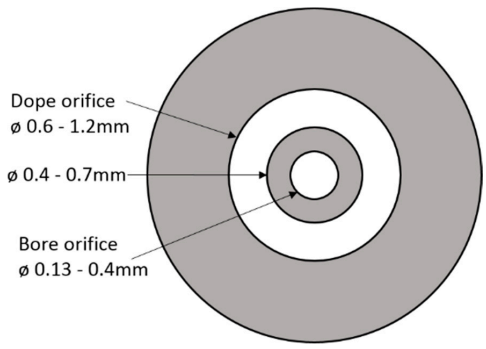

Figure 3. Spinneret type and range of different dimensions used for spinning of CAHF.

Table 1. Optimized parameters for spinning, pre-treatment and carbonization processes.

Parameter	Values	Units
	Dope Solution	
Composition	22.5 CA/5 PVP/72.5 NMP	wt%
flow rate	0.4	L/h
Temperature	RT (20–23)	°C
	Bore Fluid	
Composition	30/35 H_2O–65/70 NMP	vol%
flow rate	0.2	L/h
Temperature	RT (20–23)	°C
	Other Parameters	
Air gap	25	mm
Coagulation medium/T	H_2O/RT (20–23)	°C
Godet bath temperature	25–40	°C
Collection wheel	10	°C
Take up speed	14	m/min
	Post-Treatment	
Water wash	10 °C	24 h
Glycerol wash	7.5 vol% in water (20 °C)	24 h
Deacetylation	0.075 M NaOH (aqueous sol.) diluted with 10 vol% IP	2.5 h
After wash	7.5 wt% glucose (20 °C)	30 min
Drying	T: 40–45 °C, RH: 90% → ambient	16 h
	Carbonization	
Temperature	550–650 °C, 2 h soak	
Medium	N_2 or CO_2	0.7–1.9 L/min

2.3.1. Fiber Collection Methods and Water Wash

Different types of collection methods were tried; however, only two methods that had a great effect on membrane morphology after deacetylation, drying and carbonization, are being reported here.

Squared Collection Wheel

Figure 4 presents the collection methods of CA hollow fibers. Four specially made stands "fiber carrier" were connected on a rotating shaft of the rig in such way that fibers were kept straight on each fiber carrier along the length and a sharp bending radius (avoiding the kink) was provided on the edges of the carrier. In order to promote the solvent exchange, a water bath with the continuous flow was present in such way that each fiber carrier was immersed in the bath while rotating on the shaft. After completion of the spinning process, clamps were applied on both sides/ends of the fiber carrier and fibers were cut (on the bends) with a sharp knife to separate the wheel into 4 individual carriers (nicknamed "Guitars").

These fiber carriers applied some tension on the fibers, but they were designed to allow some contraction of the fibers to occur (sliding bottom part). The clamps on each end of the carrier were adjusted in such way that bore side of the fiber was open to exchange the solvent efficiently during water wash. Allowing some of the solvent exchange in a water bath, the wheel was left rotating for 2 h after clamping and cutting the fibers. The temperature of the water in the water bath was 10 °C. The fibers washed with 10 °C while on collection wheel for two hours and then in the water bath with continuously flowing water overnight gave the same properties as for 30 °C and 3 h wash. The water at 10 °C was easily available, therefore, most of the batches were washed overnight with cold water. Then fiber carriers were removed from the stand and placed in horizontal position in a water bath

overnight so that all fibers were dipped in the bath, but not touching the bottom. A continuous flow (1.5 L/min) of fresh water was supplied to remove the solvent from the bath.

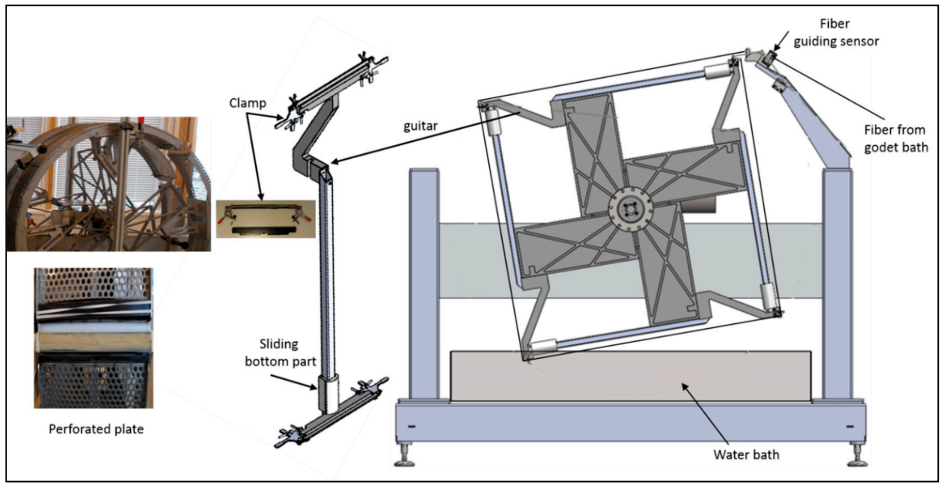

Figure 4. Collection wheel: Four fiber carriers attached to a rotating shaft (right side), perforated plate photos (left side).

Circular Wheel with Perforated Collecting Plate

There is a trade-off between how long time the fiber stays on the wheel (aging by bore solution) and production efficiency, and this may determine the diameter of the collection wheel, the number of fiber layers or the take-up speed. An easy escape of water is favorable as it results in the suppression of macrovoids formation in the CA matrix. To enhance the efficiency of solvent exchange process during spinning process, two perforated circular plates (with the same width (25 cm) as the fiber carriers) were used to collect the fibers. Each plate was making half of the wheel's circumference. A halfpipe made of acrylonitrile butadiene styrene (ABS) tubing (32 mm outer diameter (OD)) was attached to the gap between the perforated plates by 2 elastic bands (GUMA 120 × 8 mm). Foam was pre-fixed (glued in the halfpipe to conduct water). This halfpipe was placed at a level which prevents sharp bending of the collected fibers. A polycarbonate plate and an elastic band were used to make a loose clamp on the edges of each wheel half to ease the fiber endings and allow bore solution to exchange with water, as shown in Figure 4 (left hand side). The other half of the ABS pipe (made in a similar way) was placed on top of the fibers. Fibers were water-washed for 30 min in this way before clamping and moving them on the carriers. On completion of each spinning session, the fibers were transferred to two fiber carriers (2 m long each). Figure 4 shows the photo of such plates and fiber carriers. After clamping fibers on the carriers, they were placed in a horizontal bath for further water wash overnight to promote the removal of the bore solvent.

2.3.2. Glycerol Wash

After water wash, the CA hollow fibers were soaked horizontally in glycerol solution overnight to remove (solvent exchange) the residual NMP in the fibers, and to prevent the largest pores and bore side from collapsing. Different concentrations of 5, 8, 10, and 15 vol% of glycerol in water were studied to see the effect on cellulose fibers, and ultimately carbon fibers, regarding shape and performance of the membrane. The glycerol solution was circulated by a pump in a cross-pattern (the inlet and outlet of the pump were immersed diagonally on opposite sides in the bath) to ensure good mixing and aid the solvent exchange process. The fiber carriers were immersed in the bath in such a way that all fibers were well below the liquid surface, but not touching the bottom of the bath.

2.3.3. Deacetylation

The CAHF were then deacetylated with 90 vol% 0.075 M NaOH (Water) solution diluted with 10 vol% 2-propanol (isopropanol, IP) at ambient temperature for 2.5 h. Different concentrations of NaOH and dilutions of IP were tried, but it was observed that optimized degree of deacetylation of fibers was obtained by the mentioned composition. To improve mass transfer and homogeneous treatment of all fibers, liquid circulation via pumping and shaking of the bath and/or the fiber carriers were applied. It was experienced that the fibers that were not allowed to shrink during deacetylation could not give a CO_2/N_2 selectivity higher than 50 (CO_2 permeability over 100 Barrer), however, fibers allowed to move along fiber carrier length and shrink (typically, 1–3%, during the deacetylation process) improved the permeation properties of the final carbon membrane. Hence the fibers were allowed to move without restriction during deacetylation. The reaction time, concentration of base and temperature were optimized. Two stirrers were used on both ends of the carriers and circulation pump to circulate the solution in a cross-pattern to avoid any stagnant regions for the solution in the bath.

During the deacetylation process, the contact between fibers and also the bottom of the bath should be minimized as it can inhibit the reaction and partial deacetylation may result. This can ultimately destroy the whole fiber quality by making that part brittle after drying. A shaking device was installed on the fiber carriers during deacetylation to avoid the contact between fibers and the bottom of the bath.

2.3.4. Glucose Wash

Deacetylated fibers were immersed in an aqueous solution (T: 20 °C) of 7.5 wt% glucose for 30 min. The glucose solution was circulated using a pump in a cross-pattern to ensure good mixing. Direct drying after glucose wash resulted in sticky fibers. Therefore, fibers were immersed in fresh water (T: 10 °C) after glucose wash for 5 min to reduce the stickiness between the fibers.

2.3.5. Drying

Fibers were dried overnight at room temperature (20–25 °C) in a controlled humidity chamber, as shown in Figure 5. Figure 6 shows photos of fibers in various production states: (a) Fiber carriers during deacetylation, (b) fiber carriers inside drying cabinet, (c) hanging dry fibers and fibers ready for carbonization, and (d) comb to separate the fibers in equal bundles during drying. The fiber carriers were placed vertically (shown in Figure 6) inside the drying cabinet and the lock on the bottom end of the carrier was removed, allowing for shrinking of the fibers. Each fiber carrier contained 1200 fibers of 2 m length in three layers (400 fibers in each layer) and width of the total occupied surface on the carrier was 25 cm. A comb with 10 mm spacing between each tooth was used to further separate the sticky fibers (glucose effect) into equal groups, as the number of fibers in each bundle would determine the drying speed of that bundle. The effect of strand size on shrinkage of dried fiber was also studied. An extra load (averaged to 2.5 g per fiber) was added to the bottom end of the carrier. This acts as a counter force to the shrinking of the fiber clusters and assists in obtaining straight fibers. This extra load had a significant effect on the permeation properties of carbonized fibers, hence, the load was optimized in ordered to get straight fibers with good mechanical and acceptable permeation properties after carbonization.

A systematic investigation of the influences of drying parameters, such as humidity, extra load on the fibers, drying temperature was performed to obtain the straight cellulose fibers with high yield and good mechanical properties. Fibers were quality controlled after drying process by separating the broken, partially deacetylated, too curly, too brittle, and collapsed fibers from the good fibers. The good fibers were hung in bundles at ambient conditions. Storage temperature was reasonably stable, but RH was unstable due to seasonal change and no control of the internal environment. Number of days before loading the furnace for the carbonization process varied from 1–10.

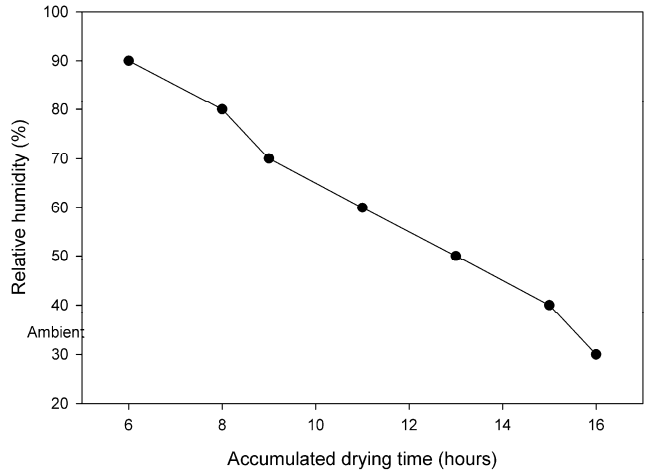

Figure 5. Accumulated time and humidity inside drying cabinet.

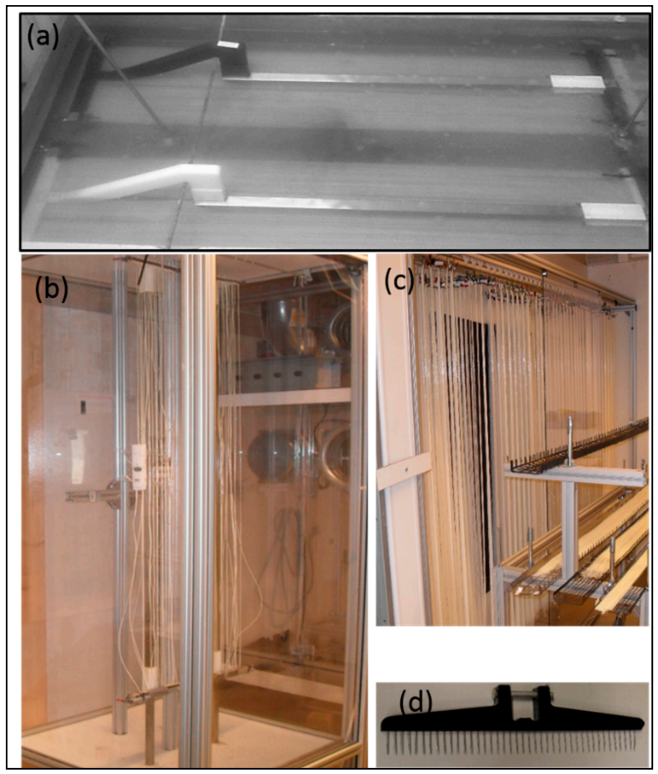

Figure 6. (**a**) Fibers lying in the deacetylation bath. (**b**) Fibers inside drying cabinet. (**c**) Hanging bundles of dry fibers and trolley with steel trays containing dry fibers. (**d**) Comb to split the fibers in equal bundles before drying.

2.3.6. Measurements of Mechanical Properties of Fibers

Tensile strength and elongation at break of the fibers were measured after different production steps (spinning, water wash, deacetylation, and drying). No sophisticated instruments were available

for the measurement of elongation at break and tensile strength of the fibers, therefore, some rough methods were used to get the estimated values for the mechanical properties of the fibers after each production step. For measurement of "elongation at break", a 30 cm long fiber was cut after each production step. The fiber was stretched (medium: Air at room temperature) with fingers above a ruler to see the length when it breaks. Tensile strength was measured by using a cylindrical dynamometer. A single loop of fiber was made around the hook (medium: Air at room temperature) immediately after the production step, and then pulled it with fingers (independent of length of the fiber). The reported values for each fiber were from an average of fourteen fiber samples of seven spinning sessions.

2.4. Carbonization

A tubular horizontal furnace (Carbolite®, three zones split furnace) was used to carbonize the deacetylated hollow fibers. These deacetylated CA hollow fibers were carbonized at 550–650 °C under N_2 or CO_2 flow (0.7–1.9 L/min) using heating rate of 1 °C/min with several dwells and the final temperature of 650 °C for 2 h. Procedure details can be found in the patents [25,26]. The detailed procedure of the pilot-scale module construction for carbon membranes is reported elsewhere [14].

2.5. Permeation Testing

For the permeation experiments discussed here, CM (0.002 m^2) modules were tested in a pilot scale "temperature and pressure rise" permeation set-up with shell side feed configuration. The system was constructed to tolerate medium range pressure single gas tests (CO_2, N_2, O_2). The mass transport properties of CHF were measured with the single pure gases CO_2 and N_2 at 5 bar feed pressure and vacuum (0.1 bar) on the permeate side. Due to fire hazard limitations, CH_4 was not tested at the membrane production facility. However, single gas CH_4 and mixed gas (40% CO_2 in CH_4) experiments were performed in a dedicated field (set-up is described in [27]). The values for CH_4 gas were obtained as: Selectivity $\alpha CO_2/CH_4 = 3 \times \alpha CO_2/N_2$.

He et al. [13] has also performed the mixed gas experiments on carbon membrane (prepared with alike protocol) and results showed that the membrane performance for CO_2 separation is the same or even higher in some cases for mixed gas as compared to single gas separation.

The performance of the membrane was evaluated by measuring the CO_2 permeance in (m^3(STP)/(m^2·h·bar)) and CO_2/N_2 selectivities (α) using Equations (1) and (2). The tests were run continues from several hours to several days, to ensure that the transient phase of diffusion was passed, and a steady state obtained (dp/dt tends to a constant). The gas permeance, P (m^3(STP)/m^2·h·bar) was evaluated using the Equation (1):

$$P = \frac{9.824.V \cdot (dp/dt)}{\Delta P \cdot A \cdot T_{exp}}. \quad (1)$$

Here, V is the permeate side volume (cm^3) that should be measured using a pre-calibrated permeation cell as reported elsewhere [28,29]. However, the permeate side volume for this study was estimated by the tube length and cylinder volume on the permeate side. dp/dt and A are the collection volume pressure increase rate (mbar/s) and total active area of membrane (cm^2) respectively, ΔP (bar) the pressure head and T_{exp} (K) is the temperature for the experiment. The ideal selectivity was defined as the ratio of the pure gas permeances, as shown in Equation (2):

$$\propto_{A/B} = \frac{P_A}{P_B}. \quad (2)$$

3. Results and Discussion

3.1. Effect of Spinning Parameters

Some initial observations during the spinning process were recorded when NMP was replaced by DMSO in the same ratio of the dope solution. For example, extrusion with DMSO as a solvent

and bore fluid H_2O/DMSO 15/85 *v*/*v*% gave higher uptake rate, which indicated greater porosity or less wall thickness. DMSO in bore fluid was also washed out faster than NMP, resulting in a firm and stronger fiber. It was observed that fibers spun at 25–30 °C in coagulation bath gave curly fibers after drying, however, applying 50 °C in the coagulation bath resulted in straight fibers after drying (free-hanging fibers). High temperature improved the mass transfer in coagulation bath and the time before polymer solidification became shorter.

After carbonization of fibers (650 °C, N_2 0.7–1.9 L/min), which were spun on the fiber carriers, they appeared to have an uneven surface and being more brittle than the fibers spun with NMP solvent. Permeance and selectivity were much lower. However, the carbonization of the fibers spun on the circular wheel with perforated plates resulted in a smooth surface and fibers being more flexible (could be looped down to 10 mm diameter). The permeance of these fibers was however so high (macrovoids) that there was no selectivity. Fu et al. [30] spun hollow fibers using a dope solution of DMSO/cellulose acetate butyrate and reported that fibers, when spun at high temperature (50 °C), had higher roughness on the outer surface. However, their membranes spun at 25 °C had a smooth outer surface, due to slow mass transfer rate.

No further experiments were performed with DMSO in the dope solution. Figure 7 shows the scanning electron microscopic (SEM) images of the DMSO based CA hollow fibers. The macrovoids could easily be seen in the walls of the spun CAHF and these fibers did not have enough selectivity. It was observed that it is difficult to mend macrovoids during the carbonization process. Furthermore, chemical vapor deposition (CVD) was used to enhance the performance of prepared carbon membranes and it was concluded that fibers obtained using NMP had better properties compared to fibers prepared using DMSO.

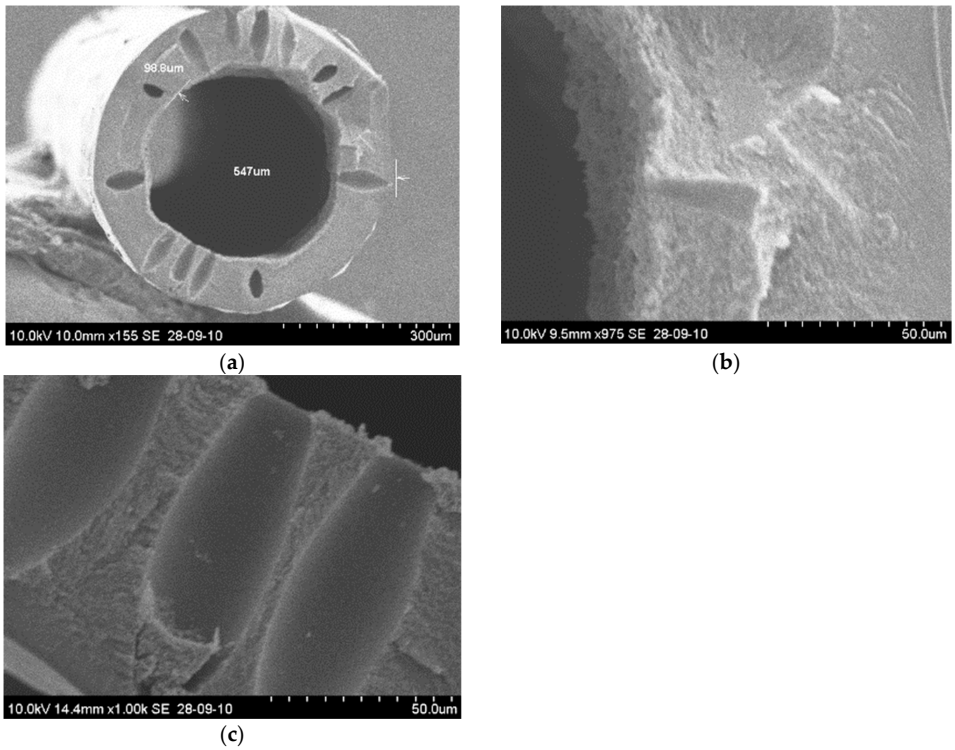

Figure 7. (**a**) CAHF cross section-72.5% dimethylsulfoxide (DMSO) in the dope solution; (**b**) Inner edge of the fiber; (**c**) Macro-voids on the wall magnified.

The rest of the batches were spun using NMP solvent in the dope solution. The CAHF spun with NMP gave high quality fibers with promising permeation properties. The SEM images of NMP based CAHF can be seen in Figure 8. The coagulation bath temperature of 25 °C resulted in the fiber wall more porous on the bore side. Pure water in the bore coagulant results in a thick and dense inner wall, which is not desired as the feed is introduced at the shell side of the fibers and the inner structure is only acting as a support. Bore solution containing up to 70% NMP have successfully been used, resulting in a porous lumen structure of the fiber, which is desired to minimize the gas transport resistance.

The effect of two different bore solvents and their compositions are presented in Figure 9. It can be seen that the membranes spun with 85% DMSO had lowest CO_2 permeability with a CO_2/CH_4 selectivity of 4 as compared to 85% NMP, which had higher permeability, 10 Barrer, and selectivity of 135. Increase in concentration of DMSO improved the permeability of CO_2, but the maximum value measured was 25 Barrer at 95% DMSO in bore fluid. Whereas membranes spun with bore solution containing 65 and 70% of NMP showed CO_2 permeability of 256 Barrer and 144 Barrer with CO_2/CH_4 selectivity of 156 and 172 respectively, as shown in Figure 9.

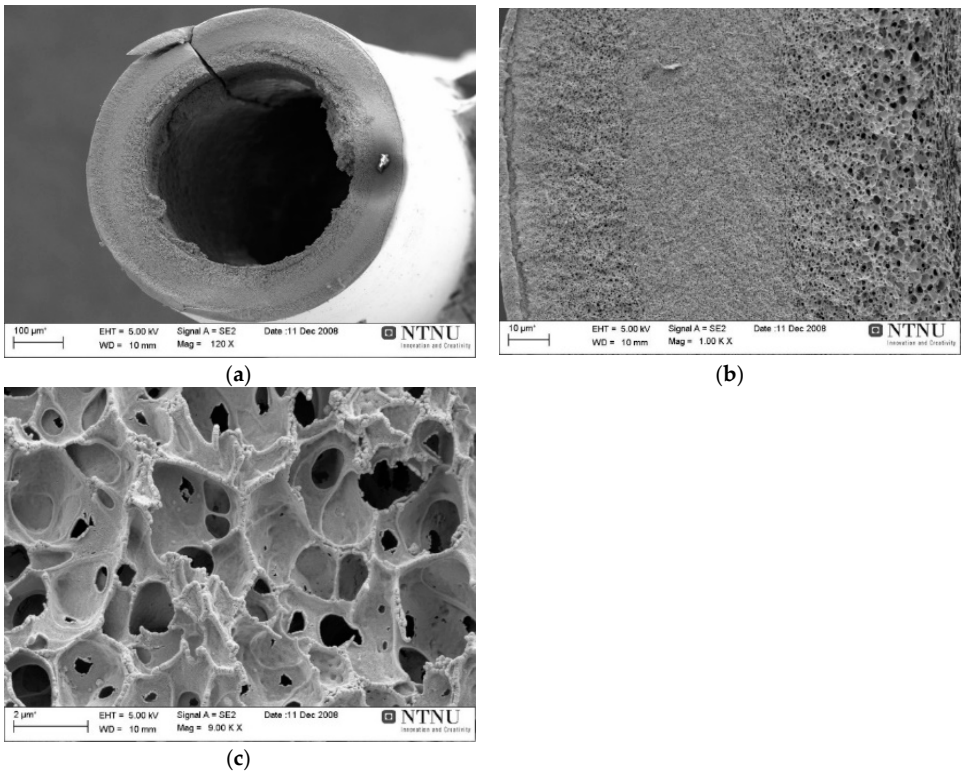

Figure 8. (**a**) CAHF cross-section-72.5% NMP in dope solution; (**b**) Wall magnified; (**c**) Wall inner edge magnified.

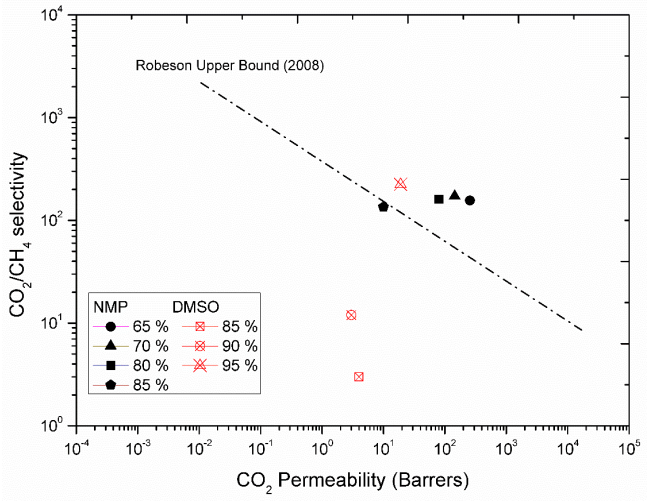

Figure 9. Effect of bore solvent and bore composition on gas permeation properties.

The outer diameter (OD) and wall thickness (WT) of some fiber samples from different spinning-sessions were measured. The length of the vertically hanging fibers were 2 m with the extra load on the bottom during drying, thus the variation in OD and WT of the fibers along fiber length was expected. The OD and WT of CHF and CM were measured at three different positions of the fiber: Top, middle, and bottom. Variation in the values and a mean value with standard deviation is shown in Figure A2 of Appendix A.

3.2. Effect of Water and Glycerol Treatment

To remove the solvent more efficiently with water, different methods were tried: Temperature, circulation with pump and stirring. It was observed that 3 h water wash at 30 °C with circulation gave good gas permeation properties of the membrane after carbonization.

Adsorbing the desired amount of glycerol into the pores of the fibers and increase the temperature (20 °C) helped to improve both the gas permeation properties, as well as mechanical properties of the carbon fibers. Fibers treated with 10 and 20% glycerol solution (circulating) gave carbon membrane with CO_2 permeability below 20 Barrer and CO_2/N_2 selectivity of 40. Similar results were obtained when fibers were not treated with glycerol and in this case, most of the fibers were collapsed after the drying process. However, the CO_2 permeability was above 200 Barrer with a selectivity of 50 for CO_2/N_2 when fibers were soaked in circulating 5 vol% glycerol aqueous solution (T: 20 °C) overnight.

3.3. Effect of Deacetylation

The rate of deacetylation depends on the diffusion velocity of OH^- ions inside the CAHF matrix and substitution reaction rate with an acetyl group. It is expected that the smaller the fiber, the faster the deacetylation. Fibers deacetylated for 2.5 h at ambient temperature gave good mechanical properties after drying and permeation properties above Robeson upper bound 2008 [31] after carbonization. Longer than 2.5 h deacetylation time resulted in a more morphological change in the pores of the fibers and decreased CO_2 permeability after carbonization. The deacetylation parameters for similar kind of process at laboratory scale has been investigated by orthogonal experimental design in a recently published study [32]. Fibers deacetylated for less time than 2.5 h gave brittle and curly fibers after both deacetylation (yield after drying <50% of good fibers) and carbonization. It may be due to the partial deacetylation of CAHF. The fiber surface may be fully deacetylated, however, non/partially deacetylated inner part of the fiber may cause different drying rates on both surfaces which ultimately

would result in curly or brittle fibers. The CO_2 permeability of the subsequent carbon fibers was below 30 Barrer with a CO_2/N_2 selectivity of less than 10. Similar results regarding mechanical and permeation properties of fibers were obtained when deacetylation was conducted in aqueous solution or 5 vol% IP dilution of 0.075 M NaOH for 2.5 h. The surface of the fibers might be deacetylated, but the base molecules could not penetrate the fibers to hydrolyze the inner part. Hence, the resulting dried fibers were brittle and dense. In 90 vol% 0.075 M NaOH solution diluted with 10 vol% Isopropanol solution, the results indicated that the deacetylation was more homogenous and optimal for required permeation properties. This may be due to the swelling of CA with IP, providing a more open structure for the base to penetrate into the fiber. Liu et al. [20] have also observed that deacetylation in an aqueous solution of NaOH, appears to be complete on the fiber surface, making them hydroxyl-rich and leaving an acetyl-rich core. Whereas, in case of NaOH/EtOH solution, base molecules can penetrate the fiber to deacetylate the fiber more homogenously both on the surface and internally.

Due to the high sensitivity of the process, the attempts to lead an optimal deacetylation (instead of full) may deteriorate a uniformity and repeatability in cellulose fibers properties. There are too many parameters starting from non-uniformity of the initial cellulose acetate, external parameters as temp., mixing conditions etc., which may change from batch to batch or even within the same batch. This uncertainty leads to some uncontrolled final chemical composition. The deacetylation in 90 vol% 0.075 M NaOH solution diluted with 10 vol% Isopropanol solution provided dried cellulose fibers possessing good mechanical properties and yield was consistently over 80%. The SEM images of deacetylated hollow fiber are shown in Figure 10. These hollow fibers with optimized deacetylation gave stronger carbon fibers (loop with diameter: 8 mm) with permeation properties above Robeson upper bound 2008.

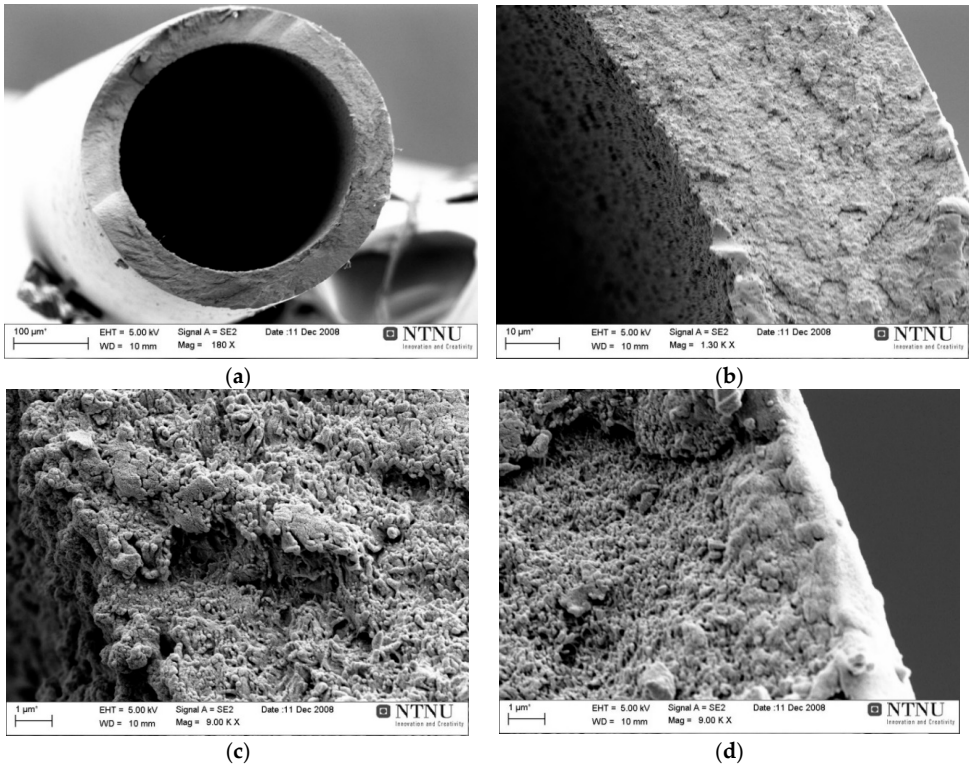

Figure 10. (**a**) Regenerated CHF after deacetylation of CAHF/cross section (**b**) wall magnified (**c**) wall inner edge magnified (**d**) wall outer edge magnified.

3.4. Effect of Glucose Wash

It was important to preserve and protect the natural micro porous structure of cellulose hollow fibers against irreversible collapse, which may occur during the drying process. Direct drying of deacetylated fibers caused the curliness and highest shrinkage (difference in length of fiber when treating with the additive solution and fiber length after drying) of hollow fiber membranes resulting in dense membranes with very low CO_2 permeability. Jie et al. [24] also performed natural drying of cellulose fibers and they found that the membrane was too dense to give any gas permeation after drying.

It was found that cellulose fibers immersed in 7.5% glucose (aqueous) solution gives straight fibers with good mechanical properties after drying. Glucose molecules having suitable size entered most of the micro pores of the cellulose and was entrapped and engrafted easily. Glucose addition provided stiffness to the fibers and minimized the curliness, but had the disadvantage of making the fibers sticky when they were still wet. It might be possible to use some non-stick agents like those used in paper and food industry, but it will then be important that all traces of this product are then burnt off during carbonization and should not affect the gas permeation properties of the fibers. Nine different types of additives and eleven various types of solvents were used both individually and in combination with each other to study their effect on fiber shrinkage. Results are shown in Figure A3. Effect of different solvent treatment (aqueous solutions) (after deacetylation) on shrinkage of dried cellulose fibers—Figure A6 in Appendix A. Glycerol can also be used instead of glucose and it has similar effect on fibers after drying. However, it was observed that drying time increases when several fibers together on a carrier (instead of single fiber) were treated with glycerol. Glycerol with its high viscosity and boiling point accumulates on the bottom part of the fibers and it was hard to obtain homogenously dried fiber. The carbon fibers obtained after glucose treatment had good separation performance and mechanical properties. One theory may be that glucose (structure) behaves like cellulose during carbonization process, which results in carbon fibers with required properties.

3.5. Dry Fibers

The length of the fiber strands varied somewhat depending on their position on the collection wheel. Hence, when the fibers were put on the "fiber carrier" they may not all have the same level of initial tension applied to them.

Dry cellulose fibers (fiber color, length, shape etc.) gave the first hint to how uniformly the fibers were processed. The effect of drying process (using the protocol shown in Figure 5) on different size of the bundles are shown in Figure 11. The results show that fibers with smallest bundle size gave the long and straight fiber after drying due to equal distribution of load at the bottom. The most likely explanation is that the smaller clusters of fibers dried quicker, hence more stretch. The fibers distributed in smaller than 10 mm bundle were longer, but collapsed in the bottom part of the fiber due to too much stress of the load. The bundle size was kept at almost 10 mm to enhance the yield of dried cellulose fibers.

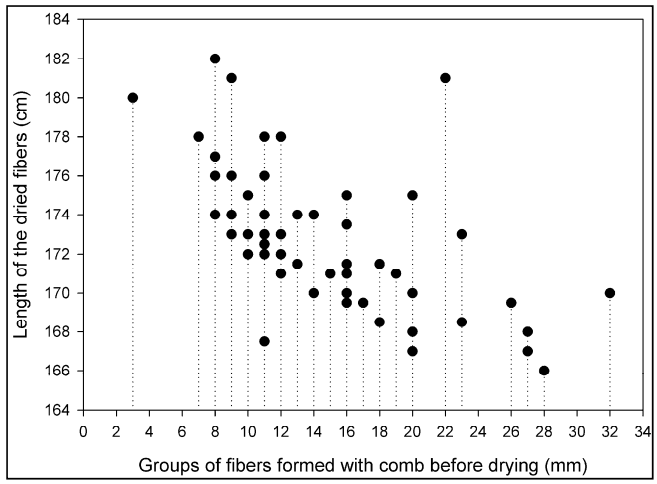

Figure 11. Drying effect on the bundle size of the cellulose fibers.

The effect of relative humidity (RH) is shown in Figure 12. The straightness was graded a visual level range from 1–10, where 10 was very straight fiber and 1 very curly fiber. Useful fibers were defined as those fibers, which could be used for further carbonization process. Figure 12 shows that RH during drying had a direct effect on the straightness and usefulness of the dried cellulose fibers. The fibers dried at RH over 50% at ambient temperature were straight and a high yield was obtained. It was observed that slow drying overnight with RH changing from 90 to ambient maximized the yield of the dried cellulose fibers. Figure 13 presents the yield of 460 spinning sessions of cellulose fibers dried using the drying protocol, as shown in Figure 5.

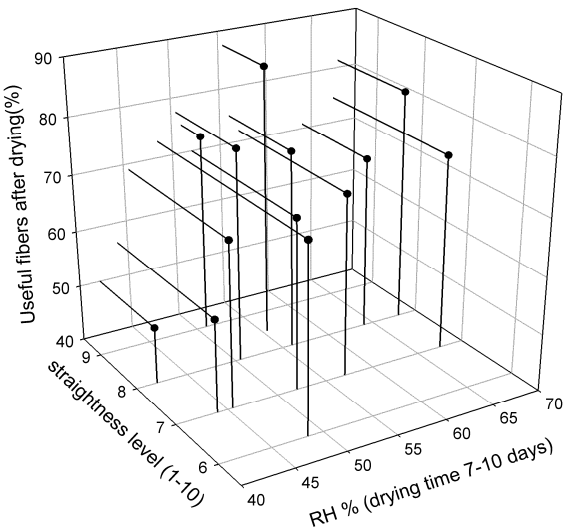

Figure 12. Effect of humidity on straightness and usefulness of the dried cellulose fibers. RH, relative humidity.

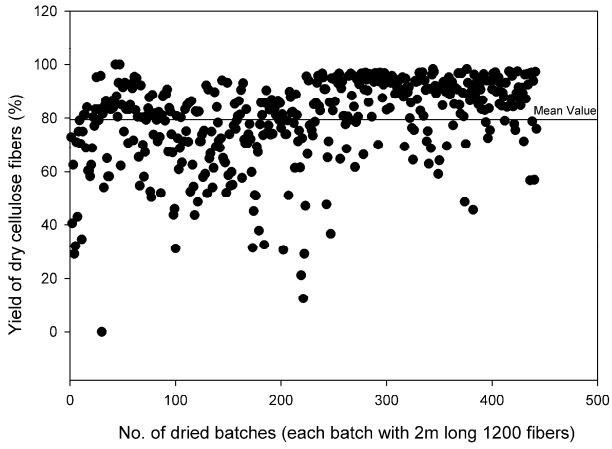

Figure 13. Yield (%) of 460 spinning-sessions of dried cellulose: RH (90–40%) and Temp (20–25 °C).

Mechanical properties of fibers after different production steps are shown in Figure 14. It shows that fibers after drying, possessed a maximum value of 1.9 N for tensile strength and minimum value 35% for elongation at break. Whereas the fibers after deacetylation, water wash, and glucose wash, showed minimum tensile strength, which was almost half of the value compared to the fibers just after spinning. The maximum value of elongation at break was measured after glucose treatment.

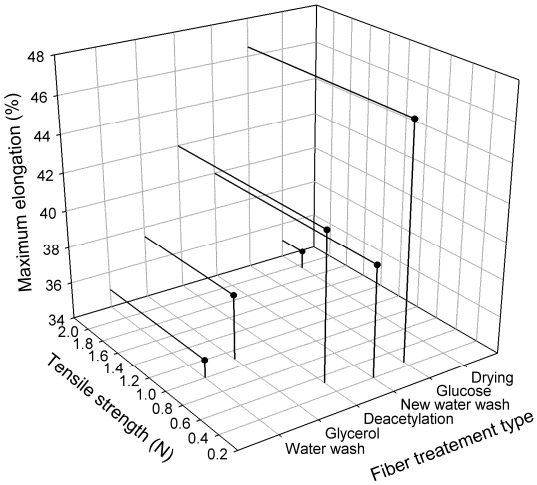

Figure 14. Mechanical properties of fiber after different production steps.

3.6. Carbonization and Gas Permeation Results

The final good carbon fibers should not be perfectly straight, but preferably having waves (i.e., wavelength > 10 cm) in order to (i) improve the gas flow pattern in the module, and to (ii) handle thermal expansion or shrinkage without breakage. However, curls (bends with a diameter less than 5 cm, i.e., ca 2× bundle diameter), kinks and loops must be eliminated. Gas permeation results of some batches dried at different RH are shown in Figure 15. These are small scale modules with an effective area of 0.002 m^2 for each module. Details about pilot scale module construction, gas permeation performance and pore tailoring of the membranes after carbonization are reported elsewhere [14,33]. It was observed that fibers dried in RH: 65% → 35% when drying overnight at ambient temperature

(23 °C) produced lowest number of carbon fibers. However, the gas permeation properties of these fibers were better compared to the fibers dried in RH: 55% → 35%. The maximum number of good fibers possessing both high gas permeation properties and mechanical properties were obtained at RH: 85% → 35%. These results indicate that slow drying of fibers at high RH humidity prevents the pore structure of dried cellulose fibers. It could be because along the cellulose fiber, water exists in two states: As bonded water (strong hydrogen bonds with cellulose molecules) and as free water (surrounded by the bonded water and no contact with the cellulose molecules). In the natural drying at lower RH: 55% → 35%, the water evaporated quite fast and the water-cellulose bonds were strong enough to pull the cellulose structure in a region with more dense/collapsed structure. However, in slow drying at higher RH: 85% → 35%, it could be that the hydrogen bonds of water-cellulose pulled the cellulose structure closer and closer until new hydrogen bonds between cellulose chains were formed, and keeping the pores structure stable as the free water evaporated gradually.

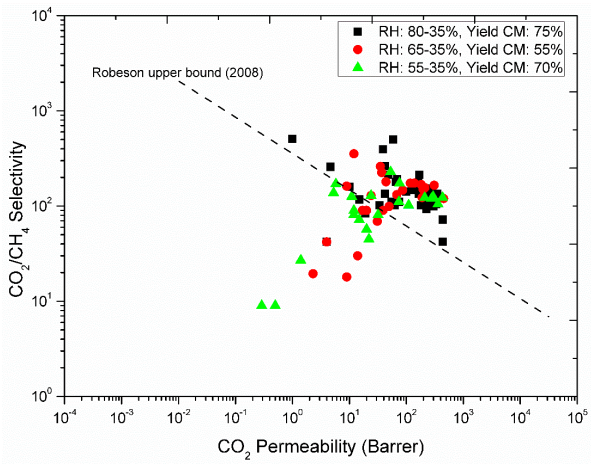

Figure 15. Gas permeation properties of carbon hollow fibers from regenerated cellulose precursor (RH: 80–35%; Black squares, RH: 65–35%; Red circles, RH: 55–35%; green triangles).

4. Conclusions

A pilot-scale system to produce regenerated cellulose hollow fiber membrane is reported in the current study. These regenerated CHF were used as precursors to produce high performance carbon membranes. Asymmetric CAHF with average outer diameter 515 μm and a wall thickness of 85 μm were spun in a dry/wet spinning process. The effect of DMSO and NMP as solvents in dope solution was studied. It was found that fibers spun with DMSO contain macrovoids on the wall. However, the fibers spun with NMP gave high quality fibers with promising (above Robeson upper bound 2008) gas permeation properties. The influence of DMSO and NMP as bore solvent on gas permeation properties was also reported. It was found that the increase in the concentration of DMSO improves the permeability of CO_2, but the maximum value measured was 25 Barrer at 95% DMSO in bore fluid. Whereas, membranes spun with bore solution containing 65% and 70% of NMP showed CO_2 permeability of 256 Barrer and 144 Barrer with CO_2/CH_4 selectivity of 156 and 172 respectively. The spun-CAHF underwent water wash and glycerol treatment to prevent the pores before they were transformed into regenerated cellulose through deacetylation process. It was found that fibers water washed overnight and then treated with 5% glycerol (aqueous) solution overnight give high performance carbon membranes with good mechanical properties. The deacetylation process was optimized by adjusting the different parameters (NaOH concentration, type of solvent, temperature, stirring, reaction duration, etc.) to achieve cellulose fibers with high yield on a pilot scale system. Optimized deacetylation of spun-CA hollow fibers (CAHF) was achieved by using 90 vol%

0.075 M NaOH aqueous solution diluted with 10 vol% Isopropanol for 2.5 h at ambient temperature. The number of collapsed and curly fibers were reduced with minimum shrinkage after drying process by the treatment of 7.5% glucose after deacetylation process. Drying conditions (temperature, relative humidity, rate of drying, stretch in fiber during drying) were optimized to achieve maximum (>95%) number of successful cellulose fibers. Relative humidity (RH) protocol for drying was improved after an investigation of different RH experiments. Separation performance results showed that RH changing from 80% to 35% at room temperature overnight gave maximum separation (above Robeson upper bound 2008) performance for the subsequent carbon hollow fibers. Tensile strength and maximum elongation of fibers were measured after each treatment. The pilot scale results showed that high performance carbon membranes can be made from regenerated cellulose (a relatively inexpensive precursor). This work identifies bottlenecks required for different unit operations in the preparation of a precursor for a carbon membrane with acceptable properties.

Author Contributions: S.H., J.A.L. and A.L. performed the experiments. S.H. wrote the manuscript and all authors contributed substantially to the revision of the manuscript.

Funding: This research work is gathered over the years by the support of different funding sources, among others, Norwegian Research Council and Innovation Norway.

Acknowledgments: The authors are very grateful to John Anders Hamnes for excellent work on the spinning of hollow fiber membranes. The authors would also like to thank The Department of Chemical Engineering at NTNU for providing the possibility to work with this article.

Conflicts of Interest: The authors declare no conflict of interest.

Appendix A.

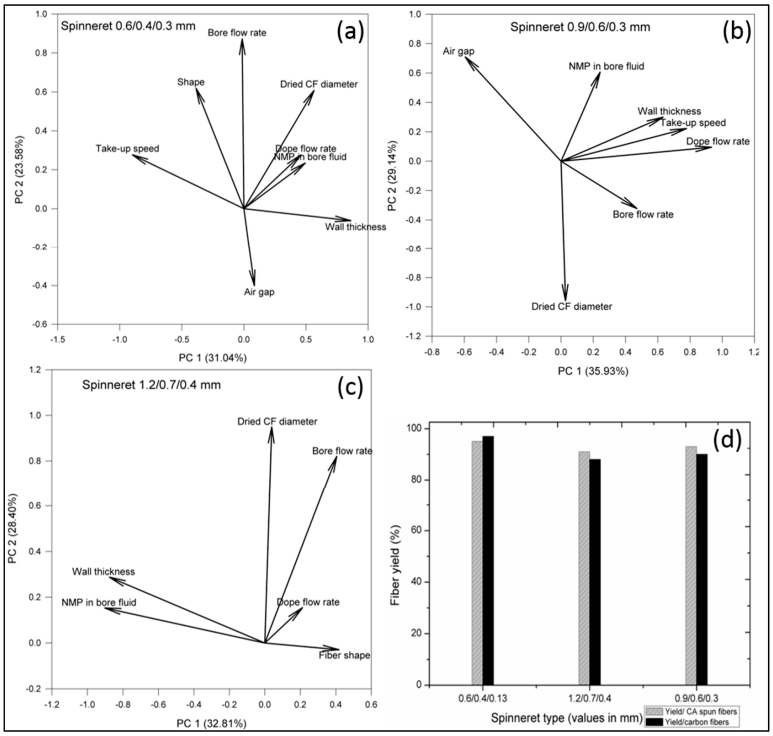

Figure A1. Principal component analysis (PCA) of three different types of spinnerets and resulting fiber yield.

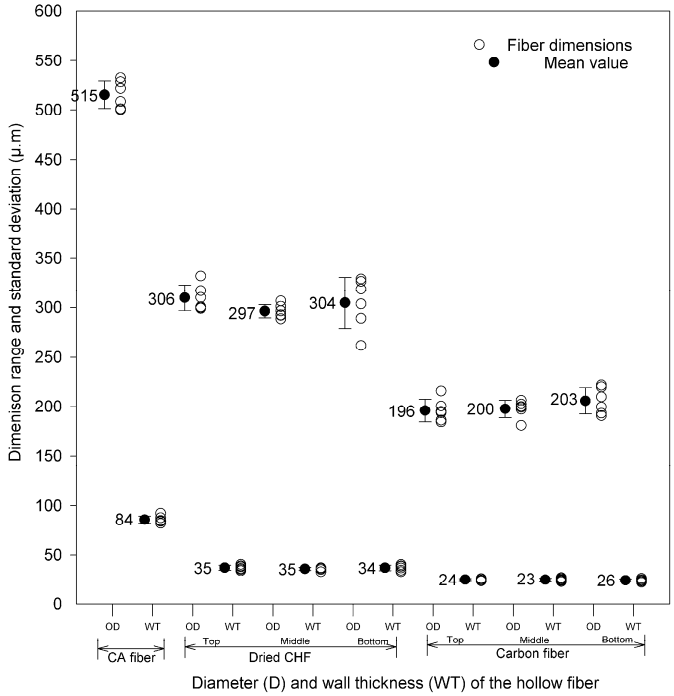

Figure A2. Outer diameter (OD) and wall thickness (WT) of CAHF, CHF, and CM at different positions of the fiber.

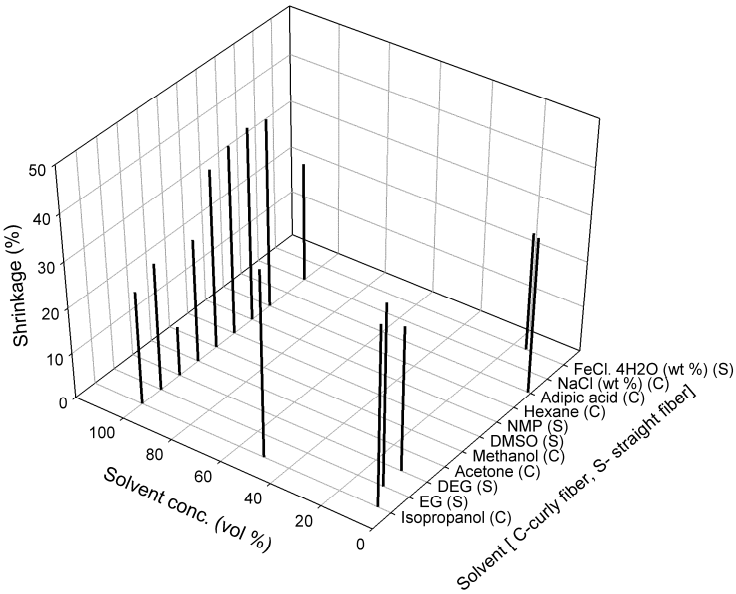

Figure A3. Effect of different solvent treatment (aqueous solutions) (after deacetylation) on shrinkage of dried cellulose fibers.

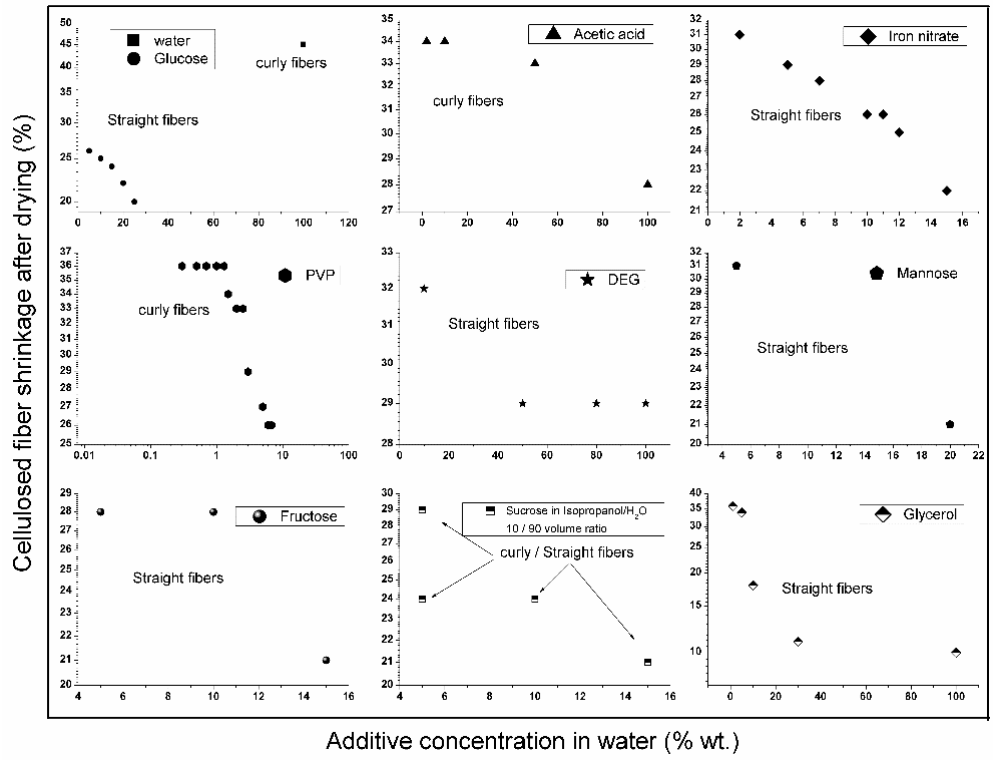

Figure A4. Effect of different additives (after deacetylation) on shrinkage of dried cellulose fibers.

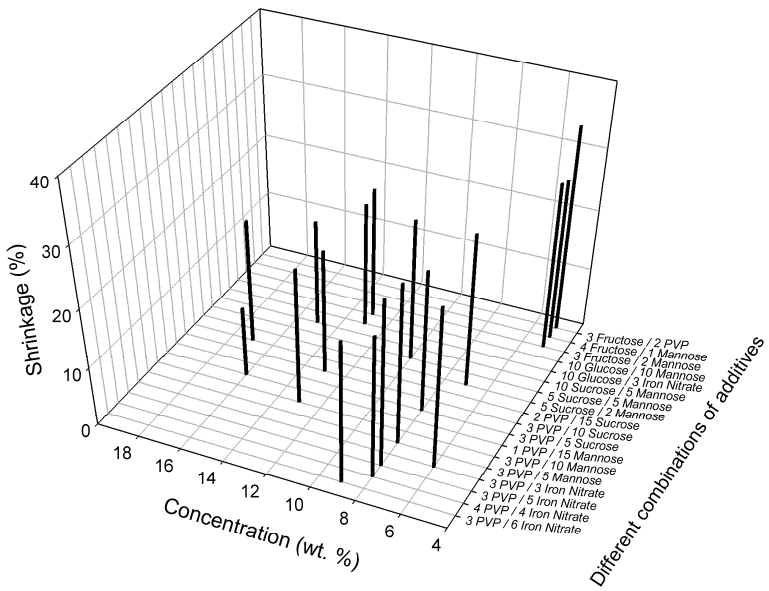

Figure A5. Combination of different additives (after deacetylation) effecting the shrinkage of dried cellulose fibers.

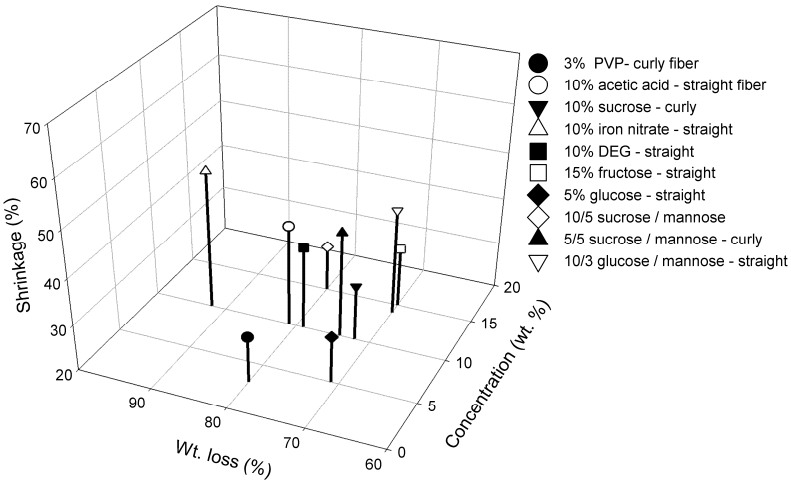

Figure A6. wt% loss and shrinkage after carbonization process when different additives were used after deacetylation.

References

1. Ash, R.B.; Baker, R.W.; Barrer, R.M. Sorption and surface flow in graphitized carbon membranes—I. The steady state. *Proc. R. Soc. Lond. Ser. A Math. Phys. Sci.* **1967**, *299*, 434–454. [CrossRef]
2. Aylmore, L.A.G.; Barrer, R.M. Surface and volume flow of single gases and of binary gas mixtures in a microporous carbon membrane. *Proc. R. Soc. Lon. Ser. A Math. Phys. Sci.* **1966**, *290*, 477–489. [CrossRef]
3. Koresh, J.E.; Sofer, A. Molecular sieve carbon permselective membrane. Part I. Presentation of a new device for gas mixture separation. *Sep. Sci. Technol.* **1983**, *18*, 723–734. [CrossRef]
4. Soffer, A.; Gilron, J.; Saguee, S.; Hed-Ofek, R.; Cohen, H. Process for the Production of Hollow Carbon Fiber Membranes. Patents EP0671202B1, 4 July 1995.
5. Sun, N.; Swatloski, R.P.; Maxim, M.L.; Rahman, M.; Harland, A.G.; Haque, A.; Spear, S.K.; Daly, D.T.; Rogers, R.D. Magnetite-embedded cellulose fibers prepared from ionic liquid. *J. Mater. Chem.* **2008**, *18*, 283–290. [CrossRef]
6. Lie, J.A.; Hägg, M.-B. Carbon membranes from cellulose: Synthesis, performance and regeneration. *J. Membr. Sci.* **2006**, *284*, 79–86. [CrossRef]
7. Kawamoto, H.; Murayama, M.; Saka, S. Pyrolysis behavior of levoglucosan as an intermediate in cellulose pyrolysis: Polymerization into polysaccharide as a key reaction to carbonized product formation. *J. Wood Sci.* **2003**, *49*, 469–473. [CrossRef]
8. Idris, A.; Ismail, A.F.; Shilton, S.J. Optimization of cellulose acetate hollow fiber reverse osmosis membrane production using Taguchi method. *J. Membr. Sci.* **2002**, *205*, 223–237. [CrossRef]
9. Cao, S.; Shi, Y.; Chen, G. Influence of acetylation degree of cellulose acetate on pervaporation properties for MeOH/MTBE mixture. *J. Membr. Sci.* **2000**, *165*, 89–97. [CrossRef]
10. Shieh, J.-J.; Chung, T.S. Effect of liquid-liquid demixing on the membrane morphology, gas permeation, thermal and mechanical properties of cellulose acetate hollow fibers. *J. Membr. Sci.* **1998**, *140*, 67–79. [CrossRef]
11. Puleo, A.C.; Paul, D.R.; Kelley, S.S. The effect of degree of acetylation on gas sorption and transport behavior in cellulose acetate. *J. Membr. Sci.* **1989**, *47*, 301–332. [CrossRef]
12. Yamashita, Y.; Endo, T. Deacetylation behavior of binary blend films of cellulose acetate and various polymers. *J. Appl. Polym. Sci.* **2006**, *100*, 1816–1823. [CrossRef]
13. He, X.; Lie, J.A.; Sheridan, E.; Hägg, M.-B. Preparation and characterization of hollow fiber carbon membranes from cellulose acetate precursors. *Ind. Eng. Chem. Res.* **2011**, *50*, 2080–2087. [CrossRef]
14. Haider, S.; Lindbråthen, A.; Lie, J.A.; Andersen, I.C.T.; Hägg, M.-B. CO_2 separation with carbon membranes in high pressure and elevated temperature applications. *Sep. Purif. Technol.* **2018**, *190*, 177–189. [CrossRef]

15. He, X.; Hägg, M.-B. Structural, kinetic and performance characterization of hollow fiber carbon membranes. *J. Membr. Sci.* **2012**, *390–391*, 23–31. [CrossRef]
16. He, X.; Hägg, M.-B. Hollow fiber carbon membranes: Investigations for CO_2 capture. *J. Membr. Sci.* **2011**, *378*, 1–9. [CrossRef]
17. He, X.; Hägg, M.-B. Hollow fiber carbon membranes: From material to application. *Chem. Eng. J.* **2013**, *215–216*, 440–448. [CrossRef]
18. Jie, X.; Cao, Y.; Lin, B.; Yuan, Q. Gas permeation performance of cellulose hollow fiber membranes made from the cellulose/*N*-methylmorpholine-*N*-oxide/H_2O system. *J. Appl. Polym. Sci.* **2004**, *91*, 1873–1880. [CrossRef]
19. Qin, J.-J.; Li, Y.; Lee, L.-S.; Lee, H. Cellulose acetate hollow fiber ultrafiltration membranes made from CA/PVP 360 K/NMP/water. *J. Membr. Sci.* **2003**, *218*, 173–183. [CrossRef]
20. Liu, H.; Hsieh, Y.-L. Ultrafine fibrous cellulose membranes from electrospinning of cellulose acetate. *J. Polym. Sci. Part B Polym. Phys.* **2002**, *40*, 2119–2129. [CrossRef]
21. Son, W.K.; Youk, J.H.; Lee, T.S.; Park, W.H. Electrospinning of ultrafine cellulose acetate fibers: Studies of a new solvent system and deacetylation of ultrafine cellulose acetate fibers. *J. Polym. Sci. Part B Polym. Phy.* **2004**, *42*, 5–11. [CrossRef]
22. Olaru, N.; Olaru, L. Cellulose acetate deacetylation in benzene/acetic acid/water systems. *J. Appl. Polym. Sci.* **2004**, *94*, 1965–1968. [CrossRef]
23. Yamashita, Y.; Endo, T. Deterioration behavior of cellulose acetate films in acidic or basic aqueous solutions. *J. Appl. Polym. Sci.* **2004**, *91*, 3354–3361. [CrossRef]
24. Jie, X.; Cao, Y.; Qin, J.-J.; Liu, J.; Yuan, Q. Influence of drying method on morphology and properties of asymmetric cellulose hollow fiber membrane. *J. Membr. Sci.* **2005**, *246*, 157–165. [CrossRef]
25. Lie, J.A.; Hägg, M.-B. Carbon Membranes. Patent US20100162887 A1, 1 July 2010.
26. Sheridan, T.B.E.; Lie, J.A.; Hägg, M.-B. Carbon Membranes from Cellulose Esters. Patent US8394175 B2, 20 March 2013.
27. He, X. Development of Hollow Fiber Carbon Membranes for CO_2 Separation. Ph.D. Thesis, Norwegian University of Science and Technology, Trondheim, Norway, 2011.
28. Lin, W.-H.; Vora, R.H.; Chung, T.-S. Gas transport properties of 6fda-durene/1,4-phenylenediamine (ppda) copolyimides. *J. Polym. Sci. B Polym. Phys.* **2000**, *38*, 2703–2713. [CrossRef]
29. Lie, J.A. Synthesis, Performance and Regeneration of Carbon Membranes for Biogas Upgrading—A Future Energy Carrier. Ph.D. Thesis, Norwegian University of Science and Technology, Trondheim, Norway, 2005.
30. Fu, X.Y.; Sotani, T.; Matsuyama, H. Effect of membrane preparation method on the outer surface roughness of cellulose acetate butyrate hollow fiber membrane. *Desalination* **2008**, *233*, 10–18. [CrossRef]
31. Robeson, L.M. The upper bound revisited. *J. Membr. Sci.* **2008**, *320*, 390–400. [CrossRef]
32. He, X. Optimization of deacetylation process for regenerated cellulose hollow fiber membranes. *Int. J. Polym. Sci.* **2017**, *2017*, 3125413. [CrossRef]
33. Haider, S.; Lindbråthen, A.; Hägg, M.-B. Techno-economical evaluation of membrane based biogas upgrading system: A comparison between polymeric membrane and carbon membrane technology. *Green Energy Environ.* **2016**, *1*, 222–234. [CrossRef]

Appendix F

Paper II

Pilot – scale production of carbon hollow fiber membranes from regenerated cellulose precursor: Part II- Carbonization procedure

Paper published in Membranes Journal 8(2018) 105

membranes

MDPI

Article

Pilot–Scale Production of Carbon Hollow Fiber Membranes from Regenerated Cellulose Precursor-Part II: Carbonization Procedure

Shamim Haider, Jon Arvid Lie, Arne Lindbråthen and May-Britt Hägg *

Department of Chemical Engineering, Norwegian University of Science and Technology (NTNU), 7491 Trondheim, Norway; haider@ntnu.no (S.H.); jonarvidlie@gmail.com (J.A.L.); arne.lindbrathen@ntnu.no (A.L.)

* Correspondence: may-britt.hagg@ntnu.no; Tel.: +47-93080834

Received: 17 September 2018; Accepted: 12 October 2018; Published: 15 October 2018

Abstract: The simultaneous carbonization of thousands of fibers in a horizontal furnace may result in fused fibers if carbonization residuals (tars) are not removed fast enough. The optimized purge gas flow rate and a small degree angle in the furnace position may enhance the yield of high quality carbon fibers up to 97% by removing by-products. The production process for several thousand carbon fibers in a single batch is reported. The aim was developing a pilot-scale system to produce carbon membranes. Cellulose-acetate fibers were transformed into regenerated cellulose through a de-acetylation process and the fibers were carbonized in a horizontally oriented three-zone furnace. Quartz tubes and perforated stainless steel grids were used to carbonize up to 4000 (160 cm long) fibers in a single batch. The number of fused fibers could be significantly reduced by replacing the quartz tubes with perforated grids. It was further found that improved purge gas flow distribution in the furnace positioned at a 4-degree to 6-degree angle permitted residuals to flow downward into the tar collection chamber. In total, 390 spun-batches of fibers were carbonized. Each grid contained 2000–4000 individual fibers and these fibers comprised four to six spun-batches of vertically dried fibers. Gas permeation properties were investigated for the carbon fibers.

Keywords: molecular sieve; regenerated cellulose; carbonization process; gas separation

1. Introduction

Polymeric membrane-based gas separation process had already been proven commercially [1,2] when Koresh and Soffer [3–6] produced and reported the first carbon molecular sieve (CMS) membranes in the 1980s. Although polymeric membranes still dominate the market for gas separation due to a low production cost [1,7], the applications of these membranes are restricted by fairly low performance (meaning the inevitable trade-off between selectivity and permeability [7]) and usually poor chemical and thermal resistance. On the contrary, carbon membranes prepared from their polymeric precursor membrane have shown both excellent separation performance as well as thermal and chemical resistance when investigated in different applications [8–12].

Since CMS are a relatively new class of membranes, most of the reported research is done on a laboratory scale [10,13–23] and there are limited data available on commercial success [24,25]. The major challenges to commercially produce these membranes are that most of the precursors being used (polyimides, polyetherimide, phenolic resin etc. [26]) are relative expensive materials or are obtained only at a laboratory scale. They have low mechanical strength (especially shear strength) and high production cost [27]. The aim of this study was to develop a cheaper process to produce CMS membranes on a pilot-scale. Cellulose esters and in particular cellulose acetate (CA) have a

relatively low cost and have been widely used in the membrane industry [28,29]. However, direct carbonization of CA results in discontinuous carbon (more like a powder) since the intermediate product levoglucosane [30] is not formed during carbonization. Hence, the CA must be deacetylated to form "regenerated cellulose" after the membrane casting process, e.g., the dry-wet spinning process. In 1995, Soffer et al. [31] patented the protocol for the carbonization of cellulose precursor. Carbon Membranes Ltd. (Arava, Israel) produced cellulose-based carbon hollow fiber modules on a pilot scale to successfully recover SF_6 in dielectric environments, but the company was closed after a few years [24,32,33].

CMS membranes from regenerated cellulose precursor have shown excellent gas permeation properties on both the lab and pilot scale [13,14,18,25,34–36]. MemfoACT AS (Trondheim, Norway), which is a company that has closed down, produced regenerated cellulose-based carbon membranes on semi-commercial plant using a multi-step production method (spinning of CA fibers, solvent-exchange, deacetylation, solvent-rinsing, drying, carbonization, module construction, and gas permeation testing) [12].

Carbonization is a critical step in the process of forming carbon membranes and the resulting pore structure (which depends on the carbonization steps and morphology of precursor) will determine the separation properties of the resulting membrane. The gases and tars liberated upon carbonization depend on the chemical composition of the precursor and can include CO_2, CO, H_2, N_2, NOx, and H_2O. A carbon residue is also formed by condensation of polynuclear aromatic compounds and expulsion of side chain groups [37]. If these by-products are not removed fast enough, they can deposit it in the carbon matrix, which makes it denser (very low flux) and, in the case of thousands of fibers, they may fuse together [38].

Generally, the carbonization furnace is used in horizontal orientation with one or three heating zones and a quartz tube reaction chamber. The loading of thousands of hollow fibers in a horizontal quartz tube would result in fused fibers (unusable) because of uneven distribution of purge gas flow (described below) in the tube and then residual products staying under the fibers makes them stick together.

To overcome the problem of fused fibers, Karvan et al. [39] tested a pilot-scale system with a vertically oriented furnace to carbonize the precursor hollow fibers. They carbonized 242 fibers using a "loop system" to suspend the fibers individually in the vertical position to reduce the possibility of fibers contacting during carbonization and to promote the flow of purge gas and by products. The maximum survival rate of fibers was 93% and the rest of the fibers were broken on the top. The fiber broke due to softening of the material, which transitioned from glassy to the rubbery state. These fibers had 66% lower permeance of CO_2 and 16% decreased CO_2/CH_4 selectivity when compared to their laboratory/bench scale carbon hollow fibers.

The production process for several thousand carbon fibers in a single batch is being reported for the first time ever. MemfoACT AS carbonized regenerated hollow fibers in a 3-zone horizontal furnace. They used different types of perforated stainless-steel flat trays to carbonize up to 4000 (160 cm long) fibers in a single batch with maximum survival of 95%. Fiber shrinkage during carbonization was 30% to 35%. The permeation properties of carbonized fibers were almost similar or even higher in some batches when compared to the lab-scale process. In total, 390 spun batches of fibers were carbonized using quartz tubes and perforated plates to investigate and enhance the survival rate of carbonized fibers. The purge gas flow distribution in all directions of the fibers was clearly improved by using perforated plates. Hence, the aim of the research by MemfoACT AS was to use a relatively inexpensive, environmentally-friendly membrane material (CA) to make carbon membranes at a semi-industrial scale with maximum successful fibers and acceptable gas separation performance. However, the focus of this paper is more on the carbonization process that was used by MemfoACT AS and briefly describes the precursor preparation. The performance of produced CM and the survival rate of each batch is also reported. Predicting the cost of carbon membrane modules is difficult because of the lack of commercial precedent. Polymeric hollow-fiber membranes are assumed to cost

roughly \$20–50/m^2. The cost of carbon membranes is far more uncertain. It is expected that carbon membranes cost between one-order and three-orders of magnitude more per unit of the membrane area compared to polymeric membranes [1,40,41]. This would make the range a rather daunting \$200–50,000/m^2. However, the goal of MemfoACT was to produce regenerated cellulose-based carbon membranes in the range of \$100–200/m^2. The details about the production cost and techno-economic feasibility of CM-based on a pilot scale production price has been discussed in our previously reported work [25,27,42].

2. Experimental

2.1. Preparation of Precursor Fibers

A dope solution consisting of CA, *N*-methylpyrrolidone (NMP), and polyvinylpyrrolidone (PVP, M_W 10,000 from Sigma Aldrich, Oslo, Norway) (CA 22.5%/NMP 72.5%/PVP 5%, all *w*/*w*) was prepared. A bore solution consisting of water/NMP in different ratios was used as an internal coagulant while water at 50 °C was used as an external coagulant for the spun fibers. A well-known dry/wet spinning process was used on a pilot scale spinning set up, delivered by Philos Korea, to spin the CA hollow fibers. Each batch consisted of 2 m long 1200 fibers. The fibers were treated with aqueous solution of glycerol for 24 h to completely wash out the bore solvent from the fibers and to preserve the porosity of the fibers. To deacetylate CA fibers, they were then immersed for 2.5 h in a 90 vol % 0.075 M NaOH aqueous solution diluted with 10 vol % Isopropanol. The regenerated cellulose fibers were treated with 7.5% glucose solution (aqueous) for 30 min to reduce the shrinkage and curliness of fibers after the drying process. The number of days before loading the furnace for the carbonization process varied from 1 to 10. Figure 1 shows the schematic diagram of the hollow fiber spinning process.

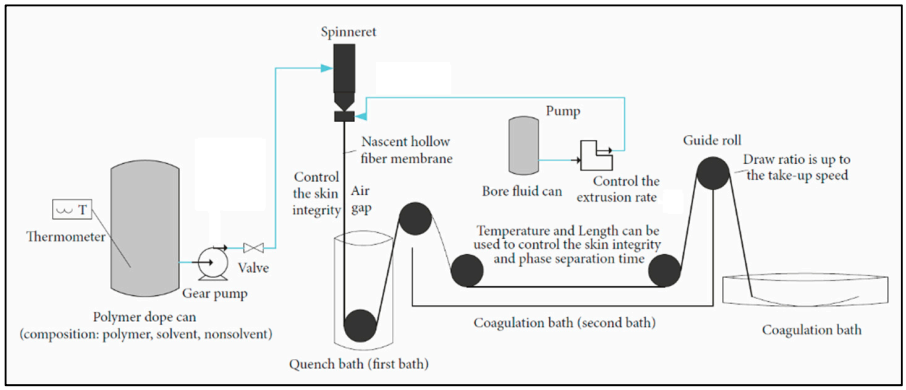

Figure 1. Schematic diagram of the hollow fiber spinning process.

2.2. Fiber Loading in the Furnace and Carbonization Procedure

2.2.1. Description of the Furnace

The furnace used in this work was specifically made (Model: Carbolite special HZS 12/150/2400, bought from VWR International AS, Hope Valley, England) with three independently controlled heating zones. A custom-built stand under the furnace was used to adjust the height accordingly. The height of the furnace could be adjusted independently on each end. The drawing of the furnace is shown in Figure 2. A quartz tube with outer diameter (OD) of 150 mm, 5 mm wall thickness, and 3000 mm in length and seven smaller quartz tubes with 34 mm OD, 2 mm wall thickness, and 2700 mm in length were purchased from Chemi-Teknik AS, Oslo, Norway. One end of the bigger tube was sealed with gasket and stainless-steel flange. However, the other end was used for loading/unloading of

the small quartz tubes and gas inlet/outlet connections. Glass wool (can withstand 800 °C) was used for an insulation purpose and was provided by Rockwool Colnite AS, Oslo, Norway. Gaskets and stainless-steel clamps as well as cup/flanges were custom-built in the workshop of Norwegian university of Science and Technology. A complete drawing of the furnace system is presented in Figure 3 along with photographs of the furnace. Gas flow controllers were bought from Aalborg USA and gases were delivered by Yara Praxair AS, Trondheim, Norway.

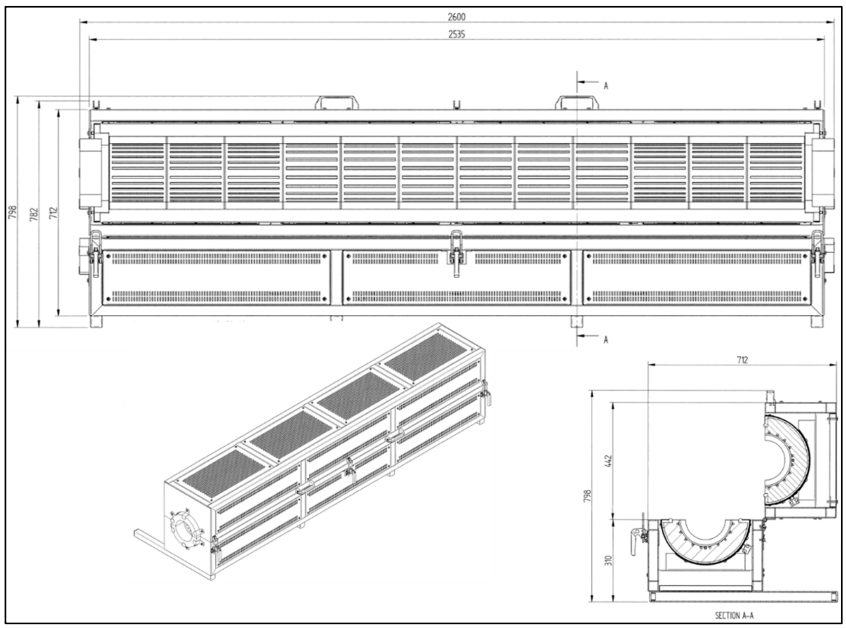

Figure 2. Drawing of 3-zone furnace with dimensions (mm) (Source: Carbolite).

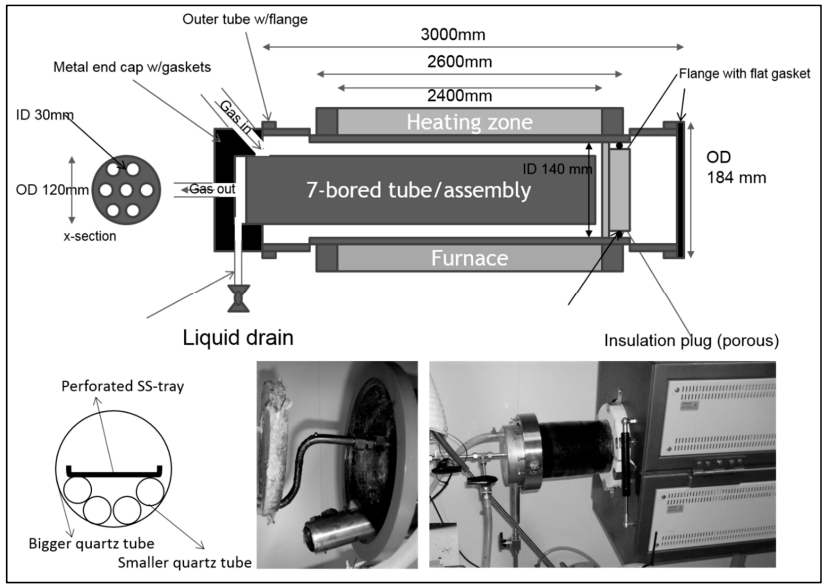

Figure 3. Drawing of furnace, bigger quartz tube, smaller quartz tube assembly and photographs of the system with carbonization in progress.

Two types of 2 m long perforated plates (purchased from Nisjemetall AS, Røyken, Norway) with square openings (10×10 mm^2 and 20×20 mm^2) and width of 120 mm were also used to carbonize the hollow fibers.

2.2.2. Procedure for Carbonization

Different types of collection methods were tried. However, only two methods that had a great effect on membrane morphology after deacetylation, drying, and carbonization are being reported here.

Loading the Furnace

The angle between support/level and furnace/tube was set to 6° by raising the closed end of the furnace to enhance the flow of residue downward. 1–7 quartz tubes were filled with 500 to 1000 fibers in each tube. A thread with a loose knot around the fibers was used to pull the fibers inside the quartz tubes. The thread was removed after fibers are inserted. An insulation plate was cut OD 120 mm and holes were made according to the template (honey comb arrangement), which is shown in Figure 3 (number of tubes loaded, 30 mm hole diameter), a 32 mm OD hole for the tar drain tube, and a 3/8" OD sweep gas tube. Insulation plate along with quartz tubes were pushed inside the bigger/furnace tuber into the heating zone of the furnace (46–48 cm from the edge of the furnace tube).

In the case of using the perforated plate/grid, the grid was filled with 1600 to 4000 fibers. The fibers were distributed as equally as possible on the grid with the layer thickness across the width of the grid becoming as constant as possible. The upper end of the fiber (the upper end during the drying of cellulose fibers) was placed at an upstream end of the grid (the end of the furnace tube where preheated purge gas enters). Flat grids were unstable when placed directly into the furnace tube. Therefore, four smaller quartz tubes were used as support inside the furnace tube in the bottom of grids (also shown in Figure 3). It also helped to protect the inner wall of the furnace tube from scratches (stainless-steel grids) and provided distance between purge gas and the grid. The grid was then pushed into the heating zone of the furnace (46–48 cm from the edge of the furnace tube).

The inlet of the purge gas (flowing into the furnace) tube was placed in between the middle support tubes and the outlet end was pushed through the insulation plate (demonstrated in Figure 4). Then the tar drain tube was inserted into the insulation plate, which makes an angle so that the tar flows to the end cup/flange of the furnace. This is shown in Figure 3. The flange, gasket, and metal cup were greased with Loctite 8104. The purge gas inlet tube is by design welded to the cup and coupled with a tube inside the furnace through a tight silicon tube (ca 40 mm long), as illustrated in Figure 4. Two clamp halves were mounted, holding the cup, with two screws so that both halves gently touched each other. The screws in the clamps were tightened very gently, avoiding high momentum, to protect the quartz tube. Figure 5 shows the photograph of the perforated plates loaded with fibers, which are ready for carbonization.

All the valves separating the furnace from the rest of the gas lines were closed. Then the vacuum pump was turned on followed by slow opening of the valve between the pump and the furnace. Then the system was checked for any possible leakage. The system was left to evacuate overnight, which normally yields a pressure <10 mbar.

Carbonization

After evacuating the air out of the system, N_2 or CO_2 flow of 0.8 L/min was supplied through a gas flow controller. The flow was gradually increased to 1.9 L/min to fill the oven. As soon as the pressure inside the furnace tube reached just above the atmospheric pressure (1.1–1.2 atm), the valve to the exhaust trap and the valve to the tar trap was slowly opened. H_2O/NMP in the volume ratio of 4/1 was used as an exhaust trap on the outlet of the furnace. For tar absorption, 10% triethyleglycol (TEG) in water was used and an outlet from both the exhaust trap and the tar trap was then connected to the ventilation. Gas flow was varied for a few batches to optimize, according to the fiber holders (no. of quartz tubes or SS-grid), but it was always kept in the superficial velocity range of 1 to 10 cm/min [38].

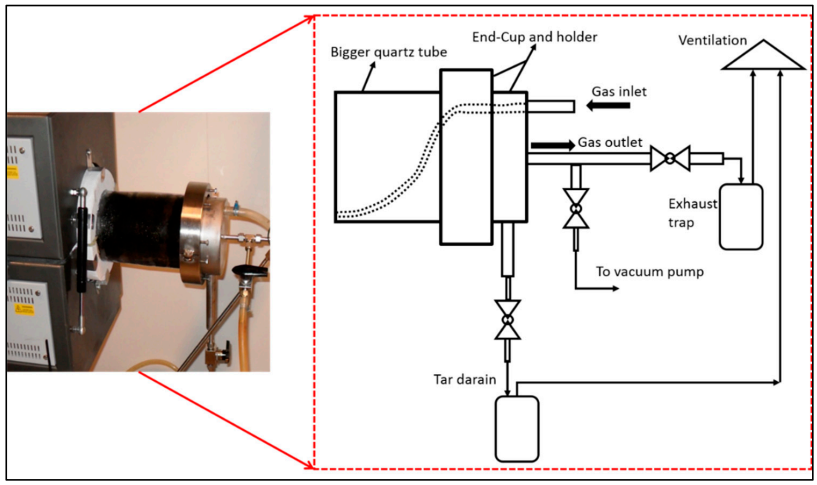

Figure 4. A photograph (on **left**) and a schematic diagram (on **right**) of end-cup and holder on the fiber loading-end of the furnace tube.

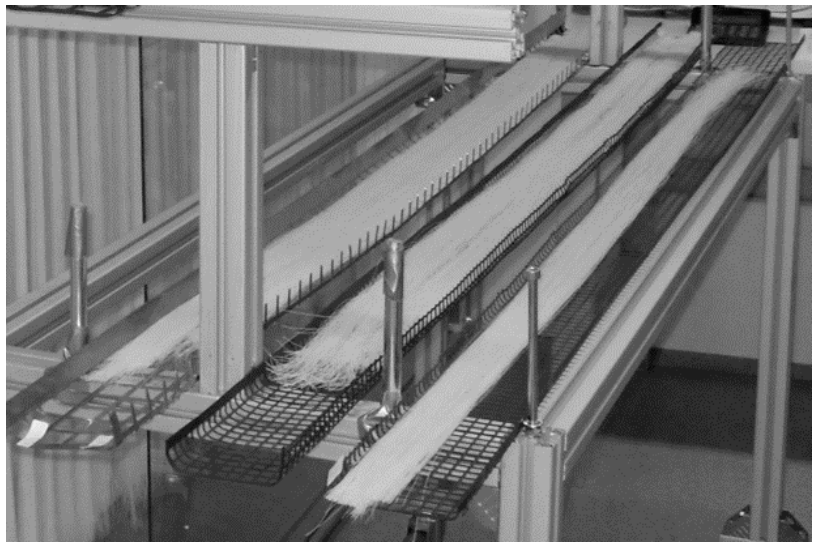

Figure 5. Perforated plates with square openings (10 × 10 mm^2) and (20 × 20 mm^2).

The carbonization protocol (as illustrated in Figure 6) was then started. At the end of the protocol, the system was left to cool naturally and gas continued to flow at the original flow rate. When the furnace temperature was 70 °C or below, the gas flow was stopped and both traps (exhaust and tar) were disconnected. Because the cooling of the furnace may create a slight vacuum inside, the liquid in the exhaust trap is thus hindered to flow into the furnace tubes or tar trap. Quartz tubes/grids were pulled out of the furnace tube and fibers were stored on a clean surface (a plain paper). Then fibers were left to degas overnight before they were further processed. The stainless-steel grid did not need any washing after carbonization since there was no residue stuck on the grid. However, the quartz tube needed washing after each carbonization cycle.

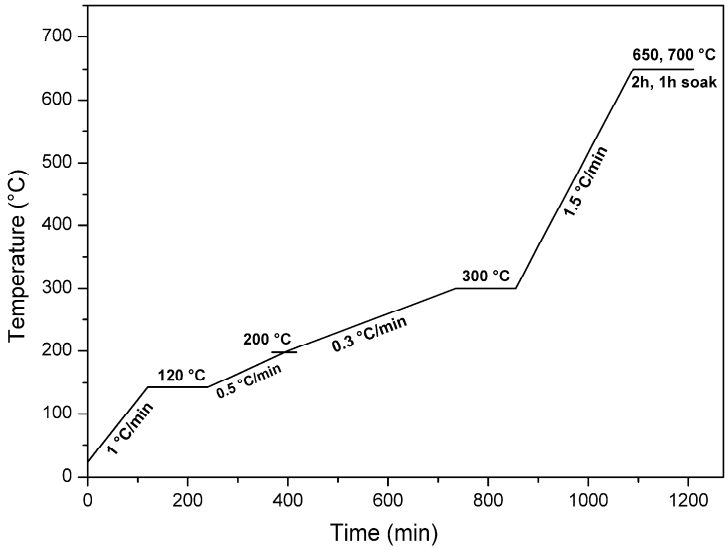

Figure 6. Carbonization protocol used by MemfoACT AS.

2.3. Permeation Testing

For the permeation experiments discussed here, CM (0.002–2 m^2 for each module) modules were tested in a permeation set-up with a shell side feed configuration. The mass transport properties of CM were measured with the single pure gases CO_2, N_2, CH_4, and mixed gas (40% CO_2 in CH_4) at 5 bar feed pressure (ambient temperature: 20–23 °C) and with or without vacuum on the permeate side. He et al. [14] has also performed the mixed gas experiments on the carbon membrane (prepared with a similar protocol) and results showed that the membrane performance for CO_2 separation is the same or even higher in some cases for mixed gas as compared to single gas separation. The carbon membranes prepared by MemfoACT AS also showed similar results. The values for CH_4 gas were found to give a selectivity $\alpha\ CO_2/CH_4 = 3{\cdot}\alpha\ CO_2/N_2$.

The performance of the membrane was evaluated by measuring the CO_2 permeance in [m^3(STP)/(m^2 h bar)] and CO_2/N_2 selectivities (α) by using Equations (1) and (2). The tests were run from several hours to several days to ensure that the transient phase of diffusion was passed and the steady state obtained (dp/dt tends to a constant). The gas permeance, P [m^3(STP)/($m^2{\cdot}$h·bar)], was evaluated by using Equation (1).

$$P = \frac{9.824\ V{\cdot}(dp/dt)}{\Delta P{\cdot}A{\cdot}T_{exp}} \tag{1}$$

In this case, V is the permeate side volume (cm^3) that can be measured with a pre-calibrated permeation cell reported elsewhere [15,40]. However, the permeate side volume for this study was estimated by the tube length and the cylinder volume on the permeate side. dp/dt and A are the collection volume pressure increase rate (m bar/s) and the total active area of the membrane (cm^2), respectively. ΔP (bar) is the pressure head and T_{exp} (K) is the temperature for the experiment. The ideal selectivity was defined as the ratio of the pure gas permeance, which is shown in Equation (2).

$$\propto_{A/B} = \frac{P_A}{P_B} \tag{2}$$

3. Results and Discussion

3.1. Fiber Morphology and Successful Fibers

Figure 7a–c shows the scanning electron microscopic (SEM, Zeiss SUPRA 55VP, NTNU) images of the carbon hollow fiber membrane. The average diameter of carbon fibers was 210 μm with wall thickness of 23 μm. Carbonization is a critical step and varying carbonization conditions would result in a dissimilar carbon matrix for each carbonized batch of hollow fibers.

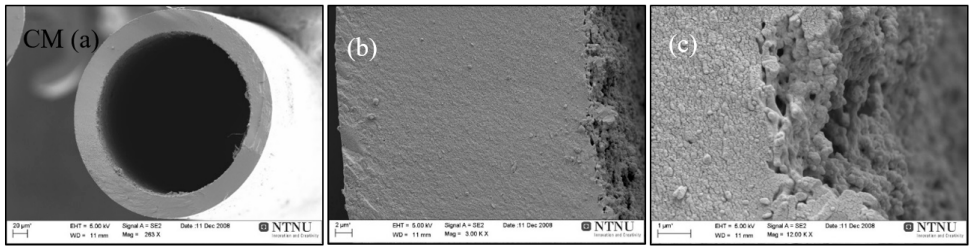

Figure 7. SEM images of carbon hollow fiber membrane (CM), (**a**) cross section, (**b**) wall magnified, and (**c**) inner edge of the wall magnified.

The final carbon fibers should not be perfectly straight but should preferably have waves (i.e., wavelength >10 cm) to (i) improve the gas flow pattern in the module and to (ii) handle thermal expansion or shrinkage without breakage. The color of carbonized fibers gave the first insight to evaluate if the fibers were processed as required. The carbonized bundle should be shiny, which means that surface of carbon fibers is free from low-molecular products (tars) of cellulose pyrolysis. The residual tars caused the fibers to stick together, which resulted in their embrittlement. To make a qualitative test on the carbonized bundle of fibers, some quick mechanical examinations were performed. The optimal bundle of carbon fibers should easily separate into individual carbon fibers with a gentle hand. The fiber bundle was shaken in a careful and gentle way by holding on one end, so any broken fibers could fall out. The procedure was repeated by holding the other end of the bundle the same way. Carbonization was considered successful if the broken fibers do not exceed 2% of the total fibers in the bundle. Fiber strength was tested by a simple loop diameter method. A loop made of an individual carbon fiber was slowly tightened while measuring the diameter simultaneously until the fiber was broken. An acceptable average minimal diameter should not exceed 10 mm. Sampling was performed on different parts of the fibers as well as from the middle and outer part of the bundle to evaluate the uniformity of its mechanical properties.

Figure 8 summarizes the results of 390 spun-batches, which are carbonized both in the quartz tubes and on the SS-grid. As can be seen in Figure 8, on average, 40% of the total carbonized fibers and fibers in the quartz tubes were fused and unusable. However, some batches exceeded to 60% of fused fibers. The brittle fibers obtained from the same batches were in the range from 0% to 30%. The percentage of curly and collapsed fibers (not shown here) was between 0% and 5%. Hence, the "survival rate" of these batches was very low (<10%). It was assumed (i.e., % of good fibers) that honey comb arrangement of quartz tubes might create more uniform conditions in cross-section within each bundle, but it was observed that the unequal flow rate of gas was distributed in each bundle/tube. Therefore, most of the residual produced during carbonization stayed inside the bundle, which resulted in fused and brittle fibers. Using an angle on furnace (4–6° by raising the closed end of the furnace to enhance the flow of residue downward) improved the rate of survival but still could not produce successful fibers consistently. The residual amount was also different in all batches depending on the changed parameters during precursor preparation or the number of fibers in each carbonization batch. It could be noted that the survived fibers were always on the top of the bundle and those in the bottom part was fused.

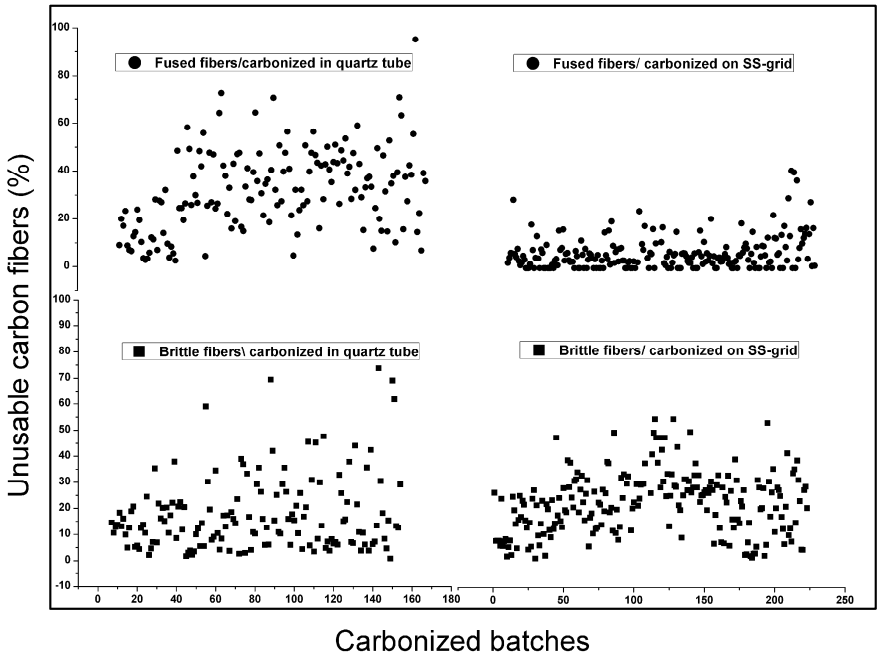

Figure 8. Fused and brittle fibers after carbonization, results with quartz tube (**left**), and results with SS-grid (**right**).

The number of fused fibers were significantly reduced when carbonized on the perforated SS-grids, which is shown in Figure 8. Usually each perforated SS-grid contained 2000–4000 individual fibers and these fibers included 4–6 spun-batches of vertically dried regenerated cellulose fibers. Initially, all fibers on the grid were placed in the same direction (top side during drying) for all batches. After several carbonizations, it was observed that the fibers fused more only on one side of the bundle (top side). Hence, the dried batches were arranged on an SS-grid in an alternating order (top of one batch in one direction neighboring with the bottom of the other batch and so on). It improved the number of survival fibers but there were still some fused fibers in each bundle. Then a perforated grid with bigger openings (20×20 mm^2) was used, which increased, and the results were almost similar as with previous grid (10×10 mm^2). It was found that fibers on the bottom of the bundle touching to the grid and specifically sections of the fibers in contact with SS-grid were sometimes fused and got stuck with the grid. That portion of the fibers became brittle and pulling it away from the bundle (separating the fibers) would break the fibers. Although numerous batches had zero fused fibers, it was still challenging to keep the consistent production rate. While gas distribution was improved by the use of grids, there were still some sections where the pressure drop was higher (fibers not equally dispersed on grid) and gas was not able to isolate the fiber-tar-fiber and fiber-tar-grid connections.

The carbonized hollow fibers should be sufficiently strong, flexible, and uniform to produce bigger commercially modules with high packing density. The challenge during carbonization is the fiber brittleness. As shown in Figure 8, both carbonization methods (fibers inside quartz tube and on SS-grid) had almost a similar number of brittle fibers. These fibers could not be looped into the 10 mm diameter before they broke. This was used as the definition of brittleness in this study. There may be two possible reasons for the brittle carbon fibers: (1) varying properties of the precursor in each batch, e.g., partial deacetylation, fast drying at lower relative humidity (40–30%), etc. (2) surface of carbon is not fully free from low-molecular products (tar). In future research, a continuously rotating perforated tube (SS or glass) is suggested for the carbonization of big batches. This would help distribute the

gas equally in a more efficient way, remove the residual tar, and avoid the continuous contact of fibers with tube and each other. Furthermore, a model to estimate the gas flow pattern inside the carbonization chamber would be very helpful to manipulate the gas distribution inside the chamber for a homogenous flow.

3.2. Gas Permeation Properties

The separation properties of the resulting membrane will be determined by the pore structure formed during carbonization. It was observed that a high temperature (700 °C) carbonization resulted in a dense membrane with decreased CO_2 permeability (up to 20 Barrer) and high CO_2/CH_4 selectivity (above 200). Yet, 650 °C final temperature improved the permeation properties of the resulting carbon membranes by sacrificing some of the selectivity.

Figure 9 presents the permeation results of the carbon hollow fiber membrane prepared from regenerated cellulose hollow fibers. As shown in Figure 9, some batches were carbonized under the CO_2 atmosphere. Despite good permeation properties, the resulting fibers possessed very weak mechanical properties. Fibers carbonized under vacuum had lower CO_2 permeability and selectivity values than when prepared in CO_2 or N_2 atmosphere. The membranes prepared in the N_2 atmosphere exhibited high performance (as shown in Figure 9) and good mechanical properties. Therefore, the rest of the batches were exposed to the N_2 atmosphere during carbonization. Geiszler and Koros [38] reported that an inert gas atmosphere resulted in a more open but a less selective CMS matrix compared to vacuum carbonization. They explained this with acceleration in the carbonization process due to an increased gas phase heat and mass transfer. The same authors also observed that the CO_2 purge produced a highly porous, nonselective membrane by oxidizing the carbon and ten times reduction in purge gas flow rate caused a decrease in the permeate flux, which was presumable by the deposition of tar (carbon) either on the membrane surface or in the pores. Based on our own observations where carbonization in the CO_2 atmosphere with previously mentioned flow rates looked promising, reasonable permeability and selectivity was achieved. The yield of produced carbon fibers was significantly reduced due to weak mechanical properties.

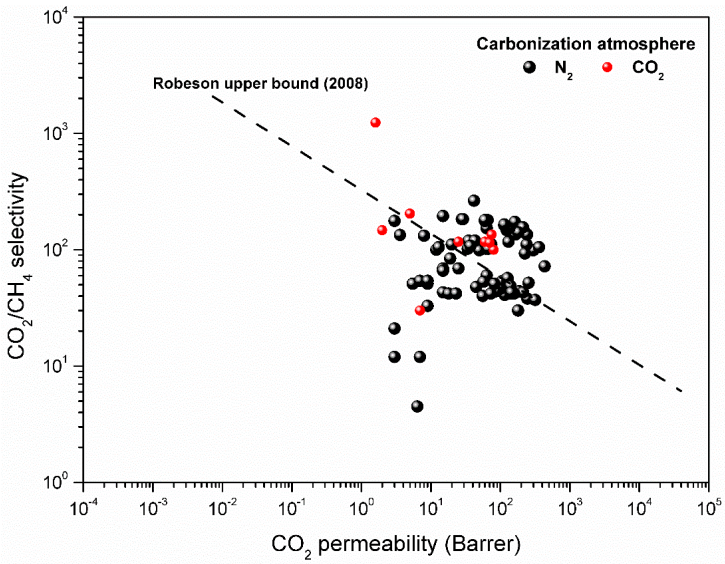

Figure 9. Separation performance of carbon hollow fiber membrane when carbonized under N_2 and CO_2 atmosphere (Final temperature: 650 °C) (1 Barrer = 2.736×10^{-9} m^3(STP) m/m^2 bar h).

As already stated, the N_2 atmosphere was chosen to be used for the rest of the batches. The optimized flow rate of purge gas yielded mechanically strong fibers with acceptable gas permeation properties. CM produced on a pilot-scale plant showed equal or higher performance as compared to the laboratory scale carbon membranes in CO_2-CH_4 separation. The performance of produced fibers is comparable with the previously reported work [13–15,17]. The results presented in Figure 9 are for the smaller (~0.002 m^2 of each module) modules. However, the bigger modules with an effective area of 2–2.5 m^2 of each module were made and used to produce vehicle fuel from biogas. The performance of these bigger modules was enhanced further by a chemical vapor deposition (CVD) process. Details about the construction of bigger modules, performance, CVD procedure, and aging of these modules were reported elsewhere [25]. Preparation of regenerated cellulose-based carbon membranes, characterization, and the performance of these modules on a laboratory scale has already been reported [14]. The carbonization process is not stable enough to achieve the same results for each fiber in each batch. However, the idea of this work was to keep the variance minimal within and between batches. It is important to note that the results shown in Figure 9 were obtained by testing several fibers from different batches. The performance of different fibers picked up from different batches varies. This varying performance may be due to a change in the structure that might have occurred during the preparation of precursor fibers or through the carbonization process. In each bundle of carbonized fibers, there might be a gradient of tar build up. In some cases where membrane performance is below the upper bound, it seems that a smaller number of open pores are available for gas permeation. During carbonization, it might be that tar have stuck the fiber surface to reduce the number of open pores, which ultimately declined the performance of the membrane. However, in other batches, the chosen fiber for permeation testing might have had more open pores.

Karvan et al. [39] reported that fibers carbonized on a pilot scale plant in a vertically-oriented furnace had 66% lower permeance of CO_2 and 16% decreased CO_2/CH_4 selectivity when compared to their laboratory/bench scale carbon hollow fibers. The gas permeation results of carbon membranes prepared by MemfoACT AS showed that horizontal orientation could give carbon membranes with a high performance. An adjustment of the furnace angle (4–6° by raising the closed end of the furnace) and a perforated plate inside the furnace increased the number of good fibers consistently by securing equal purge gas distribution and removing the residual products simultaneously.

4. Conclusions

A pilot-scale system for production of high performance carbon membranes from regenerated cellulose has been studied and reported. A relatively low-cost precursor material and a single stage carbonization process, which obtained over 90% of successful carbon fibers, made the pilot production of carbon membranes more economically attractive. The number of fused fibers was significantly reduced by replacing the quartz tubes as fiber carriers inside the furnace with perforated trays of stainless steel as fiber carriers. Separation performance of the regenerated cellulose-based carbon membranes was equal or even higher than the reported membranes produced on a laboratory scale. Fibers carbonized under a CO_2 atmosphere had lower mechanical properties compared to the fibers carbonized under an N_2 atmosphere. The carbonization process is not stable enough to achieve the same results for each fiber in each batch. However, the idea of this work was to keep the variance minimal within and between batches. A few suggestions were proposed to enhance the survival rate of good fibers with more consistency. Through careful optimization of the carbonization process (temperature, purge gas flow rate, purge gas type, and angle of the furnace), the number of fused fibers may be reduced. An adjustment of the furnace angle (4–6° by raising the closed end of the furnace) and a perforated rotating tube inside the furnace may increase the number of survived fibers consistently by securing equal purge gas distribution and removing the residual products simultaneously. Exploration of the purge gas flow pattern inside the furnace is also proposed in future work.

Author Contributions: S.H., J.A.L., and A.L. performed the experiments. S.H. wrote the manuscript and all authors contributed substantially to the revision of the manuscript.

Funding: This research work is gathered over the years by the support of different funding sources including the Norwegian Research Council and Innovation Norway.

Acknowledgments: The authors would also like to thank The Department of Chemical Engineering at NTNU for providing the opportunity to develop this paper.

Conflicts of Interest: The authors declare no conflict of interest.

References

1. Baker, R.W. Future directions of membrane gas separation technology. *Ind. Eng. Chem. Res.* **2002**, *41*, 1393–1411. [CrossRef]
2. Yan, S.; Fang, M.; Zhang, W.; Zhong, W.; Luo, Z.; Cen, K. Comparative analysis of CO_2 separation from flue gas by membrane gas absorption technology and chemical absorption technology in china. *Energy Convers. Manag.* **2008**, *49*, 3188–3197. [CrossRef]
3. Koresh, J.; Soffer, A. Study of molecular sieve carbons. Part 1.—Pore structure, gradual pore opening and mechanism of molecular sieving. *J. Chem. Soc. Faraday Trans. 1* **1980**, *76*, 2457–2471. [CrossRef]
4. Koresh, J.; Soffer, A. Study of molecular sieve carbons. Part 2.-estimation of cross-sectional diameters of non-spherical molecules. *J. Chem. Soc. Faraday Trans. 1* **1980**, *76*, 2472–2485. [CrossRef]
5. Koresh, J.E.; Sofer, A. Molecular sieve carbon permselective membrane. Part I. Presentation of a new device for gas mixture separation. *Sep. Sci. Technol.* **1983**, *18*, 723–734. [CrossRef]
6. Koresh, J.E.; Soffer, A. Mechanism of permeation through molecular-sieve carbon membrane. Part 1.—The effect of adsorption and the dependence on pressure. *J. Chem. Soc. Faraday Trans. 1* **1986**, *82*, 2057–2063. [CrossRef]
7. Robeson, L.M. The upper bound revisited. *J. Membr. Sci.* **2008**, *320*, 390–400. [CrossRef]
8. Tin, P.S.; Chung, T.-S.; Hill, A.J. Advanced fabrication of carbon molecular sieve membranes by nonsolvent pretreatment of precursor polymers. *Ind. Eng. Chem. Res.* **2004**, *43*, 6476–6483. [CrossRef]
9. Ismail, A.F.; David, L.I.B. A review on the latest development of carbon membranes for gas separation. *J. Membr. Sci.* **2001**, *193*, 1–18. [CrossRef]
10. Salleh, W.N.W.; Ismail, A.F. Carbon membranes for gas separation processes: Recent progress and future perspective. *J. Membr. Sci. Res.* **2015**, *1*, 2–15. [CrossRef]
11. Kiyono, M.; Williams, P.J.; Koros, W.J. Effect of polymer precursors on carbon molecular sieve structure and separation performance properties. *Carbon* **2010**, *48*, 4432–4441. [CrossRef]
12. Jon Arvid Lie, M.-B.H. Carbon Membranes. U.S. Patents US20100162887 A1, 1 July 2010.
13. He, X.; Hägg, M.-B. Structural, kinetic and performance characterization of hollow fiber carbon membranes. *J. Membr. Sci.* **2012**, *390–391*, 23–31. [CrossRef]
14. He, X.; Lie, J.A.; Sheridan, E.; Hägg, M.-B. Preparation and characterization of hollow fiber carbon membranes from cellulose acetate precursors. *Ind. Eng. Chem. Res.* **2011**, *50*, 2080–2087. [CrossRef]
15. Lie, J.A. Synthesis, Performance and Regeneration of Carbon Membranes for Biogas Upgrading—A Future Energy Carrier. Ph.D. Thesis, Norwegian University of Science and Technology, Trondheim, Norway, 2005.
16. Jones, C.W.; Koros, W.J. Characterization of ultramicroporous carbon membranes with humidified feeds. *Ind. Eng. Chem. Res.* **1995**, *34*, 158–163. [CrossRef]
17. Lie, J.A.; Hägg, M.-B. Carbon membranes from cellulose: Synthesis, performance and regeneration. *J. Membr. Sci.* **2006**, *284*, 79–86. [CrossRef]
18. Lie, J.A.; Hägg, M.-B. Carbon membranes from cellulose and metal loaded cellulose. *Carbon* **2005**, *43*, 2600–2607. [CrossRef]
19. Menendez, I.; Fuertes, A.B. Aging of carbon membranes under different environments. *Carbon* **2001**, *39*, 733–740. [CrossRef]
20. Xu, L.; Rungta, M.; Hessler, J.; Qiu, W.; Brayden, M.; Martinez, M.; Barbay, G.; Koros, W.J. Physical aging in carbon molecular sieve membranes. *Carbon* **2014**, *80*, 155–166. [CrossRef]
21. Lagorsse, S.; Campo, M.C.; Magalhães, F.D.; Mendes, A. Water adsorption on carbon molecular sieve membranes: Experimental data and isotherm model. *Carbon* **2005**, *43*, 2769–2779. [CrossRef]
22. Sanyal, O.; Zhang, C.; Wenz, G.B.; Fu, S.; Bhuwania, N.; Xu, L.; Rungta, M.; Koros, W.J. Next generation membranes—Using tailored carbon. *Carbon* **2018**, *127*, 688–698. [CrossRef]

23. Ma, X.; Swaidan, R.; Teng, B.; Tan, H.; Salinas, O.; Litwiller, E.; Han, Y.; Pinnau, I. Carbon molecular sieve gas separation membranes based on an intrinsically microporous polyimide precursor. *Carbon* **2013**, *62*, 88–96. [CrossRef]
24. Soffer, A.; Koresh, J.E.; Saggy, S. Separation Device. U.S. Patents US4685940A, 11 August 1987.
25. Haider, S.; Lindbråthen, A.; Lie, J.A.; Andersen, I.C.T.; Hägg, M.-B. CO_2 separation with carbon membranes in high pressure and elevated temperature applications. *Sep. Purif. Technol.* **2018**, *190*, 177–189. [CrossRef]
26. Salleh, W.N.W.; Ismail, A.F. Carbon hollow fiber membranes derived from pei/pvp for gas separation. *Sep. Purif. Technol.* **2011**, *80*, 541–548. [CrossRef]
27. Haider, S.; Lindbråthen, A.; Hägg, M.-B. Techno-economical evaluation of membrane based biogas upgrading system: A comparison between polymeric membrane and carbon membrane technology. *Green Energy Environ.* **2016**, *1*, 222–234. [CrossRef]
28. Qin, J.-J.; Li, Y.; Lee, L.-S.; Lee, H. Cellulose acetate hollow fiber ultrafiltration membranes made from ca/pvp 360 k/nmp/water. *J. Membr. Sci.* **2003**, *218*, 173–183. [CrossRef]
29. Son, W.K.; Youk, J.H.; Lee, T.S.; Park, W.H. Electrospinning of ultrafine cellulose acetate fibers: Studies of a new solvent system and deacetylation of ultrafine cellulose acetate fibers. *J. Polym. Sci. Part B* **2004**, *42*, 5–11. [CrossRef]
30. Kawamoto, H.; Murayama, M.; Saka, S. Pyrolysis Behavior of Levoglucosan as an Intermediate in Cellulose Pyrolysis: Polymerization Into Polysaccharide as a Key Reaction to Carbonized Product Formation. *J. Wood Sci.* **2003**, *49*, 469–473. Available online: https://link.springer.com/article/10.1007/s10086-002-0487-5 (accessed on 13 October 2018). [CrossRef]
31. Soffer, A.; Gilron, J.; Saguee, S.; Hed-Ofek, R.; Cohen, H. Process for the Production of Hollow Carbon Fiber Membranes. Patents EP0671202B1, 4 July 2001.
32. Drioli, E.; Barbieri, G.; Brunetti, A. *Membrane Engineering for the Treatment of Gases: Gas Separation Issues with Membranes*; RSC Publishing: Cambridge, UK, 2011; Volume 2, p. 180, ISBN 978-1-78262-874-3.
33. Lagorsse, S.; Magalhães, F.D.; Mendes, A. Carbon molecular sieve membranes: Sorption, kinetic and structural characterization. *J. Membr. Sci.* **2004**, *241*, 275–287. [CrossRef]
34. He, X.; Arvid Lie, J.; Sheridan, E.; Hägg, M.-B. CO_2 capture by hollow fibre carbon membranes: Experiments and process simulations. *Energy Procedia* **2009**, *1*, 261–268. [CrossRef]
35. He, X.; Hägg, M.-B. Hollow fiber carbon membranes: Investigations for CO_2 capture. *J. Membr. Sci.* **2011**, *378*, 1–9. [CrossRef]
36. He, X.; Hägg, M.-B. Hollow fiber carbon membranes: From material to application. *Chem. Eng. J.* **2013**, *215–216*, 440–448. [CrossRef]
37. Barton, T.J.; Bull, L.M.; Klemperer, W.G.; Loy, D.A.; McEnaney, B.; Misono, M.; Monson, P.A.; Pez, G.; Scherer, G.W.; Vartuli, J.C.; et al. Tailored porous materials. *Chem. Mater.* **1999**, *11*, 2633–2656. [CrossRef]
38. Geiszler, V.C.; Koros, W.J. Effects of polyimide pyrolysis conditions on carbon molecular sieve membrane properties. *Ind. Eng. Chem. Res.* **1996**, *35*, 2999–3003. [CrossRef]
39. Karvan, O.; Johnson, J.R.; Williams, P.J.; Koros, W.J. A pilot-scale system for carbon molecular sieve hollow fiber membrane manufacturing. *Chem. Eng. Technol.* **2013**, *36*, 53–61. [CrossRef]
40. Lin, W.-H.; Vora, R.H.; Chung, T.-S. Gas transport properties of 6fda-durene/1,4-phenylenediamine (ppda) copolyimides. *J. Polym. Sci. B Polym. Phys.* **2000**, *38*, 2703–2713. [CrossRef]
41. Koros, W.J.; Mahajan, R. Pushing the limits on possibilities for large scale gas separation: Which strategies? *J. Membr. Sci.* **2000**, *175*, 181–196. [CrossRef]
42. Haider, S.; Lindbråthen, A.; Lie, J.A.; Hägg, M.-B. Carbon membranes for oxygen enriched air—Part II: Techno-economical analysis. *Sep. Purif. Technol.* **2018**, *205*, 251–262. [CrossRef]

Appendix G

Paper III

Regenerated cellulose-based carbon membranes for CO_2 separation; Durability and aging under miscellaneous environments

Paper published in Journal of Industrial & Engineering Chemistry 70 (2019) 363-371

Journal of Industrial and Engineering Chemistry 70 (2019) 363–371

Contents lists available at ScienceDirect

Journal of Industrial and Engineering Chemistry

journal homepage: www.elsevier.com/locate/jiec

Regenerated cellulose based carbon membranes for CO_2 separation: Durability and aging under miscellaneous environments

Shamim Haider, Arne Lindbråthen, Jon A. Lie, May-Britt Hägg*

Department of Chemical Engineering, Norwegian University of Science and Technology, NTNU, 7491 Trondheim, Norway

ARTICLE INFO

Article history:
Received 5 February 2018
Received in revised form 15 October 2018
Accepted 31 October 2018
Available online 10 November 2018

Keywords:
Carbon membrane
Gas separation
Biogas
Module housing
H_2S exposure

ABSTRACT

Predictive models regarding the aging effect on membrane separation properties are required to estimate the membrane life time with acceptable permeability and selectivity for the respective application. The current article is reporting an insight into this topic regarding the aging of regenerated cellulose-based carbon hollow fibres (CHF) mounted in a membrane module when they were exposed to real biogas in three different fields. CHF were exposed to biogas for almost one year with H_2S content extending from 0 to 2400 ppm, and gas permeation tests for single gases, N_2, CO_2, CH_4, and O_2 were analysed periodically at the membrane production facility. CHF storage methods under miscellaneous dry environments like air, vacuum, CO_2, etc. were studied. The air flow through bore side of the CHF under controlled conditions had a regenerative effect on the membrane permeability, and the membrane performance was quite steady until after 150 days under laboratory environment.

Introduction

Carbon molecular sieve (CMS) membranes were first reported by Koresh and Soffer in the 1980s, and after a couple of years, the first company called Carbon Membranes Ltd. was based in Israel [1]. As of now, extensive attempts involve the development of new strategies for producing CMS membrane with improved CO_2–CH_4 separation performance, finding cheaper and environmentally friendly raw materials. Most of the work reported has been performed at laboratory scale and, to the best of our knowledge, very limited work has been reported on the actual industrial exposure of CMS membranes when in contact with H_2O, H_2S, higher hydrocarbons, aromatic compounds and aging of carbon membranes under these harsh environments. CMS membranes appear to be vulnerable to oxidation, humidity and pore blockage resulting in pore constrictions that make it hard for gas molecules to permeate through the membrane [2].

Carbon membranes are known to age, and extended exposure to various molecules such as H_2O and O_2 change the effective pore size by physical or chemical sorption, hence modifying the performance of the membrane. The vulnerability of CMS membranes to water is a complex phenomenon. Carbon surfaces are basically hydrophobic; however, the microporous walls of the carbon membrane will quickly become partially covered with an oxygen containing functional group which hence results in the membrane having a hydrophilic character. Therefore, once the first layer of water molecules is adsorbed, adsorbate–absorbate interactions promote further adsorption of more water through hydrogen bonds [3,4]. This results in a reduction in capacity of the membrane, and hence is a serious problem for the industrial application of carbon membranes as most feed streams contain some humidity. Jones and Koros [5] reported that performance losses were minimum for carbon membranes prepared at 550 °C as compared to the one pyrolyzed at 500 °C when tested in the range of 23–85% humidity. Xu et al. [6] have recently reported the importance of physical aging showing that physical aging appears to be the leading source for rapid changes of transport properties at the early stage after the membrane fabrication. It may happen due to shrinkage of pores over time to achieve a thermodynamically stable state. Wenz and Koros [7] have recently reported the postsynthetic modification method to suppress the physical aging by tuning the pores of carbon membranes. Chemical sorption involves chemical bonds, usually C–O bonds, and the bonding forces here are stronger than van der Waals forces (physical bonding), making removal of these components more complex and energy demanding [8,9].

Okamoto et al. [10] carbonized asymmetric hollow fiber membrane of a polyimide from 3,3′,4,4′-biphenyltetracarboxylic dianhydride and aromatic diamines in the N_2 atmosphere at 500–700 °C. Carbon membranes prepared at 600–630 °C showed good stability in

* Corresponding author.
E-mail address: may-britt.hagg@ntnu.no (M.-B. Hägg).

https://doi.org/10.1016/j.jiec.2018.10.037
1226-086X/

the separation of propylene/propane and 1,3-butadiene/*n*-butane. The membranes hardly changed the performance, when stored for 1 week at room temperature. Campo et al. [11] have described the flat sheet carbon molecular sieve membrane produced from commercially available cellophane paper which is regenerated cellulose obtained by the viscose process. The authors claim the membrane showed no signs or aging upon exposure to oxygen and water. It has been shown that storing carbon membranes in an inert environment such as nitrogen prior to use is advantageous [9].

MemfoACT AS, a spin-off company from the Norwegian Univ. of Science and Tech. founded in 2008 (closed in 2015) produced an efficient and compact system for biogas upgrading to fuel quality bio-methane based on carbon hollow fibres (CHF) membranes using deacetylated cellulose acetate (CA) as precursor. These membranes were exposed to real biogas at three different biogas fields in Norway, Field 1 (F1) with H_2S <5 ppm in the feed gas, Field 2 (F2) also with H_2S <5 ppm and Field 3 (F3) with H_2S: 150–2400 ppm in the raw biogas. CHF installed, demonstrated excellent initial performance, but a significant drop (up to 70% in CO_2 permeance) was observed after one year of exposure at F1. This highlights the importance of concern with respect to aging for the carbon membrane. Anderson et al. [12] have reported the effect of H_2S on polyfurfuryl alcohol based carbon membranes. It is important to understand the stability and aging of CMS membranes when stored under different conditions (static aging) and while in operation (dynamic aging). The experience of CHF to mentioned conditions and their effect on membrane performance is important to understand for the actual industrial applications of CHF and is the motivation and focus of the current work. It is however important to stress that the current study reports the performance of regenerated cellulose based CHF membranes at low pressure The high pressure process is discussed elsewhere [13]. Real biogas exposure results also indicated that the membrane was mechanically stable at actual industrial conditions. However, the brittleness of hollow fibers remained a challenge. The mechanical strength of carbon membranes may be enhanced using some fillers in the precursor [14]. The challenges experienced with the regenerated cellulose derived CMS membranes may be different that of other precursors. As an example, Zhang et al. [15] have reported the excellent stability of a polyimide based precursor for carbon hollow fiber membranes when operated over 100 bar It is hence important to remember that CMS is not a single material but a family of materials where the achieved separation properties may be determined by choice of precursors and processing conditions. Detailed characterization of the CMS membranes studied here, are more closely reported in Refs. [16–18] using FTIR and SEM.

The principal objective of the described study is hence to obtain a better understanding of the durability and aging of the cellulose derived carbon membrane performance when exposed to real field biogas and H_2S. In the current work the aging effect on the performance of CHF when stored under different conditions is also reported, such as vacuum, open air, CO_2 atmosphere, dark place and cold place (4 °C). CHF membranes were exposed to field biogas for maximum 350 days and the membrane performance was measured before and after the exposure. Lab-scale study of *dynamic aging* (membrane under controlled conditions and a continuous gas flow through the membrane), *static aging* (membrane lying inside the lab, no control of the flow) and *intermediate aging* (mix of the dynamic and static aging, further discussed below) using bore side-feed configuration is also presented. The gas permeation results indicate that dynamic aging under certain environments is helpful preventing the membrane performance better than static aging.

Experimental

Carbon hollow fibers preparation

The precursor for CHF was prepared using cellulose acetate (CA, M_W 100,000 from ACROS Organics Belgium) by the dry/wet phase inversion process in a pilot scale spinning set up delivered by Philos Korea. Process details are described elsewhere [19]. A dope consisting of CA mixed with *N*-methylpyrrolidone (NMP: purity >99.5% from Merck Norway) and polyvinylpyrrolidone (PVP: M_W 10,000 from Sigma Aldrich Norway) was used to spin CA hollow fibers. CA hollow fibers were deacetylated batch-wise with a mix solution of NaOH (>99% from VWR Norway) in short chain alcohol. Then deacetylated CA hollow fibers were carbonized at 550 °C under N_2 flow in a tubular furnace. The carbonization protocol had a heating rate of 1 °C/min with several dwells and the final temperature of 550 °C for 2 h. Fig. 1 shows the schematic of carbonization process to form carbon hollow fibers from cellulose precursor. The detailed description of carbonization process can be found in Ref. [20].

CHF storage environments and conditions

The carbon fibers were stored in different environments before mounted in a module.

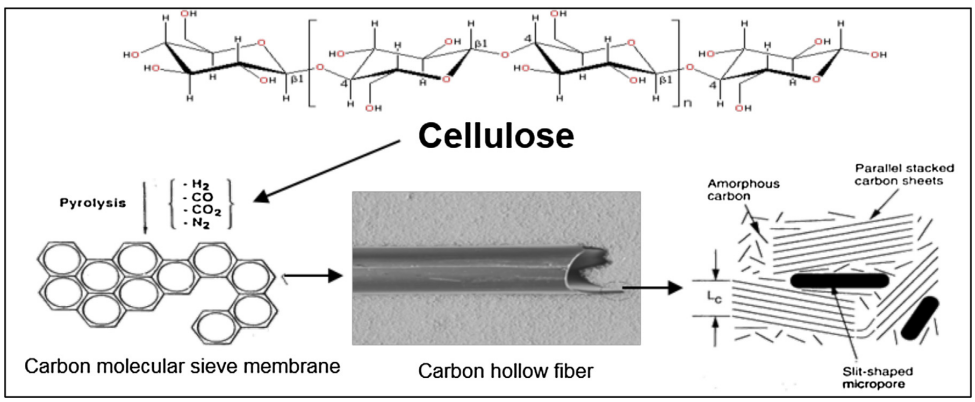

Fig. 1. Regenerated cellulose precursor to form carbon hollow fibers.

Storage in air (ambient temperature)

Different air environments were tested at ambient temperature (21 ± 2 °C):

- Stored in open air inside lab.
- Rolled in plain paper lying on open shelf.
- Rolled in plain paper lying inside cabinet (dark place; a chemical storage cabinet with dimension as; H: 1990 × W: 1000 × B: 435 MM)
- Rolled in aluminum foil lying on open shelf.
- Rolled in aluminum foil inside cabinet (dark place).
- Rolled in tightly packed aluminum foil lying on open shelf.
- Rolled in tightly packed aluminum foil lying under dark fume hood.
- Rolled in plain paper lying under dark fume hood.

Storage under vacuum (ambient temperature)

- Stored under vacuum lying inside ABS tube.
- Stored in vacuum bag in dark place inside cabinet.
- Stored in vacuum bag under the light.

Storage under CO_2 atmosphere (ambient temperature)

- Stored under CO_2 lying inside ABS tube.

Gas permeation experiments

Gas permeation tests in laboratory

The issues of porosity and surface polarity also come into play when considering the orientation of the membrane in relation to the feed stream. Generally, for the modules described here, the gas is fed into the membrane using a shell side flow configuration, having permeate gas coming from bore side. But in the study of dynamic aging, feed air was transported through the membrane using bore side feed to understand the most influential conditions which promote aging and the most critical time for aging depending on the environment the membrane is exposed to.

Two identical modules (M1 and M2 with an effective area of 0.02 m^2 for each module) were prepared and tested using a continuous (dynamic) flow of air. The feed pressure used in this study was slightly above atmospheric pressure (1.4 bar) at 24 °C temperature in a standard pressure-rise set up as described in Refs. [21,22]. Permeability tests were carried out on each module separately and were recorded at different time intervals. Each test was carried out over a time span (650 h) until linearity was established. This ensured that the aging process continued with a constant flow of air through the system. No other gases were tested for these two modules.

The useful information that can be obtained from this study is a calculation of the flow rate in accordance with the Reynolds number (R_e). Using this information, the pressure drop can also be calculated due to a change in thickness of the boundary layer [23]. The pressure at the feed end including the pressure loss was estimated and compared to that of the experimental feed pressure applied to assess the pressure loss due to aging. Three different types of pressure are considered when evaluating the estimated feed pressure. They are the pressure loss due to sudden contraction, i.e., the flow going from the inlet tube to the entrance of the membrane. Secondly, the friction losses within the membrane due to the gas flow through the fiber. Thirdly, the loss due to the expansion from the permeate side to the atmosphere. The estimated feed pressure at the feed side was calculated using a Fanning-type expression [24].

Intermediate aging (aging with no feed flow). Following a period of 28 days, permeation tests were conducted on Module 1 as a function of dynamic aging. The pump was then disconnected from the module at the feed end and the module was exposed to the atmosphere, undergoing a period of static aging (ambient temperature). A vacuum remained on the permeate side of the module, to prevent the adsorption of air on the remainder of the gas unit. Thus, this combination of dynamic and static aging was termed intermediate aging.

Real biogas field exposures (small scale pilot plant)

Field 1 (F1). Some of the CHF membrane modules exposed to F1 were modified using chemical vapor deposition (CVD), oxidation and reduction process. All other membrane modules studied in this article are non-modified carbon hollow fibers prepared as described in Section "Carbon hollow fibers preparation". In total 31 modules of the area ranging from 0.5 to 2 m^2 of each module were installed on F1 biogas plant for a period ranging from 25 to 212 days to separate biomethane from raw biogas mixture. Gas permeation measurements were performed with pure gas (CO_2 and N_2) at the membrane production facility, using 5 bar feed pressure against vacuum on permeate side in ambient temperature (closed-volume setup). These permeation tests on the membrane module were conducted before and after the module was exposed to biogas field, and the results were analyzed to evaluate the aging effect of real biogas on CHF. Fig. 2 shows the process diagram of F1 and F2. F3 was similar but had no H_2S removal system.

The composition of a biogas depends strongly on the substrate type and the digestion conditions. Table 1 shows the biogas source and contents of biogas produced on three different fields. The biogas, in all three cases, was fully saturated with water. However, the water was removed from the feed gas, before exposed to membranes, to keep it below %RH of 30 which is considered as a safe relative humidity for carbon membranes [5]. Proteins and other sulfur containing materials produce H_2S in the digestion process which is a poisonous and corrosive gas. It was expected that high loading of H_2S may cause the chemisorption and ultimately reduce the performance of the membrane. Therefore, the H_2S contents were reduced to <20 ppm (fuel standard requirement) in field F1 and F2. Table 1 shows the loading of H_2S in different fields and the amount of H_2S exposed to the membranes.

Field 2 and Field 3. One membrane module with an effective area of 0.08 m^2, which had been gas permeation tested for single gas CO_2, N_2, O_2 and CH_4 in the laboratory, was installed at F3, where the CHF were exposed to a real biogas containing H_2S from 150 to 2400 ppm. H_2S concentration was varying each day depending

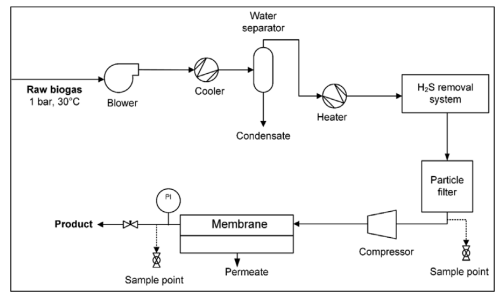

Fig. 2. Biogas separation process using CHF membrane at Field 1, 2 and 3. (F3 did not have H_2S removal system).

Table 1
Biogas source and its composition in different fields.

Biogas source	Food waste F1	Food waste, fish oil F2	Sewage, municipal waste F3
Component	(mole %)		
Methane (CH_4)	64 ± 3	62 ± 6	59 ± 3
Carbon dioxide (CO_2)	30–35	32–44	38–44
Nitrogen (N_2)	<1	<1	ca. 2
Oxygen (O_2)	ca. 0	ca. 0	ca. 1
H_2S feed loading (ppm)	150–1000	0–2000	150–2400
H_2S at membrane inlet (ppm)	<5	<5	150–2400
H_2O in feed, 35 °C (g/Nm^3)	~32	~32	~32
H_2O at membrane inlet (%RH)	~20	10	~20

upon the source of biogas in the anaerobic digester. After 30 days, the module was brought back to the laboratory and tested for the above-mentioned single gases and installed again at F3. After exposure of 120 days at F3, the module was tested for single gas and installed at F2 where less concentration of H_2S (<5 ppm) was present, as the biogas was passing through the adsorption column containing silica gel for H_2S removal. After continuous exposure of 100 days at F2, the CHF membrane module was tested for single gases in the laboratory. After the tests, it was again installed at F3 for additional 50 days for high concentration exposure of H_2S. The reason for this procedure was to understand if biogas containing less concentration could regenerate the hollow fibers effected by high concentration of H_2S.

Difference between steel housing and ABS housing. Stainless steel (SS) with all its advantages, is still a costly material to use commercially in membrane assembly. To achieve an economical solution for module housing, Acrylonitrile Butadiene Styrene (ABS) material was used to make a CHF module. Both SS (effective area: 0.05 m^2) and ABS (effective area: 0.015 m^2) modules were installed at F3 for high concentration exposure of H_2S, and gas permeation tests for single gases, CO_2, N_2, and CH_4 were performed before and after exposure to analyze the aging effect on membranes inside both materials.

Results and discussion

Aging under different conditions

The difficulty in carrying out any type of aging experiment on bundles of these CHF in a module is that the membranes cannot be tested immediately after carbonization, as the time required to prepare the modules is a minimum of 6 h. The epoxy resin requires this duration of time to set. Placing the module directly in the gas testing unit under vacuum, would cause distortion of the epoxy resin, break the seal and hence the gas would permeate through the fibers as well as the module resulting in an inaccurate evaluation of permeability.

The first permeation tests were thus carried out 9 days after the CHF had been prepared. It has been reported by Menendez and Fuertes [8] that the permeability values of carbon membranes drops by nearly 50% after 1 day due to aging and following a certain period of time, then the reactive sites are saturated and then permeability remains constant. Hence, the aging reported in the current work is investigated after an aging of 9 days. Membranes in which the permeability varies due to severe aging, is not an option for large-scale use. Thus, following module assembly, mounting the module into the gas permeation unit and allowing time for a short evacuation period, the fibers had already undergone a significant aging, and it will be of interest if high performance can be recovered.

The aging effect on the CO_2 permeability of carbon membrane stored under different conditions is shown in Fig. 3 and summary of the results is presented in Table 2. To analyze the performance stability of the stored CHF, the gas permeation properties were measured systematically during this storage period. CHF after carbonization were rolled in a plain paper and kept on an open shelf inside the lab for all batches until the first module was prepared and permeation test was performed. Fig. 3(a) presents the four sets of CHF which are rolled in plain paper and then stored at different conditions. The decline in CO_2 permeability is fastest for the fibers lying on an open shelf, whereas slowest in the fibers stored inside the cabinet, which decelerated the chemisorption phenomena by reducing the O_2 supply inside the cabinet. Apparently, membrane performance losses here are due to chemisorption of O_2, rather than other contaminants.

Fig. 3(b) shows the CO_2 permeability loss over time for CHF rolled inside aluminum foil and stored under different conditions. Coldness (4 °C) was not helpful in preventing or slowing the performance loss of the membranes. Not surprisingly, the identical effect as Fig. 3(a) was observed for the CHF rolled in aluminum foil and stored inside the cabinet. In all cases, membrane performance becomes constant after all unstable sites on carbon had reacted or stabilized by the formation of oxygen surface groups.

The storage of CHF under vacuum was helpful in keeping the membrane performance to some extent. Fig. 3(c) illustrates the change in CO_2 permeability when CHF were stored under vacuum in different conditions. Fibers stored inside an ABS tube under vacuum slowed down the aging effect until first 28 days and then performance remained constant for next 32 days. First permeation test was performed 10 days after the carbonization and then fibers were stored under vacuum, which explains that some reactive sites of carbon surface had formed oxygen surface groups during first 10 days reducing CO_2 permeability from 74 to 33 Barrer, however applying vacuum helped in slowing down and further preventing chemisorption of O_2, when stored inside ABS tube. CHF stored in vacuum bag did not help to prevent the aging and that was due to small leakages present in vacuum bags. Fig. 3(d) shows the aging comparison for CHF stored under CO_2 atmosphere and in open air. It was observed that fibers stored under CO_2 environment lost the performance faster than fibers stored under open air inside the lab. Hayashi et al. [25] reported a membrane carbonized at 700 °C and they studied the stability of membrane in air at 100 °C for 30 days. They observed that permeances decreased in the initial stage of the oxidation but were regenerated by a post-heat-treatment at 600 °C for 1–4 h. Lagorsse et al. [9] studied the effect of air on CMS membrane and reported that the formation of new constrictions arising from chemisorption of oxygen had a noticeable influence on penetrants with critical dimensions close to the critical pore size resulting in higher loss of the N_2 permeance as compared to CO_2 and similar behavior was observed in this study.

Dynamic, intermediate and static aging

The aim of this study was to understand the aging phenomena when membranes are lying under ambient environment (air). The

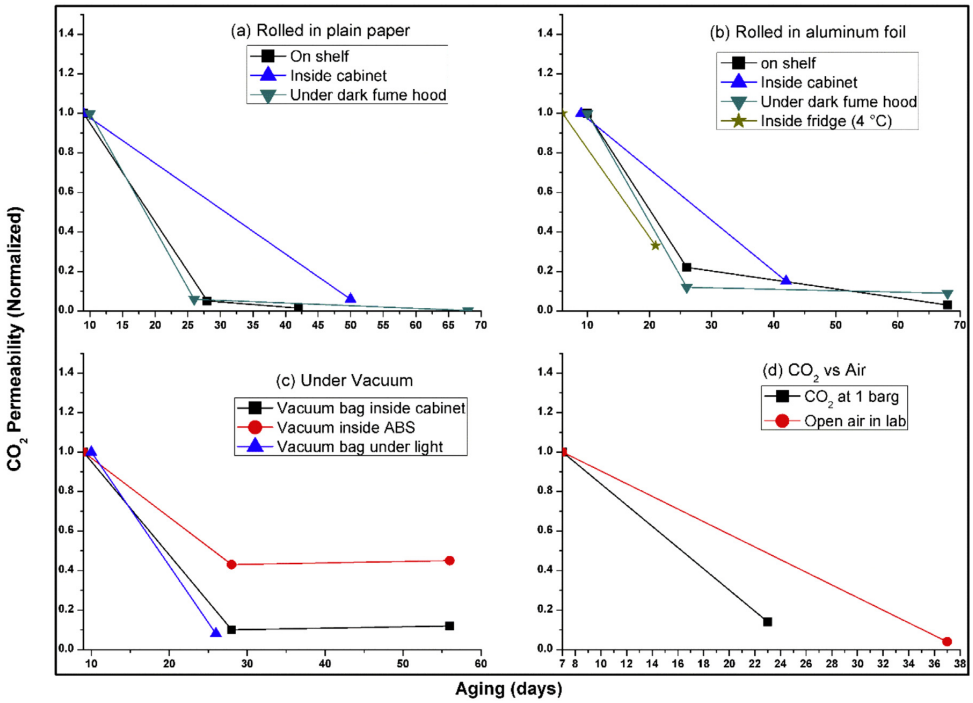

Fig. 3. Storage of CHF under different environments.

more focus of the work was about the collective permeance of air through the membrane. The individual O_2 and N_2 permeabilities were not measured in these experiments. In Fig. 4, the scatter plot is to show the trend of air permeability through the membrane. The results showed that both modules are following the same trend.

The slope for aging is hard to define as many variables are involved here. The degree of freedom can be reduced by controlled environment as in dynamic aging in this study. With bore feed orientation as depicted from the graph in Fig. 4, there is only a slight change in permeability over a time of 650 h. The slight changes between each module are most likely attributed to the variation in fiber diameter and hence wall thickness, as slight variations in the pre-treatment stages can result in variations of the membrane permeability. It is evident that there is no decrease in permeability, indicating that this dynamic source of air has an inhibitory effect on aging. Following, approximately 100 h of aging, there is an increase in permeability and after 200 h of aging, there is a stabilization period, in which the permeability remains within a range of 50–60 Barrer. The air flow under controlled environment had a regenerative effect on the membranes to restore the permeability which was lost due to physical aging (narrowing of pores due to matrix shrinkage and/or pore clogging caused by dust and moist) during first nine days until the module was prepared

Table 2
Effect of storage conditions and storage time on CO_2 permeability of regenerated cellulose-based CFM.

Storage conditions	Duration (days)	CO_2 permeability loss (%)	Fig. no.
Rolled in plain paper			
On shelf	42	98.5	3(a)
Inside cabinet	50	93.5	3(a)
Under fume hood in darkness	68	99.7	3(a)
Rolled in aluminum foil			
On shelf	70	96.9	3(b)
Inside cabinet	42	85.1	3(b)
Under fume hood in darkness	68	91.4	3(b)
Inside fridge (4 °C)	21	66.7	3(b)
Under vacuum			
In Vacuum bag inside cabinet	56	88.0	3(c)
In ABS tube under vacuum	56	55.4	3(c)
In vacuum bag under light	26	91.2	3(c)
Under CO_2 at 1 bar	23	86.0	3(d)
Open air inside lab	37	96.0	3(d)

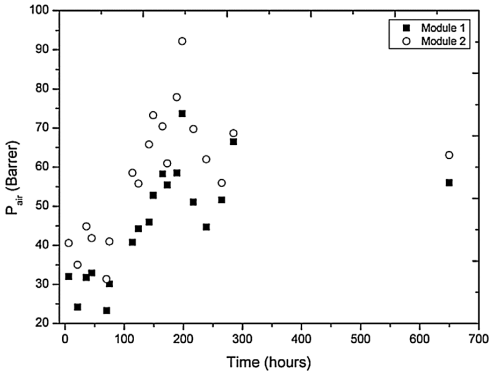

Fig. 4. Permeability values for air as a function of time (dynamic aging). Two similar modules were tested to ensure validity of the study.

and installed for testing. Some studies have shown that high fractional free volume polymer precursor based carbon membranes may change pore structure due to physical aging, like glassy polymer membranes [6,26]. After recovering the permeability, controlled environment helped to keep it at a constant value. Physical aging at this point would be considered zero in this case. The rate of physical aging depends on the ratio of the driving force, i.e. the displacement of the specific volume from its equilibrium value, and the relaxation time for the sample, which is a function of temperature and the material's current free volume state.

As shown in Fig. 5, there was no significant change in permeability over an 11-day period following a 27-day period of dynamic aging. The temperature was then monitored and recorded in accordance with the room temperature (22–25 °C) at the time of each experiment. From the presented results in Fig. 5, it can be seen that the dynamic atmosphere had an inhibitory effect on the aging process.

Pressure drop calculations

Given the similarity in velocity and inner diameters of both Module 1 and 2, the Reynolds number of 423 and 442 were evaluated respectively, which shows that flow is laminar [27].

The quantified pressure values at various points of the membrane are correlated to give Δp^2 in Pa^2, as shown in Table 3. From the data shown in Table 3, it is evident that the estimated feed pressures, p_{est}, of 1.35×10^5 and 1.38×10^5 Pa are within close

Table 3
Data correlating the pressures at various sections of the membrane. These values have been used to estimate the feed pressure, p_{est} and compared with the experimental feed pressure, p_{exp}.

Module	Δp^2 (Pa^2)	Δp (Pa)	p_{est} (Pa)	p_{exp} (Pa)
1	8.35×10^9	9.14×10^4	1.35×10^5	1.40×10^5
2	9.16×10^9	9.57×10^4	1.38×10^5	1.40×10^5

range of the experimental feed pressures, p_{exp}, of 1.40×10^5 Pa for Module 1 and 2, respectively. This indicates that the flow rate is maintained and the accumulation of a boundary layer due to adsorption of molecules such as O_2 present in the air flow is minimized. Hence, aging of the membrane is reduced using this type of flow system.

Static study

Fig. 6 illustrates the data recorded for the static aging experiment. The first permeation test was not carried out until 9 days of aging had occurred. As mentioned earlier, during module assembly, mounting the module into the gas permeation unit and allowing time for a short evacuation period, the fibers had undergone a significant aging. CHF used to prepare this module, Module 3, were prepared from the same batch as those used in Module 1 and 2, and thus were expected to have similar performance. Fibers were stored in the lab environment all the time.

As depicted in Fig. 6, the permeability of Module 3 decreased exponentially as fibers underwent a further period of aging between day 10 and day 141. However, from day 41 to day 141, the change in permeability remained very small. The relatively small fluctuation in permeability from day 41 to 141 indicates that the largest effect of aging had occurred, and the permeability was relatively stable for this membrane after day 41.

Analysis of the changes in permeability from day 41 to day 141 appears quite similar for the membranes exposed to intermediate aging followed by static aging. However, the average decrease in permeability from day 1 for the module that is exposed to the only static environment is hard to determine from the slope of permeability as a function of time, as shown in Fig. 6. Only a good enough estimation can be made by considering the slope from day 41 to 141. But that estimation is not good enough to understand the life expectancy of the membrane. From the Figs. 5 and 6, apparently, it can be expected that the membranes exposed to the static environment are aging at a rate faster than those previously exposed to a dynamic air supply and then to a static

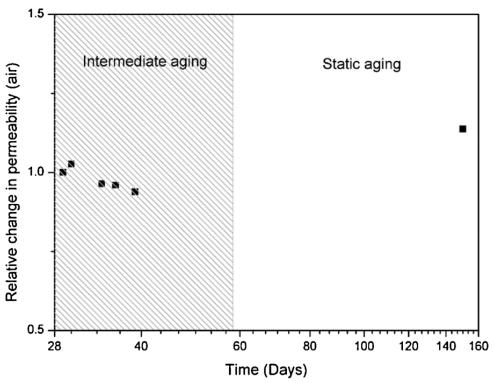

Fig. 5. Permeability values of air as a function of time for Module 1 containing carbon membranes previously used in the dynamic aging study.

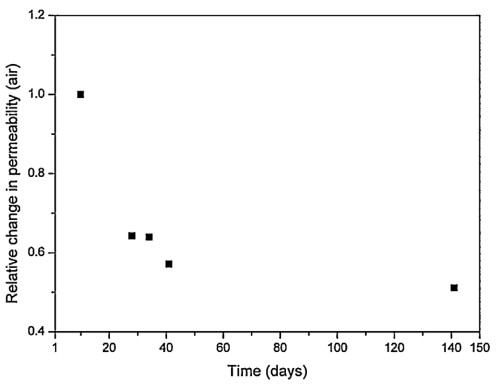

Fig. 6. Permeability data plotted as a function of time, for the static aging study.

environment. Hence, this confirms the positive effect that a dynamic air source has on slowing down the aging process. However, as mentioned previously, in order for this to be a viable process for industry, the process of aging should be kept to a minimum. Although a dynamic air flow has this effect, financially, the cost of this process should be evaluated before applying it at large scale.

Real biogas exposure

This chapter presents the results of exposing the carbon membranes to biogas from three different plants F1–F3.

Exposure to F1

Table S1 in supporting information summarizes the permeability loss of CO_2 and N_2 after CHF exposed to real biogas with H_2S <5 ppm. It can be seen in Fig. 7 and table S1 in supporting information that most of the modules lost CO_2 permeability in the range of 20–50%, even though the exposure time for these modules is varying from 25–210 days. It explains that after oxygen adsorption (whether during module preparation or in a later stage) CHF start stabilizing without further loss in performance. Membrane modules showing 20% loss after 210 days may have lost the performance already and close to saturation point before they were tested the first time for gas permeation.

Exposure to F2 and F3

Fig. 8shows the change in permeability of N_2, CO_2, CH_4 and O_2 with the time for CHF exposed to F2 (H_2S: <5 ppm) and F3 (H_2S: 150–2400 ppm). Results indicate that after 30 days with high H_2S concentration, CHF lost 22% CH_4 permeability, however, CO_2 permeability increased resulting in good membrane performance for CO_2-CH_4 separation, and so did increase the O_2 and N_2 permeabilities. It can be speculated that CH_4 molecules filled the carbon micropores and prevented the access to oxygen, thus resulting in enhanced performance of the membrane. However, after four months with a high concentration of H_2S, CHF showed degraded performance with 70% loss in CO_2 permeability, which may be the result of micropore blockage. Adsorption onto activated carbon is one of the methods that is used to clean the biogas when pressure swing adsorption (PSA) is used to upgrade the biogas. The

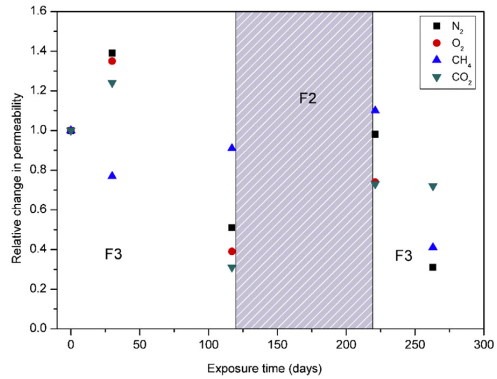

Fig. 8. Relative change in permeability of N_2, CO_2, O_2 and CH_4 when CHF are exposed to high H_2S concentration.

reason for decreased performance of carbon membrane at F2 may be the high loading and adsorption of H_2S on carbon. Consequently, regeneration of carbon membrane is needed to restore the lost performance. The membrane module was then installed at F2 with low H_2S for regeneration and it was observed that after 100 days exposure, membrane recovered 40% CO_2 permeability without any extra regeneration treatment. O_2, N_2, and CH_4 permeabilities were also increased. Again, exposure of 50 days at F3 showed no effect on CO_2 permeability, whereas N_2 and CH_4 permeabilities were decreased. O_2 permeation was not measured for the final experiment. It can be assessed from the exposure at F2 and F3, that high H_2S concentration reduced the membrane performance, but in some way, membrane regenerated itself to some extent under real biogas conditions. CHF membranes need to be regenerated during separation process and this extra step adds complexity and cost to the process. Anderson et al. [12] have reported the effect of H_2S on polyfurfuryl alcohol based carbon membranes. The PFA based carbon membranes showed that CO_2 permeance was reduced by 7% in the presence of H_2S (partial pressure: 0.3 kPa) in the feed when membrane was performing at 35 °C for almost 5 h. The loss in CO_2/N_2 selectivity was only 2%.

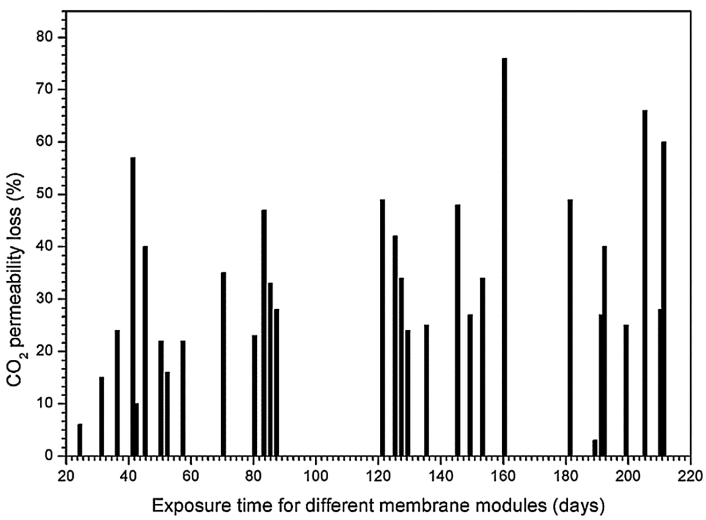

Fig. 7. Percent loss in CO_2 permeability for different CHF modules in different exposure time at F1.

A non-adsorbable gas like H_2 or He could be used in purging the membrane for removal of contaminants, but this is adding cost and extra line to the process for the treatment. Another alternative is N_2, however in ultra-microporous membranes, the kinetics of transport of N_2 may be too slow and if separation application does not involve N_2, then nitrogen itself will constitute a contaminant that could take a couple of hours to leave the pore structure of the membrane [9]. The objective of this purging study by exposing membrane to real biogas stream with high and low H_2S concentration was to regenerate and clean the membrane by removing contaminants adsorbed physically. Thus, the additional cost could be avoided in the industrial application of carbon membranes.

Effect of module material housing

As mentioned earlier, the focus of this study is to make the CHF membranes viable and economical for industrial applications. The exposure to high H_2S concentration was to understand if CHF can survive this harsh condition and H_2S removal unit could be used after membrane separation, which would reduce the cost of the unit because of less gas flow on retentate as compared to feed flow. The intention to study the SS housing and ABS housing was primarily to understand the effect of H_2S and aging of the membrane and finally to reduce the cost of the module. Biogas primarily deals with CO_2–CH_4 separation, but before the gas is exposed to the membrane, pretreatment is performed to remove impurities like H_2S and water. The same task is performed for natural gas separation, so research published on natural gas upgrading can also be applied to biogas upgrading. Schell et al. [28] studied a process for biogas treatment using cellulose acetate spiral-wound membranes for 18 months and reported that no significant differences were seen between the permeation of landfill gas with and without pretreatment, however, the authors suggested that gas pretreatment could prolong the service lifetime of membranes.

The internal corrosion of carbon steel in the presence of hydrogen sulfide represents a significant problem for both oil refineries and natural gas treatment facilities. Surface scale formation is one of the important factors governing the corrosion rate. The scale growth depends primarily on the kinetics of scale formation which is proportional to the sulfide concentration.

One module with SS-housing and one with ABS-housing were installed at F3 with high H_2S concentration and single gas permeation tests were performed in the lab afterwards. Fig. 9 shows the SS-module and single gas permeation results for N_2, CO_2, and CH_4. Both N_2 and CO_2 were stable for the first 20 days and then N_2 permeability started increasing, whereas CO_2 remained almost constant for first two months. CH_4 permeability increased 2.4 times within first 24 h and results were same even after 18 days before it dropped very quickly in the next 10 days. The reason for the loss in CH_4 permeability may be the pore clogging with H_2S and CO_2. Only CO_2 was tested after 30 days and it can be seen that CO_2 permeability started declining after two months of exposure at F3 until the membrane lost 90% of CO_2 permeability in 350 days. In comparison with Fig. 8, here the membrane module is exposed to only high H_2S concentration so more chances of pore clogging which resulted in 90% loss of CO_2 permeability. However, in Fig. 8, exposure to F2 with low H_2S concentration had a regenerative effect on the membrane and CO_2 permeability loss was 25% after 260 days.

Fig. 10 presents the effect of ABS-housing and results for single gas permeation are very like Fig. 9 except CH_4 permeability, which seems declining slower in the case of ABS-housing. The reason expected here could be the H_2S concentration varying every day on biogas field F3 (150–2400 ppm). So, the physical aging (clogged micro pores) effect was slightly different for both modules. Results from Figs. 9 and 10 show that ABS-housing has the same effect as

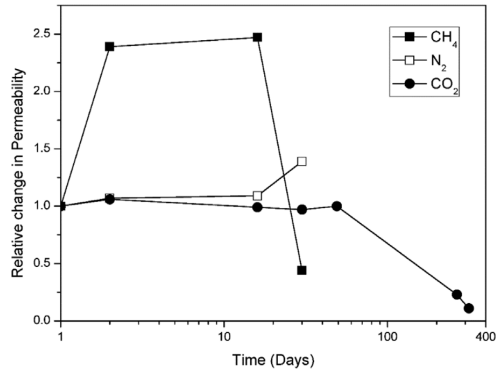

Fig. 9. Single gas permeability for CHF in a stainless-steel module housing.

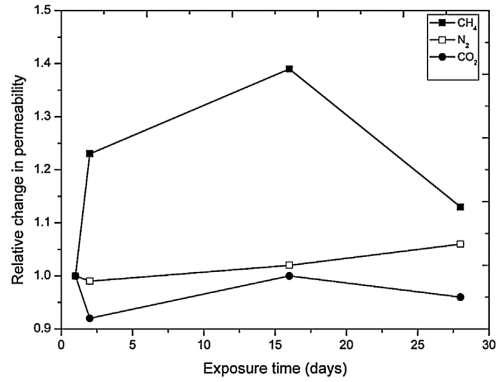

Fig. 10. Single gas permeability for CHF in ABS module housing.

SS-housing and it could be used for making modules of CHF. If CHF module needs to be modified with heat treatment processes like thermal regeneration or CVD for pore tailoring, then temperature limitations for ABS-housing and sealing epoxy should be measured. However, ABS housing is suitable for electrothermal regeneration since ABS is non-conductive.

Conclusions

Regenerated cellulose based carbon hollow fibers CHF were stored under different environments. Membranes stored in lab condition and CO_2 atmosphere lost the CO_2 permeability by more than 80% within the first 30 days. CHF stored in ABS tube under vacuum were stable after losing 65% CO_2 permeability in one month, and fibers lost their permeability very fast when stored in air at low temperature (4 °C).

Dynamic aging, as defined earlier "aging under controlled environment and continuous gas flow through the membrane", had a promising regenerative effect on the membranes to recover some permeability. The fibers which underwent dynamic aging were not susceptible to static aging anymore. They showed the same performance even after 128 days when stored in the laboratory environment. In total, 31 modules of area 0.5–2 m^2 for each module were used to separate biogas in actual biogas field for days ranging from 25 to 212. Most of these modules lost 40% permeability of CO_2 within a few days after installation and were

stable afterwards. CHF were mechanically stable at 20 bar in real industrial conditions.

Further real gas exposure was performed in two biogas fields by exposing CHF to the H_2S in the sequence high–low–high concentrations. Adsorption of H_2S on carbon membrane may significantly reduce the performance over time. It was observed that the membranes installed at high H_2S (150–2400 ppm) concentration lost CO_2 permeability by up to 65% in 125 days, and 55% of this lost permeability was regenerated by exposing membrane to a biogas field with low H_2S (<5 ppm) concentration for 100 days. When this membrane was installed again on high concentration field, the CO_2 permeability was stable for the next 50 days. The biogas-field results showed that high loadings of H_2S increase the aging effect on carbon membranes. Hence, the pre-treatment of biogas is required to bring down the H_2S contents before the upgrading process.

However, it is important to note that aging behavior of carbon membranes may depend on the precursor and the manufacturing conditions used. Carbon membranes with e.g. different structure and surface chemistry will behave differently as shown by other researchers. Thus, it would be useful in the future study to do a direct comparison of carbon molecular membranes from different precursors and manufacturing conditions to better understand the behavior of CMS in biogas application.

Module casing, SS-housing or ABS-housing did not affect the membrane performance significantly. If CHF module needs to be modified with heat treatment processes like thermal regeneration or CVD for pore tailoring, then temperature limitations for ABS-housing and sealing epoxy should be measured. However, ABS housing is suitable for electrothermal regeneration since ABS is non-conductive.

Acknowledgments

The authors are very grateful to Ms Cathrine Hval Carlsen for excellent laboratory work on the carbon hollow fiber membranes. The authors would also like to thank The Department of Chemical Engineering at NTNU for providing the possibility to work with this article.

Appendix A. Supplementary data

Supplementary data associated with this article can be found, in the online version, at https://doi.org/10.1016/j.jiec.2018.10.037.

References

[1] J. Koresh, A. Soffer, J. Chem. Soc. Faraday Trans. 1 76 (0) (1980) 2457.
[2] S.M. Saufi, A.F. Ismail, Carbon 42 (2) (2004) 241.
[3] S. Lagorsse, M.C. Campo, F.D. Magalhães, A. Mendes, Carbon 43 (13) (2005) 2769.
[4] M.C. Campo, S. Lagorsse, F.D. Magalhaes, A. Mendes, J. Membr. Sci. 346 (1) (2010) 26.
[5] C.W. Jones, W.J. Koros, Ind. Eng. Chem. Res. 34 (1) (1995) 158.
[6] L. Xu, M. Rungta, J. Hessler, W. Qiu, M. Brayden, M. Martinez, G. Barbay, W.J. Koros, Carbon 80 (2014) 155.
[7] G.B. Wenz, W.J. Koros, AIChE J. 63 (2) (2017) 751.
[8] I. Menendez, A.B. Fuertes, Carbon 39 (5) (2001) 733.
[9] S. Lagorsse, F.D. Magalhães, A. Mendes, J. Membr. Sci. 310 (1–2) (2008) 494.
[10] K.-i. Okamoto, S. Kawamura, M. Yoshino, H. Kita, Y. Hirayama, N. Tanihara, Y. Kusuki, Ind. Eng. Chem. Res. 38 (11) (1999) 4424.
[11] M.C. Campo, F.D. Magalhaes, A. Mendes, J. Membr. Sci. 350 (1–2) (2010) 180.
[12] C.J. Anderson, W. Tao, C.A. Scholes, G.W. Stevens, S.E. Kentish, J. Membr. Sci. 378 (1) (2011) 117.
[13] S. Haider, A. Lindbråthen, J.A. Lie, I.C.T. Andersen, M.-B. Hägg, Sep. Purif. Technol. 190 (Suppl C) (2018) 177.
[14] W. Li, S.A.S.C. Samarasinghe, T.-H. Bae, Ind. Eng. Chem. 67 (2018) 156.
[15] C. Zhang, G.B. Wenz, P.J. Williams, J.M. Mayne, G. Liu, W.J. Koros, Ind. Eng. Chem. Res. 56 (37) (2017) 10482.
[16] J.A. Lie, M.-B. Hägg, J. Membr. Sci. 284 (1–2) (2006) 79.
[17] J.A. Lie, Phd. Thesis Synthesis, Performance and Regeneration of Carbon Membranes for Biogas Upgrading — a Future Energy Carrier, Norwegian University of Science and Technology, Trondheim, 2005.
[18] X. He, M.-B. Hägg, J. Membr. Sci. 390–391 (Suppl C) (2012) 23.
[19] M.-B.Hägg. J. A. Lie, Patent; Carbon Membranes, US20100162887 A1, 2010.
[20] S. Haider, J.A. Lie, A. Lindbråthen, M.-B. Hägg, Membranes 8 (4) (2018) 97.
[21] K. Adachi, W. Hu, H. Matsumoto, K. Ito, A. Tanioka, Polymer 39 (11) (1998) 2315.
[22] K.C. O'Brien, W.J. Koros, T.A. Barbari, E.S. Sanders, J. Membr. Sci. 29 (3) (1986) 229.
[23] M. Mulder, Basic Principles of Membrane Technology, 2nd ed., Kluwer Academic Publishers, Dordreacht, 1996 p. 564.
[24] N.C. Mehta, J.M. Smith, E.W. Comings, Ind. Eng. Chem. 49 (6) (1957) 986.
[25] J.-i. Hayashi, M. Yamamoto, K. Kusakabe, S. Morooka, Ind. Eng. Chem. Res. 36 (6) (1997) 2134.
[26] X. Ma, S. Williams, X. Wei, J. Kniep, Y.S. Lin, Ind. Eng. Chem. Res. 54 (40) (2015) 9824.
[27] R.H. Perry, Perry's Chemical Engineers Handbook, 7th ed., McGraw-Hill, New York, 1997.
[28] W.J. Schell, C.D. Houston, Energy Prog. 3 (1983) 96.

Appendix H

Paper IV

CO_2 separation with carbon membranes in high pressure and elevated temperature applications

Paper published in Separation and Purification Technology 190 (2018) 177-189.

Separation and Purification Technology 190 (2018) 177–189

Contents lists available at ScienceDirect

Separation and Purification Technology

journal homepage: www.elsevier.com/locate/seppur

CO_2 separation with carbon membranes in high pressure and elevated temperature applications

Shamim Haider[a], Arne Lindbråthen[a], Jon Arvid Lie[a], Ingerid Caroline Tvenning Andersen[b], May-Britt Hägg[a,*]

[a] Norwegian University of Science and Technology, NTNU, Department of Chemical Engineering, 7491 Trondheim, Norway
[b] Metrohm Nordic AS, 1363 Høvik, Norway

ARTICLE INFO

Keywords:
Carbon membrane
Pore tailoring
Module construction
Thermal expansion
Membrane simulations

ABSTRACT

Carbon hollow fibers (CHF) were fabricated by carbonization of deacetylated cellulose acetate precursor. To enhance membrane permeation properties, pore structure was tailored by means of an oxidation and reduction process followed by chemical vapor deposition with propene. Permeation properties using shell-side feed configuration of 70 modules (0.2–2 m^2) for both CHF and modified carbon hollow fibers (MCHF) were investigated for single gases, N_2 and CO_2 at high pressure (2–70 bar feed vs 0.05–1 bar permeate pressure) and temperature from 25–120 °C. Maximum CO_2 permeance value for a MCHF module was recorded 50,000 times higher as compared to prior modification, and CO_2/N_2 selectivity was improved 41 times in comparison with CHF for the same module. Results indicated that carbon membranes are hardly effected by high pressure, but significant drop in CO_2 permeability was observed at elevated temperature. Simulations of CO_2/CH_4 separation by MCHF and polymeric membranes were conducted based on Aspen Hysys® integrated with ChemBrane, and the process was optimized for cost calculation based on membrane area and compression energy. Simulation results indicated that the required separation can be achieved by a single stage process for MCHF, while a two-stage process is needed for the polymeric membranes.

1. Introduction

Methane is the main component of natural gas which also contains undesired components, such as CO_2, H_2O, N_2 and H_2S. The removal of these impurities is vital to meet the pipeline specification, and for this application the membranes fit well to selectively separate out CO_2 from the high-pressure gas mixture. This separation is the focus of this work. The demand for natural gas demand has increased by around 2.7% per year over the last decade with a total consumption of 3.47 trillion cubic meters in 2015, and this consumption drives a worldwide market of over $5 billion per year for new natural gas separation equipments. The market for gas separation membranes is expected to grow from US$ 150 million in 2002 to around US$ 750 million in 2020 [1–3].

The CO_2 needs to be separated to meet pipeline specifications (< 2%) as it is corrosive, reduces the calorific value of natural gas and increases compression cost for transport of the gas [4]. Amine absorption is considered the most mature technique to separate out CO_2, but the limitation of regular maintenance and continuous operator care hinder the use of amine absorber-strippers at distant locations [5]. Membrane separation has advantages like the compact modular design, simple operation, small footprints, low capital and operational cost, environmentally friendliness and easy maintenance [3]. However, membrane processes have < 5% of the natural gas sweetening market, as this technology is still facing challenges to overcome the plasticization and degradation of the membrane (caused by H_2O, CO_2, C_{4+} hydrocarbons and aromatic compounds). There is a further limitation of the membranes to process small/medium gas flows (< 50,000 Nm^3/h) [4,6]. The natural gas stream is typically treated at their elevated pressure of 30–60 bar and may also contain impurities like mist of higher hydrocarbons and fine particles that can easily deposit on the membrane surface. Most of the commercially available membranes are polymeric and some of these membranes have shown high performance for CO_2/CH_4 separation, but high-pressure separations are still a challenge as these membranes are plasticized under high pressure or high CO_2 concentration operations, and there are more chances of elevating market shares if other membrane materials are commercially produced [4–9].

Inorganic membranes with excellent thermal and chemical stabilities have been reported by many researchers. Particularly, carbon membranes have shown higher permeability and selectivities than commercially available polymeric membranes and have

* Corresponding author.
E-mail address: may-britt.hagg@ntnu.no (M.-B. Hägg).

http://dx.doi.org/10.1016/j.seppur.2017.08.038
Received 6 June 2017; Received in revised form 15 August 2017; Accepted 15 August 2017
Available online 16 August 2017

advantages in high pressure and temperature applications [8,10–14]. Permeation through carbon membranes is accomplished by the adsorption of gas molecules and activated transport through selective pore openings.

The increase in performance (permeability and selectivity of a preferred gas) of the membrane cuts the capital cost, as less area is required to treat the same volume of gas. Numerous methods are being used to enhance the performance of carbon membranes and most of them involve changing precursor, precursor geometry, and pyrolysis conditions. Variations in these factors offer desirable carbon membrane morphology and tailored microstructure resulting in desired permeation properties [15–23]. A recent study has reported CO_2/CH_4 pure gas selectivity of 204 (CO_2 permeability of 83.1 Barrer) using PBI/Kapton as precursor [13]. Very limited data is available about the pore tailoring method after the pyrolysis. The CO_2 permeance of 0.021 (m^3(STP)/m^2 bar h) and CO_2/CH_4 selectivity of 246, improved by pore tailoring technique of previously pyrolyzed hollow fibers has been reported [10].

The objective of this work is to explore the potential applicability of carbon hollow fibres (CHF) membranes at elevated pressure and temperature. Additionally, membrane pore tailoring was performed by using CVD and thermal treatment to obtain optimum selectivity and improved performance of previously pyrolyzed fibers. Despite high performance and mechanical stability of carbon hollow fiber membranes at high pressure and temperature, limited research has been done on this topic [24–27]. These authors [14] performed high pressure (70 bar) experiments with a CO_2-CH_4 mixture, and they showed that carbon membranes offer selectivity and mechanical stability also at this pressure. Kruse et al. [28] have recently reported high pressure testing of carbon tubular membranes at 200 bar for a binary mixture of CO_2 with O_2, N_2 or He which showed promising results for high pressure and high temperature applications.

This research work addresses the comparison of the CHF performance with the performance of modified carbon hollow fibers (MCHF). The permeation properties of MCHF were enhanced by changing the pore geometry using oxidation, chemical vapor deposition (CVD) and reduction processes. Furthermore, module construction process for high pressure–temperature applications is reported in the current work. These modules were tested to separate CO_2 at high pressure and elevated temperature. Finally, simulations were performed and discussed to estimate the economics of membrane process in natural gas separation application. The CHF were synthesized at a pilot scale plant using regenerated cellulose precursor, pyrolyzed in presence of N_2 at 550 °C, and the membrane modules were tested at a maximum pressure of 70 bar and maximum a temperature of 120 °C in order to study the effect on membrane performance and durability of both fibers and potting material. Further, some experiments were performed to understand the bore side feed configuration effect and the burst pressure for the carbon hollow fibers. Burst pressure value for the MCHF was calculated as 700 bar using Barlow's equation (based on the measured tensile strength of the MCHF).

2. Experimental

2.1. Materials

Acros Organics (Belgium) supplied cellulose acetate (CA: M_w 100,000) and 1-Methyl-2-pyrrolidone (NMP: Mw 99.13). Polyvinylpyrrolidone (PVP: M_w 10,000) was purchased from Sigma Aldrich (Norway). Ionic exchanged water was used for coagulation. Epoxy for module construction was received from Loctite (Norway). Steel piping was obtained from Brødrene Dahl, Norway. Steel housing and flanges were specially designed by MemfoACT AS. Gas cylinders for permeation testing were purchased from Yara Praxair: 99.96% purity for single gases (Norway).

2.2. Preparation of carbon hollow fibers

The carbon hollow fiber membrane which was investigated is a semi-commercial membrane, produced by MemfoACT AS (Norway), a company which has now closed down. The average pore size of the membrane is about 4 Å. The precursor is CA which is mixed with NMP and PVP to make dope solution. CA hollow fibers were synthesized using the dry-wet spinning process at a commercial scale plant, delivered by Philos, Korea. The prepared hollow fibers were then treated with NaOH for deacetylation. Then a tubular furnace (Carbolite®) was used to carbonize the deacetylated fibers. Procedure details for the production can be found in the patent by Hagg and Lie [29]. The protocol was optimized with respect to mechanical properties of the carbon membranes and its separation properties.

2.3. Construction of high-pressure CHF module

This chapter provides details on module construction, choice of epoxy, repair of broken fibers inside a module, and finally gas separation testing which is the ultimate quality control.

2.3.1. Potting/Sealing

Membrane modules were constructed using up to 3000 carbon hollow fibers with outer diameter between 0.15 and 0.25 mm. The length of the finished module was 800 mm. Manually sorted fibers were bundled loosely with wool thread so that fibers are held together while inserting in the stainless-steel tube as shown in Fig. 1(a). The outer diameter of the SS-pipe was 32 mm with 1.5 mm of wall thickness. Edges of the tube were trimmed to smoothen the surface so that the small ending parts/end plug (named smart plugs here, see Fig. 1(b and e)) can be glued on. Then the fiber bundle was carefully pulled through the tube and a thread was tied onto the section of the bundle facing up. Then a piece of duct tape was placed on the bottom side as shown in Fig. 1(b). The module side with dead end fibers (1 b) was first exposed to extra fast curing adhesive (Loctite 9455) for fiber ends clogging, so that the sealing glue (Loctite 9483) was not sucked into the fibers. The fibers in the module was adjusted to be freely suspended inside the module (not touching the duct tape in the bottom facing smart plug). The module was fixed vertically in a clamp and glued by filling adhesive in the right amount to achieve a hermetic sealing. A period of 24 hrs was required for the glue to fully cure at room temperature. However, three hours were sufficient to turn the module upside down and glued the other end. A plastic cup with the same diameter as the steel tube was used to prepare a glue plug with a significant length of fibers suspended within the plug. Loctite 9483 was filled through the holes in the smart plug until glue reached the gas holes. Fig. 1(d) presents the specially designed smart plug used on "open endings" side of the fibers and a glue plug with fiber endings (white dots) is shown on the top.

When sealing is cured after 24 h at room temperature, hack saw, chisel together with rubber hammer was used to open the fiber endings on the top side of the module. After opening all fibers, modules were tested for any leakage.

2.3.2. Selective clogging

CHF were quality controlled after carbonization regarding straightness, length and broken fibres by hand sorting and throwing away all broken, too short, collapsed and fused fibres. However, it is not attainable, at least currently to prevent some broken or damaged fibres to remain in the fibre bundle when the membrane package in Fig. 1(a) is produced. This leads to a bundle consisting of three principal fibre types (good fibres, broken fibres, and surface damaged fibres) randomly distributed. It has been investigated, the possibility of using what is known as selective clogging of faulty fibres. The idea of this process is reported elsewhere [30], however, the procedure was developed at MemfoACT. The outline of this process is indicated in Fig. 2.

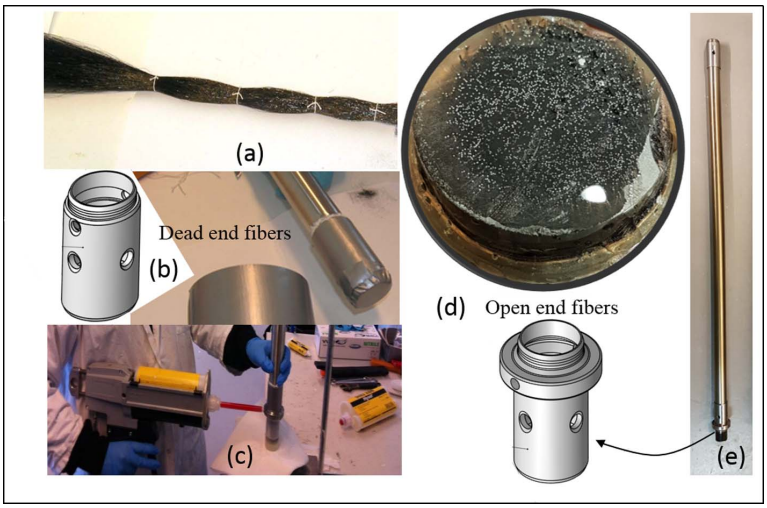

Fig. 1. CHF module construction process, (a) CHF loosely bundled with thread, (b) smart plug and dead end potting, (c) filling glue on top end of the fibers (d) Open end fibers and smart plug (e) Module ready for testing broken or damaged fibers.

The membrane package is partly mounted into a pressure vessel in such a manner that the fibre end is exposed to the surroundings. By applying vacuum to the outer surface of the fibre, the lift flow force in the failed fibre types can easily be estimated using the Hagen Poiseuille equation (Eq. (1)) if surface effects are ignored. However, the inner fibre diameter is only 0.19 mm (190 μm) so the capillary forces can most likely not be ignored, and the capillary rise (or lowering) is estimated via the Pascal equation (Eq. (2)), which requires knowledge about both surface tension of glue on carbon (our carbon consists of randomly oriented graphene sheets).

$$\frac{dx}{dt} = \Delta P \frac{r^2}{8\eta x}\phi, x = \sqrt{\Delta P \frac{r^2 \cdot t}{8\eta}} \tag{1}$$

where x is the penetration height, ΔP is the pressure difference (~1 bar), r is the internal radius of the fibre (95 μm), t is the time the pressure works (approximated as the pot life of the glue) and η is the viscosity of the liquid mixed glue.

$$x = \frac{2g.\cos\theta}{r.\rho.\gamma} \tag{2}$$

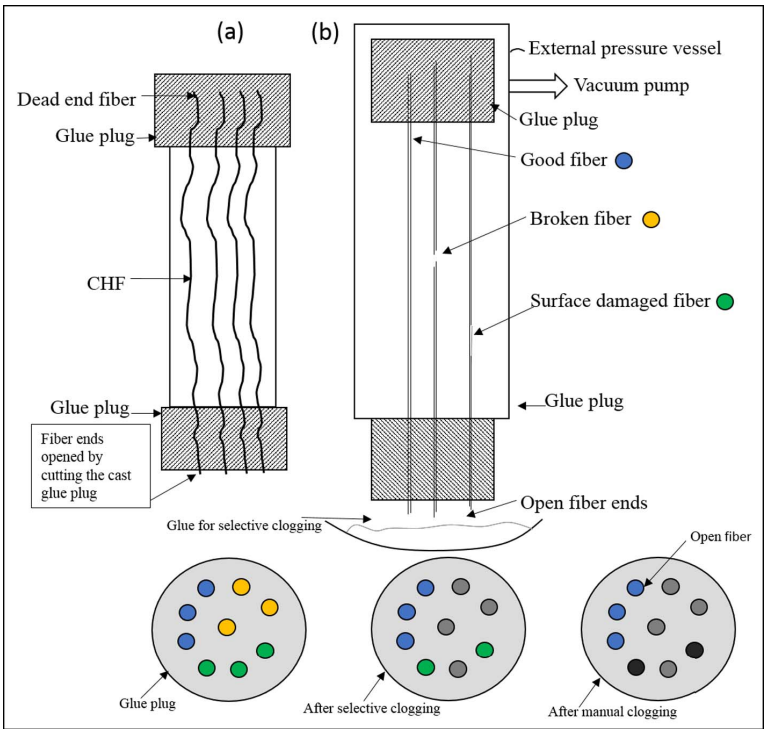

Fig. 2. (a) Membrane Package, (b) Selective clogging of failed fibers in membrane package.

where γ is the surface tension of glue on carbon, θ is contact angle between glue and carbon, ρ is density of glue, g is the acceleration of gravity.

As shown in Fig. 2, fibres marked as blue are good fibres, yellow are broken fibres, green colour represents the surface damaged fibres, and grey colour is showing clogged fibres after selective clogging process. Loctite 9492 and 9484 was used for selective clogging. As shown in Fig. 2(b), the membrane module was clamped in upside down position. The glue was mixed in a pot and kept under the module in such a way that the fibre endings from the glue plug of the module are dipped in it. Now apply the vacuum for 1–2 minutes so that the required penetration is achieved and let it cure. Then cut the glue plug up to 3–5 cm in length depending upon the glue type. The glue types used here have the penetration rise in this range for the good fibres. Now all the broken fibres are clogged because these fibres have maximum penetration rise. It is difficult to estimate the exact penetration rise for the surface damaged fibres. In practice, only 30–40% surface damaged fibres were clogged by selective clogging process. Therefore, manual clogging was done to identify and block the remaining damaged fibres. For the manual clogging, the module was clamped facing open fibres endings in upward direction. Slight over pressure than atmospheric pressure was applied instead of vacuum. Then soap or thin layer of liquid water was poured on the glue plug to identify the fibres with fastest flow (making the bubbles faster). Using magnifying glass, the fibres with fastest gas flow were marked with a coloured marker. Now wipe the liquid and apply the vacuum again before using some instant glue (Loctite 3040 here) on marked fibres. In case of manual clogging (dark grey fibres), more than one fibre (including good fibres) is blocked while clogging the one defected fibre as fibres are packed closely together. Therefore, this process reduces the membrane effective area as well.

Several glue types were tested for selective clogging application by studying both self-penetration of glue and forced penetration (under vacuum). Some of the glues are shown in table 1. It was determined that the requirements for a suitable glue that could be used for selective clogging are as follows in prioritized order:

1. The glue must have an overall forced penetration height of about 10 cm.
2. The capillary rise alone must not be more than 1 cm.
3. The glue should cure into a solid plug inside the fibres (not form a gel, or plastic/ rubber).
4. Preferably cure within an hour (at least enough to be removed from the vacuum)
5. For analytical purposes, it is an advantage that the glue has a colour other than clear or black.

2.3.3. Permeation testing

For the permeation experiments discussed here, CHF modules were tested in a pilot scale temperature and pressure rise permeation system with shell side feed configuration. The system was constructed to tolerate high pressure single gas tests (CO_2, N_2, O_2). The mass transport properties of CHF were measured with the single pure gases CO_2 and N_2 at different feed pressure and experiments were carried out with no sweep on the permeate side. He et al. [31] has performed the mixed gas experiments on carbon membrane (prepared with alike protocol) and results showed that the membrane performance for CO_2 separation is the same or even higher in some cases for mixed gas as compared to single gas separation. Due to fire hazard limitations, CH_4 was not tested at the membrane production facility, only in a dedicated field. Therefore, the values for CH_4 gas are estimated values (selectivity α $CO_2/CH_4 = 3{\cdot}\alpha$ CO_2/N_2), as shown in table 2.

Table 1
Types of glue tested for selective clogging.

Glue type	Viscosity[b]	Pot life[b]	Estimated viscous height	Measured penetration	Measured capillary rise[a]
[Loctite]	[Pa s]	[s]	(Eq. (1)) [mm]	total [mm]	[mm]
3430	23	600	77	45	0
9466	35	3600	152	50	0
9455	5	420	138	90	3
9483	7	3600	341	> 140	18
3421	95	9000	146	> 100	4
9484	110	2400	70	50	0
9464	97	2000	68	20	0
9492	50	900	63	30	0

[a] The zero values can indicate capillary lowering due to a non-wetting glue (θ > 90°).
[b] Provided by suppliers

The performance of the membrane was evaluated by measuring the CO_2 permeance in [m^3(STP)/ (m^2 h·bar)] and CO_2/N_2 selectivities (α) using equations (3) and (4). A high-pressure vessel used for permeation tests is shown in Fig. 3. The tests were run from several hours to several days, to ensure that the transient phase of diffusion was passed and steady state obtained (dp/dt tends to a constant). The gas permeance, P [m^3(STP)/ (m^2·h·bar)] was evaluated using the Eq. (3).

$$P = \frac{9.824.\ V\cdot(dp/dt)}{\Delta P\cdot A\cdot T_{exp}} \tag{3}$$

Here, V is the permeate side volume (cm^3) that can be measured with a pre-calibrated permeation cell reported elsewhere [34,35]. However, the permeate side volume for this study was estimated by the tube length and cylinder volume on the permeate side. dp/dt and A are the collection volume pressure increase rate (mbar/s) and total active area of membrane (cm^2) respectively, ΔP (bar) the pressure head and T_{exp} (K) is the temperature for experiment. The ideal selectivity was defined as the ratio of the pure gas permeances as shown in Eq. (4).

$$\alpha_{A/B} = \frac{P_A}{P_B} \tag{4}$$

2.4. Pore size adjustment

The CHF modules after permeation tests were modified to enhance the membrane performance. For this purpose, modules were installed in a custom designed rig to allow the potting material (temperature limitations) to remain outside the heated area, with integrated external cooling of the potting during the process. The Fig. 4 illustrates the steps followed in this work, as also explained in the patent held by Soffer et al. [30].

The virgin carbon will most likely have too narrow pores to yield a feasible permeability, and the whole membrane wall thickness is expected to contribute to mass transfer resistance. Thus, the overall permeance of the carbon is infeasible low for practical usage. Due to the narrow pores, the selectivity is expected to be high (i.e. the selectivity of CO_2 over methane is normally more than 100)

A mild oxidation in synthetic air at about 300 °C for a defined time will cause the pores to widen. The internal pore surface of the carbon is now obviously in a highly-activated condition, and will most likely exhibit a rapid clogging if exposed to water or any other hydrogen bonding molecules. (The carbon in this condition is surface wise like a process aged carbon. Hence, this and the following steps might also be modified to be a regeneration technique for the degenerated modules. The process is normally referred to as thermal regeneration)

The surface is deactivated using hydrogen at ca 500 °C, which will widen the pores slightly more. The permeance of the carbon is now significantly increased (normally, several orders of magnitude higher) and the selectivity is now expected to approach unity.

Chemical vapor deposition (CVD) using propene for a short time will cause a new layer of carbon to be generated on all accessible surfaces. The thickness of this layer is a strong function of reaction time and hence a thin layer of new virgin carbon with calculable thickness is

Table 2
Membrane permeances and selectivities used in this work.

Membrane type	Permeance, (m^3(STP)/(m^2 h bar)) [GPU[c]]		Selectivity	Wall thickness (μm)	Ref.
	CO_2	CH_4	CO_2/CH_4		
CHF[a]	4.14E-07 [1.51E-04]	6.89E-08 [2.52E-05]	6	41	This work
MCHF[b]	2.12E-02 [7.748]	8.53E-05 [3.12E-02]	249	41	This work
Polyimide	5.60E-02 [20.46]	1.70E-03 [6.21E-01]	33	125	[32]
CA	1.40E-01 [50.12]	9.10E-03 [3.326]	15	130	[3,33]

[a] carbon hollow fibers without pore tailoring/modification.
[b] carbon hollow fibers after pore tailoring process
[c] 1 GPU = 2.736E-03 (m^3(STP)/(m^2 h bar))

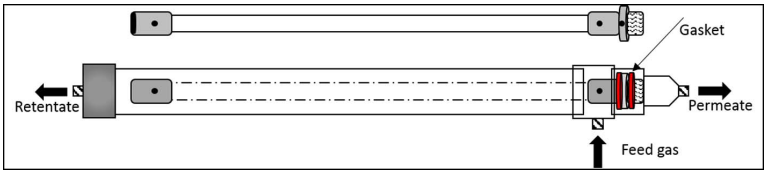

Fig. 3. Membrane module in high pressure vessel for permeation testing.

achieved. This will lead to a decrease in flux and an increase in selectivity. Subsequent post oxidation and reduction may be needed to achieve the desired transport properties for the membrane module.

In this study, the post oxidation has been scrutinized, applying the concept of full factorial experimental design to investigate the influence of air pressure, air flow and reaction time. The design consisted of two levels and two replicas for the three parameters, in total 16 tests. Reaction time was 15–90 min, pressure difference over membrane was 1 bar against vacuum and 1.4 bar against vacuum, and airflow 1.5–12 l/h as shown in table 3.

2.4.1. Procedure for pore tailoring process

Fig. 5 presents the set-up used for post oxidation–reduction and CVD process. The module was connected within the furnace, in a way that the sealing glue is kept outside the oven as shown in Fig. 5. Glue cannot withstand temperature above 150 °C, therefore it was kept cold by chilled water. An insulation between furnace and heat exchanger was also applied. Then module and lines connected to the module were evacuated using vacuum pump down to 50 mbar. To start first post-oxidation, the gas (synthetic air) bottle was opened and pressure/flow values were adjusted per protocol (e.g. 1 bar and 10 ml/min). The oven was programmed for the protocol (e.g. 4 °C/min to 300 °C, dwell 180 min, cooling) and turned on. When the temperature in the cooling sequence is below 100 °C, the vacuum pump was switched off and the gas supply was stopped. Now 2nd heating sequence was started using N_2 atmosphere using same protocol until it reached 500 °C, then switched the gas to H_2 for first post-reduction process and kept for 30 min. After post-reduction, CVD was started using propene gas and then the cooling process was initiated swapping again to N_2 until the temperature goes down to 300 °C for the 2nd post-oxidation process as shown in table 3. The module can be removed from the oven when the temperature is below 40 °C.

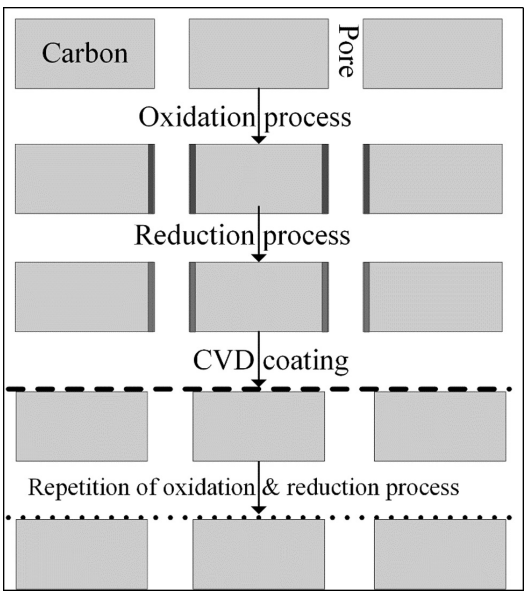

Fig. 4. Steps followed for pore tailoring of CHF.

Table 3
Parameters used for Post Oxidation-reduction and CVD process.

Gas type	Heating rate [a] /Temperature	Pressure [b] (bar)	Gas flow [b] (l/hr)	Duration (min)
Heating 1				
Synthetic air[a]	4 °C/min	1.4 bar	< 1	[b]
Postoxidation 1				
O_2 (20%)[a]	300 °C	1.4 bar	< 1	[b]
Heating 2				
N_2[a]	4 °C/min	1.5 bar	< 1	[b]
Postreduction 1				
H_2[a]	500 °C	1.4 bar	< 1	30[a]
CVD				
Propene[a]	500 °C	1.1 bar	1.5–12	[b]
Cooling 1				
N_2[a]		1.2 bar	< 1	[b]
Postoxidation 2				
O_2 (20%)[a]	300 °C	1 bar	< 1	[b]
Heating 3				
N_2[a]	4 °C/min		< 1	[b]
Postreduction 2				
H_2[a]	500 °C		< 1	30[a]

[a] Fixed parameter.
[b] varying parameter.

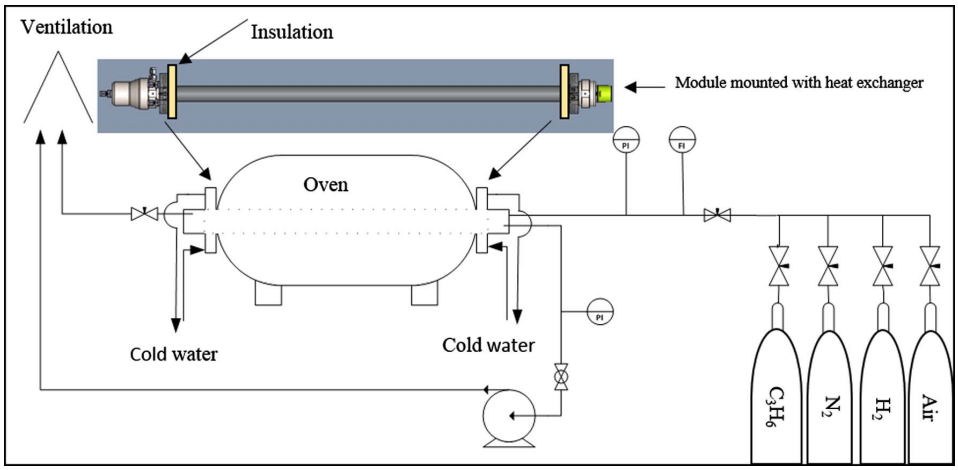

Fig. 5. Post oxidation and CVD process.

3. Simulation basis and process conditions

The following basis and assumptions were used to simulate the membrane process performance:

- Countercurrent gas transportation without sweep on permeate side has been used in all hollow fibre membrane modules.
- Membrane simulation model (Chembrane) was integrated into 9 V Aspen Hysys®. This model, developed at NTNU, uses fourth-order Runge-Kutta method to calculate the flux along membrane length, and then iteration over permeate values to converge to a solution.
- CO_2 (0–50%) is considered in the gas stream entering the membrane system. Process conditions used in simulations are shown in Table 4. Due to the limitation caused by plasticization, CA membranes are simulated for maximum 30% CO_2 contents in feed at 50 bar, whereas maximum 50% CO_2 is considered for other membranes [36]. Permeabilities and selectivities used in simulations are shown in Table 2.
- The adiabatic efficiency of the compressors is modelled as 75%.
- A single stage process can obtain methane recovery over 97.5% with MCHF, so this membrane is simulated for single stage, and other membranes are simulated for two stages. Simulating a two-stage system, permeate from the first stage is compressed to 51 bar and taken as the input for second stage membrane. Then rejection/retentate stream at 50 bar from the second stage is recycled back to mix with feed stream which is already at 50 bar. A two stage system is shown in Fig. 6.
- In a two-stage system CO_2 obtained on "permeate 2" is 97.5% pure and can be used further for re-injection in enhanced oil recovery process or some other application. In order to reduce the compression capacity/duty for CO_2, the pressure for permeate 2 is kept at 4 bar in these simulations (as membrane area is assumed to be cheaper than an extra stage of the compressor at low pressure).

Table 4
Process conditions used in simulations.

Feed composition	0–50 % CO_2, balance CH_4
Feed flow rate (Nm^3/hr)	300
CH_4 purity in product (%)	98
CH_4 loss (%)	2.5
Feed pressure (bar)	50
Temperature (°C)	25
Flow pattern in membrane module	Countercurrent

4. Results and discussion

Thermal expansion is a critical parameter and to understand the stability of CHF in applications where they are exposed to varying temperature conditions, it is important to study the thermal expansion behavior of the CHF. Thermal stability of CHF in responding to change in temperature from 43-400 °C was studied.

4.1. Thermal expansion of the CHF

CHF were placed into a thermos thread hole in an alumina thermocouple tube and cut into the right length so that 10 mm of the fiber was visible over thermocouple tube. Close clamping of the fibers was avoided so that thermal expansion difference would not introduce mechanical distortion. Thermocouple tube stood into a 3 mm hole in a steel slab. The sample was placed in an optical dilatometer (MIZURA HTM, Expert Systems) and heated at a rate of 2 °C/min in the air till it reached the set point of 400 °C. The sample was filmed during the entire heating and cooling cycle. The sample was held at 400 °C for 5 minutes. Fig. 7 is the snapshots from heating cycle. It indicates that the fibers are intact and stable up to 374 °C. Above this temperature, the change is probably because of oxidation.

4.2. CHF and MCHF (Performance difference)

A total of 70 CHF modules of effective area range 0.2–2 m^2 for each module (pore size might be in range 3–5 Å as it was not detected by TEM and BET), were modified to study the effect of pore tailoring process and separation performance of CHF and MCHF. The result is shown in Fig. 8. Single gas N_2 and CO_2 permeation tests were performed (using standard pressure-rise set up [37]) before and after modification at 23 °C, 5 bar feed (shell-side configuration) pressure and vacuum on permeate side. Permeation results measured by pressure increase method indicated that overall performance of all modules was improved after physicochemical treatment of the membrane surface, and performance for most of the MCHF is high above the Robeson's upper bound 2008 as shown in Fig. 8 [38]. Maximum permeance value for a MCHF module was recorded (module 16), which was 50,000 times higher than prior to modification. CO_2/CH_4 selectivity was improved 41 times in comparison with pre-modified fibers of the same module. This selectivity and permeance value is used in the simulation section. In a few modules, selectivity was reduced after surface treatment and the reason may be that the chemical vapor deposition process did not

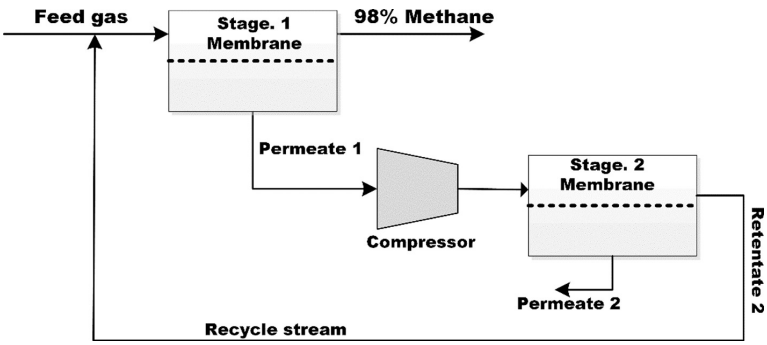

Fig. 6. Two stage membrane process.

create a sufficient layer on all the fibers, or that the oxidation–reduction process opened the pores too void before or after the CVD process. Numerical values of CO_2/CH_4 selectivity, CO_2 permeabilities, membrane area for CHF and MCHF are shown in table A1 of Appendix A. The modules referred in Fig. 8 all contain between 200–2000 fibers.

4.3. High pressure testing

The permeation properties of MCHF were also examined at elevated temperature and pressure. A membrane module consisting of two modified hollow fibers was used for high pressure experiments to understand the behavior of pure gas CO_2 and N_2 permeation (fluxes) at seven different pressure set points for shell-feed configuration as shown in Fig. 9. All experiments were done at 1 bar pressure on the permeate side. Both CO_2 and N_2 flux remained almost constant with increase in pressure. Rao et al. [39] explained that with very strong adsorbing or non-permanent gases pore blocking can occur at high pressure resulting in high selectivity. Permeabilities of N_2 and CO_2 changes, but the effect is much smaller and it explains that the dominant mechanism here is molecular sieving, which is not being effected by pressure. It was found

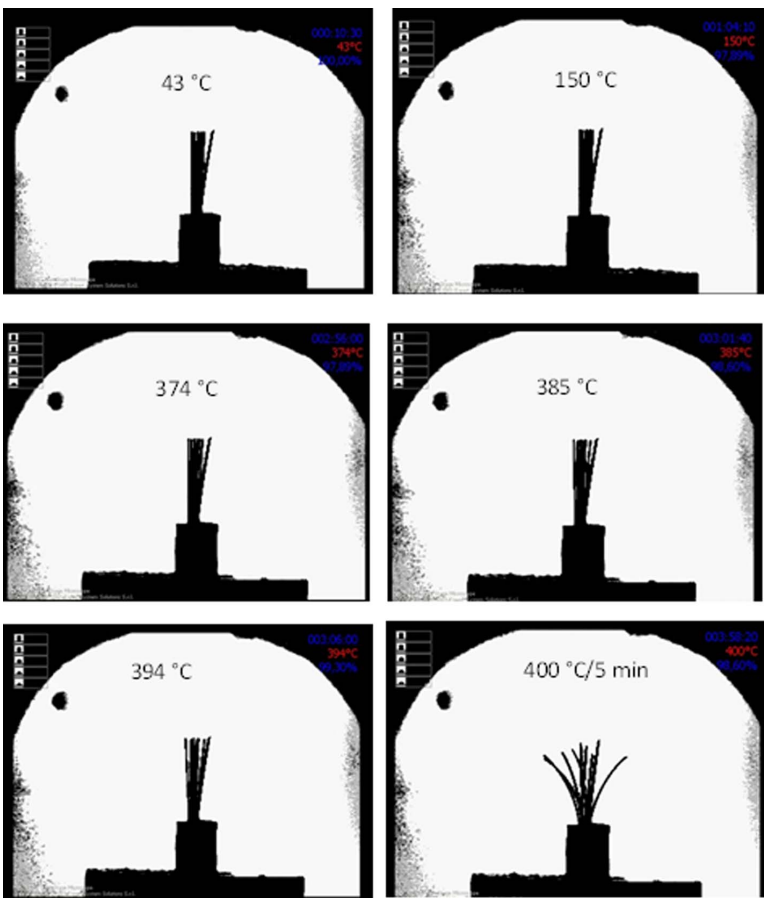

Fig. 7. Snapshots of the thermal expansion of CHF.

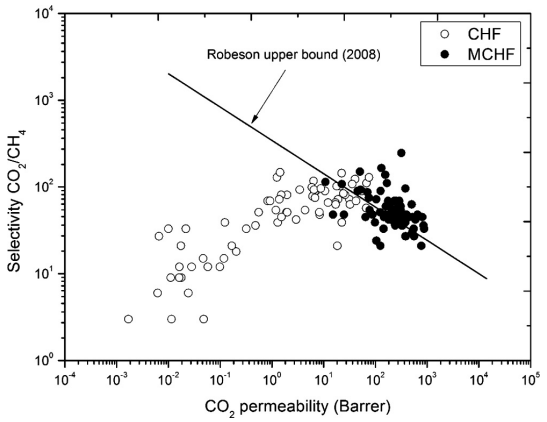

Fig. 8. Separation performance of CHF and MCHF (1 Barrer = 2.736.10E−09 m^3(STP) m/m^2 bar h).

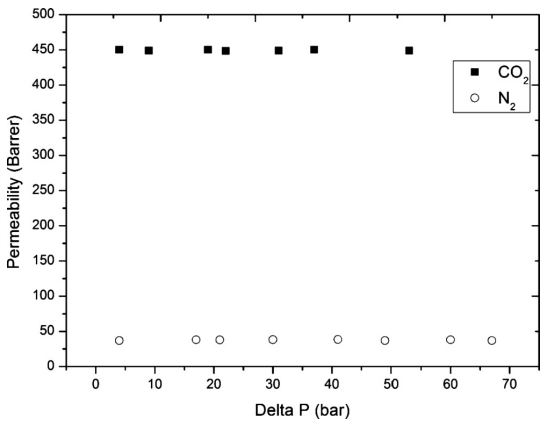

Fig. 9. CO_2 and N_2 permeability at elevated pressure (T: 23 °C).

Table 5
Economic parameters.

Membrane type	CA	Polyimide	MCHF
Cost $/$m^2$	25	50	100
Compressor cost ($)	$ 8700 × (HP[a])$^{0.82}$		

[a] HP is the installed horse power for the installed compressor.

that the carbon membrane is not swollen by high partial pressures of CO_2. Fibers were fed to shell side, however, pressures higher than 70 bar were not tested at our facility due to HSE (health and safety executive) limitations. Although in the later stage, dynamic mechanical properties of MCHF were measured and then burst pressure was calculated by using Barlow's formula (Eq. (5)). Then fibers were kept bore side fed at 60 bar (10% CO_2 in N_2) for 1 hour. It was observed that fibers are quite stable when fed through bore side as well.

$$P = \frac{2S \cdot T}{(OD)} \tag{5}$$

Here, P (psi) is the fluid pressure, S (psi) is allowable stress (ultimate tensile strength or yield strength can be used), T(in) wall thickness of the fiber, OD(in) is outside diameter of the fiber.

4.4. Elevated temperature testing

To investigate the temperature dependence of mass transport through the MCHF, pure gas CO_2 and N_2 has been studied between 23 and 120 °C as shown in Fig. 10. The extensive temperature span shows that CO_2 and N_2 have different transport behavior with the temperature elevation. For inert gases, the separation can be done at temperatures up to the carbonization temperature (~500–800 °C). If the operational temperature is limited by the sealing material, this may be overcome by installing heat exchangers at the module ends. As shown in Fig. 10, CO_2 permeability declines significantly almost 50% in a linear fashion when the temperature is increasing. Fuertes et al. [40] suggested that the CO_2 permeability decline at high temperature and low pressure is a result of a compensation between increasing mobility and decreasing adsorption. In contrast, the effect of temperature on N_2 permeability was very low and above 45 °C, the permeability of N_2 is almost constant.

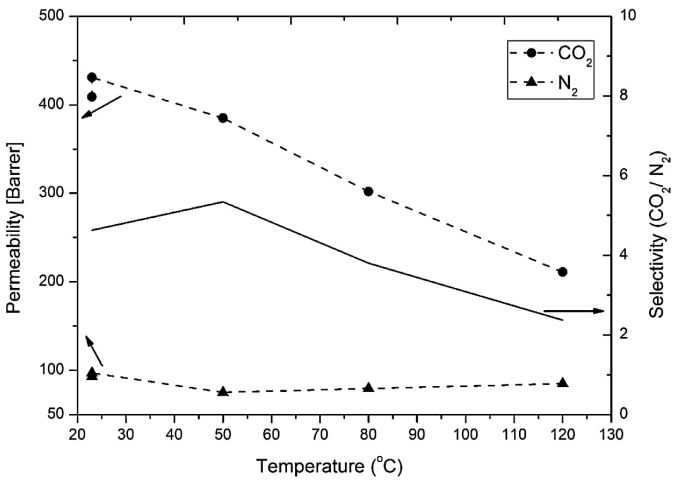

Fig. 10. Effect of temperature on the permeability of CO_2 and N_2 (P: 5 bar).

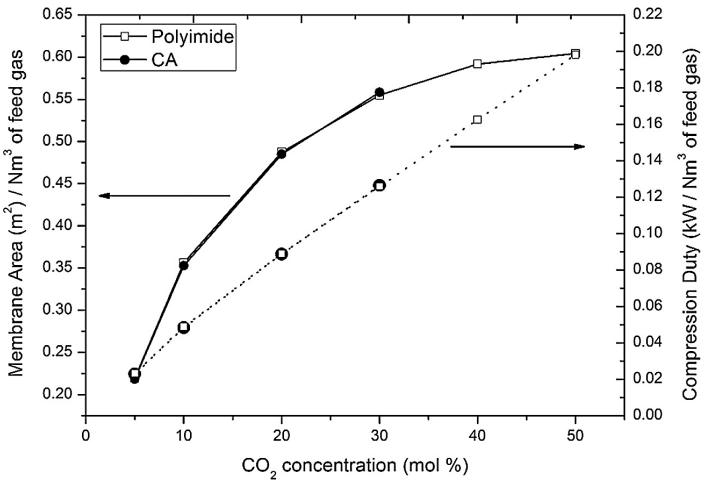

Fig. 11. Effect of CO_2 contents in feed on Area and duty for two-stage membrane system.

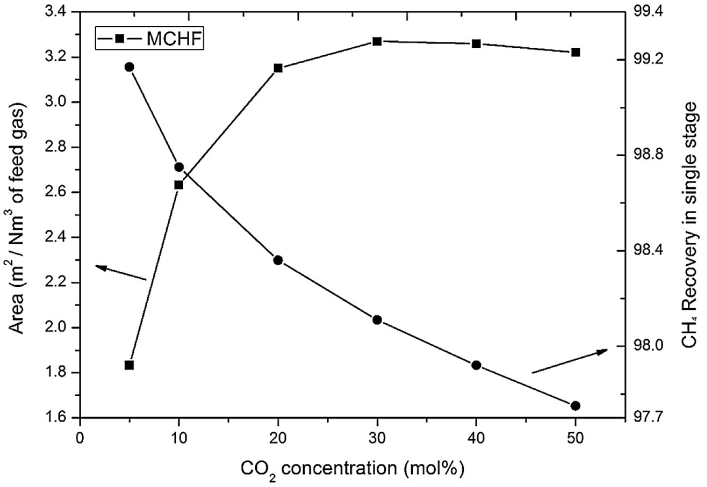

Fig. 12. Required membrane area and CH_4 recovery in a single stage MCHF system.

4.5. Simulations and economics

In this study, the effect of CO_2 contents in feed for a fixed product purity (98% CH_4) and loss (2.5% CH_4) using membranes with different efficiencies is simulated and hence the subsequent effect on total cost in form of membrane area and compression duty is evaluated. Selection of a separation process is entirely based on economic considerations. Costs must be calculated for every specific separation problem in details and it cannot be considered very general. This article gives a short capital cost comparison among MCHF, polyimide and CA membranes, which include the capital cost of the membrane and installed compressor for required duty as shown in Eq. (6). No recompression/pumping cost for the CO_2 produced is considered here. Detailed economic design and net present value (NPV) calculations for CO_2-CH_4 separation with MCHF membranes are explained in the referred article [10]. Carbon membranes are quite advanced membranes and still in the optimization process. That is why the cost per m^2 mounted into a module for MCHF is four times higher than CA as shown in table 5. This price for MCHF membranes is for carbon membranes prepared from CA (assumed as economical raw material) on a pilot scale plant (MemfoACT, Norway). This price is estimated from the pilot-scale production experience. However, the prices for polymers are taken from the data presented by W. J. Koros [41] at NTNU, Norway. These values were further used by other authors also [11,31]. Membrane properties used in simulations are shown in table 2.

$$C_{total} = C_{membrane} + C_{compressor} \quad (6)$$

The membrane performance (CO_2 permeability and selectivity) influences the CO_2 removal rate from the feed gas. The higher performance will reduce the membrane area needed for separation to achieve the product purity. In the case of polyimide, the selectivity is higher than CA, but the permeance is much lower which results in overall slightly lower performance as compared to CA. In simulations, pressure for permeate one (Fig. 6) is kept at 1 bar for both CA and polyimide membranes. In the case of polyimide membrane, the optimized pressure can achieve the selectivity-driven region by increasing area on the first stage and reducing compression energy on 2nd stage (considering membrane area is cheaper than compression energy). Fig. 11 shows that area required for both polyimide and CA is almost same for different CO_2 concentrations in the feed gas. Due to low selectivity, it is not possible to achieve required product purity in a single stage while using CA or polyimide membrane system. Therefore, a two-stage system is

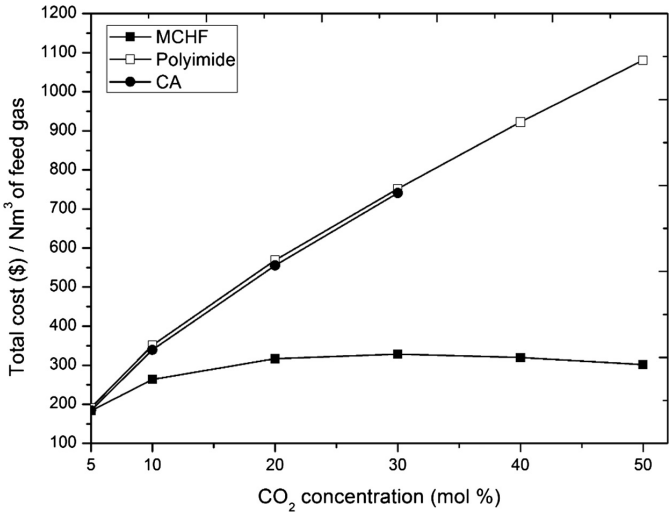

Fig. 13. Total cost per Nm^3 of feed for CA and polyimide two-stage membrane process and MCHF single stage process.

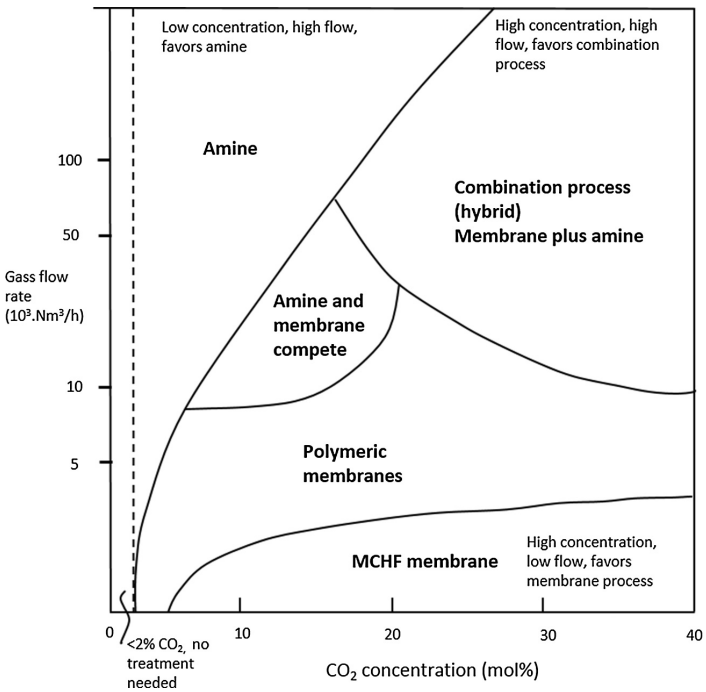

Fig. 14. MCHF application region in "gas flow rate and CO_2 concentration diagram" adopted from Baker and Lokhandwala [5].

needed for required CH_4 purity and recovery and in that case, and compression is needed on 2nd stage to achieve the pipeline pressure for recycle stream as shown in Fig. 6. This compression duty is shown in Fig. 11 which is alike for both CA and polyimide membranes.

The modified carbon membranes offer high efficiency in a one stage process reducing methane losses, footprint, and energy consumption as shown in Fig. 12. Results indicate that CH_4 recovery of 99.2% can be achieved in a single stage with MCHF membrane system when 5% CO_2 is present in the feed gas. Required area is almost constant from 20% and higher contents of CO_2 in natural gas. The data in Fig. 6 depends on pressure ratio, which is fixed here at 50/1 bar.

For the natural gas facility, in the case of single stage separation, the largest cost item is the membrane and associated housing for high pressure, because there is not any compression cost associated with natural gas feed, which is already at high pressure. But in the case of two stage membrane system, the need for compression of recycle stream adds up the cost as shown in Fig. 13. From the results, for the natural gas stream, increasing the membrane performance (both permeability and selectivity) reduces the process complexity by achieving the goal in a single stage and hence reduces the total cost. Although MCHF membrane price is higher than polyimide and CA membranes, still the separation process with MCHF is economical

and offers small foot prints owing to only single stage requirement. Carbon hollow fiber membranes are still in the development phase, and the membrane price will most likely be reduced by further optimization of the carbon membrane production and modification process in the future.

4.6. Carbon membrane applications

Membranes have been widely used in natural gas treating to pipeline specification and enhanced oil recovery (EOR), where CO_2 is removed from an associated natural gas stream and reinjected into the oil field to improve oil recovery. Carbon membranes have the ability to separate gases based on small differences in the size and shape of the gas molecules and separation performance is higher than conventional polymeric membranes. High CO_2 concentration and low flow favour carbon hollow fibres membrane processes. Stand-alone membrane systems are ideal for small distributed fields with small gas flows ($<$ 20 million scfd/ $<$ 23,600 Nm^3/h). Membrane area is dictated by the percentage of acid gas removal rather than absolute acid gas removal, and small variations in feed acid gas content hardly change the sales-gas purity. In the case of MCHF, the membrane has high performance which keeps the membrane far into the selectivity driven region and the installed area is not much effected by CO_2 contents in the feed. Simulation data showed that installing a MCHF membrane area for 20% CO_2 contents can work for CO_2 range of 1–50% with less than 1% loss in both purity and recovery. Installing membrane area for equal or below 5% CO_2 contents brings it into the pressure ratio driven region and additional compression cost adds up, (pipeline purity and recovery) if actual CO_2 concentration increases in the line. A schematic plot (adopted from Baker and Lokhandwala [5]) illustrating the effect of gas flow rate and CO_2 composition on the choice of the separation process is shown in Fig. 14.

5. Conclusion

Cellulose acetate hollow fibers were spun and deacetylated with NaOH at a pilot scale facility. These hollow fibers were carbonized in N_2 environment up to 550 °C based on a multi-dwell carbonization protocol. Numerous potting glue types were tested to make stable modules of CHF for high pressure and elevated temperature permeation testing. A potting/sealing procedure with selective clogging and thermal expansion of CHF were presented. Permeation properties of CHF were investigated for the single gases CO_2 and N_2 at the pilot facility. Due to fire hazard limitations, CH_4 was not tested at membrane production facility, only in the lab. CHF modules were further modified to enhance the permeation properties by tailoring pore structure with an oxidation–reduction process and forming a new thin selective layer of carbon using CVD with propene. The MCHF showed attractive permeation properties for CO_2, N_2, and CH_4 at elevated temperature and pressure conditions. It appeared that permeation properties for CO_2/CH_4 remained almost constant by increasing pressure up to 70 bar, but significant decline (almost 50%) in CO_2 permeability was observed when the temperature was increased up to 120 °C. Using permeation results for MCHF simulations were conducted based on Aspen Hysys® integrated with ChemBrane. The CO_2/CH_4 separation process was optimized based on membrane area and compression duty to calculate the cost for the given CH_4 purity and recovery. A cost comparison for MCHF, polyimide, and CA membranes was presented, which showed that MCHF can do CO_2/CH_4 separation in a single stage, making the process economical and simple as compared to polymeric membranes where a complex two stage system is required to do the same separation. Offering high permeability and high CO_2/CH_4 selectivity, MCHF is far into the selectivity driven region and simulation data showed that a MCHF system designed for 20% CO_2 contents in feed can separate the range of 1–50% CO_2 contents in the feed with less than 1% loss in purity and recovery. The successful high-pressure (up to 70 bar) testing of MCHF is encouraging and industrially relevant for many high-pressure applications, such as CO_2 removal from natural gas.

Acknowledgement

The authors would like to thank The Department of Chemical Engineering at NTNU for providing the possibility to work with this article.

Appendix A. Appendix

See table A1.

Table A1
Carbon hollow fibers and Modified carbon hollow fibers performance.

		CHF		MCHF	
No.	Area	Selectivity	CO_2 Permeability	Selectivity	CO_2 Permeability
	(m^2)	CO_2/CH_4	Barrer	CO_2/CH_4	Barrer
1	1.0	21	1.75E−02	60	1.60E+02
2	0.8	33	2.18E−02	48	2.46E+01
3	0.7	12	2.81E−02	24	1.05E+02
4	0.8	12	1.63E−02	39	9.82E+01
5	1.0	18	2.05E−01	45	6.47E+01
6	0.9	9	1.11E−02	69	1.76E+02
7	1.0	3	4.80E−02	72	1.04E+02
8	0.7	6	2.43E−02	54	3.10E+02
9	1.0	15	4.68E−02	138	1.55E+02
10	0.8	27	6.59E−03	60	3.08E+02
11	1.1	9	1.78E−02	45	1.78E+02
12	0.7	3	1.15E−02	69	2.52E+02
13	0.8	9	1.61E−02	51	1.23E+02
14	1.0	3	1.69E−03	57	2.62E+02
15	1.0	12	5.76E−02	42	5.96E+02
16	0.9	6	6.20E−03	246	3.18E+02
17	1.1	51	5.57E−01	48	3.39E+02
18	1.0	12	9.88E−02	165	1.31E+02
19	1.3	15	1.18E−01	21	1.25E+02

(continued on next page)

Table A1 *(continued)*

		CHF		MCHF	
No.	Area	Selectivity	CO_2 Permeability	Selectivity	CO_2 Permeability
20	1.1	21	1.68E−01	42	2.93E+02
21	1.1	51	1.92E+00	45	2.45E+02
22	1.0	51	1.97E+00	42	1.80E+02
23	1.5	72	3.14E+01	36	2.42E+02
24	1.4	90	7.09E+00	39	2.90E+02
25	1.5	39	1.24E−01	48	8.76E+01
26	1.4	33	3.19E−01	39	2.35E+02
27	1.5	54	1.19E+00	48	2.40E+02
28	1.4	72	1.90E+01	42	2.52E+02
29	1.4	81	2.59E+01	39	3.80E+02
30	1.6	48	8.39E+00	36	3.23E+02
31	1.7	69	8.27E−01	36	3.34E+02
32	1.7	36	4.83E−01	57	2.80E+02
33	1.9	66	1.69E+01	45	2.94E+02
34	1.6	84	2.41E+01	27	3.87E+02
35	1.1	39	1.30E+00	45	3.06E+02
36	1.5	87	6.62E+00	54	7.70E+01
37	1.5	63	3.25E+01	27	3.81E+02
38	1.7	54	4.37E+00	60	1.89E+02
39	1.6	63	1.70E+01	48	2.77E+02
40	1.7	66	1.22E+01	21	7.71E+02
41	1.4	90	5.45E+01	30	5.16E+02
42	1.5	69	4.22E+01	27	5.60E+02
43	1.4	129	1.25E+00	45	1.46E+02
44	0.3	117	6.36E+00	33	1.44E+02
45	0.3	123	4.04E+01	36	8.55E+02
46	0.3	111	6.76E+01	33	8.76E+02
47	0.2	78	6.09E+00	33	5.51E+02
48	0.2	144	2.23E+01	48	4.02E+02
49	0.2	39	2.25E+01	45	5.20E+02
50	0.2	42	2.94E+00	96	3.82E+02
51	0.2	69	9.22E−01	69	2.88E+02
52	0.2	102	2.08E+01	48	1.53E+02
53	0.2	51	8.30E+00	93	5.16E+01
54	0.3	99	5.89E+00	108	2.25E+01
55	0.3	93	3.46E+00	150	5.03E+01
56	0.3	108	3.56E+01	45	4.54E+02
57	0.3	129	7.56E+01	48	6.55E+02
58	0.2	90	1.06E+01	69	2.32E+02
59	0.3	102	1.79E+01	45	8.05E+02
60	0.2	75	6.82E+00	63	5.04E+02
61	0.2	81	1.96E+00	111	1.68E+02
62	0.2	81	1.52E+00	66	1.85E+02
63	0.3	93	6.49E+00	51	2.03E+02
64	0.1	147	1.44E+00	114	1.08E+01
65	0.3	72	1.39E+00	90	1.26E+02
66	0.3	96	8.83E+00	48	2.99E+02
67	0.9	45	1.53E+00	90	4.57E+01
68	1.0	21	1.84E+01	75	7.52E+01
69	0.9	57	6.65E+01	87	7.02E+01
70	1.1	33	1.00E−02	48	1.51E+01

References

[1] British Petroleum, British Petroleum Statistical Review of World Energy. 65th ed. 2016. https://www.bp.com/content/dam/bp/pdf/energy-economics/statistical-review-2016/bp-statistical-review-of-world-energy-2016-full-report.pdf (accessed 12.02.2017).

[2] U.S. Energy Information Administration EIA-0383, Annual Energy Outlook with projections to 2040, 2015. https://www.eia.gov/outlooks/aeo/pdf/0383(2015).pdf (accessed 15.01.2017).

[3] R.W. Baker, Future directions of membrane gas separation technology, Ind. Eng. Chem. Res. 41 (2002) 1393–1411, http://dx.doi.org/10.1021/ie0108088.

[4] R.W. Baker, Membrane Technology and Applications, 2nd ed., John Wiley & Sons Ltd., California, 2004, p. 338.

[5] R.W. Baker, K. Lokhandwala, Natural gas processing with membranes: an overview, Ind. Eng. Chem. Res. 47 (2008) 2109–2121, http://dx.doi.org/10.1021/ie071083w6.

[6] M. Mulder, Basic Priciples of Membrane Technology, 2nd Ed., Kluwer Academic Pulishers, Netherlands, 1996.

[7] X. He, T.-J. Kim, M.-B. Hägg, Hybrid fixed-site-carrier membranes for CO2 removal from high pressure natural gas: membrane optimization and process condition investigation, J. Membr. Sci. 470 (2014) 266–274, http://dx.doi.org/10.1016/j.memsci.2014.07.016.

[8] W.N.W. Salleh, A.F. Ismail, Carbon membranes for gas separation processes: Recent progress and future perspective, J. Membr. Sci. Res. 1 (2015) 2–15 http://www.msrjournal.com/article_12301.html.

[9] T.-J. Kim, H. Vrålstad, M. Sandru, M.-B. Hägg, Separation performance of PVAm composite membrane for CO2 capture at various pH levels, J. Membr. Sci. 428 (2013) 218–224, http://dx.doi.org/10.1016/j.memsci.2012.10.009.

[10] Y. Kusuki, H. Shimazaki, N. Tanihara, S. Nakanishi, T. Yoshinaga, Gas permeation properties and characterization of asymmetric carbon membranes prepared by pyrolyzing asymmetric polyimide hollow fiber membrane, J. Membr. Sci. 134 (1997) 245–253, http://dx.doi.org/10.1016/S0376-7388(97)00118-X.

[11] S. Haider, A. Lindbråthen, M.-B. Hägg, Techno-economical evaluation of membrane based biogas upgrading system; a comparison between polymeric membrane and carbon membrane technology, Gr. En. Env. 1 (2016) 222–234, http://dx.doi.org/10.1016/j.gee.2016.10.003.

[12] M. Yoshimune, K. Haraya, CO_2/CH_4 mixed gas separation using carbon hollow fiber

membranes, En. Proc. 37 (2013) 1109–1116, http://dx.doi.org/10.1016/j.egypro.2013.05.208.
[13] S.S. Hosseini, et al., Enhancing the properties and gas separation performance of PBI–polyimides blend carbon molecular sieve membranes via optimization of the pyrolysis process, Sep. Pur. Tech. 122 (2014) 278–289, http://dx.doi.org/10.1016/j.seppur.2013.11.021.
[14] D.Q. Vu, W.J. Koros, S.J. Miller, High pressure CO2/CH4 separation using carbon molecular sieve hollow fiber membranes, Ind. Eng. Chem. Res. 41 (2002) 367–380, http://dx.doi.org/10.1021/ie010119w.
[15] K. Briceño, D. Montané, R. Garcia-Valls, A. Iulianelli, A. Basile, Fabrication variables affecting the structure and properties of supported carbon molecular sieve membranes for hydrogen separation, J. Membr. Sci. 415–416 (2012) 288–297, http://dx.doi.org/10.1016/j.memsci.2012.05.015.
[16] H.-H. Tseng, K. Shih, P.-T. Shiu, M.-Y. Wey, Influence of support structure on the permeation behavior of polyetherimide-derived carbon molecular sieve composite membrane, J. Membr. Sci. 405–406 (2012) 250–260, http://dx.doi.org/10.1016/j.memsci.2012.03.014.
[17] W.N.W. Salleh, A.F. Ismail, Effect of Stabilization Condition on PEI/PVP-Based Carbon Hollow Fiber Membranes Properties, Sep. Sci. Tech. 48 (2013) 1030–1039, http://dx.doi.org/10.1080/01496395.2012.727938.
[18] A.C. Lua, Y. Shen, Preparation and characterization of polyimide–silica composite membranes and their derived carbon–silica composite membranes for gas separation, Chem. Eng. J. 220 (2013) 441–451, http://dx.doi.org/10.1016/j.cej.2012.11.140.
[19] M. Teixeira, M. Campo, D.A. Tanaka, M.A. Tanco, C. Magen, A. Mendes, Carbon–Al_2O_3–Ag composite molecular sieve membranes for gas separation, Chem. Eng. Res. and Desig 90 (2012) 2338–2345, http://dx.doi.org/10.1016/j.cherd.2012.05.016.
[20] C.W. Jones, W.J. Koros, Carbon molecular sieve gas separation membranes-I. Preparation and characterization based on polyimide precursors, Carbon 32 (1994) 1419–1425, http://dx.doi.org/10.1016/0008-6223(94)90135-X.
[21] A.B. Fuertes, T.A. Centeno, Carbon molecular sieve membranes from polyetherimide, Micropo. Mesopo. Mater. 26 (1998) 23–26, http://dx.doi.org/10.1016/S1387-1811(98)00204-2.
[22] J.E. Koresh, A. Soffer, Mechanism of permeation through molecular-sieve carbon membrane. Part 1.-The effect of adsorption and the dependence on pressure, J. Chem. Soc. Faraday Trans. 1: Phy. Chem. Cond. Phases 82 (1986) 2057–2063, http://dx.doi.org/10.1039/F19868202057.
[23] R. Steiner, Microfiltration and Ultrafiltration - Principles and Applications, in: L.J. Zeman, A.L. Zydney, Marcel Dekker, New York, 1996, 648 Seiten, Zahlr. Abb. u. tab., geb., $ 185,-, ISBN 0-8247-9735-3. Chemie Ingenieur Technik, 69, 1997, 1479–1479 doi: 10.1002/cite.330691022.
[24] R. Swaidan, X. Ma, E. Litwiller, I. Pinnau, High pressure pure- and mixed-gas separation of CO_2/CH_4 by thermally-rearranged and carbon molecular sieve membranes derived from a polyimide of intrinsic microporosity, J. Membr. Sci. 447 (2013) 387–394, http://dx.doi.org/10.1016/j.memsci.2013.07.057.
[25] E.P. Favvas, Carbon dioxide permeation study through carbon hollow fiber membranes at pressures up to 55 bar, Sep. Pur. Tech. 134 (2014) 158–162, http://dx.doi.org/10.1016/j.seppur.2014.07.041.
[26] G. Härtel, T. Püschel, Permselectivity of a PA6 membrane for the separation of a compressed CO_2/H_2 gas mixture at elevated pressures, J. Membr. Sci. 162 (1999) 1–8, http://dx.doi.org/10.1016/S0376-7388(99)00066-6.
[27] W. Ogieglo, L. Upadhyaya, M. Wessling, A. Nijmeijer, N.E. Benes, Effects of time, temperature, and pressure in the vicinity of the glass transition of a swollen polymer, J. Membr. Sci. 464 (2014) 80–85, http://dx.doi.org/10.1016/j.memsci.2014.04.013.
[28] N. Kruse, et al., Carbon membrane gas separation of binary CO2 mixtures at high pressure, Sep. Pur. Tech. 164 (2016) 132–137, http://dx.doi.org/10.1016/j.seppur.2016.03.035.
[29] M.-B. Hägg, J.A. Lie, Carbon Membranes, patent US patent 20100162887 A1, 2010. https://www.google.ch/patents/US20100162887.
[30] A.A. Soffer, J. Gilron, H.Cohen, Separation of Linear from Branched hydrocarbons using a Carbon Membrane. US parent 5914434 A, 1999. http://www.google.no/patents/US5914434.
[31] X. He, J.A. Lie, E. Sheridan, M.-B. Hägg, Preparation and characterization of hollow fiber carbon membranes from cellulose acetate precursors, Ind. Eng. Chem. Res. 50 (2011) 2080–2087, http://dx.doi.org/10.1021/ie101978q.
[32] G. Dong, H. Li, V. Chen, Factors affect defect-free Matrimid® hollow fiber gas separation performance in natural gas purification, J. Membr. Sci. 353 (2010) 17–27, http://dx.doi.org/10.1016/j.memsci.2010.02.012.
[33] C. Liu, R. Bai, Preparation of chitosan/cellulose acetate blend hollow fibers for adsorptive performance, J. Membr. Sci. 267 (2005) 68–77, http://dx.doi.org/10.1016/j.memsci.2005.06.001.
[34] W.-H. Lin, R.H. Vora, T.-S. Chung, Gas transport properties of 6FDA-durene/1,4-phenylenediamine (pPDA) copolyimides, J. Polym. Sci. B Polym. Phys. 38 (2000) 2703–2713, http://dx.doi.org/10.1002/1099-0488(20001101)38:21<2703::AID-POLB10>3.0.CO;2-B.
[35] J.A. Lie, Synthesis, performance and regeneration of carbon membranes for biogas upgrading – a future energy carrier, Norwegian University of Science and Technology, 2005 PhD thesis.
[36] G. Valenti, A. Arcidiacono, J.A. Nieto Ruiz, Assessment of membrane plants for biogas upgrading to biomethane at zero methane emission, Biom. Bioenerg. 85 (2016) 35–47, http://dx.doi.org/10.1016/j.biombioe.2015.11.020.
[37] K.C. O'Brien, W.J. Koros, T.A. Barbari, E.S. Sanders, A new technique for the measurement of multicomponent gas transport through polymeric films, J. Membr. Sci. 29 (1986) 229–238, http://dx.doi.org/10.1016/S0376-7388(00)81262-4.
[38] L.M. Robeson, The upper bound revisited, J. Membr. Sci. 320 (2008) 390–400, http://dx.doi.org/10.1016/j.memsci.2008.04.030.
[39] M.B. Rao, S. Sircar, Nanoporous carbon membrane for gas separation, Gas Sep. Pur. 7 (1993) 279–284, http://dx.doi.org/10.1016/0950-4214(93)80030-Z.
[40] A.B. Fuertes, T.A. Centeno, Preparation of supported asymmetric carbon molecular sieve membranes, J. Membr. Sci. 144 (1998) 105–111, http://dx.doi.org/10.1016/S0376-7388(98)00037-4.
[41] W.J. Koros, Membrane opportunities and challenges for large capacity gas andvapour feeds, European Membrane Society's 20th Summer School, 2003, NTNU, Trondheim, Norway.

Appendix I

Paper V

Vehicle fuel from biogas with carbon membranes; a comparison between simulation predictions and actual field demonstration

Paper published in Green Energy & Environment 3(2018) 266-276.

Available online at www.sciencedirect.com

ScienceDirect

Green Energy & Environment 3 (2018) 266–276

www.keaipublishing.com/gee

Research paper

Vehicle fuel from biogas with carbon membranes; a comparison between simulation predictions and actual field demonstration

Shamim Haider [a], Arne Lindbråthen [a], Jon Arvid Lie [a], Petter Vattekar Carstensen [b], Thorbjørn Johannessen [a], May-Britt Hägg [a,*]

[a] *Norwegian University of Science and Technology, NTNU, Department of Chemical Engineering, 7491 Trondheim, Norway*
[b] *Oksenøyveien 8, 1360 Fornebu, Norway*

Received 8 December 2017; revised 21 March 2018; accepted 22 March 2018
Available online 30 March 2018

Abstract

The energy contents of biogas could be significantly enhanced by upgrading it to vehicle fuel quality. A pilot-scale separation plant based on carbon hollow fiber membranes for upgrading biogas to vehicle fuel quality was constructed and operated at the biogas plant, Glør IKS, Lillehammer Norway. Vehicle fuel quality according to Swedish legislation was successfully achieved in a single stage separation process. The raw biogas from anaerobic digestion of food waste contained 64 ± 3 mol% CH_4, 30–35 mol% CO_2 and less than one percent of N_2 and a minor amount of other impurities. The raw biogas was available at 1.03 bar with a maximum flow rate of 60 $Nm^3\ h^{-1}$. Pre-treatment of biogas was performed to remove bulk H_2O and H_2S contents up to the required limits in the vehicle fuel before entering to membrane system. The membrane separation plant was designed to process 60 $Nm^3\ h^{-1}$ of raw biogas at pressure up to 21 bar. The initial tests were, however, performed for the feed flow rate of 10 $Nm^3\ h^{-1}$ at 21 bar. The successful operation of the pilot plant separation was continuously run for 192 h (8 days). The CH_4 purity of 96% and maximum CH_4 recovery of 98% was reached in a short-term test of 5 h. The permeate stream contained over 20 mol% CH_4 which could be used for the heating application. Aspen Hysys® was integrated with ChemBrane (in-house developed membrane model) to run the simulations for estimation of membrane area and energy requirement of the pilot plant. Cost estimation was performed based on simulation data and later compared with actual field results.

Keywords: Biogas upgrading; Pilot-scale demonstration; Membrane separation: Process simulations

1. Introduction

Industrial development and increased human population have globally led to a rising demand for energy with a growth rate of about 2% per year [1,2]. Oil and gas are the major sources of energy today and the complexity of the fossil fuel energy market always involves the risk of energy crisis emerging for political or the other reasons, like in the mid-1970s, and then recently in 2015 [1–3]. Renewable energy sources like biogas, wind and solar are inexhaustible compared to fossil fuels which are decreasing continuously over time. Although the reserves of fossil fuels are still significant, the questions related to climate change will enforce a change of energy usage. Renewable technologies are making relatively fast progress and expected to increase significantly (30–80%) in 2100 [2,4].

Biogas is a valuable renewable energy source and forms naturally, e.g. under anaerobic conditions such as in small lakes or flooded fields, in the sediments of the sea floor, and in the stomachs of ruminants. It can be produced by microbial digestion of organic material (agricultural waste, manure, municipal waste, sewage, food waste, etc.) in the absence of

* Corresponding author.
E-mail address: may-britt.hagg@ntnu.no (M.-B. Hägg).

https://doi.org/10.1016/j.gee.2018.03.003

oxygen [5,6]. The major components are methane (CH_4) and carbon dioxide (CO_2) with traces of H_2S, some other gases and vapors [7,8]. The most common applications of biogas are for heating, combined heat and power generation and usage as a vehicle fuel. Other applications which are studied or tested are injection into the natural gas grid and H_2 production for fuel cells.

A study on different utilizations of biogas reports that biogas upgrading to fuel quality gives the highest portion of exportable energy with a medium range (10%) energy demand [9]. In the aforesaid statement, upgrading was done with membrane process. Sweden is one of the countries that widely developed biogas as an energy source after the energy crisis in the 1970s, and today is the leading nation when it comes to biogas as vehicle fuel with projected yearly consumption of 1 TWh in 2020, in comparison with 100 GWh in 2002 [10,11]. A simplified configuration of sustainable energy production is shown in Fig. 1 [6].

Biogas is widespread throughout the world in abundance where there is farming, and people are living. To use biogas as vehicle fuel, it must be upgraded to certain required specifications. The corrosive components (water vapor and sulphur) present in biogas must be removed. The CO_2, which is one of the major components in the biogas, needs to be separated from the biogas because it dilutes/lowers the heating value of the gas. This results in reduced burning capacity which, in return, affects the performance of the engine [12].

Both CO_2 and H_2S present in raw biogas yield corrosive products in the presence of moisture (carbonic acid and sulfurous acid). For extracting the energy carrier (methane) from biogas, membrane separation constitutes one of the attractive separation technologies and is the focus of the current study. A pilot-scale membrane separation unit was installed at a biogas (from food waste) production field in Norway to obtain the fuel quality bio-methane according to the Swedish fuel quality standards [13,14].

The membrane is a perm selective barrier which separates two phases and restricts transport of various molecules in a selective manner. In the case of biogas upgrading, membrane separation is based on the difference in permeation rate of methane and carbon dioxide due to the difference in molecular size, shape, and interaction with membrane material. The process to produce biomethane should be inexpensive and simple to control. Commercially available membranes for CO_2/CH_4 separation are mostly polymeric membranes, and these membranes do not have high enough separation factor (selectivity) to achieve a high recovery and purity of CH_4 in a single stage [15]. The amount of energy required for biogas upgrading is a key factor when selecting a technology for this purpose [16,17]. In this work, carbon membranes were applied in the pilot plant as an economically possible separation solution. Most of the work reported on carbon membranes was done at laboratory scale, and very limited work has been reported for these membranes on real gas industrial exposure. Carbon membranes have shown promising separation properties at laboratory scale, and these membranes are stable at high pressure and temperature [18–25]. The novelty of this work is to assess regenerated cellulose-based carbon hollow fiber membranes with high CO_2 permeability and CO_2/CH_4 selectivity in pilot scale biogas upgrading application. Biogas upgrading process, with the reported carbon membranes, is an energy efficient process and high purity methane (vehicle fuel quality) with high recovery can be obtained in a single stage separation process.

Biogas upgrading process consists of two main stages: (1) pretreatment process to remove trace components (H_2O, H_2S) to meet the fuel standards and (2) the membrane process to separate CO_2. A detailed description of the biogas plant can be found in the references [16,17,23]. This article reports the carbon hollow fiber pilot-scale module design used for biogas upgrading to vehicle fuel quality and testing of these membranes at the biogas field, Glør IKS, in Norway.

Process simulation is used to operate the model/limitation of the system before a new system is built or altered. The model can be redesigned, experimented and optimized in a way which would be too expensive or impractical to do in the actual system itself. Aspen HYSYS®, a process modeling tool, was integrated with ChemBrane (in-house membrane model described elsewhere [26,27]) to design the membrane separation process for biogas upgrading. Results obtained at the

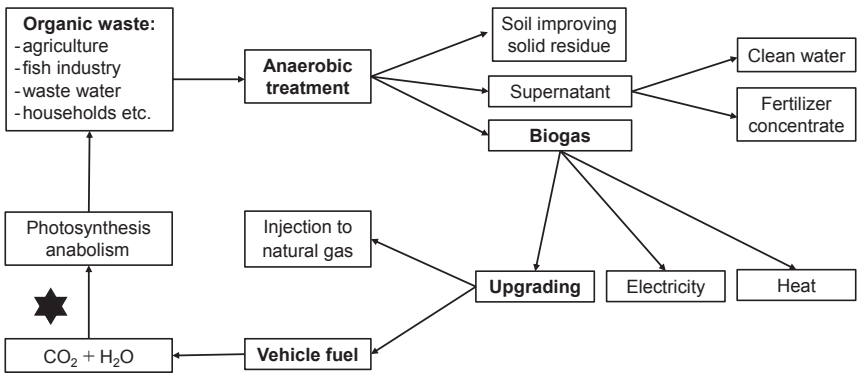

Fig. 1. Simplified configuration of sustainable energy production; turning waste into a resource [6].

membrane production facility were used in the model to optimize the process in the valuation of the required energy and membrane area. Total capital investment and production cost of the process were estimated based on supplier price quotations and simulation data. However, the price for each unit operation is presented as percent of total capital investment and production cost here. This work sums up the membrane module design, simulation predictions, and then, the actual field results in terms of membrane performance and total capital investment/production cost of the process.

2. Experimental

2.1. Carbon hollow fibers (CHF) preparation

The precursor for CHF was prepared using regenerated cellulose acetate (CA) by the dry/wet phase inversion process in a pilot-scale spinning set up delivered by Philos Korea. A dope consisting of CA mixed with N-methylpyrrolidone (NMP) and polyvinylpyrrolidone (PVP) was used to spin CA hollow fibers. CA hollow fibers were deacetylated batch-wise with a mix solution of NaOH in short chain alcohol. Then the deacetylated dried CA hollow fibers were carbonized at 550 °C under N_2 flow in a tubular 3-zone furnace. The carbonization protocol had a heating rate of 1 °C min^{-1} with several dwells and the final temperature of 550 °C for 2 h. Process details were described elsewhere [22].

2.2. Biogas composition and vehicle fuel quality

The raw biogas feed originates from microbial anaerobic digestion of food waste. Raw biogas composition is shown in Table 1. Untreated biogas was fed to a biological H_2S scrubber, and a slip stream of the treated biogas was fed to the membrane pilot plant.

For the biogas to be used as vehicle fuel, it must meet certain quality requirements/standards. Norway does not have its own fuel quality legislation yet, therefore, Swedish standards were used to acquire vehicle fuel with carbon membrane separation process as both countries have an alike climate. The requirements for clean biogas used as vehicle fuel according to Swedish standards is shown in Table 2. According to the legislation, an odorant must be added into flammable gas to ensure that the gas can be smelled below 20% of the lower explosion limit. Tetrahydrothiophene was used as an odorant to the upgraded biogas in this study.

Table 1
Composition of raw biogas obtained from anaerobic digestion of food waste.

Component	Food waste (mole%)
Methane (CH_4)	64 ± 3%
Carbon dioxide (CO_2)	30–35%
Nitrogen (N_2)	< 1%
Oxygen (O_2)	ca. 0%
Hydrogen sulfide (H_2S)	1000 ppm
Water (H_2O), 35 °C	ca. 32 g Nm^{-3}

Table 2
The requirement for vehicle fuel quality; Swedish legislation [13,14].

Components	Standard
CH_4 (Vol%)	96–98
H_2O (mg Nm^{-3})	< 32
Dew point (°C)	−60 °C at 250 bar (g)
$CO_2 + O_2 + N_2$ (Vol%)	< 4
O_2 (Vol%)	< 1
H_2S (ppm)	< 23

2.3. The carbon membrane pilot plant

The high performance of carbon membranes measured, at laboratory scale, indicated that CO_2–CH_4 separation process may have a very high recovery of methane (> 98%) and high CH_4 content (96%) in a single stage process. The carbon membrane production cost is higher compared to polymeric membrane technologies, as the production process is not yet fully optimized at commercial scale. But the high recovery results in a lower operational cost of the process which compensates to a certain extent for the cost of the membrane.

2.3.1. Biogas upgrading process

In principal, the raw biogas is compressed, bulk water is removed by means of a chiller (dew point: 4 °C at 1 bar), gas is reheated and then led through the membrane system. Carbon membranes are more selective for CO_2 relative to CH_4, therefore, in the biogas upgrading process CO_2 from the feed biogas passes through the membrane (low pressure side/permeate) and CH_4 remains on the high-pressure side (retentate). Hence, the retentate is the desired product. The ratio of permeate flow rate and feed flow rate is defined stage cut (q_p/q_f). Biomethane purity in the retentate stream depends on (1) CO_2/CH_4 selectivity, (2) pressure ratio on both sides of the membrane and (3) stage cut. Carbon hollow fiber membranes possess high CO_2/CH_4 selectivity and can be operated at high pressure, thus a sufficiently high-pressure ratio can be achieved if required. However, the necessity is determined by process design and economic considerations. H_2S and water need to be removed from the biogas stream prior to the membrane and this is done in pre-treatment section as shown in Fig. 2. Pre-treatment is a vital part of the process to meet the fuel standards and enhance the life time of the upgrading plant together with membranes.

The process flowsheet of the upgrading process with essential components is shown in Fig. 2, and operating conditions are shown in Table 3. The biogas upgrading pilot plant, containing carbon hollow fiber membrane, was operated to achieve fuel quality biomethane. The plant was designed to process 60 Nm^3 h^{-1} of raw biogas at pressure up to 21 bar. The initial tests reported here were performed for the feed flow rate of 10 Nm^3 h^{-1} at feed pressure 21 bar and vacuum on permeate side. The raw biogas was available at 1.03 bar and a blower was used to increase the pressure up to 1.3 bar. An activated charcoal system was used to remove most of the H_2S and bring it down to 5 ppm in the biogas stream. To ensure the

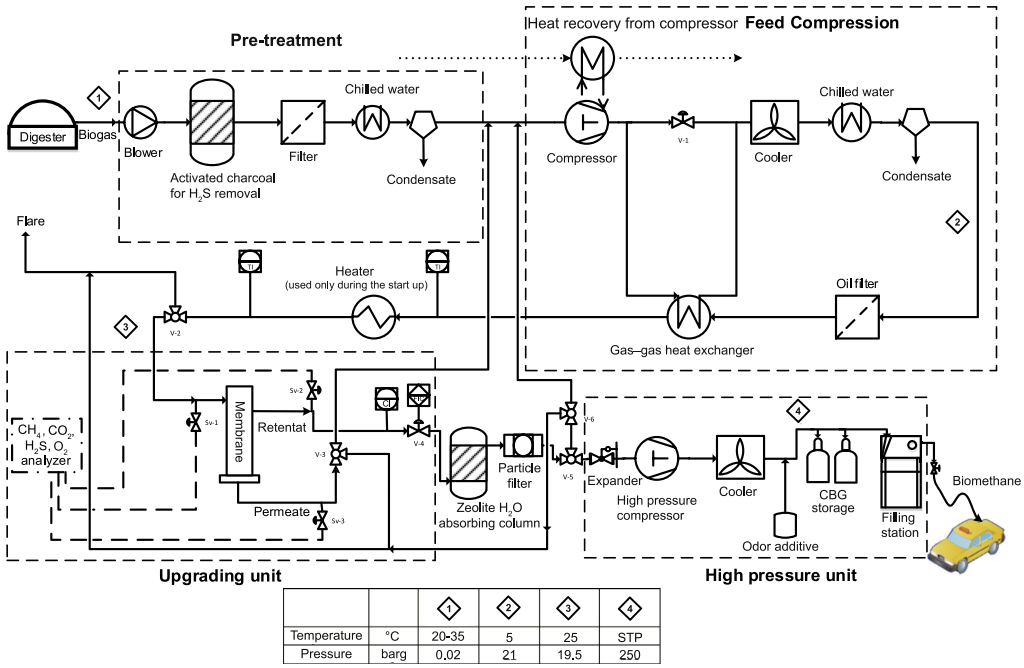

		①	②	③	④
Temperature	°C	20-35	5	25	STP
Pressure	barg	0.02	21	19.5	250

Fig. 2. Process flowsheet of biogas upgrading pilot plant based on carbon hollow fiber membrane.

Table 3
Operating conditions used in biogas upgrading pilot-plant.

Parameter	Value	Unit
Feed flow rate	10	$Nm^3\ h^{-1}$
Biogas pressure at blower inlet	1.03	bar
Biogas pressure at blower outlet	1.3	bar
Biogas pressure at compressor inlet	1.3	bar
Biogas pressure at compressor outlet	21	bar
Permeate pressure	0.1	bar
Temperature	20–25	°C
CH_4 in product	96	%
CH_4 recovery	98	%
H_2S in biogas feed	< 5	ppm

compressor safety, in form of scale formation or deposition of charcoal inside the compressor, a filter was present after H_2S removal system to remove the entrained particulates of activated charcoal. Then the water knockout through temperature swing (TS) at 4 °C and 1 bar was introduced just before the feed to the compressor to reduce the water level in the feed gas. The raw biogas was compressed to 21 bar with the mechanical reciprocating compressor (oil-free with 4-radial cylinders and external oil lubrication pump). Another chiller and an oil filter shown after compressor were part of the compression unit. They were not installed separately. In the case of carbon membranes, less than 40% relative humidity (RH) is satisfactory [21,28] as the performance of carbon membrane deteriorates at higher RH, so (partly)drying is needed. However, as a precaution, a heater was introduced just before membrane unit. The compressor oil, in case of any leakage from lubrication side, may deposit on the membrane surface and thus have a deleterious effect on the membrane performance, therefore several oil filters were used downstream to remove oil from the compressed feed gas. The compressed biogas then entered a cylindrical multi-module (shown in Fig. 3) containing 24 medium sized carbon hollow fiber modules (≈ 0.5–2 m^2 each). A single stage separation configuration was successfully tested to obtain 96% CH_4 and a significant amount of data was collected. The membrane feed gas temperature was regulated by an electric heater, and the pressure was controlled by a modulating valve (v-4 in Fig. 2, a globe valve with K vs. 2.5, supplied by Samson). The membrane pressure, temperature, flow of the

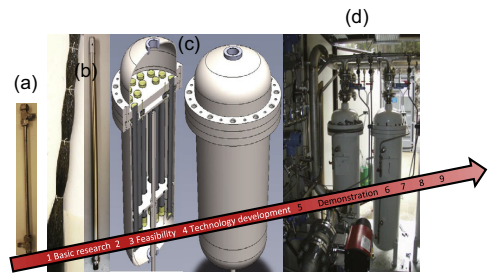

Fig. 3. Technology readiness level according to the EU commission/Up-Scaling from lab to pilot-scale; (a) lab scale module, (b) medium sized module, (c) Multimodule, (d) Membrane Pilot plant.

two outlet streams, permeate and retentate, were monitored with instruments as shown in Table 4. Online infrared analyzers (GD10P from Simtronics ASA) were used to monitor the composition of permeate stream only. However, another online gas analyzer (SSM 600C from Pronova) was available to measure composition of only one stream at a time, feed, retentate or permeate. A handheld gas analyzer GA 2000 from Geotechnical Instruments UK, was used at each site to have an estimation of the actual biogas composition. The analyzer can detect: Methane (0–100%), CO_2 (0–100%), O_2 (0–25%), H_2S (0–500 ppm). No more thorough analysis of trace compounds in the gases was performed. To accomplish the dew point: −60 at 250 barg in the final product, a zeolite-H_2O absorbing column was installed followed by a particle filter prior to the high-pressure compressor. The purpose of particle filter was to retain zeolite particles entering high pressure compressor. High-pressure compression up to 250 bar and odor addition was performed before storage of the vehicle fuel.

2.3.2. Multi-module system assemblage

A multi-module system (MMS) was comprised of up to 24 medium sized modules, of which, each module was made up of up to 2000 carbon hollow fibers, which were tested for strength in bundles with effective area ranging from 0.5 to 2 m^2. The outer diameter of the hollow fiber is in the range of 150–300 micron and a wall thickness of 30–50 micron. Feed is on the shell side of the module (outer membrane surface) and permeate flows internally (bore side) along the fibers. The assemblage, testing and performance of each medium sized module are reported elsewhere [25]. The MMS was designed in a way to accomplish maximum efficiency of the membranes. The structural strength, low fouling tendency, membrane replacement and ease to clean the MMS were important considerations for its application in a biogas upgrading plant. The MMS size was 0.324 m in diameter and 1 m in active length and consisting of three parts: (1) the vertical tank having both feed, retentate connecting ports and three legs with screws to secure it to the skid. (2) Middle part to insert the medium sized modules and, consisting of two round plates with holes according to the outer diameter of the medium sized modules. One partition plate on the top to separate the permeate section from feed section and 2nd partition plate between feed and retentate also helping to hold the modules firmly and avoid bumping into each other. (3) The lid on the top with permeate connection. The arrangement of the medium sized modules inside the MMS is shown in Fig. 3c. Photographs of the biogas upgrading plant are shown in Fig. 4. After the assembly and before fitting the lid, each of the medium sized module was tested again for any leakage (fiber breakage) using air pressure and soap water.

Fig. 4. Photographs showing the biogas upgrading membrane plant.

The MMS were pressurized and filled with gas by adjusting the feed, retentate and permeate valves manually in the initial stage. The valves were adjusted to fill gas in such a way that fibers achieve gentle treatment on the surface and there is no excessive pressure difference between feed and retentate across the partition plate inside the MMS.

3. Simulations and cost estimations

3.1. Simulation basis

Based on laboratory results, a single stage membrane configuration without recycle stream was examined and optimized by computer simulations before the execution of the pilot plant operation. The process configuration in simulation software "Aspen HYSYS" is illustrated in Fig. 5.

Then following basis and assumptions were used to simulate the membrane process performance:

Table 4
List of main instruments and measuring range.

Instrument	Model	Supplier	Measuring range	Accuracy
Dedicated product gas analyzer	GD 10P	Simtronics ASA	CO_2: 0–100%	± 3%
Handheld gas analyzer	GA 2000	Geothecnical instruments	CH_4: 0–100%	± 3%
			CO_2: 0–100%	± 3%
			O_2: 0–25%	± 1%
			H_2S: 0–500 ppm	± 5%
Online gas analyzer	SSM 6000C	Pronova	CH_4: 0–100%	± 2%
			CO_2: 0–100%	± 2%
			O_2: 0–25%	± 2%
			H_2S: 0–5 ppm	± 5%
			H_2: 0–1000 ppm	± 5%
Temperature transmitter	TT-Classe A	Officina Orobiche	−30–+350 °C	± 0.15 °C
Dew point transmitter	DP-001	Michell Instruments	−100–+20 °C	± 1 °C
Pressure transmitter	3051S	Emerson	1–275 bara	0.025% of span

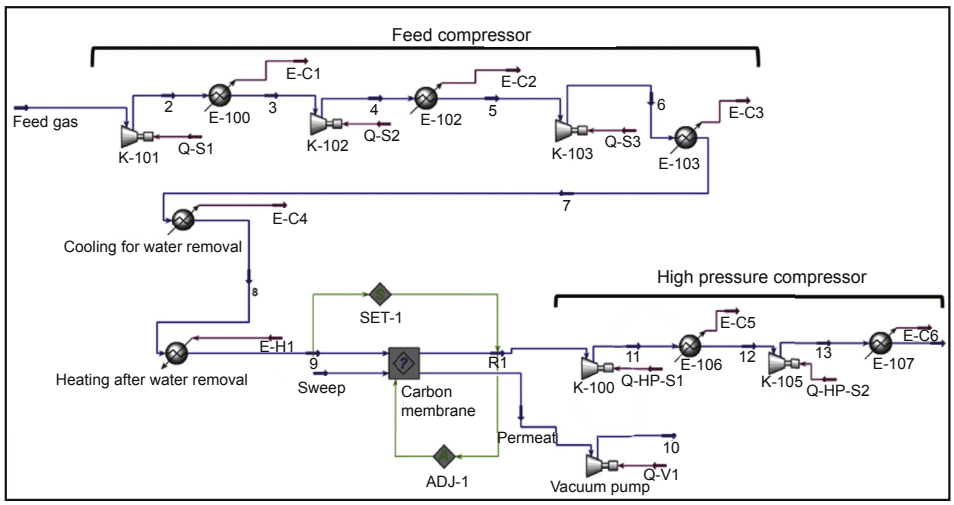

Fig. 5. Single stage process for biogas upgrading with carbon membranes.

Table 5
Process operating conditions used in the simulations.

Feed composition	35–40% CO_2, balance CH_4
Feed flow rate ($Nm^3\ h^{-1}$)	60
CO_2 permeability (Barrer[a])	300
CO_2/CH_4 selectivity	100
CH_4 purity in product (%)	96
Feed pressure (bar)	21
Permeate pressure (bar)	0.1
Temperature (°C)	25
Flow pattern in membrane module	Countercurrent

[a] 1 Barrer = 2.736E-09 (m^3(STP).m)/(m^2.bar.h).

- Countercurrent gas flow pattern without sweep on permeate side was used in all hollow fiber membrane modules.
- In-house made membrane simulation model (Chembrane) was integrated into 6 V Aspen Hysys®. This model, developed at NTNU, uses fourth-order Runge-Kutta method to calculate the flux along membrane length, and then iteration over permeate values to converge to a solution.
- CO_2 composition (40–45%) balance with CH_4, was considered in the feed biogas stream entering the membrane system. Process conditions used in simulations are shown in Table 5. Permeabilities and selectivities used in simulations are also shown in the same table.
- The adiabatic efficiency of the compressors was modeled as 75%.

3.2. Economic parameters

The economic calculations may differ considerably, as they are justified by the data available and cost model. An economic evaluation was performed to assess the total capital investment and production cost of the biogas upgrading plant. A single stage biogas upgrading process with installed carbon

Table 6
General assumptions for economic calculations [23].

	Values	Units
Energy prices		
Electricity	0.06	€ kWh^{-1}
Vehicle gas	0.33	€ Nm^{-3}
Methane content	60	%
Financial assumptions		
Membrane cost	161	€ m^{-2}
Installed compressor cost (CC)[a]		€ 7100 × $(HP)^{0.82}$
High pressure compressor cost (CBGC)[a]		$C_{comp,ins} = 912.\ (W_{comp})^{0.9315}.\ f_m.\ f_i.\ f_{inst}$ [29]
Internal rate of return (IRR)	5	%
Depreciation	15	Yrs
Operating percentage	96	%
Total hours in operation	8409.6	h/yr
Normal supervision	416	h/yr
Membrane life time	5	Yrs

[a] Cooling system was included in the compression unit.

membranes with given performance, cannot recover all the CH_4 coming from the biogas. Consequently, this CH_4 will be lost in the permeate stream. Therefore, the cost of the lost CH_4 was not included in the cost of upgrading process. General assumptions used to evaluate the economics of the upgrading unit are presented in Table 6. A detailed description of the economic analysis and net present value are reported elsewhere [23].

4. Results and discussion

4.1. Multimodule membrane system

The first trial was run relatively quickly, using one MMS comprising medium sized membrane modules of low permeance, and a feed flow rate of 4 $Nm^3\ h^{-1}$ was applied. The CO_2/CH_4 selectivity obtained in this run was quite low, and high permeance was recorded compared to the values estimated from individual module testing and MMS results at the production facility. Two reasons were considered: firstly, the trial was run for too short time, and it is unlikely that the permeate stabilizes so quickly, therefore, relatively low selectivity was obtained in the beginning. Stabilizing the permeate concentration for the low permeance modules may take days, due to long residence time on the permeate side of the MMS. Secondly, due to fiber breakage as carbon hollow fibers being self-supported hold relatively poor mechanical stability.

The plant was stopped, and MMS was opened to check the fiber breakage. Each medium-sized module was tested using air pressure and soap water to find the leakage in the modules as shown in Fig. 6. Many broken fibers were found which ultimately were manually clogged using epoxy “Loctite 3090” and the procedure in detail is reported somewhere else [25]. It was considered that vibration from compressor could break the fibers as many of the broken fibers were found close to the support legs of MMS where vibration effect was at maximum. Therefore, the membrane skid was damped down to reduce the vibration amplitude defecting the brittle fibers and operation was started again.

Several measurements over a period of some days were made. One MMS with an estimated membrane area of 2.5 m^2 was tested for four days (cumulative operation time) to determine the membrane performance. Fig. 7 presents the results of this module with cumulative operation time. Feed pressure was gradually increased to obtain a required pressure of 21 bar. Depending on the composition of the raw biogas, H_2S was removed upstream of the feed gas compressor. All measurements were made at 21 bar feed pressure and vacuum on the permeate side. CH_4 contents in feed, retentate and permeate streams are shown graphically along with flow rates in Fig. 7. The concentration of CH_4 in retentate stream increased to 78 (maximum CO_2/CH_4 selectivity of 7) in the beginning but suddenly started decreasing and the flow of the product stream (retentate) reduced. A very high permeate flow with no CO_2/CH_4 selectivity was measured which indicated fiber breakage in the module. The broken fibers were clogged, and the operation was started up again. This time membranes were showing some selectivity (during 50–65 h plant operation time), but the value was very low as compared to the laboratory results. After few hours, some fibers broke again and the same composition as feed was detected on permeate stream, hence, the plant operation was stopped once more. Hence the first three operations were not successful with respect to achieve high selectivity due to the fiber breakage problems as shown in Fig. 9.

These initial problems of fiber breakage were solved, and in the fourth test the pilot plant was run for eight days at stable conditions and measurements were done periodically both by an online infrared analyzer and a portable analyzer. The plant was working as expected by giving required vehicle fuel quality as shown in Fig. 8. The results in Fig. 8 show that CH_4 concentration in the feed, retentate and permeate streams and flow rate of each stream was almost constant during the cumulative test period of 192 h. The concentration of CH_4 in the product stream was 96 mol% (CH_4 loss: 2–4%) throughout

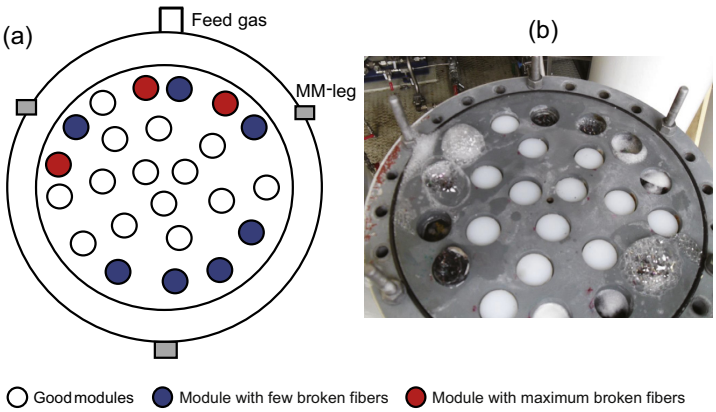

Fig. 6. (a) Arrangement of small modules into a big multi-module (MMS) (b) leakage testing and manual clogging of each module inside MMS.

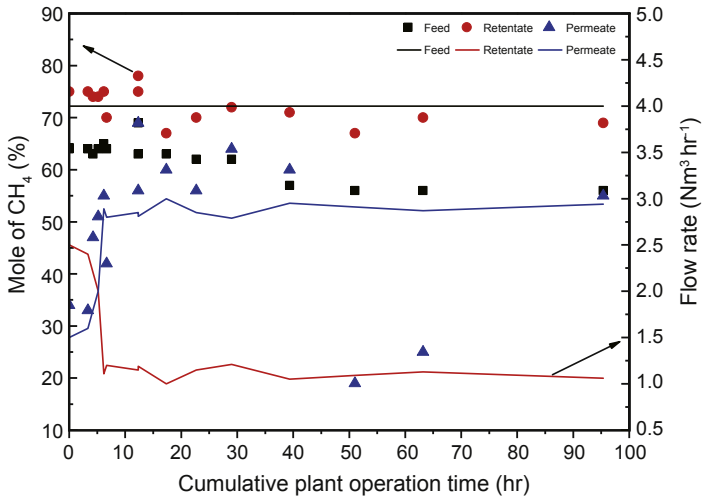

Fig. 7. Results of one MMS, tested for feed flow: 4 $Nm^3\ h^{-1}$.

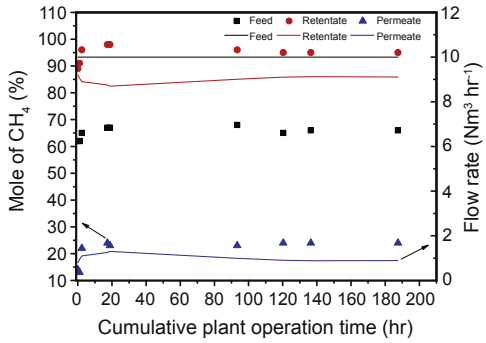

Fig. 8. Carbon membrane separation process for biogas upgrading; Flow rates as "solid lines" and CH_4 contents as "dots" in the graph.

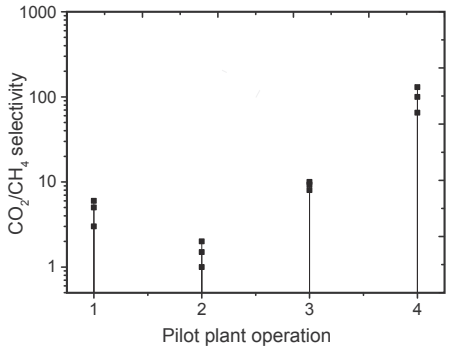

Fig. 9. CO_2/CH_4 selectivity during different operational runs of pilot plant. For the three first runs there were some fiber breakage, hence low performance resulted.

this time, and maximum selectivity for CO_2/CH_4 was measured 130 as shown in Fig. 9. The Robeson plot shows the trade-off between permeability and selectivity for gas pairs through a membrane. For the gas pair CO_2 and CH_4, it shows clearly that both high purity and high recovery cannot be attained in a single stage with a polymeric membrane [30]. Therefore, a two-stage system with recycle may usually be needed to achieve high purity and recovery of the product. But a high-performance membrane (showing both high CO_2 permeability and CO_2/CH_4 selectivity), may achieve both high purity and recovery of the product in a single stage process with optimized process conditions. Thus, the feed pressure of 21 bar (against the 0.1 bar in permeate) the required methane purity (96%) and recovery (98%) of the product was achieved in a single stage process (estimated through simulations before installation). Fig. 9 presents the CO_2/CH_4 selectivity achieved during the different set of operations. As already mentioned, the first three operations were not successful and very low selectivity was achieved due to the fiber breakage problem. This was however resolved and the plant was working as expected by giving required quality vehicle fuel (plant operation 4 in Fig. 9). The effective membrane area was significantly reduced due to the manual clogging process of broken fibers. The modules with a high number of damaged fibers were later replaced by the good performing modules. After installation of the good modules, the membrane area that was lost due to clogging was only about 1–2% of the total membrane area.

4.2. Installed energy and cost of the plant

The energy values for the biogas upgrading unit were assessed for 60 $Nm^3\ h^{-1}$ plant capacity and values for the compressed natural gas unit (CNG) were considered for 40 $Nm^3\ h^{-1}$. Cost assessment is very important before the implementation of the plan. Normally the membrane cost for

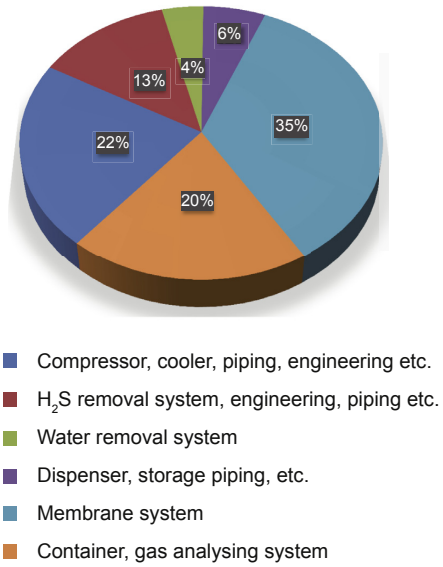

Fig. 10. Contribution of each unit in the biogas upgrading pilot plant.

polymer membrane modules is about 10–25% of the total cost [23], but the scenario is quite different in case of carbon hollow fibers. The carbon membrane production process is not optimized for commercial scale, and continuous process is not yet developed to produce the hollow fibers and to construct the modules. Therefore, a batch process was used on pilot-scale production plant which adds up the cost in terms of material usage, energy consumption, man power and working hours. Hence, the estimated membrane cost based on "small scale membrane preparation" data was 161 € m^{-2}, contributing about 35% of the total capital investment as shown in Fig. 10. Moreover, the economic assessment depends on the method of analysis and assumptions used to evaluate the final results.

Fig. 10 presents the cost of both upgrading unit and CNG package. Membrane price was assumed based on lab-scale production price, however, other costs mentioned in Fig. 10 were corrected in this paper according to the price quotations obtained from suppliers. The membranes represent the largest capital cost, while the second largest capital investment was of compression unit which made 22% of the total cost. H_2S removal with charcoal was also very costly (13% of the total cost), thus, a biological H_2S removal system is recommended for future studies. By applying these assumptions and available information, a projected net present value (NPV) of 765,189 € was estimated. A detailed description of cost analysis and NPV calculations were reported elsewhere [23]. The total capital investment for a 60 Nm^3 h^{-1} biogas upgrading pilot plant was 297,897 € and total operation & maintenance cost (production/running cost) was predicted to be 5532 € per year. Fig. 10 only presents the contribution of each unit as a percentage value of the total capital investment. The price for high pressure compressor was also added in total capital investment. However, the specific energy of high pressure compressor was 0.13 kWh/(Nm^3 of upgraded biogas) which was not included in running cost in order to make comparison with other studies. Carbon membranes used in current study possessed high performance (selectivity and permeability), therefore, very small area (10 m^2) and low specific energy was required to produce high quality vehicle fuel with high recovery of methane in a single stage separation process. Running cost of the carbon membrane based pilot plant was thus estimated 0.014 €/(Nm^3 of upgraded biogas), which is much lower than 0.05 € Nm^{-3}, the values computed by Deng et al. [15]. They reported an experimental analysis of biogas upgrading process based on CO_2 facilitated transport membranes. The two-stage membrane process with permeate recycle was proven optimal and specific energy consumption of 0.29 kWh/(Nm^3 of upgraded biogas) was estimated. Makaruk et al. [16] investigated different membrane systems for biogas upgrading process and reported specific energy consumption of 0.3 kWh/(Nm^3 of upgraded biogas), whereas Valenti et al. [17] have simulated the optimal value of specific energy from 0.33 to 0.47 kWh Nm^{-3} (depending on the layout). No vacuum pump was used on permeation side in any of the above-mentioned studies. However, biogas upgrading with carbon membranes proved that a single stage membrane system with no recycle stream, can produce vehicle fuel with specific energy consumption of 0.28 kWh Nm^{-3}. Although a vacuum pump was used (vacuum energy is also added in total specific energy usage) on permeate side for carbon membrane system, yet the total energy consumption is still lower than in all the above-mentioned studies. The energy consumption for high pressure compression was not included in any of above-mentioned studies.

4.3. Simulations and field results

To make an economically viable membrane separation process, both high permeability and high efficiency (selectivity) are needed. Carbon membranes reported here showed superior separation performance on laboratory scale experiments compared to polymeric membranes. Hence, a pilot-scale system was simulated based on the experimental results at production facility. The performance of the membranes was almost similar or even higher in some operations for biogas upgrading as compared to simulated values. The total capital investment was quite close to the projected values based on simulations. The membrane cost was considered 80 € m^{-2} in the simulations based on knowledge from pilot-scale production at MemfoACT AS. However, the brittleness of hollow fibers remained a challenge and the total cost of the membrane was almost doubled when required membrane area was in operation at the biogas facility. Hence, the total capital investment and production cost increased because of that extra membrane area. The energy consumption by the compressor and vacuum pump, product (methane) purity and methane recovery were very much comparable with the simulated results.

4.4. Challenges and suggestions

Although the carbon membrane pilot plant successfully obtained the vehicle fuel, there are still challenges that need consideration. The manually sorted and randomly packed hollow fibers of carbon membranes had smaller mass transfer-coefficients than those for regular dense packings (polymeric hollow fibers). Flow through the randomly packed hollow fiber bundle could be highly nonuniform. Membrane effective area was very much reduced due to selective and manual clogging. Furthermore, regions, where fibers come in close contact, may create sections of high pressure drop. The gas velocity through these regions is much lower than the velocities in the regions where fiber spacing is larger, yielding higher mass transfer coefficient in these regions. On the other hand, in high velocity regions, there are increased chances of fiber breakage if any weak point occurs on the fiber surface. It may result in flow-channels formation and hence, bypassing effect which would result in selectivity loss. The MMS design for 24 medium size modules was not most efficient in this development phase of the operation. It could have been easier with individual module housing instead of MMS housing in order to isolate and treat the modules with bad performance separately. The process of dismantling the MMS to take out the medium sized module, finding and clogging of the broken fibers, and again assembling the MMS increased the probability of fiber breakage in neighboring modules inside MMS and the entire process was time consuming as well. The shell-side feed configuration might have damaged the fibers due to high pressure feed flow. Bore-side feed configuration might have been more efficient in the MMS system. The membrane production cost at semi-industrial production plant was about 80 € m^{-2}, but due to a decrease in membrane effective area, the membrane cost doubled for the biogas pilot plant, which ultimately increased the total capital investment and production cost of the plant. The mentioned problems must be solved before a successful hollow fiber membrane module sees the market.

5. Conclusions

A multimodule system containing 24 medium sized modules, was successfully installed and operated at 21 bar feed pressure to obtain vehicle fuel from biogas. The carbon hollow fiber membranes achieved 97 mol% CH_4 with 98% CH_4 recovery in a single stage process. Pretreatment of biogas was performed prior to membrane separation to meet the fuel quality standards according to the Swedish legislation. The pretreatment consisted in removing H_2S with charcoal bed and H_2O removal by temperature swing and zeolite absorption. The plant operation was run successfully for 8 days and membranes used in this study yielded consistent results. It was observed that shell-side feed configuration was not very efficient in the MMS because the fibers could damage or break with high pressure feed flow. A bore-side feed configuration may give better results. Simulations were conducted to estimate area and energy requirement for the pilot plant. Total capital investment and production cost were estimated based on simulated data. The membrane cost was considered 80 € m^{-2} in the simulations based on pilot-scale production at MemfoACT AS. However, the brittleness of hollow fibers remained a challenge and the total cost of the membrane was almost doubled when required membrane area was installed and in operation at biogas facility. Hence, the total capital investment and production cost increased only because of that extra membrane area needed. However, the high recovery resulted in a lower operational cost of the process which compensated to a certain extent for the cost of the membranes. The running cost was much lower (0.014 € Nm^{-3} of biogas upgraded) than the polymeric membranes (0.05 € Nm^{-3}) reported in literature. The energy consumption by the compressor and vacuum pump, product (methane) purity, and methane were very much comparable with the simulated results. As far as carbon membrane-based biogas upgrading is concerned, the future membrane development should focus on improved mechanical properties of the membrane fibers and bore-side feed configuration should possibly be applied.

Conflict of interest

There is no conflict of interest.

Acknowledgements

Glør IKS, Norway, is gratefully acknowledged for providing the opportunity to test the carbon hollow fiber multi module membranes on pilot-scale. The authors would also like to thank The Department of Chemical Engineering at NTNU for providing the possibility to work with this article.

References

[1] World Energy Review, Statistical Review of World Energy, BP. https://www.bp.com/content/dam/bp/en/corporate/pdf/energy-economics/statistical-review-2017. (Accessed 29 September 2017).
[2] Carbon capture and storage EU, Predicted rise in global energy demand. http://www.zeroemissionsplatform.eu/extranet-library/publication/226-zepop-ed.html. (Accessed 3 October 2017).
[3] K. Kanjilal, S. Ghosh, Resour. Pol. 52 (2017) 358–365.
[4] A. Demirbas, Energ. Source. Part B 4 (2009) 212–224.
[5] P. Weiland, Appl. Microbiol. Biot. 85 (2010) 849–860.
[6] J.A. Lie, Synthesis, Performance and Regeneration of Carbon Membranes for Biogas Upgrading – a Future Energy Carrier (PhD. thesis), NTNU, Trondheim, 2005.
[7] M.Å. Maltesson, Biogas för fordonsdrift - kvalitetsspecifikation, kommunikations forskningsberedningen (KFB4), Stockholm (in Swedish), 1997.
[8] K. Wågdahl, Chalmers Tekniska Högskola, Sweden, 1999.
[9] R. Rautenbach, K. Welsch, J. Membr. Sci. 87 (1994) 107–118.
[10] P. M, Utvärdering av uppgraderingstekniker för biogas, Lund/Malmö (in Swedish), 2003.
[11] J. Forsberg, Biogas Grid in Mälardalen Valley, Malmö, 2014, p. 6.
[12] S. Bari, Renew. Energy 9 (1996) 1007–1010.
[13] H. Consult as, Forprosjekt: Biogassoppgradering; vurdering av ulike teknologier for oppgradering av biogass fra Nye Mjøsanlegget (in Norwegian), Norway, 2013, p. 12 av 47.
[14] M. Svensson, National Biomethane Standards (SGC), 2014.
[15] L. Deng, M.-B. Hägg, Int. J. Greenh. Gas Control 4 (2010) 638–646.

[16] A. Makaruk, M. Miltner, M. Harasek, Separ. Purif. Technol. 74 (2010) 83–92.
[17] G. Valenti, A. Arcidiacono, J.A. Nieto, Biomass Bioenergy 85 (2016) 35–47.
[18] W.N.W. Salleh, A.F. Ismail, J. Membr. Sci. Res. 1 (2015) 2–15.
[19] Y. Kusuki, H. Shimazaki, N. Tanihara, S. Nakanishi, T. Yoshinaga, J. Membr. Sci. 134 (1997) 245–253.
[20] T.-J. Kim, H. Vrålstad, M. Sandru, M.-B. Hägg, J. Membr. Sci. 428 (2013) 218–224.
[21] D.Q. Vu, W.J. Koros, S.J. Miller, Ind. Eng. Chem. Res. 41 (2002) 367–380.
[22] M.-B. Hägg. J.A. Lie, Patent, US20100162887 A1, 2010.
[23] S. Haider, A. Lindbråthen, M.-B. Hägg, Green Energy Environ. 1 (2016) 222–234.
[24] S.S. Hosseini, M.R. Omidkhah, A. Zarringhalam Moghaddam, V. Pirouzfar, W.B. Krantz, N.R. Tan, Sep. Purif. Technol. 122 (2014) 278–289.
[25] S. Haider, A. Lindbråthen, J.A. Lie, I.C.T. Andersen, M.-B. Hägg, Sep. Purif. Technol. 190 (Suppl. C) (2018) 177–189.
[26] D. Grainger, Development of Carbon Membranes for Hydrogen Recovery (PhD. thesis), NTNU, Trondheim, 2007.
[27] D. Grainger, M.-B. Hägg, Fuel 87 (2008) 14–24.
[28] I. Menendez, A.B. Fuertes, Carbon 39 (2001) 733–740.
[29] A. Lindbråthen, D.R. Grainger, M.B. Hägg, Sep. Sci. Technol. 42 (2007) 3049–3070.
[30] L.M. Robeson, J. Membr. Sci. 320 (2008) 390–400.

Appendix J

Paper VI

Techno-economical evaluation of membrane based biogas upgrading system: A comparison between polymeric membrane and carbon membrane technology

Paper published in Green Energy & Environment 1(3) (2016) 222-234.

Available online at www.sciencedirect.com

ScienceDirect

Green Energy & Environment 1 (2016) 222–234

www.keaipublishing.com/gee

Research paper

Techno-economical evaluation of membrane based biogas upgrading system: A comparison between polymeric membrane and carbon membrane technology

Shamim Haider, Arne Lindbråthen, May-Britt Hägg*

Norwegian University of Science and Technology, NTNU, Department of Chemical Engineering, 7491 Trondheim, Norway

Received 1 September 2016; revised 21 October 2016; accepted 22 October 2016
Available online 31 October 2016

Abstract

A shift to renewable energy sources will reduce emissions of greenhouse gases and secure future energy supplies. In this context, utilization of biogas will play a prominent role. Focus of this work is upgrading of biogas to fuel quality by membrane separation using a carbon hollow fibre (CHF) membrane and compare with a commercially available polymeric membrane (polyimide) through economical assessment. CHF membrane modules were prepared for pilot plant testing and performance measured using CO_2, O_2, N_2. The CHF membrane was modified through oxidation, chemical vapour deposition (CVD) and reduction process thus tailoring pores for separation and increased performance. The post oxidized and reduced carbon hollow fibres (PORCHFs) significantly exceeded CHF performance showing higher CO_2 permeance (0.021 m^3(STP)/m^2 h bar) and CO_2/CH_4 selectivity of 246 (5 bar feed vs 50 mbar permeate pressure). The highest performance recorded through experiments (CHF and PORCHF) was used as simulation basis. A membrane simulation model was used and interfaced to 8.6 V Aspen HYSYS. A 300 Nm^3/h mixture of CO_2/CH_4 containing 30–50% CO_2 at feed pressures 6, 8 and 10 bar, was simulated and process designed to recover 99.5% CH_4 with 97.5% purity. Net present value (NPV) was calculated for base case and optimal pressure (50 bar for CHF and PORCHF). The results indicated that recycle ratio (recycle/feed) ranged from 0.2 to 10, specific energy from 0.15 to 0.8 (kW/Nm^3_{feed}) and specific membrane area from 45 to 4700 (m^2/Nm^3_{feed}). The high recycle ratio can create problems during start-up, as it would take long to adjust volumetric flow ratio towards 10. The best membrane separation system employs a three-stage system with polyimide at 10 bar, and a two-stage membrane system with PORCHF membranes at 50 bar with recycle. Considering biomethane price of 0.78 $/$Nm^3$ and a lifetime of 15 years, the techno-economic analysis showed that payback time for the best cascade is 1.6 months.

Keywords: Carbon membrane; Biogas upgrading; Techno-economical analysis; NPV calculations

1. Introduction

Combustion of fossil fuel to meet the ever-increasing energy demand has resulted in depletion of natural resources [1]. At the same time, greenhouse gas emissions, especially CO_2 produced by combustion of fossil fuel, is a major source of the contribution to global warming and climate change [2–4]. Development and use of renewable energy have become of major importance for long-term sustainability. By the year 2020, it is predicted in a Swedish case study that almost 20% of energy will be produced from renewable sources [5].

Biogas produced by microbial digestion of farm waste or sewage waste contains high concentrations of methane, which could be combusted to meet the energy and power demands. The biogas produced by microbial digestion of waste consists of several gases among which CH_4 and CO_2 account for most

* Corresponding author.
E-mail address: hagg@ntnu.no (M.-B. Hägg).

http://dx.doi.org/10.1016/j.gee.2016.10.003

of the volume fraction. Other gases including H_2S, N_2, O_2 and water vapours coexist in traces. Depending upon the raw material, digestion procedure and process condition, the CO_2 concentration in biogas can reach up to 50%. This high concentration of CO_2 significantly reduces the calorific value of biogas [6–9]. The produced biogas needs to be enriched in methane ($CH_4 > 95\%$) by removing CO_2 and other impurities from the gas [10,11].

The CO_2 can be removed from a gas stream by many different techniques. Some of the most investigated techniques for the upgrading of biogas involve CO_2 capture by physical or chemical absorption in liquid, pressure swing adsorption, membrane technology or cryogenic separation [7,12–16]. Among all these techniques, membrane technology offers several advantages like the compact modular design, small footprint, low capital and operational cost, simple operation and easy maintenance [17–19]. Due to these advantages, biogas upgrading by using membrane technology has gained a lot of attention. Much work has been done in the development of a competitive membrane material for different gas separation applications during the last two or three decades. The most important factor in membrane separation is the membrane material. Different materials have been suggested, here is only referred to a few representing both polymers and carbon membranes [20–23].

A novel carbon hollow fibre (CHF) membrane was synthesized at NTNU using cellulose acetate as a precursor, which was de-acetylated to cellulose prior to the carbonization process. The CHF membrane showed high performance and potential to become an economically viable solution for biogas purification [24]. Their membrane showed high CO_2/CH_4 selectivity and good CO_2 permeance. These CHF membranes were developed and tested on a pilot scale for biogas by MemfoACT AS a company which has now closed down. The CHF membranes showed promising results and attractive properties for biogas upgrading under real test conditions at a biogas plant in Southern Norway. The modules of 2 m^2 area were made to test the membrane performance at the pilot plant. The plant was capable of processing 20 Nm^3/h of biogas. CHF membrane modules with feed on the shell side, showed weak mechanical properties when tested at high pressure, and many broken fibres inside the module were observed. Secondly, the potting which should bind that many fibres together at high pressure was not god enough and more research was needed. Modules with a small number of fibres (a few cm^2 modules) tested in the laboratory showed good mechanical properties up to 70 bar. CHF membranes displayed a CO_2/N_2 selectivity of 30 with a CO_2 permeance of 5.5E-3 $m^3(STP)/m^2$ h bar. A further modification was done by applying oxidation, CVD, and reduction process on CHF membranes, which dramatically increased the CHF membrane performance (CO_2/N_2 selectivity of 82 and CO_2 permeance of 2.1E-2 $m^3(STP)/m^2$ h bar).

The major separation in biogas upgrading process is CO_2/CH_4 separation. The membranes for CO_2/CH_4 separation are based on solution-diffusion mechanism, there is usually a trade-off between CO_2 separation selectivity and permeability. The Robeson plot in Fig. 1 shows that a membrane with high CO_2 selectivity usually has low permeability [25,26].

The process to produce biomethane should be inexpensive and simple to control. Commercially available membranes for CO_2/CH_4 separation are mostly polymeric membranes, and these membranes do not have high enough separation factor (selectivity) to achieve a high recovery of CH_4 in a single stage. The amount of energy required for biogas upgrading is a key factor when selecting a technology for this purpose. Due to low selectivity but high permeance of commercial membranes, big recycle stream has to be treated if high recovery (99.5% of CH_4) and pipeline spec (97.5% CH_4) has to be reached in the two-stage system. This results in high costs due to the compressor price and compressor duty while in operation. The process operating cost can be reduced by optimization of feed pressure, inter stage pressure and recycle flow. A three-stage membrane separation could also be helpful to achieve high recovery and purity; however, operational complexity regarding intermediate pressure and biogas components concentration, suggest that adjustment of these variables is the key towards optimization. Plasticization inhibits the polymeric membranes to a threshold pressure [27], whereas CHF membrane has shown a stable performance and no plasticization up to 50 bar or even higher [28,29].

Many researchers have been conducting Simulations and modelling of multi-stage membrane systems to evaluate and optimize membrane systems for CO_2 capture [30–37]. Baker et al. [17] have provided a guideline for conducting simulations on commercially available membranes, which also shows the comparison between membrane system and amine absorption process. Baker suggested that membrane technology is suitable in small (less than 6000 Nm^3/h) and medium scale (6000–50,000 Nm^3/h) processes.

This study intends to demonstrate biogas upgrading with membrane separation technology. Permeance and selectivity of gases in polymeric membranes for biogas upgrading is

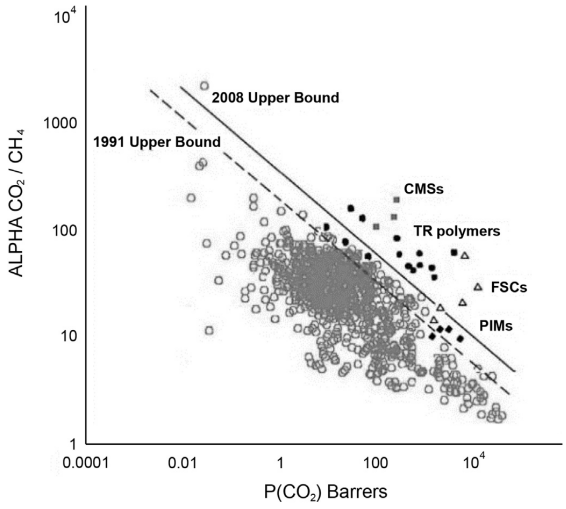

Fig. 1. Robeson upper bounds for CO_2/CH_4 membrane separation [31].

abundantly available in the literature. However, similar data for carbon membranes has seldom been reported. Various modular configurations containing membranes with different CO_2 selectivities, have been investigated in the current study, using HYSYS simulations for optimal performance and minimum energy consumption. Considering that the membrane separation system fulfils the German national standard for biogas as vehicle fuel, the evaluation focus to achieve 99.5% CH_4 recovery and 97.5% CH_4 purity. The important parameters such as compressor duty, recycle ratio (recycle/feed) and membrane area are discussed. In the end, techno-economical evaluation of the entire plant, including running costs and net present value (NPV) have been calculated. The purpose of this study is to present an economically viable scheme to upgrade biogas by using membranes with high CH_4 recovery. Biogas composition depends on the source of the gas as shown in Table 1 [6].

2. Material and methods

2.1. Materials

Acros Organics (Belgium) supplied cellulose acetate (CA) and 1-Methyl-2-pyrrolidinone, while 99.5% (NMP) and PVP (Polyvinylpyrrolidone) were purchased from Sigma–Aldrich (Norway). Ionic exchanged water was used for coagulation.

2.2. Hollow fibre preparation

Using a dry-wet spinning process at commercial scale plant, delivered by Philos Korea, cellulose acetate hollow fibres (CAHFs) were spun from a dope composed of CA/NMP/PVP. CAHF were soaked in water and glycerol solution respectively after the spinning process. CAHF were deacetylated with NaOH/isopropanol/water solution and then dried in a humidity-controlled environment. Carbon hollow fibres (CHFs) were prepared by the carbonization of deacetylated CAHF in the presence of CO_2 and N_2. Details of this membrane preparation are given in the patent held by Hägg and Lie [24].

2.3. Modification

The pore size of CHF membrane, already mounted into a module with stainless steel casing, was tailored to enhance the membrane separation properties. The Fig. 2 illustrate the steps followed in this work, as also reported in the patent held by Soffer et al. [38]. The durability, mechanical stability at operating conditions and separation efficiency of CHF membrane increased appreciably after oxidation and reduction process (PORCHF). The first oxidation step will produce quite large membrane pores with fairly low selectivity, then chemical vapour deposition (CVD) was performed using propylene to coat the membrane surface with a thin polymeric layer closing the pores again. The oxidation process was then repeated to open (tailoring) the pores in the newly formed layer to fit the molecular sieving of the gases in question (here CO_2–CH_4), finally followed by a reduction process, which reduced the aging of the membrane by stabilizing the pores.

Table 1
Biogas composition from various sources [6].

Component	Farm plant	Sewage digester	Landfill
CH_4	55–58	61–65	47–57
CO_2	37–38	34–38	37–41
N_2	Trace	Trace	1–17
O_2	Trace	Trace	0–2
H_2S	<1	<1	<1
H_2O	4–7	4–7	4–7
Aromatic hydrocarbon	Trace	Trace	Trace

2.4. Transport mechanism and membranes used in this work

The mass transport properties of CHF and PORCHF were measured with the single pure gases CO_2, O_2, and N_2 at different feed pressure and experiments were carried out without sweep gas on the permeate side. He et al. has performed the mixed gas experiments on the same type of carbon membrane (same protocol) and results indicated that the membrane performance for CO_2 separation is the same or even higher in some cases for mixed gas as compare to single gas separation [39]. Due to fire hazard limitations, CH_4 was not tested at membrane production facility, only in the lab. Therefore, the values for CH_4 gas are estimated values (three times of N_2 selectivity) in this work based on work done by He et al (Fig. 6 of the article) [39]. The performance of the membrane was evaluated by measuring the CO_2 permeance in m^3(STP)/(m^2 h bar) and CO_2/N_2 selectivities (α) using the Eqs. (1) and (2).

$$\frac{q_{p,i}}{A_m(p_h x_i - p_l y_i)} = \frac{q_p y_{p,i}}{A_m(p_h x_i - p_l y_i)} = \frac{J_i}{(p_h x_i - p_l y_i)} = \frac{P_i}{l} \quad (1)$$

$$\propto = \frac{P_i}{P_j} \quad (2)$$

where J (m^3(STP)/m^2 h) is the flux of gas component i, q_p is the volume of the permeating gas (i) (m^3(STP)/h), P_i is the permeability of gas component i ((m^3(STP)/m^2 h bar), P_h and P_l are feed and permeate side pressures (bar), x_i and y_i are the mole fractions of component i on the feed and permeate sides and A_m (m^2) is the membrane area [36].

A benchmarking polymeric membrane is considered for comparison, as a future biogas upgrading membrane with a 1 μm thick selective layer, having a permeability of 100 barrer and a selectivity of 100 for CO_2/CH_4, which is above Robeson upper bond 2008. Gas permeation properties of CHF and PORCHF with other membranes used in the simulation of this work, are shown in Table 2.

3. Process description and simulation method

3.1. Pre-treatment of biogas

As shown in Table 1, raw biogas contains several impurities, like water, dust, H_2S, CO_2, siloxanes, hydrocarbons,

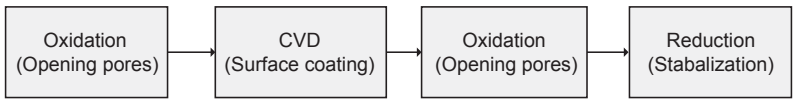

Fig. 2. Steps followed for membrane pore tailoring.

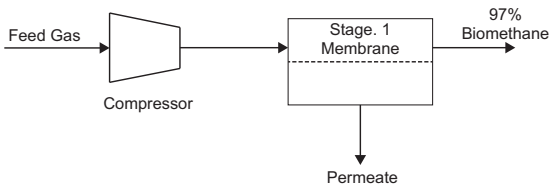

Fig. 3. Single stage membrane process.

NH_3, oxygen and several other components that must be removed in order to increase the membrane lifetime to avoid corrosion of the upgrading system and to comply for the biogas being approved as biomethane for vehicle fuel. Some membrane materials like polyimide have high permeability and can work in the presence of components which often are harmful to the membrane, like H_2S and H_2O [41]. As shown in Table 1, Impurities like H_2S and aromatic hydrocarbons need to be removed before biogas encounter the carbon membrane.

Biogas is usually saturated with water, and the amount of water which needs to be removed depends on how much water is allowed to enter into the compressor and membrane system. This water can be removed before entering the compressor or after membrane separation prior to high-pressure compression for vehicle fuelling or pipeline requirements. In the case of carbon membranes, less than 30% relative humidity (RH) is acceptable [29]. However, the presence of water may influence the separation of the other components, and it was documented that the permeability of N_2 increased and CO_2 decreased for CHF and PORCHF at 50% RH. When the fibres were again dried, it was observed that the permeability of CO_2, N_2 and selectivity of CO_2/N_2 slightly increased as compared to the initial values before the membrane was exposed to high humidity.

Biogas can contain up to 3000 ppm H_2S, which is a very high amount to expose the membranes to. Different techniques are used to remove sulphur from biogas: silica gel, activated carbon, iron sponge and biological filtration. Polyimide membranes, unlike CHF and PORCHF, have high H_2O and H_2S permeability, which make it suitable for biogas upgrading process without special pre-treatment as these components will permeate with CO_2 [42]. However, biomethane as a vehicle fuel (German legislation) demands sulphur contents below 4 ppm and water dew point of $-10\ ^{\circ}C$ at 200 bar, which require pre-treatment in both carbon and polyimide membrane separation process as considered in this work. It can be expected that biogas contains traces of organic components such as alkanes, halogenated hydrocarbons, ketones, aromatic compounds, siloxane, alkyl sulphides and alcohols depending on the substrate used for anaerobic digestion [42,43]. Toluene, an aromatic hydrocarbon, is usually detrimental to the membrane, and it significantly decreased CO_2 permeability and CO_2/N_2 selectivity when tested at 100 ppm for CHF. The PORCHF membrane showed a significant increase in permeability of CO_2, whereas selectivity of CO_2/N_2 decreased. Heptane showed the similar effect as toluene when tested 1000 ppm for both CHF and PORCHF. However, the presence of methanol significantly lowered the permeability and CO_2/N_2 selectivity in both CHF and PORCHF. The presence of 300 ppm toluene on polyimide membranes decreased the CO_2 permeability significantly and a slight decrease in CO_2/CH_4 selectivity was observed by Wind et al. [44]. Many of these components have not yet been tested and will need further investigations. With the presently available membranes, it was

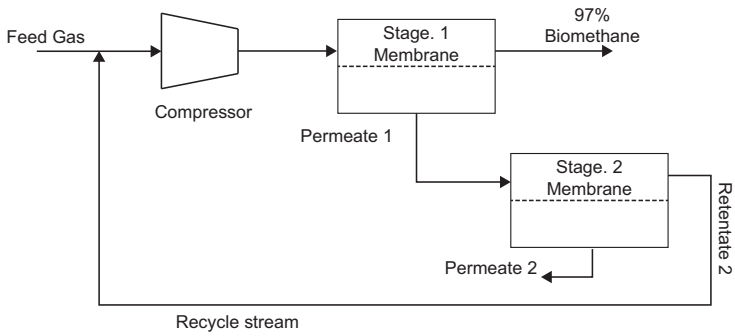

Fig. 4. Two stage membrane process.

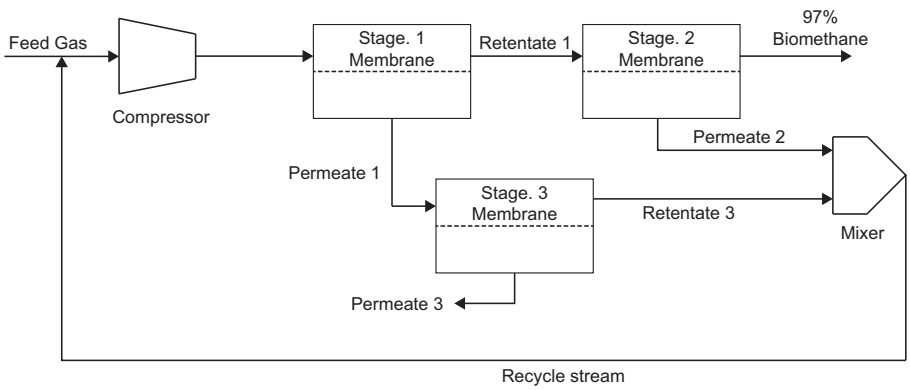

Fig. 5. Three stage membrane process.

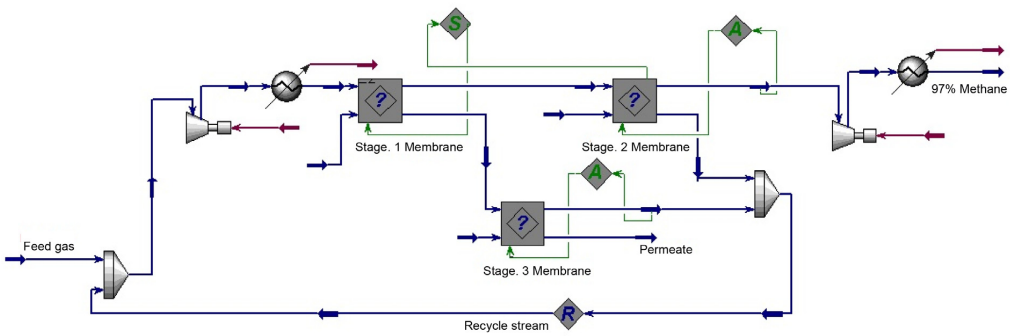

Fig. 6. A three-stage membrane system integrated into Aspen HYSYS.

concluded that pre-treatment is needed before the membrane is exposed to biogas.

3.2. Membrane configurations

3.2.1. Three cases

Membrane processes may vary with respect to operational units, their arrangement and applied process conditions. Three different cases were evaluated in this study.

3.2.1.1. Single stage membrane process. A membrane system using only one stage to separate biogas for required methane recovery and purity has been simulated. Polyimide membrane is a commercially available membrane with modest selectivity, and in order to judge the separation performance of this membrane, using only one stage simulation at 10 bar feed pressure is evaluated (Fig. 3).

3.2.1.2. Two-stage membrane process. To maximize the recovery of biomethane from biogas, a two-stage system has been simulated using all four membrane types with different selectivities. The permeate from the first stage enters into the second stage membrane to recover more CH_4. Retentate from second stage mix with feed in the form of recycle stream prior to the

Table 2
Gas permeation properties used in this work.

Membrane type	Permeance, (m^3(STP)/(m^2 h bar)) [GPU], (m^3(STP)/(m^2 h bar)) 1 GPU = 2.736E-3			Single gas selectivity		Ref.
	CO_2	CH_4	N_2	CO_2/CH_4	CO_2/N_2	
Polyimide hollow fibre	5.6E-2 [20.5]	1.7E-3 [0.62]	6.0E-4 [0.22]	33	31	[40]
CHF	5.5E-3 [2.02]	6.1E-5 [0.0224]	1.8E-4 [0.0673]	90	30	This work
PORCHF	2.1E-2 [7.75]	8.6E-5 [0.0315]	2.6E-4 [0.0943]	246	82	This work
Benchmarking polymeric membrane	1.4E-2 [5.01]	1.4E-4 [0.0501]	4.1E-4 [0.15]	100	33	See text

compressor for better CH_4 recovery (Fig. 4). There is no compression between the stages and the pressure of permeate 1 is adjusted with flow valve at Retentate 2. The pressure at permeate 1 was kept at a constant value for the specific feed pressure, obtained with formula as shown in Eq. (3). The basis of the formula is to maximize the pressure ratio (hence maximum perm purity) on both stages simultaneously by setting the interstage retentate. It was observed that the intermediate pressure value acquired, gave optimized membrane area for required purity and recovery of CH_4.

$$P_{interstage} = \sqrt{\left(P_{feed} \cdot P_{permeate2}\right)} \quad (3)$$

3.2.1.3. Three-stage membrane process. A three-stage membrane system may give better separation and reduce energy demand [45]. A three-stage configuration is shown in Fig. 5. Evonik Fibres Gmbh has applied for the patent of this configuration, and according to the patent, no one but Evonik can use a membrane with a CO_2/CH_4 selectivity of 30 or higher on the first stage [46]. Considering this patent is accepted, the energy demand of the process may increase by 0.027 kWh/Nm^3 for other membrane providers. The three-stage system is simulated and economically evaluated here by using polyimide membranes.

3.3. Simulation basis

- NTNU has an in-house membrane simulation model (Chembrane) which can easily be integrated into Aspen HYSYS. This model uses fourth-order Runge–Kutta method to calculate the flux along membrane length, and then iteration over permeate values to converge to a solution. ChemBrane model is integrated into 8.6 V Aspen HYSYS for all simulations in this work.
- Countercurrent gas transportation without sweep on permeate side has been used in all hollow fibre membrane modules. Literature data shows that counter current flow exhibits the superior separation and uses lowest membrane area in hollow fibre module design. This module design is very efficient and has a high packing density (can be up to 30,000 m^2/m^3 for certain designs) [47].
- The Peng Robinson sour fluid package was used.
- In order to run the simulations smoothly, only separation of the main components CH_4 (50–70%) and CO_2 (50–30%) is considered in the gas stream entering the membrane system. But techno-economic evaluation includes H_2S removal, water removal and dust removal system.
- Intermediate pressure (inlet pressure for the stage 2 membranes in two-stage configuration and inlet pressure for the stage 3 membranes in three-stage configuration) is kept same for different membranes to balance the complexity of the system. Effect of intermediate pressure and sweet gas has already been studied by Deng et al. [31].
- The adiabatic efficiency of the compressors is modelled as 75%.

3.4. Process conditions

A water-saturated biogas stream of 300 Nm^3/h with 3000 ppm of H_2S is considered as a base-case. Biogas enters into biological H_2S remover for bulk removal down to between 50 and 100 ppm and passes further through activated charcoal, where H_2S is taken down to below 1 ppm. The refrigeration process followed by zeolite molecular sieve is used to remove water from biogas in order to achieve a dew point of −10 °C at 200 bar. Biogas is compressed (single stage compression is used in simulations but multi stage compression with inter stage cooling is considered in cost calculation) to required feed pressure (6, 8, 10 bars and all pressure values are absolute in this work) and then filtered to remove dust and oil droplets before entering the membranes. Biogas is fed to the membrane and the resulting biomethane is compressed up to 250 bars before it is stored for further usage as a vehicle fuel (see Table 3). A three-stage simulation using ChemBrane model in Aspen Hysys is shown in Fig. 6.

3.4.1. Effect of N_2

Using biological desulfurization may result in the addition of air components in the biogas stream. CH_4 and N_2 have close selectivity value for commercially available membranes, which makes it difficult to remove N_2 from CH_4 to achieve required CH_4 purity. CHF membranes and PORCHF membranes have shown CH_4/N_2 selectivity of 3, making it less vulnerable to N_2 in the gas stream. Only PORCHF membrane with the two-stage system has been simulated including N_2. The intermediate pressure needed some extra optimization to get required results. N_2 concentration in feed and operating conditions is shown in Table 4.

3.5. Cost estimation and economic parameters

Accurate economic assessment of any process depends on available design details, a method of analysis used for calculation and accuracy of available cost data. Therefore, the economic calculations may differ considerably, as they are justified by the data available and also cost model. An economic evaluation was performed to assess the different membranes and their configurations, by taking capital cost,

Table 3
Process conditions and feed composition used in this work.

Process conditions used in simulation	
Feed composition	30–50% CO_2, balance CH_4
Feed flow rate (Nm^3/h)	300
CH_4 purity in product (%)	97.5
CH_4 recovery (%)	99.5
S total	<4 ppm
Water dew point	−10 °C at 200 bar
Feed pressure (bar)	6, 8, 10
Intermediate pressure in two stage (bar)	2.45, 2.82, 3.16
Intermediate pressure in three stage (bar)	2.45, 2.82, 3.16
Flow pattern in membrane module	Countercurrent
Biogas delivery pressure (bar)	250

Table 4
N_2 concentration in feed and operating pressure.

N_2 in feed	Feed pressure	Intermediate pressure
%	bar	bar
0	10	4.24
0.5	10	4.24
1	10	3.7
1.5	10	3.55
2	10	2.95
2.1	10	2.95

operating cost, pre-treatment cost and high-pressure compression (CBG) cost into account. A high recovery of biomethane is achieved, resulting in a very small fraction of CH_4 loss with permeate stream (CO_2). Thus CO_2 obtained on permeate side is 99% pure and could be used for other applications. The price for the CO_2 is not considered in this economical assessment. Table 5 is showing process parameters for economic assessment of a biogas upgrading process.

4. Results and discussion

4.1. Membrane configurations

A constant pressure of 10 bar was applied to the feed gas with different CO_2 concentration to see the influence on recovery and membrane area. The result (Fig. 8) shows that methane loss is high up to 17% when 30% CO_2 is present in the feed at the applied operating conditions, and methane recovery decreases with increase in CO_2 content in the feed as shown in Fig. 7. The single stage system, as expected gives the lowest recovery; therefore, multiple stage system with recycle is discussed in the further results.

The feed pressure has a big effect on required membrane area for different CO_2 concentrations in the feed as shown in Fig. 9. The results show that higher the CO_2 present in the feed, less area is required in this case to reach the targeted product (CH_4) specifications. Area needed at low feed pressure (here 6 bar) is more sensitive to the feed concentration. Fig. 9 demonstrates the required area for a two-stage separation system of polyimide membrane with varying CO_2 loadings under a set of applied pressure. Results indicate that required area per Nm^3 of feed gas under different concentrations of CO_2 in the feed is three times higher when operating feed pressure is decreased from 10 bar to 6 bar. The effect of CO_2 concentration in the feed gas is more sensitive at low pressure—this is as expected in this range when considering the basic equations.; here it shows the decline in required membrane area from 175 m^2/Nm^3 to 125 m^2/Nm^3 when increasing from 30- to 50% CO_2, whereas, at 8 and 10 bar pressure, the area is almost constant. The product purity is affected by selectivity limited region at 6 bar (Separation factor vs permeate purity plot of Weller–Steiner equation [53]). When the pressure is 8 bar or higher, the product purity is in the pressure ratio limited region. Two-stage membrane separation cascade using a polymeric membrane with CO_2/CH_4 selectivity of 100 is presented in Fig. 10.

Table 5
Process parameters for economic assessment of biogas upgrading plant [51,52] ($ used in this work is US).

Total plant investment (TPI)	
Polymeric membrane cost (PMC)	$ 20/m^2 [31,33,48,49]
Carbon membrane cost (CMC_o)	$ 100/m^2
Installed compressors cost (CC)	$ 8700 × $(HP/\eta)^{0.82}$
High pressure compressor cost (CBGC)	$C_{comp,ins} = 912 \cdot (Wcomp)^{0.9315} \cdot f_m \cdot f_i \cdot f_{inst}$ [50]
Fixed cost (FC)	$PMC/CMC_o + CC + PTC + CBGC$
Base plant cost (BPC)	1.12 × FC
Project contingency (PC)	0.2 × BPC
Total facility investment (TFI)	BPC + PC
Start-up cost (SC)	0.10 × VOM
TPI	TFI + SC
Annual variable operating and maintenance cost (VOM)	
Contract and material maintenance cost (CMC)	0.05 × TFI
Local taxes and insurance (LTI)	0.015 × TFI
Direct labour DL, cost based on 8 h/day	$ 15/h
Labour overhead cost (LOC)	1.15 × DL
Utility cost (UC) ($/kWh)	0.07/kWh
VOM	CMC + LTI + DL + LOC + MRC + UC
Other assumptions	
Membrane life for polyimide (t)	7.5 years
Membrane life for carbon (t)	5 years
Biomethane sales price ($)	$ 0.8/Nm^3
Nominal interest rate (%)	6%
Depreciation (t)	15 years
LCC/LCI factor (ordinary annuity factor)	9.7122
Plant availability (%)	96%
CO_2/CH_4 in feed (%)	40/60

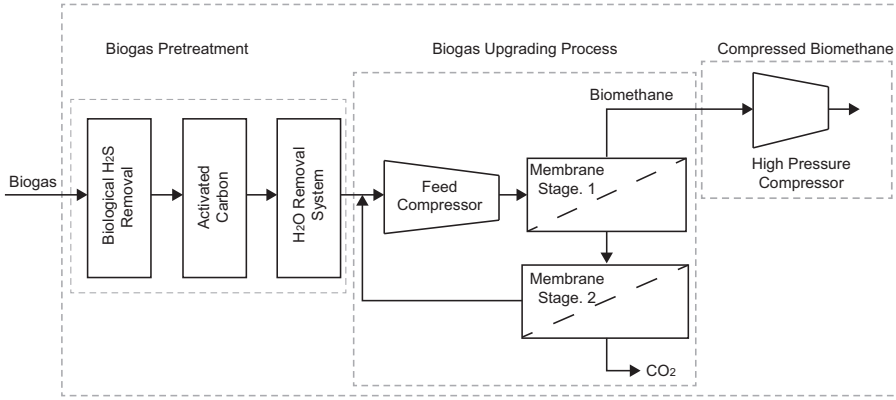

Fig. 7. Schematic diagram of biogas upgrading system.

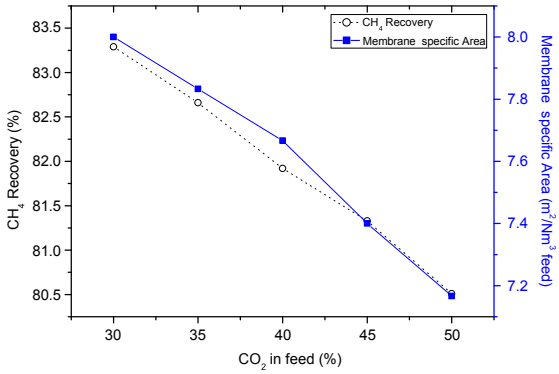

Fig. 8. A single stage separation with polyimide membrane (10 bar, 23 °C).

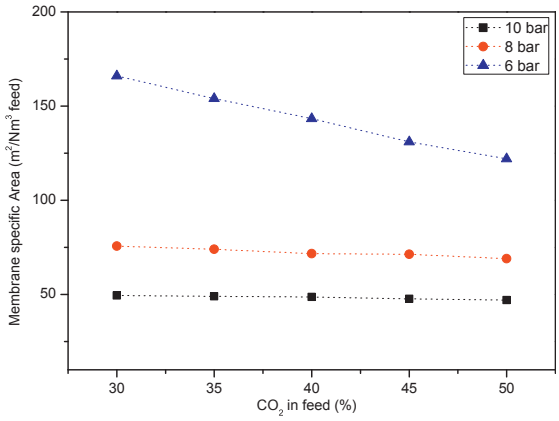

Fig. 9. Two-stage membrane separation cascade (Polyimide membrane, T: 23 °C).

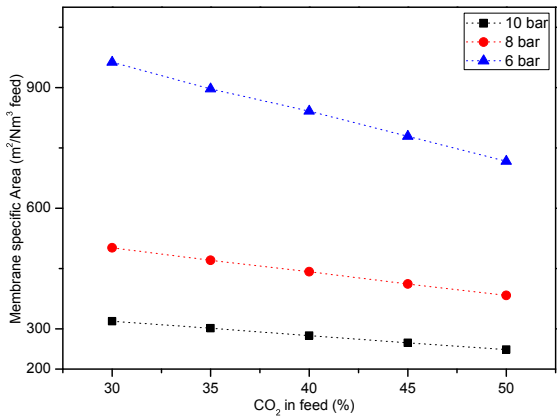

Fig. 10. Two stage membrane separation cascade (selectivity 100, T: 23 °C).

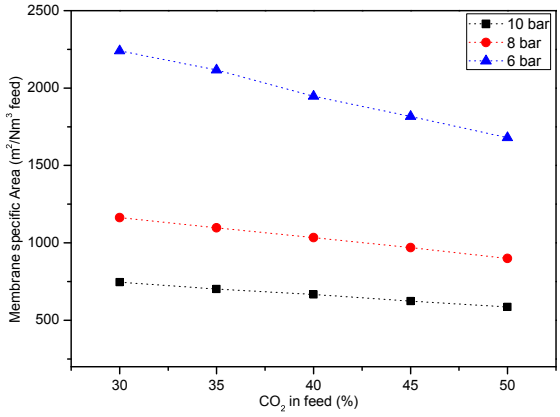

Fig. 11. Two stage membrane separation cascade (CHF membrane, T: 23 °C).

Required area per Nm^3 of feed is lowest when feed pressure is 10 bar and 50% CO_2 is present in the feed—this is according to theory for solution-diffusion separation. Fig. 11 shows the results for two-stage CHF membrane separation and a linear decline in required membrane area can be observed for different CO_2 loadings. Maximum area is required when feed pressure is 6 bar and the feed concentration of CO_2 is 30%. A similar trend is observed in the case of

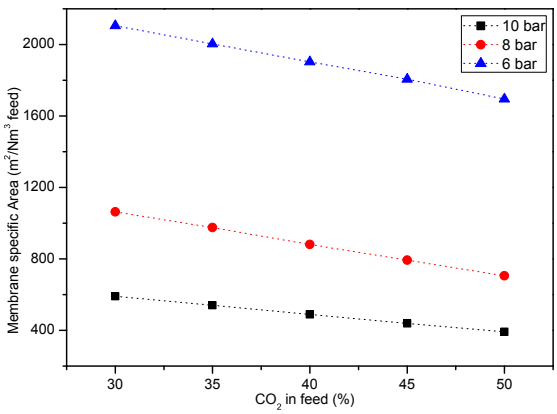

Fig. 12. Two stage membrane separation cascade (PORCHF membrane, T: 23 °C).

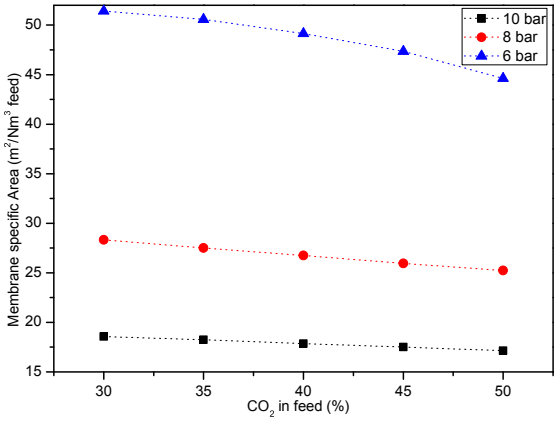

Fig. 13. Three stage membrane separation cascade (Polyimide membrane, T: 23 °C).

two-stage PORCHF membrane cascade (Fig. 12). Results presented in Figs. 9–12 show that change in required membrane area under a set of CO_2 loadings is significant when feed pressure is low (6 bar). However, when pressure is high (10 bar) the trend line looks almost straight for Fig. 9 and the variation in the area (Figs. 10–12) is not very high. Fig. 13 shows the results for a three stage membrane separation using polymeric membranes. In membranes, the performance is a trade-off between selectivity and permeability, and productivity is a function of material property and thickness of the membrane [54]. Assuming a selective wall thickness of 1 μm for polyimide membrane and 20 μm for carbon membranes, it was observed that carbon membrane requires >13 times larger area when same operational conditions are applied as for the polymeric membrane. A three-stage polyimide system requires the lowest area, which is three times less than the two-stage polyimide system. The area against different CO_2 loadings shows a linear decline for CHF and PORCHF membranes when CO_2 increases in the feed, whereas the curve is more visible in case of three stage polyimide membrane.

4.2. Recycle stream and compression duty

Operating cost of a biogas upgrading process depends largely on the compressor duty, and the recycle ratio (recycle/feed) higher than 1 can increase this compression energy requirement to a higher level. Results obtained by the simulation of different membranes with two and three stage configurations are plotted in Figs. 14 and 15. The Fig. 14 (a), demonstrates the recycle ratio at 6 bar feed pressure, which is seven for the two stage polyimide membrane system and it would result in high operating cost; in the form of compression energy and also, a compressor with high capacity is required to treat the total volume of the gas which would increase capital cost as well. Whereas, the recycle ratio is below one (Fig. 14 (a)) for PORCHF membrane system and the compression duty required for this system is one fourth of the amount required for two stage polyimide system as shown in Fig. 15 (a). The efficiency of a membrane system increases with high selectivity as it can be seen from the recycle ratio and specific duty plots. The data shows that PORCHF having highest selectivity gives lowest recycle ratio and the required specific duty values. It was observed that the recycle ratio decreases in CHF and PORCHF membranes unlike polyimide membranes with high CO_2 present in the feed. It is very important to choose an optimal point where capital investment and running cost are low and the system is efficient at the same time. The increasing of feed pressure to 8 bar results in lower recycle ratio and energy demand. However, for two stage polyimide membranes, recycle ratio is still quite high especially when 50% CO_2 is present in the feed as shown in Fig. 14 (b). The Fig. 15 (b) indicates that the specific duty required is still four times higher for the polyimide membrane system as compared to PORCHF system. Plasticization effect inhibits polyimide membrane to go to high pressures [27], so maximum pressure tested for polyimide membrane systems is 10 bar in this section of work, which shows high recycle ratio in two-stage configuration as shown in Fig. 14 (c). The three-stage system with polyimide shows recycle ratio about 1 for 8 bar and 10 bar simulations, and the specific energy demand for three stage polyimide is double as compare to PORCHF membrane system.

4.3. Effect of N_2

It seems impossible to get fuel quality with this polyimide membrane if up to 2.5% N_2 is present in the feed biogas, as infinite membrane area would be required to separate out 100% CO_2, whereas PORCHF membrane can tolerate more N_2 due to high CH_4/N_2 selectivity as compared to polyimide membrane as shown in Fig. 16. The curve of area and duty in Fig. 16 is expected to be asymptotical, which leads to infinite area and compression duty requirement in the presence of high N_2 percentage in feed biogas. The presence of more N_2 would result in increased recycle ratio to achieve required fuel (CH_4) purity and recovery, which again leads to high membrane specific area and compression duty.

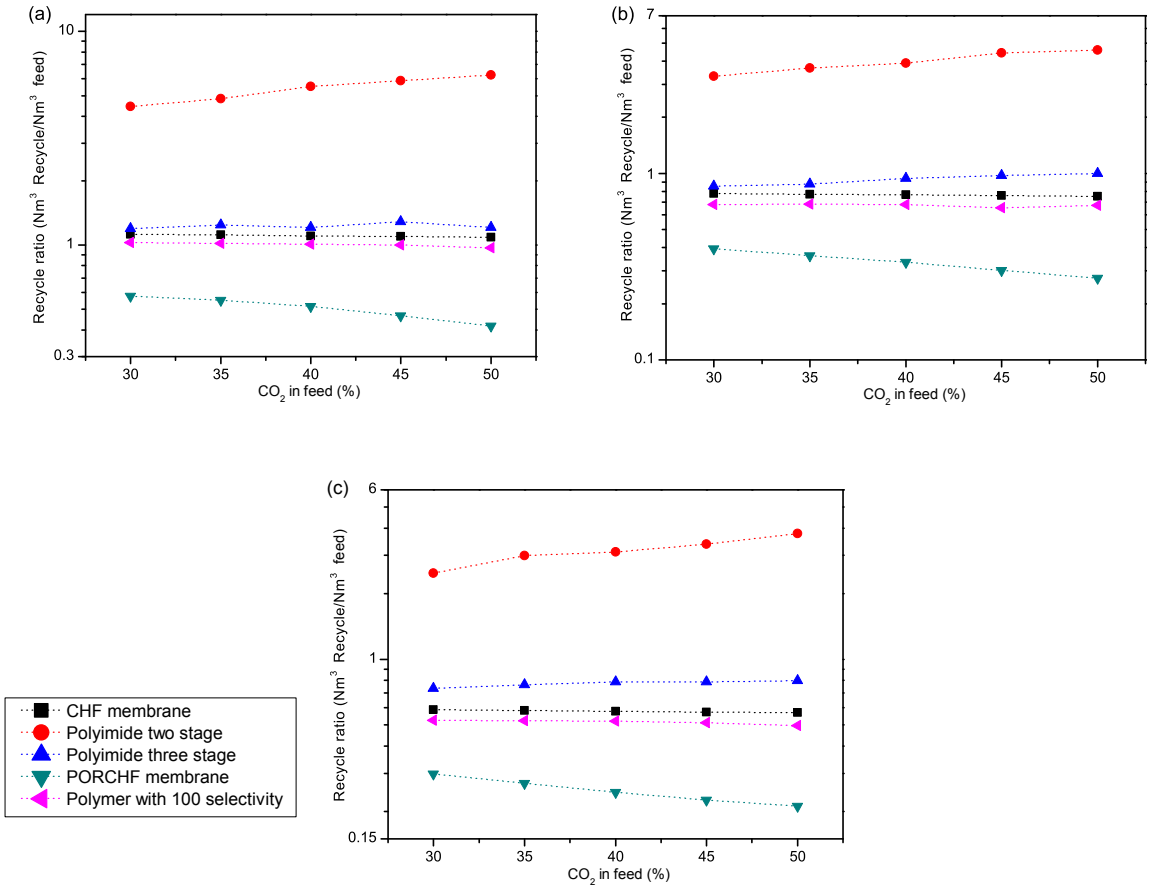

Fig. 14. Recycle ratio at different CO_2 loadings in feed at 23 °C, (a) at 6 bar, (b) at 8 bar, (c) at 10 bar.

4.4. Cost calculation

4.4.1. Processing cost

Processing cost has been considered as the sum of capital and operating cost to calculate the price of compression duty and area for membrane systems over 15 years. The Fig. 17 shows the processing cost of compression energy and area per Nm^3 of upgraded biomethane for a two-stage polyimide membrane system. The effect of big recycle ratio can be seen in the form of high processing cost here for two-stage polyimide system. Even though the membrane cost is quite low, the cost of energy in capital investment and costs during running time is very high. The required processing cost is reduced to one-fourth by using a three-stage system for polyimide membrane as shown in Fig. 18. The effect of membrane efficiency is more prominent in Figs. 19 and 20 with CHF and PORCHF membranes, showing considerably low processing cost related to energy consumption, whereas the effective membrane area required is five-fold higher than for polymeric membranes. Considering $ 20/m^2 for polymeric membranes and $ 100/m^2 for carbon membrane, results show that membrane area can increase 30%–80% of total investment if optimal pressure is not applied on the upgrading plant.

4.4.2. Net Present Value (NPV) calculation

The NPV calculation includes pre-treatment, upgrading part and high-pressure compression on biomethane to the fuel standard. Considering that different material has specific advantages, an optimal pressure value has been applied on both carbon and polymeric materials to calculate the NPV in cost estimation. Fig. 21 shows NPV at 10 bar pressure for polyimide two-stage and three-stage system. Carbon membranes have shown a stable performance under different CO_2 loadings, with no plasticization up to 50 bar [28]. It can be seen from the NPV results that optimal pressure for carbon membrane is 50 bar or higher. For NPV calculations, 50% CO_2 concentration in the feed is considered.

A three-stage polyimide membrane system has been calculated to have a maximum NPV of $ 9.3 M at 10 bar,

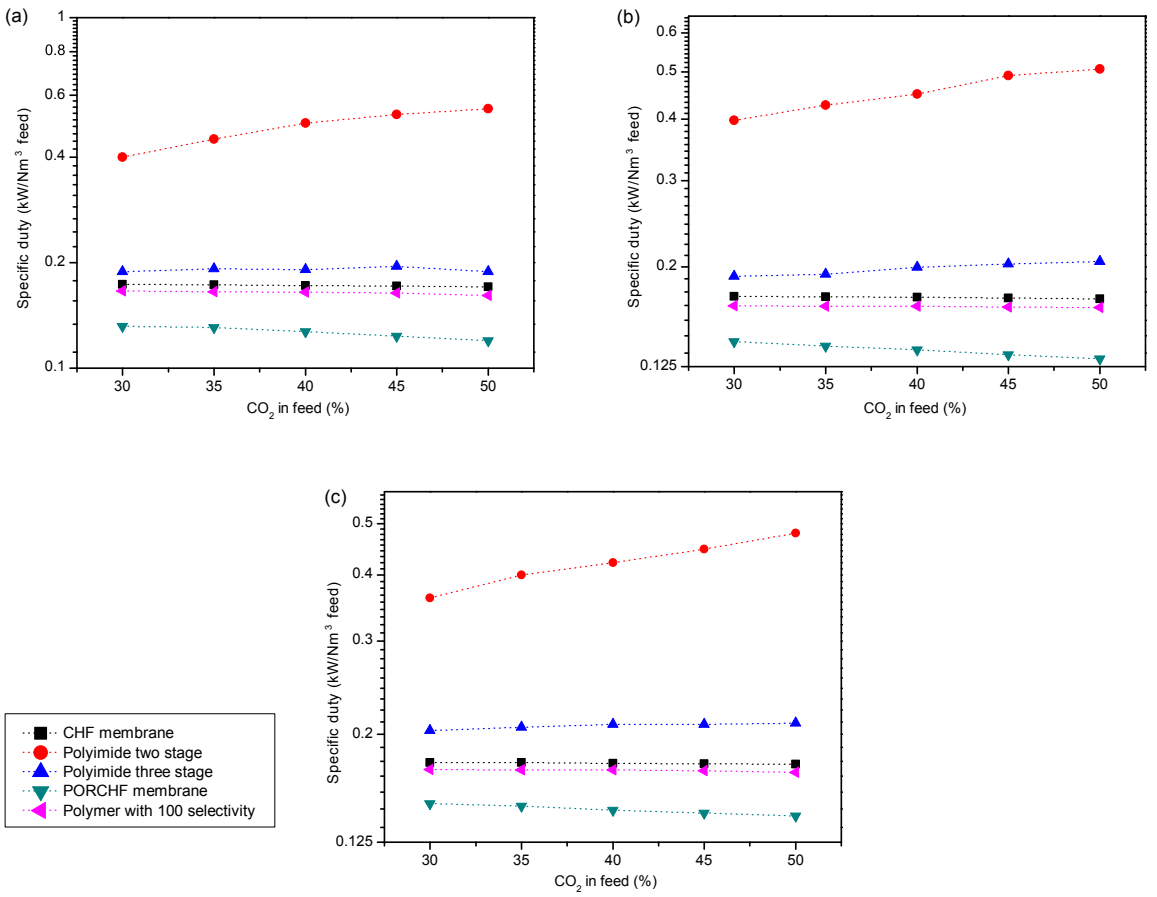

Fig. 15. Specific Compression duty at different CO_2 loadings in feed at 23 °C, (a) at 6 bar, (b) at 8 bar, (c) at 10 bar.

whereas PORCHF membrane system looks competitive with an NPV of $ 7.4 M. The resulting lower NPV value for PORCHF is due to high membrane cost and estimated for a lifetime of 5 years in comparison with 7.5 years of polyimide membranes. However, this price can be reduced by optimizing the membrane production process (The production process was not fully optimized for the pilot scale production of CHF and PORCHF at the company MemfoACT).

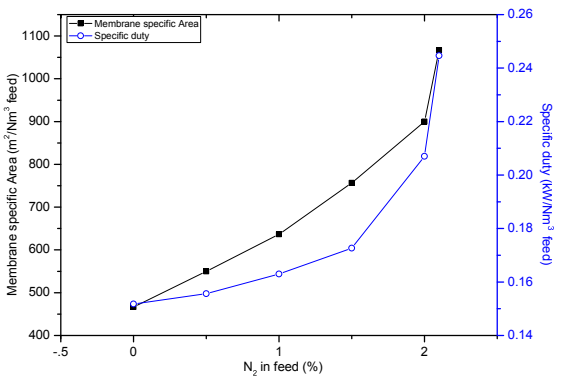

Fig. 16. Effect of N_2 concentration in feed gas (10 bar, 23 °C).

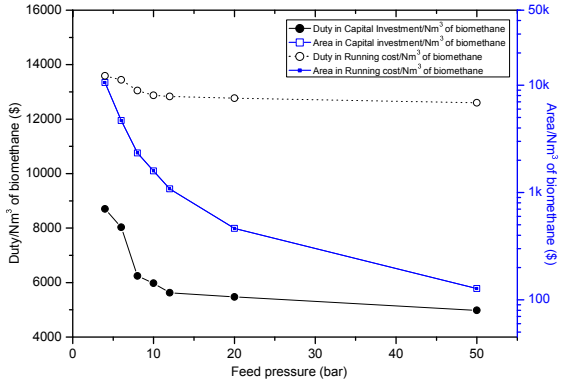

Fig. 17. $ for duty & area in processing cost, (two stage polyimide).

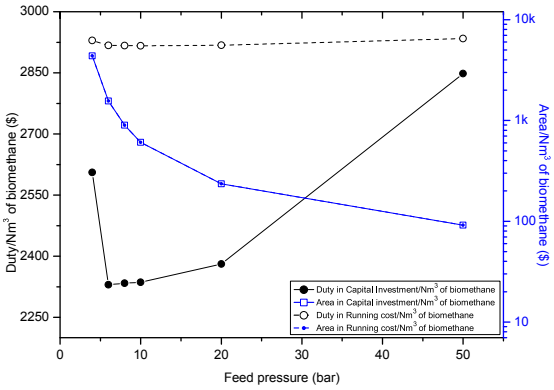

Fig. 18. $ for duty & area in processing cost, (three stage polyimide).

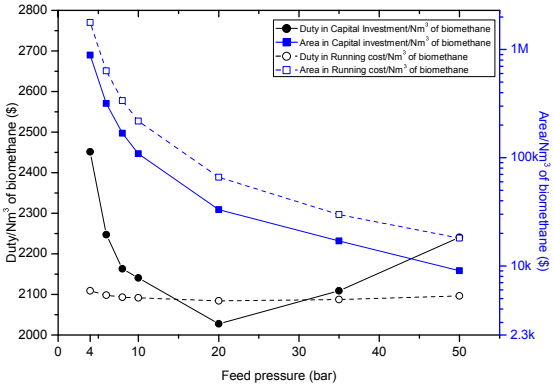

Fig. 19. $ for duty & area in processing cost, (two stage CHF).

4.4.3. Sensitivity analysis

Assuming an optimized process producing PORCHF at a price of $ 60/m^2 instead of $ 100/m^2 and a membrane lifetime of 7.5 years will give NPV for PORCHF of $ 8.8 M. and applying 70 bar pressure, then it can increase NPV for PORCHF over $ 9 M as shown in Fig. 22.

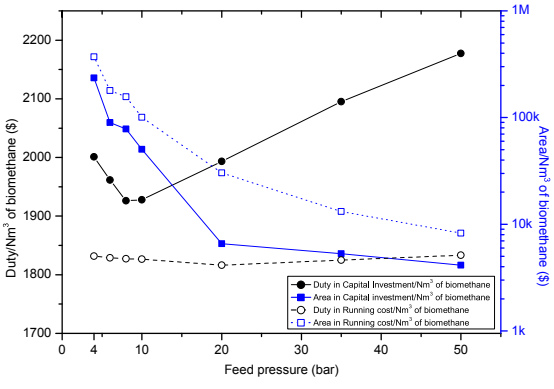

Fig. 20. $ for duty & area in processing cost, (two stage PORCHF).

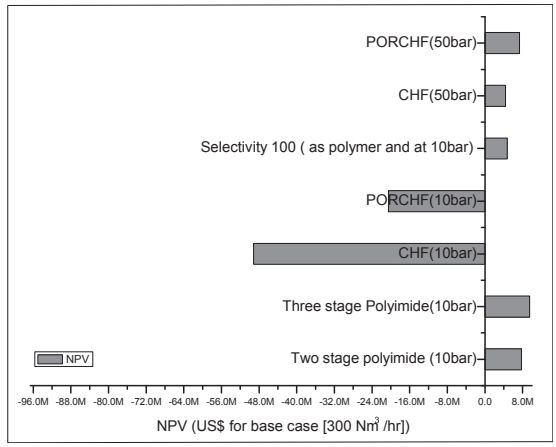

Fig. 21. NPV calculated for optimal pressures.

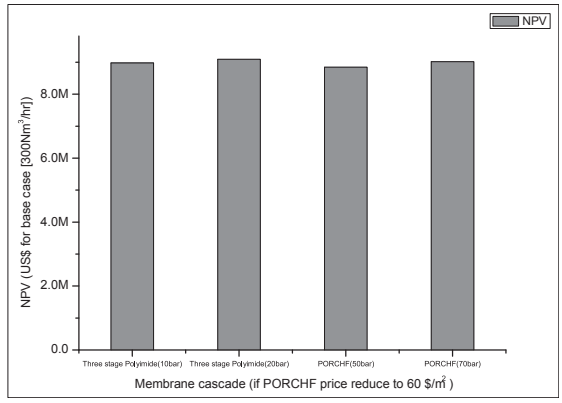

Fig. 22. NPV comparison of three stage polyimide and PORCHF membrane.

5. Conclusions

In this study, it was found that the two-stage cascade process with recycle using a polyimide membrane was not economically viable for biogas upgrading due to high recycle ratio, and thus resulting in high operating cost, whereas the three stage polyimide membrane system is quite feasible in order to obtain fuel quality of biomethane. Carbon hollow fibre membrane and modified carbon hollow fibres produced on a pilot plant were tested to obtain the same fuel quality in two stage cascade, and these membranes consumed 22% less energy as compared to three-stage polyimide system. The drawback of these membranes is, however, the production cost, which is 5-fold higher than the assumed costs of a polyimide membrane. The optimization in the production process and choosing an optimal operating pressure can reduce the

capital cost for CHF and PORCHF membranes, whereas the operating cost can be reduced by increasing the membrane life through regeneration of carbon fibres by applying CVD process if pore clogging is the problem. In the case of fibre breakage, the broken fibres may be plugged in the module. Instant boosting with electrical regeneration applying low voltage and direct current (DC) has been documented as successful, but the effect of this regeneration procedure on the aging of the membrane is not sure.

Conflict of interest

There is no conflict of interest in the reported work; not between the acknowledged researchers, authors or mentioned companies.

Acknowledgements

The authors are very grateful to Ms Ingerid Caroline Tvenning Andersen for excellent laboratory work on the carbon hollow fiber membranes and Dr. Muhammad Saeed for fruitful discussion. The authors would also like to thank The Department of Chemical Engineering at NTNU for providing the possibility to work with this article.

References

[1] Z. Song, C. Zhang, G. Yang, Y. Feng, G. Ren, X. Han, Renew. Sustain. Energy Rev. 33 (2014) 204–213.
[2] R.H. Williams, Toward zero emissions from coal in China, China Cl. Energy Forum, Beijing, 2001.
[3] M. SoltaniehS, K. Thambimuthu, J.C. Abanades, Special Report on CO_2 Capture and Storage, (IPCC), 2005.
[4] H. Yang, Z. Xu, M. Fan, R. Gupta, R.B. Slimane, A.E. Bland, I. Wright, J. Environ. Sci. 20 (2008) 14–27.
[5] Anon, Swedish Case Studies, Swedish Gas Association, 2008.
[6] S. Rasi, A. Veijanen, J. Rintala, Energy 32 (2007) 1375–1380.
[7] J.B. Holm-Nielsen, T. Al Seadi, P. Oleskowicz-Popiel, Biores. Tech. 100 (2009) 5478–5484.
[8] S.S. Hosseini, N. Peng, T.S. Chung, J. Membr. Sci. 349 (2010) 156–166.
[9] L. Yingjian, Q. Qi, H. Xiangzhu, L. Jiezhi, Sustain. Energy Technol. Assess. 6 (2014) 25–33.
[10] M. Scholz, M. Alders, T. Lohaus, M. Wessling, J. Membr. Sci. 474 (2015) 1–10.
[11] A. Molino, M. Miglion, B. Bikson, G. Giordano, G. Braccio, Fuel 107 (2013) 585–592.
[12] L. Yang, X. Ge, C. Wan, F. Yu, Y. Li, Renew. Sustain. Energy Rev. 40 (2014) 1133–1152.
[13] E. Ryckebosch, M. Drouillon, H. Vervaeren, Biomass Bioenerg. 35 (2011) 1633–1645.
[14] A. Wellinger, A. Lindberg, Biog. Upgrad. Utilisat., 2005 [Internet] IEA Bioenerg. Task 24.
[15] D.A. Ken Krich, J.P. Batmale, J. Benemann, B. Rutledge, D. Salour, Natural Gas in California, Clear Concepts, California, 2005, pp. 47–69.
[16] B. Rutledge, White Paper, California Biog. Ind. Assess, vol. 38, West-Start-Calstart, Pasadena, USA, 2005.
[17] R. Baker, Membr. Tech. (2001) 5–10.
[18] Z. Dai, R.D. Noble, D.L. Gin, X. Zhang, L. Deng, J. Membr. Sci. 497 (2016) 1–20.
[19] A.L. Kohl, R. Nielsen, Gas Purif, fifth ed., Gulf Pub. Co, Houston, Texas, 1997.
[20] J.A. Lie, M.B. Hägg, J. Membr. Sci. 284 (2006) 79–86.
[21] J. Ahmad, M.B. Hägg, J. Membr. Sci. 427 (2013) 73–84.
[22] S. Kim, S.H. Han, Y.M. Lee, J. Membr. Sci. 403–404 (2012) 169–178.
[23] Y. Zhang, J. Sunarso, S. Liu, R. Wang, Int. J. Greenh. Gas. Control. 12 (2013) 84–107.
[24] J.A. Lie, M.B. Hagg. (US20100162887A1, 2010), chap. US 2010/0162887 A1.
[25] L.M. Robeson, J. Membr. Sci. 320 (2008) 390–400.
[26] L.M. Robeson, J. Membr. Sci. 62 (1991) 165–185.
[27] S. Kanehashi, T. Nakagawa, K. Nagai, X. Duthie, S. Kentish, G. Stevens, J. Membr. Sci. 298 (2007) 147–155.
[28] N. Tanihara, H. Shimazaki, Y. Hirayama, S. Nakanishi, T. Yoshinaga, Y. Kusuki, J. Membr. Sci. 160 (1999) 179–186.
[29] D.Q. Vu, W.J. Koros, S.J. Miller, Ind. Eng. Chem. Res. 41 (2002) 367–380.
[30] A. Makaruk, M. Miltner, M. Harasek, Sep. Purif. Technol. 74 (2010) 83–92.
[31] L. Deng, M.B. Hägg, Int. J. Greenh. Gas. Control. 4 (2010) 638–646.
[32] C. Micale, Energy Proced. 82 (2015) 971–977.
[33] J.A. Lie, T. Vassbotn, M.B. Hagg, D. Grainger, T.J. Kim, T. Mejdell, Int. J. Greenh. Gas. Control. 1 (2007) 309–317.
[34] D. Grainger, M.-B. Hägg, Fuel 87 (2008) 14–24.
[35] X. He, J. Arvid Lie, E. Sheridan, M.-B. Hägg, Energy Proced. 1 (2009) 261–268.
[36] A. Hussain, M.-B. Hägg, J. Membr. Sci. 359 (2010) 140–148.
[37] B. Belaissaoui, Y. Le Moullec, D. Willson, E. Favre, J. Membr. Sci. 415–416 (2012) 424–434.
[38] A. Soffer, H. Cohen, US005914434A vol. US005914434A, Carbon Membr. Ltd., Arava, Israel, 1999.
[39] X. He, J.A. Lie, E. Sheridan, M.B. Hägg, Ind. Eng. Chem. Res. 50 (2011) 2080–2087.
[40] F. Falbo, F. Tasselli, A. Brunetti, E. Drioli, G. Barbieri, Braz. J. Chem. Eng. 31 (2014) 1023–1034.
[41] M. Scholz, T. Melin, M. Wessling, Renew. Sustain. Energy Rev. 17 (2013) 199–212.
[42] M. Harasimowicz, P. Orluk, G. Zakrzewska-Trznadel, A.G. Chmielewski, J. Hazard. Mater. 144 (2007) 698–702.
[43] P. Weiland, Appl. Microbiol. Biot. 85 (2010) 849–860.
[44] J.D. Wind, D.R. Paul, W.J. Koros, J. Membr. Sci. 228 (2004) 227–236.
[45] S.P. Kaldis, G. Skodras, G.P. Sakellaropoulos, Fuel Process. Technol. 85 (2004) 337–346.
[46] M. Ungerank, G. Baumgarten, M. Priske, H. Roegl, US20130098242A1 vol. US 20130098242A1, Evonik Fibres Gmbh, 2013.
[47] M. Mulder, Basic Principles of Membrane Technology, Springer, Netherlands, 1996.
[48] W.J. Koros, Membrane opportunities and challenges for large capacity gas andvapour feeds, in: European Membrane Society's 20th Summer School, NTNU, Trondheim, 2003.
[49] X. He, C. Fu, M.-B. Hägg, Chem. Eng. J. 268 (2015) 1–9.
[50] A. Lindbråthen, D.R. Grainger, M.B. Hägg, Sep. Sci. Technol. 42 (2007) 3049–3070.
[51] M.S. Peters, K.D. Timmerhaus, Plant Design and Economics for Chemical Engineers, McGraw-Hill, New York, 1991.
[52] W.D. Baasel, Preliminary Chemical Engineering Plant Design, Van Nostrand Reinhold, New York, 1990.
[53] D.J. Stookey, C.J. Patton, G.L. Malcolm, Effects of Separation Factor and Pressure Ratio on Permeate Purity (Membranes Separate Gases Selectivity), Chemical Engineering Progress, 1986.
[54] W.J. Koros, R. Mahajan, J. Membr. Sci. 175 (2000) 181–196.

Appendix K

Paper VII

Carbon membranes for oxygen enriched air –Part I: Synthesis, performance and preventive regeneration

Paper published in Separation and Purification Technology 204 (2018) 290-297.

Separation and Purification Technology 204 (2018) 290–297

Contents lists available at ScienceDirect

Separation and Purification Technology

journal homepage: www.elsevier.com/locate/seppur

Carbon membranes for oxygen enriched air – Part I: Synthesis, performance and preventive regeneration

Shamim Haider, Arne Lindbråthen, Jon Arvid Lie, May-Britt Hägg*

Norwegian University of Science and Technology, NTNU, Department of Chemical Engineering, 7491 Trondheim, Norway

ARTICLE INFO

Keywords:
Carbon hollow fibers
Oxygen-enriched air
Online electrical regeneration

ABSTRACT

Chemisorption of oxygen on the active sites of carbon layers limits the use of carbon membranes in air separation application. A novel online electrical regeneration method was applied to prevent the active sites on carbon surface to be reacting with O_2 while the membrane was in operation. This method reduced the aging effect and the membrane showed relative stable performance with only 20% loss in O_2 permeability and 28% increase in O_2/N_2 selectivity, over the period of 135 days using various feeds containing H_2S, *n*-Hexane and CO_2-CH_4 gas. The carbon membranes reported here were produced at the pilot-scale facility by the carbonization of regenerated cellulose under optimized conditions to achieve good air separation properties. The permeation properties of the membranes were tested by single gas separation experiments at 5 bar feed pressure (50 mbar permeate) and temperature range 20–68 °C. It was observed that O_2 permeability is increasing exponentially with increase in operating temperature without significant loss in the O_2/N_2 selectivity. The O_2 permeability of 10 Barrer *(1 Barrer = 2.736E − 09 m^3(STP)m/m^2 bar h)* with O_2/N_2 selectivity of 19 was achieved at 68 °C. Thermal (80 °C), chemical (propylene) and online-electrical (10 V DC) regeneration approaches were studied to lessen the aging effect on carbon membranes.

1. Introduction

At present, the air separation market to produce pure oxygen (O_2: 95–99.99%) is dominated by cryogenic fractionation and pressure swing adsorption because current membranes are not capable of economically producing membranes with comparable purity [1]. The separation is based on the difference in permeation rates of oxygen and nitrogen through the membrane, and the performance of polymeric membranes is restricted by the trade-off between permeability and selectivity [2]. Polymeric materials may have a high permeability for O_2, but rather low O_2/N_2 selectivity (usual range 2–8), and the maximum permeate purity achievable for O_2 with these membranes seems to be 30–60% [3].

Carbon is one class of material that can offer improved performance due to molecular sieving effect. In molecular sieving, the available pore size is below the kinetic diameter of one of the gas components in the feed. This characteristic of the material increases selectivity by reducing the rotational degrees of freedom of nitrogen versus oxygen in the diffusion (kinetic) transition state. Carbon membranes (CM) can be prepared by carbonization of the precursor membranes at high temperature (550–850 °C) under vacuum or in an inert environment (Ar, He or N_2). Gas permeation properties of CM are affected by the type of precursor and carbonization conditions. Many authors have reported high selectivity and permeability of carbon membranes (CM) compared to polymeric membranes for air separation [4–7].

Although CM have reported better performance compared to polymeric membranes, the operational stability and aging are the important issues to be considered for the implementation of these carbon membranes. CM usually age very rapidly due to physical aging (pore shrinkage to achieve a thermodynamically stable structure and or physical adsorption of gas molecules) and or chemical aging (chemical bonding, usually C═O bonds) [8–11]. This aging effect may seriously reduce the permeability of a membrane and hence it is still a major problem for the industrial application of CM in air separation where the membrane is exposed to O_2 all the time.

Several techniques have been reported to achieve a stable performance of CM under oxygen environment. Menendez et al. [11] used *thermal regeneration* and found that thermal treatment of membranes at 120 °C in a vacuum could remove oxygen-containing surface groups from activated carbons. However, the regenerative effect is very brief because it leaves a surface with reactive carbon sites that can re-adsorb oxygen very quickly even at room temperature. *Chemical regeneration* requires an addition of a chemical (gas) to restore the membrane performance. Jones and Koros [12] tested purging of propylene at about

* Corresponding author.
E-mail address: may-britt.hagg@ntnu.no (M.-B. Hägg).

https://doi.org/10.1016/j.seppur.2018.05.014
Received 1 February 2018; Received in revised form 23 April 2018; Accepted 7 May 2018
Available online 08 May 2018
1383-5866/

10 bar to restore the membrane performance, however, the permeance of O_2 was not successfully recovered.

Lie et al. [13] studied *electrothermal regeneration* to enhance the permeation of CO_2 in iron-doped flat-sheet CM. They applied a direct current of 30 mA (17.5 V) on the iron-doped CM and studied the effect of pulsating electrothermal regeneration (i.e. electric current set to "on" and "off" periodically). After electrothermal regeneration, the CO_2 permeability was 65% higher compared to initial value because the sorption of gases in carbon matrix was reduced, while diffusivity was increased to a considerable extent. Nevertheless, the membrane without any regeneration showed 60% loss in permeance of CO_2.

The aim of the current study has been to exploit further the electrically conductive nature of CM to enhance or stabilize the performance of the membrane. The present paper focuses on the novel online-regeneration method to prevent the reactive/adsorption sites by supplying continuous electric current. The effect of "online electrical regeneration (regeneration parallel with separation process)" on carbon hollow fiber membranes has not been fully explored, and there is not much information available on this topic. Hence, an online regeneration (DC: 44–55 μA, 10 V) was tested in this study to achieve a stable performance of CM in air separation application. In addition, thermal and chemical regeneration methods were also pursued to find an effective, simple, and economical solution to restore the membrane performance. The term "Preventive electrical regeneration" (PER) is used for the electric regeneration in this study. PER means a continuous supply of electrical potential during membrane operation to prohibit the molecules adsorbing on the membrane surface.

2. Theory and background

2.1. Structure of carbon molecular sieve

Carbon molecular sieve (CMS) is derived from organic thermosetting precursors by heat treatment in vacuum or in an inert environment. Geiszler and Koros [14] reported that an inert gas (Ar, He or N_2) atmosphere resulted in more open, but less selective CMS matrix compared to vacuum carbonization. They explained this with acceleration in the carbonization process due to increased gas phase heat and mass transfer. By increasing the final temperature in polyimide carbonization from 550 °C to 800 °C (in vacuum of He gas), the authors observed a decrease in permeance while selectivity increased. Precursors for CMS include thermosetting resins, graphite, coal, pitch, plants and synthetic polymers [15].

Bisco and Warren [16] introduced the concept of turbostratic order for graphitic carbons. The carbon consists of turbostratic groups, where each group has several graphite layers stacked together roughly parallel and equidistant, but with each group having a random orientation as shown in Fig. 1(a). Packing imperfection between the stacked layers contains slit-like pores which give rise to the molecular sieving structure and have a bimodal pore size distribution. The edges of adjacent stacked layers are believed to make the slit-like ultra-micropores (≤ 0.7 nm), while micropores (0.7–2 nm) are formed between the planes due to the random orientation of the adjacent carbon sheets [6]. The gases may diffuse through the pores, or they may adsorb on the walls and travel through the pores by a mechanism known as surface flow [17]. The bigger, more strongly adsorbed molecules may also block the pores of smaller molecules in a phenomenon known as competitive adsorption or selective surface flow. This results in reverse selectivity; the smaller components are thus retained.

2.2. Electrical regeneration

The continuous medium of graphene sheets makes the CMS membranes electrically conductive. As shown in Fig. 1(b), each sp^2-hybridized carbon atom combines with three other sp^2-hybridized atoms to form a series of hexagonal structures, all located in parallel planes. The fourth valency, that is, the free delocalized electron, is oriented perpendicular to this plane as shown in Fig. 1(b). Unlike the sigma (σ) orbital, it is non-symmetrical and is called by convention a pi (π) orbital [18].

An adsorbed gas, such as CO_2, may be quickly and efficiently desorbed by the passage of a direct current (DC), thereby allowing for a low-energy, electric swing separation system with operational simplicity [19]. The van der Waals forces between the carbon skeleton and the adsorbent are disrupted or perhaps reversed by the electric current. This interaction most likely results from the quadrupole moment and the free electrons of CO_2. As a result, adsorbed CO_2 is released or repulsed from the micropore surface and desorption occurs. The same effect may apply to other adsorbed gases.

Electrothermal desorption is a process where the heat is generated inside the adsorbent. Hence, the heat and mass flux directions are the same, i.e. from solid to the fluid, as opposed to traditional thermal regeneration. Petkovska and Mitrovic [20] reported that electrothermal desorption is more energy efficient than conventional desorption because the fluid temperature can be substantially lower than the adsorbent temperature determining the adsorption equilibrium. They also showed that same direction of heat and mass fluxes results in better desorption kinetics. The ohmic heating enhancing desorption, probably discourage adsorption at the pore entrances. For this reason, optimization of current cycle time, to stabilize or increase the permeability of relevant gas is believed to be important.

The electrical resistance R (Ω) can be evaluated from media resistivity and its dimensions [21] as shown in Eq. (1).

$$R = \frac{\rho L}{e\ell} \tag{1}$$

where ρ is electrical resistivity of the material (Ωm), L is the length of material (m), e is the width (m) and ℓ is the thickness (m). Resistivity is

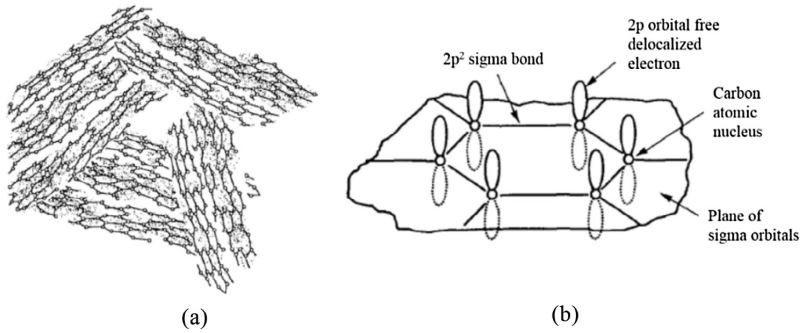

Fig. 1. (a) Structure of turbostratic graphite and (b) Schematic of sp^2 hyberdized structure of graphite sheet showing 2p free electrons [18].

defined as resistance times cross sectional area for the current flow, divided by the resistor length [22].

Electro-swing adsorption has also been reported, this is a process that takes place on beds of activated carbon material [23] and on activated carbon honeycomb monoliths [24]. In the latter process [24], an electrical current was applied to the activated carbon resulting in a localized heating of the material, which is referred to as the Joule effect. This heating, in turn, caused desorption of CO_2, much the same mechanism as thermal swing adsorption. Electro-swing adsorption had been applied commercially for removal of volatile organic compounds but not yet for gas separation processes [25].

The rationale behind the study of preventive electrical regeneration (PER) was to add ohmic heating (Ohm's law) to desorb the molecules and prevent new adsorption. Electric potential is a very strong driving force compared to pressure. It was presumed that while introducing electric current, the cross coupling of driving force and mass flow would enhance the membrane flux by reducing the adsorption of gas molecules on the pore edges.

3. Experimental

3.1. Preparation of carbon membranes

Carbon hollow fiber membranes were produced at a semi-commercial scale production plant by carbonization of regenerated cellulose precursor. Through an organized study of both precursor and carbonization parameters, protocols were developed for dope solution formation and carbonization process which are described elsewhere [13,26]. Cellulose acetate (CA), which is a biodegradable semi synthetic polymer (M_w: 100,000, ACROS, Belgium) was dissolved in 1-Methyl-2-pyrrolidone (NMP: Mw 99.13, Merck, Germany), and then mixed with polyvinylpyrrolidone (PVP: M_w 10,000, Sigma-Aldrich®, Norway) to make a dope solution. CA hollow fibers were synthesized using dry-wet spinning process using NMP and water mixture as bore solvent. The prepared CA hollow fibers were then treated with a mixture of NaOH and short chain alcohol to deacetylate the fibers. A tubular horizontal furnace (Carbolite®, 3 zones split furnace) was used to carbonize the deacetylated hollow fibers. These deacetylated CA hollow fibers were carbonized at 550 °C under N_2 flow using heating rate of 1 °C/min with several dwells and the final temperature of 550 °C for 2hrs. Carbonization protocol is shown in Fig. 2 and procedure details can be found in the patent [27]. The pilot-scale module construction procedure for CM is reported elsewhere [28]. CMS is not a single material but a family of materials where the achieved separation properties may be determined by choice of precursors and processing conditions. Detailed characterization of the CMS membranes studied here are more closely reported in references [13,22,29] using FTIR and SEM.

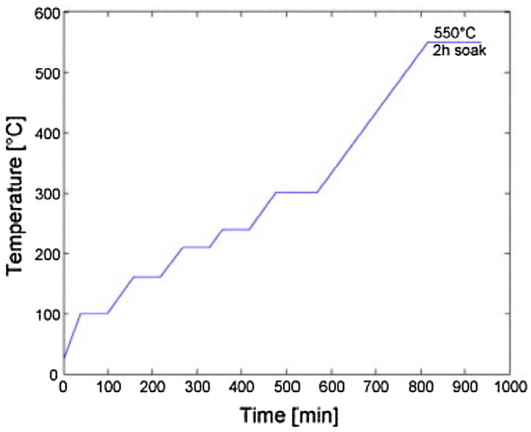

Fig. 2. Carbonization protocol based on [27,31].

3.2. Gas permeation tests

Carbon hollow fibers (effective area of 0.004 m^2) were mounted in an in-house made module, using stainless steel tubing and Swagelok® fittings. Gas permeation properties were tested using shell side feed configuration with single pure gases N_2 and O_2 at 5 bar feed pressure and vacuum on the permeate side. A set of temperature values, 20, 25, 35, 45 and 68 °C was applied to measure the temperature effect on O_2 and N_2 permeances. A standard pressure-rise setup with LabView® data logging was used for all tests. The experiments were run for several hours to ensure that steady state was obtained. For each set of the permeation tests with one temperature set point, the O_2 was run for ca. 2 h followed by N_2 which was ca. 3 h. Then system was evacuated overnight before next set of experiments were started. The gas permeance P was calculated using Eq. (2).

$$P = \frac{9.828V \cdot (dp/dt)}{\Delta P \cdot A \cdot T} \quad (2)$$

Here, V is the permeate side volume (cm^3) that can be measured with a pre-calibrated permeation cell as reported by Lin et al. [22,30], dp/dt is the collection volume pressure increase rate (mbar/s) and A is the total active area of membrane (cm^2), ΔP (bar) the pressure head and T (K) is the temperature for experiment. The ideal selectivity is defined as the ratio of the pure gas permeances as shown in Eq. (3).

$$\alpha_{A/B} = \frac{P_A}{P_B} \quad (3)$$

3.3. Aging and regeneration of carbon membranes

To study the enhanced aging effect on CM, the membrane was exposed to a biogas containing three different concentrations of H_2S as shown in Table 1.

3.3.1. Thermal and chemical regeneration

Adsorption is an exothermic phenomenon; and as a consequence the desorption is an endothermic phenomenon and energy must be supplied to desorb the adsorbents [22]. A membrane module with stainless steel housing was prepared using two carbon hollow fibers (0.0004 m^2 effective area) in the module. Single gas experiments for pure O_2 and N_2 were performed at 30 °C (2 bar feed pressure and vacuum on permeate side) to measure the reference permeability values. After determining the initial permeability values of these two gases, both sides (shell and bore) of the membranes were exposed to WCG for 24 h. The permeability of pure gases was measured again to examine the possible aging effects in the membrane.

The membranes were regenerated chemically using propylene. The CM were flushed with propylene gas for 24 h and the single gas permeation tests were performed systematically after the exposure to detect any change in membrane performance. After single gas tests, thermal regeneration was applied by heating the membrane module. The module was heated up to 80 °C and kept at this temperature for

Table 1
Different gas mixtures used to enhance the aging effect on CM.

Gas mixture name	Gas composition
Synthetic biogas (SBG)	40 ppm H_2S in a CO_2-CH_4 mixture
Worst case gas (WCG)	1% H_2S and 0.1% *n*-Hexane in biogas mixture
Real biogas field exposure (RBG)	250 ppm H2S in biogas (source: microbial digestion of slurry from waste water)
Air exposure during the storage period	Ambient air with average relative humidity 40%

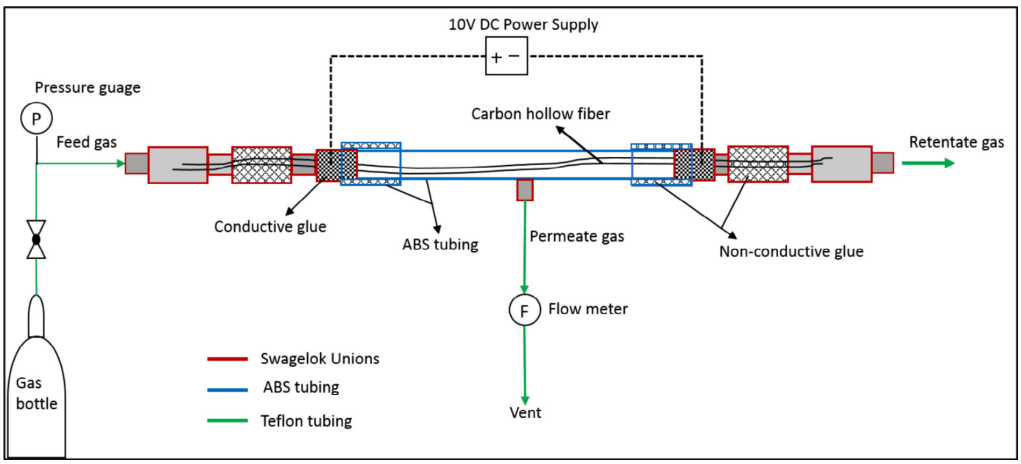

Fig. 3. Experimental setup for electrical regeneration of carbon hollow fiber membrane module.

24 h to desorb the adsorbed gas molecules in the pore structure of the membrane. Then final gas permeation tests were performed at 30 °C to see the effect of thermal regeneration.

3.3.2. Electrical regeneration

Two new membrane modules with Acrylonitrile Butadiene Styrene (ABS) housing were prepared containing two carbon hollow fibers (4 cm^2 effective area, OD: 198 μm, wall thickness, ℓ: 31 μm) in each module. A conductive glue (Eccobond 56C) was applied between carbon hollow fibers and Swagelok® fittings on each end of the module. The electric power source was connected (Alligator clips) to the external of the Swagelok ® fitting containing conductive glue on both sides of one module as shown in Fig. 3. The second module (reference module) was not connected to electric current. The conductive glue was not gas tight enough at high pressure, hence another set of Swagelok® unions were connected to a non-conductive glue on the outer section of the module. Teflon tubings were used for feed, retentate and permeate flows. Single pure gases were tested to determine the initial permeability of the membranes.

Both modules with CM were exposed on both sides (shell and bore side) to WCG for four days. Then "preventive electrical regeneration" (PER) was performed on one module and the second module was used as reference (RM) module (no electrical treatment). PER was conducted using a direct current (DC) power source and an applied voltage of 10 V which corresponds to about 45–55 μA measured amperage on carbon fibers. The current was continuously applied during the whole exposure.

Table 2 shows the steps followed during electrical regeneration of the CM. As shown, single gas tests (O_2, N_2) were performed for both the PER module (which is going to be regenerated electrically and current is on during the test) and reference module (RM). Then both modules were exposed to WCG for four days, with PER under 10 V and RM without any current. After four days voltage supply was turned off on PER module, and both modules were tested for single gases. After the single gas tests, both modules were again exposed to WCG for 14 days keeping voltage supply "on" for PER module, and then tested again for single gases afterward.

Table 2
Electrical regeneration of CM and exposure to different gases (reported in consecutive days from left to right). Single gas tests are O_2 and N_2.

Single gas tests	WCG	Single gas	WCG	Single gas	RBG	SBG
PER module	4 days, 10 V	no voltage	14 days, 10 V	no voltage	14 days, no voltage	no voltage
RM module	4 days, no voltage	no voltage	14 days, no voltage	no voltage	14 days, no voltage	no voltage

The CM modules were then installed at a real biogas plant for 14 days and exposed to the real biogas containing 250 ppm H_2S. The modules were disconnected from the biogas plant and reconnected to the synthetic biogas in the laboratory for several days. The membrane modules were then tested for single gases again to check if a stable performance had been achieved after the preventive electrical regeneration.

The electrical resistance of the carbon fibers was measured by a handheld Ohm meter to calculate the specific conductivity of the membranes. Carbon fibers obtained at different soak temperatures (550 °C. 650 °C, 750 °C) were used to measure the electric conductivity.

4. Results and discussion

4.1. Experimental findings

The impact of temperature on O_2 and N_2 permeability at constant pressure and feed flow rate is plotted in Fig. 4. The results reported are from pure gas permeation experiments. He et al. has performed the mixed gas experiments on the same type of CM (same protocol) and results indicated that the membrane performance is same or even higher in some cases for mixed gas as compared to single gas separation [32]. Singh et al. [33] also confirmed that pure gas permeation properties were within 3% of mixed gas permeation properties for the pyrolyzed hollow fibers. The trend in Fig. 4 shows that O_2 permeability is increasing exponentially with increase in temperature which is also comparable with an Arrhenius law type effect. The high permeability is a result of high diffusivity and high solubility as well, and the increase in O_2 permeability here indicates a more open molecular matrix aiding O_2 flux. Whereas, change in N_2 permeability is quite modest with an increase in temperature. Fig. 5 represents the selectivity of O_2/N_2 at varying temperatures. The carbon matrix is comprised of relatively large pores interconnected by constrictions of negligible thickness that approach the dimensions of diffusing molecules. In this case, penetrant molecules require characteristic activation energies to overcome the resistance at the constrictions. Hence, a small increase in activation energy in form of high temperature increased the activated diffusion of

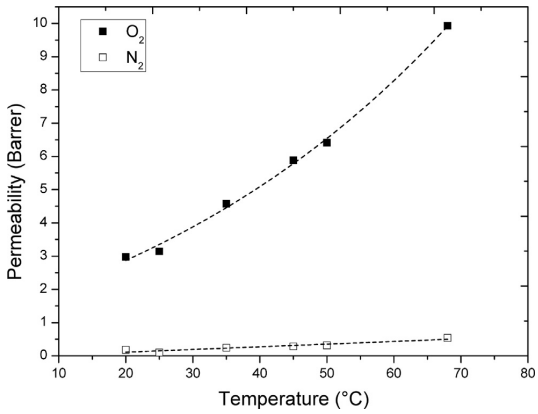

Fig. 4. Effect of temperature on O_2 and N_2 permeability (P:5 bar).

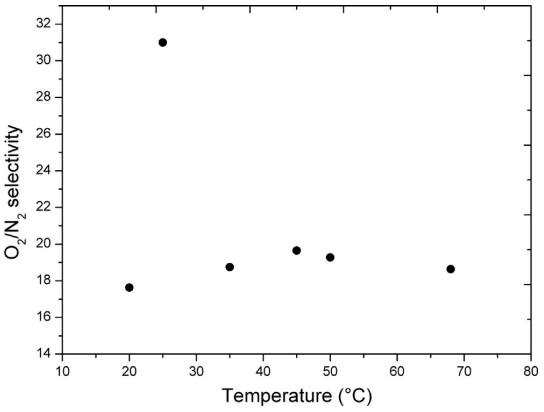

Fig. 5. Effect of temperature on O_2/N_2 selectivity (P:5 bar).

O_2 and N_2. Permeation experiments were performed at 20, 35, 45, 50 and 68 °C in order of increasing temperature. Finally, the experiment at 25 °C was performed (shown in Fig. 5) to see if the microporous structure of the membrane had changed after a ten hours direct exposure of the O_2 and finally altering the permeation properties. It was observed that O_2/N_2 selectivity increased to 31 as compared to values at 20 and 30 °C, which are 17 and 18 respectively. However, the membrane permeability for O_2 increased slightly as compared to the value at 20 °C and to some extent decreased for N_2. The small numerical value for the N_2 permeability causes this to be more vulnerable to fluctuation in the leak-rate of the setup (measured at the beginning of the test series). Hence the measured value of an O_2/N_2 selectivity of 31 at 25 °C is most likely an experimental out-layer. Fresh carbon membranes, prepared with similar protocol, were tested at 25 °C and an O_2 permeability of 32 Barrer was measured and O_2/N_2 selectivity was 10.

Hayashi et al. [34] exposed the CM (carbonized at 700 °C) to air at 100 °C for 1 month and observed that membrane permeance increased with increasing permeation temperature. They concluded that O_2 in the air reacts with the membrane and forms oxygen-containing functional groups, which are continuously decomposed to CO_2. The formation and removal of surface oxides gradually restructure the carbon layer and somewhat narrow the micropores permanently. This effect was observed in the present study as well by inclined in selectivity of O_2/N_2 without losing O_2 permeability when the membrane was tested at 25 °C as shown in Figs. 4 And 5. As explained earlier, the permeance test at 25 °C was performed after the membrane had gone through many

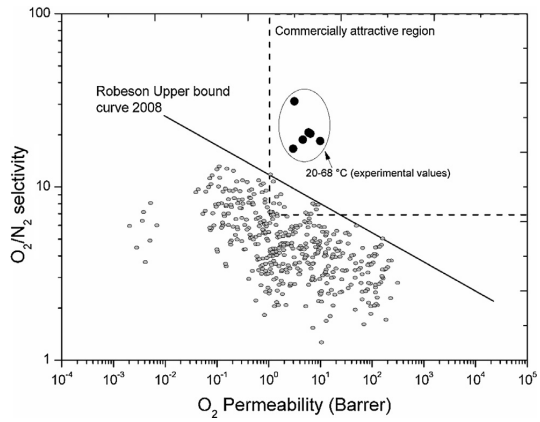

Fig. 6. O_2 permeability and O_2/N_2 selectivity of CM with respect to Robeson upper bound curve (2008) [2].

exposures of O_2, N_2, and vacuum (6 days) at different temperature and pressure conditions which helped the membrane micropores to restructure. The effect of temperature was not significant on the permeability of N_2 as it was observed for O_2. Fig. 6 presents the Robeson upper bound (2008) and as can be seen, the membrane performance for all experiments reported here, are in the commercially attractive region [2].

4.2. Regeneration

The permeation results referring to recently prepared membranes could be very misleading if the change in results is very fast over time (aging). A better evaluation could be achieved by adding a dimension of time to the membrane performance plot. To attain a commercially attractive membrane life, a stable performance is essential, and it can be achieved by membrane regeneration process. A few techniques were used here to restore the membrane performance.

4.2.1. Thermal and chemical regeneration

Results for the change in permeability of O_2 and N_2 after WCG, propylene exposure and thermal regeneration of CM are presented in Fig. 7. After 24 h exposure of WCG, the permeabilities of O_2 and N_2 declined by 30% and 40%, respectively. Chemisorption sorption occurs only on active sites; therefore, it might be that the O_2 had already

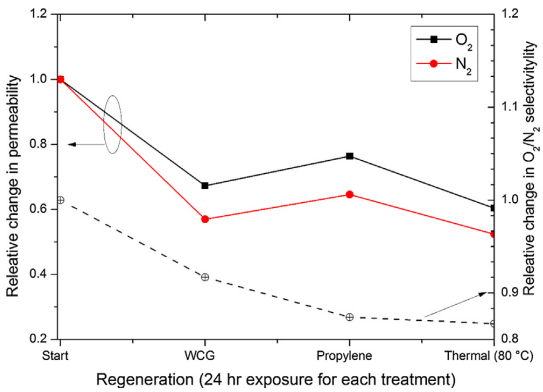

Fig. 7. Relative change in permeability and selectivity of O_2/N_2 after chemical and thermal treatment.

penetrated the micro and ultra pores of the carbon structure and occupied a large fraction of the active sites and formed covalently bounded O-bridges with the carbon. However, further blockage of pores occurred by physiosorption when H_2S, CO_2 and hexane molecules were present in WCG and adsorbed on the carbon surface. The strong aging may be explained by both a strong physiosorption of bigger molecules on the carbon surface and chemisorption in the matrix.

Flushing the module with propylene for 24 h could partially (ca. 10%) restore the lost permeability for both O_2 and N_2, but selectivity decreased further. Propylene acted as a cleaning agent by removing adsorbed compounds from carbon surface and the exposure broadened the membrane pores, thus reducing the resistance to the transport of O_2 and N_2. Physiosorption is usually a reversible process and heat of adsorption is low, therefore, the increase in permeability might be only due to the desorption of physically adsorbed molecules. The propylene may interact with carbon matrix in two ways: Firstly, it may act as a solvent, dissolving some or all the permeants that are sorbed in a carbon matrix. Compounds that possess π-bonds may also interact in another way: The high electron density in the π-bonds may cause repulsion between the π-cloud of the olefin and the π-cloud of the graphene layers making up the micropore. The result may be pore expansion and increased permeability [35,36]. This may also explain the slight increase in permeability of O_2 and N_2 over the exposure of propylene.

Thermal treatment of the membrane at 80 °C for 24 h could not regain the lost flux. Instead, the permeability values for both O_2 and N_2 decreased. It might be that all the reactive sites cleaned by propylene were occupied again by the adsorption O_2 which blocked the pores and ultimately decreased the permeability of both gases. The thermal limitations of the used epoxy in module construction prevented the use of elevated temperature in this study. Jones et al. [12] also reported that 90 °C thermal regeneration was ineffective to restore the membrane permeation properties. The oxygen chemisorbed on carbon can only be removed as CO or CO_2 at 600–800 °C. However, at this elevated temperature, the carbon structure may be changed in two ways: sintering (pore narrowing/closure) and gasification (pore widening). A stable epoxy at elevated temperatures for module construction could have helped to develop some thermal regeneration methods for the restoration of the membrane permeation properties.

4.2.2. Electrical regeneration

The final carbonization temperature had a significant effect on the specific conductivity of the material. The conductivity of resulting carbon increased with increase in soak temperature as shown in Table 3. The results in Table 3 shows that 550 °C is too low temperature to yield electrical conductive carbon fibers. The resistivity of the carbon hollow fibers, used in PER, was 0.022 Ωm (from Eq. (1)) which was somewhat higher than reported for activated carbons that is in the range 0.001–0.006 Ωm [37]. The resistivity can be used as measure of porosity. Increasing the porosity causes the drop-in electron flow. For characterizing carbon that have been treated in different ways, resistivity is therefore a possible rapid indicator. The high resistivity of CM may be defined by the high degree of porosity.

Electrical regeneration with 10 V DC yielded a positive effect for the permeability of O_2 when applied while membrane was in operation and being exposed to WCG, as shown in Fig. 8.

The permeability of O_2 increased by 15% but the effect did not last long. Later, the membrane was stored in air for five days and the membrane lost some of the permeability. After repetition of the electrical regeneration along with WCG exposure did not gain the lost permeability but rather it declined and lost 20% of the initial value after exposed to WCG for 12 days. Almost similar effect was observed for N_2 with 5% increased permeability in the first attempt of electric regeneration, as shown in Fig. 9. It might be that the applied voltage in 2nd electrical regeneration treatment was not enough to disrupt the van der Waals forces between carbon structure and adsorbed gases like O_2 and CO_2.

Table 3
Final soak temperature and specific conductivity of resulting carbon fibers.

Soak Temperature (°C)	Specific conductivity ($1/\Omega \cdot m^3$)
550	83
650	5520
750	112,000

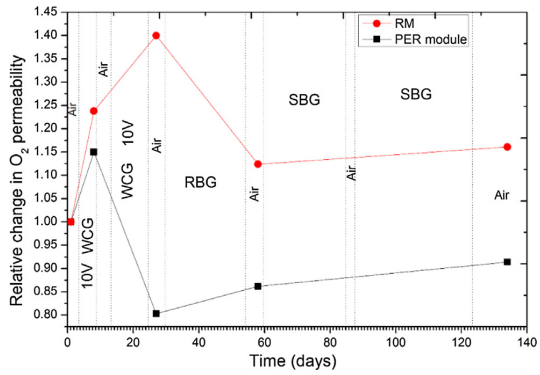

Fig. 8. Aging of CM under different environments and effect of electrical regeneration on O_2 permeability.

Although, the lost performance was partially regained after 10 days' exposure to RBG and remained steady for next 3 months. But the observed phenomenon is still unclear with respect to how the electric current desorbs the absorbed gases.

The effect of applied current was instantaneous, indicating that electrostatic repulsion was also active. Desorption or an instantaneous change would not result only by Ohmic heating. Therefore, some other factors could also be contributing in the results. One explanation for this opposite behaviour of current could be that electro potential driving force and cross coupled mass transfer were influencing the flux through the membranes. Deconvolution of electric field effects and heating effects on permeation is a challenging task. Mixed gas tests with applied current will probably provide more insight to this problem. The permeability of N_2 dropped in a continuous way after the first electrical regeneration till the end of the run (130 days) by losing 60% of the initial value.

The effect of PER was not significant compared to the RM and it might be the WCG being too potent to be counter effected by the

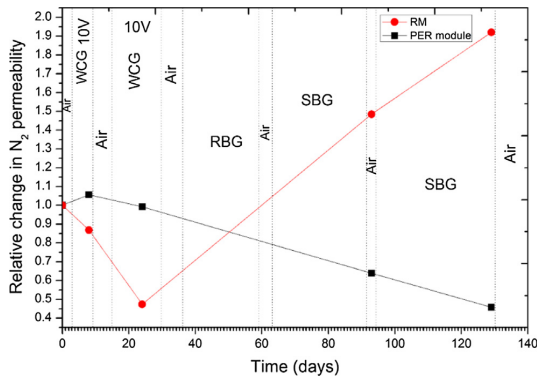

Fig. 9. Aging of CM under different environments and effect of electrical regeneration on N_2 permeability.

electric potential as conductivity of the fibers was already too low. Nevertheless, the electrical regeneration performed in this study kept the permeance of O_2 quite stable and only 20% drop in O_2 permeability was recorded during 138 days of different exposures and storage. The O_2/N_2 selectivity was 28% higher than the fresh membrane. The decreased flux of N_2 in PER may be explained by the effect of electric field. With an electric field, cross coupling is generated, which reduces the effective pore size (effect is larger for N_2) but stimulates desorption from pore walls (favorable for O_2 transport).

In the reference module, as shown in Fig. 9, N2 permeance was almost doubled after 4 months resulting 45% drop in O_2/N_2 selectivity. The results from the module exposed to PER showed that the overall performance was enhanced due to the online electrical regeneration, however, the performance of RM reduced gradually over time.

5. Conclusions

Regenerated cellulose-based carbon hollow fiber membranes produced at the pilot-scale plant demonstrated competitive air separation properties. Experimental results showed that elevated temperature operations increase O_2 permeability without significant loss in O_2/N_2 selectivity. The prepared CM had reasonable performance over a time span of about 5 months under harsh environments (air, H_2S, *n*-Hexane, CO_2, CH_4). Online preventive electrical regeneration (PER) enhanced the O_2 permeability by eliminating the aging effect on the membrane and the O_2/N_2 selectivity was also increased.

When choosing a regeneration method, both energy demand and ease of operation are key factors. Offline regenerations (thermal and chemical) has the severe drawback of potential plant shut down. If this interruption must be avoided, then one needs to have two sets of membranes. One set can be regenerated while other is in use. Both interruption of a process and or having a double set of membranes mean extra cost.

Thermal treatment up to 80 °C was not very effective and use of very high temperature would result in possible burnout of the carbon matrix. Chemical regeneration requires the use of an additional chemical (if the regenerating gas/vapor is not present in the feed stream), with the subsequent evacuation of that gas/vapor after use, and offline operations.

“Preventive” electric regeneration is the most promising method if its regeneration efficiency is reasonable because it operates constantly online but requires a small amount of energy (0.86 μW/fiber·m) and simple equipment. It also has the possibility of high heating rates. Deconvolution of electric or magnetic field effects and heating effects on permeation is a challenging task. Mixed gas tests with applied current will probably provide more insight to this problem.

However, it is important to note that aging behaviour of CM may depend on the precursor and the manufacturing conditions used. Carbon membranes with e.g. different structure and surface chemistry will behave differently as also shown by other researchers.

Acknowledgement

The authors would like to thank The Department of Chemical Engineering at NTNU for providing the possibility to work with this article.

References

[1] R.W. Baker, Future directions of membrane gas separation technology, Ind. Eng. Chem. Res. 41 (6) (2002) 1393–1411, http://dx.doi.org/10.1021/ie0108088.
[2] L.M. Robeson, The upper bound revisited, J. Membr. Sci. 320 (2008) 390–400, http://dx.doi.org/10.1016/j.memsci.2008.04.030.
[3] B.D. Bhide, S.A. Stern, A new evaluation of membrane processes for the oxygen-enrichment of air. I. Identification of optimum operating conditions and process configuration, J. Membr. Sci. 62 (1991) 13–35, http://dx.doi.org/10.1016/0376-7388(91)85003-N.
[4] C.W. Jones, W.J. Koros, Carbon molecular sieve gas separation membranes-I. Preparation and characterization based on polyimide precursors, Carbon 32 (8) (1994) 1419–1425, http://dx.doi.org/10.1016/0008-6223(94)90135-X.
[5] W. Shusen, Z. Meiyun, W. Zhizhong, Asymmetric molecular sieve carbon membranes, J. Membr. Sci. 109 (2) (1996) 267–270, http://dx.doi.org/10.1016/0376-7388(95)00205-7.
[6] J.E. Koresh, A. Sofer, Molecular sieve carbon permselective membrane. Part I. Presentation of a new device for gas mixture separation, Sep. Sci. Technol. 18 (8) (1983) 723–734, http://dx.doi.org/10.1080/01496398308068576.
[7] H. Hatori, Y. Yamada, M. Shiraishi, H. Nakata, S. Yoshitomi, Carbon molecular sieve films from polyimide, Carbon 30 (4) (1992) 719–720, http://dx.doi.org/10.1016/0008-6223(92)90192-Y.
[8] S. Lagorsse, F.D. Magalhães, A. Mendes, Aging study of carbon molecular sieve membranes, J. Membr. Sci. 310 (2008) 494–502, http://dx.doi.org/10.1016/j.memsci.2007.11.025.
[9] L. Xu, M. Rungta, J. Hessler, W. Qiu, M. Brayden, M. Martinez, G. Barbay, W.J. Koros, Physical aging in carbon molecular sieve membranes, Carbon 80 (2014) 155–166, http://dx.doi.org/10.1016/j.carbon.2014.08.051.
[10] G.B. Wenz, W.J. Koros, Tuning carbon molecular sieves for natural gas separations: a diamine molecular approach, AIChE J. 63 (2) (2017) 751–760, http://dx.doi.org/10.1002/aic.15405.
[11] I. Menendez, A.B. Fuertes, Aging of carbon membranes under different environments, Carbon 39 (5) (2001) 733–740, http://dx.doi.org/10.1016/S0008-6223(00)00188-3.
[12] C.W. Jones, W.J. Koros, Carbon molecular sieve gas separation membranes-II. Regeneration following organic exposure, Carbon 32 (8) (1994) 1427–1432, http://dx.doi.org/10.1016/0008-6223(94)90136-8.
[13] J.A. Lie, M.-B. Hägg, Carbon membranes from cellulose: synthesis, performance and regeneration, J. Membr. Sci. 284 (2006) 79–86, http://dx.doi.org/10.1016/j.memsci.2006.07.002.
[14] V.C. Geiszler, W.J. Koros, Effects of polyimide pyrolysis conditions on carbon molecular sieve membrane properties, Ind. Eng. Chem. Res. 35 (9) (1996) 2999–3003, http://dx.doi.org/10.1021/ie950746j.
[15] S.M. Saufi, A.F. Ismail, Fabrication of carbon membranes for gas separation—a review, Carbon 42 (2) (2004) 241–259, http://dx.doi.org/10.1016/j.carbon.2003.10.022.
[16] J.W. Biscoe, B.E. Warren, An X-ray study of carbon black, J. Appl. Phys. 13 (6) (1942) 364–371, http://dx.doi.org/10.1063/1.1714879.
[17] J.E. Koresh, A. Soffer, Mechanism of permeation through molecular-sieve carbon membrane Part 1 – The effect of adsorption and the dependence on pressure, J. Chem. Soc. Faraday Trans. 1: Phys. Chem. Condens. Phases 82 (7) (1986) 2057–2063, http://dx.doi.org/10.1039/F19868202057.
[18] H.O. Pierson, Handbook of Carbon, Graphite, Diamond and Fullerenes-Properties, Processing and Applications, NOYES, New Jersey, 1993.
[19] T.D. Burchell, R.R. Judkins, M.R. Rogers, A.M. Williams, A novel process and material for the separation of carbon dioxide and hydrogen sulfide gas mixtures, Carbon 35 (9) (1997) 1279–1294, http://dx.doi.org/10.1016/S0008-6223(97)00077-8.
[20] M. Petkovska, M. Mitrović, Microscopic modelling of electrothermal desorption, Chem. Eng. J. Biochem. Eng. 53 (3) (1994) 157–165, http://dx.doi.org/10.1016/0923-0467(92)02768-E.
[21] A. Subrenat, P.L. Cloirec, Adsorption onto activated carbon cloths and electrothermal regeneration: its potential industrial applications, J. Environ. Eng. 130 (3) (2004) 249–257, http://dx.doi.org/10.1061/(ASCE)0733-9372(2004) 130:3(249).
[22] J.A. Lie, Synthesis, performance and regeneration of carbon membranes for biogas upgrading – a future energy carrier, PhD. thesis (ISBN 82-471-7191-0), NTNU, Trondheim, 2005.
[23] S.H. Moon, J.W. Shim, A novel process for CO_2/CH_4 gas separation on activated carbon fibers – electric swing adsorption, J. Colloid Interface Sci. 298 (2) (2006) 523–528, http://dx.doi.org/10.1016/j.jcis.2005.12.052.
[24] R. Ribeiro, C.A. Grande, A.E. Rodrigues, Electrothermal performance of an activated carbon honeycomb monolith, Chem. Eng. Res. Des. 90 (11) (2012) 2013–2022, http://dx.doi.org/10.1016/j.cherd.2012.03.010.
[25] C.A. Grande, R.P.L. Ribeiro, E.L.G. Oliveira, A.E. Rodrigues, Electric swing adsorption as emerging CO_2 capture technique, Energ. Proced. 1 (1) (2009) 1219–1225, http://dx.doi.org/10.1016/j.egypro.2009.01.160.
[26] J.A. Lie, M.-B. Hägg, Carbon membranes from cellulose and metal loaded cellulose, Carbon 43 (12) (2005) 2600–2607, http://dx.doi.org/10.1016/j.carbon.2005.05.018.
[27] T.B. Edel Sheridan, Jon Arvid Lie, May-Britt Hagg, Carbon membranes from cellulose esters, U.S. Patent: 8394175, 2013.
[28] S. Haider, A. Lindbråthen, J.A. Lie, I.C.T. Andersen, M.-B. Hägg, CO2 separation with carbon membranes in high pressure and elevated temperature applications, Sep. Purif. Technol. 190 (2018) 177–189, http://dx.doi.org/10.1016/j.seppur.2017.08.038.
[29] X. He, M.-B. Hägg, Structural, kinetic and performance characterization of hollow fiber carbon membranes, J. Membr. Sci. 390–391 (Supplement C) (2012) 23–31, http://dx.doi.org/10.1016/j.memsci.2011.10.052.
[30] W.-H. Lin, R.H. Vora, T.-S. Chung, Gas transport properties of 6FDA-durene/1,4-phenylenediamine (pPDA) copolyimides, J. Polym. Sci. B Polym. Phys. 38 (2000) 2703–2713, http://dx.doi.org/10.1002/1099-0488(20001101)38:21<2703.
[31] M.-B.H. Jon Arvid Lie, Carbon membranes, U.S. Patent: 20100162887 A1, 2010.
[32] X. He, J.A. Lie, E. Sheridan, M.-B. Hägg, Preparation and characterization of hollow fiber carbon membranes from cellulose acetate precursors, Ind. Eng. Chem. Res. 50 (4) (2011) 2080–2087, http://dx.doi.org/10.1021/ie101978q.
[33] A. Singh-Ghosal, W.J. Koros, Air separation properties of flat sheet homogeneous

pyrolytic carbon membranes, J. Membr. Sci. 174 (2) (2000) 177–188, http://dx.doi.org/10.1016/S0376-7388(00)00392-6.
[34] J.-I. Hayashi, M. Yamamoto, K. Kusakabe, S. Morooka, Effect of oxidation on gas permeation of carbon molecular sieving membranes based on BPDA-pp 'ODA Polyimide, Ind. Eng. Chem. Res. 36 (6) (1997) 2134–2140, http://dx.doi.org/10.1021/ie960767t.
[35] Y. Finkelstein, A. Saig, A. Danon, J.E. Koresh, Encapsulation of He and Ne in carbon molecular sieves, Langmuir 19 (2) (2003) 218–219, http://dx.doi.org/10.1021/la026671n.
[36] J.E. Koresh, On the flexibility of the carbon skeleton, J. Chem. Soc. Faraday Trans. 89 (6) (1993) 935–937, http://dx.doi.org/10.1039/FT9938900935.
[37] A. Subrenat, J.N. Baléo, P. Le Cloirec, P.E. Blanc, Electrical behaviour of activated carbon cloth heated by the joule effect: desorption application, Carbon 39 (5) (2001) 707–716, http://dx.doi.org/10.1016/S0008-6223(00)00177-9.

Appendix L

Paper VIII

Carbon membranes for oxygen enriched air –Part II: Techno-economic analysis

Paper published in Separation and Purification Technology 205 (2018) 251-262.

Separation and Purification Technology 205 (2018) 251–262

Contents lists available at ScienceDirect

Separation and Purification Technology

journal homepage: www.elsevier.com/locate/seppur

Carbon membranes for oxygen enriched air – Part II: Techno-economic analysis

Shamim Haider, Arne Lindbråthen, Jon Arvid Lie, May-Britt Hägg*

Norwegian University of Science and Technology, NTNU, Department of Chemical Engineering, 7491 Trondheim, Norway

ARTICLE INFO

Keywords:
Oxygen enriched air
Carbon membrane
Simulations
Techno-economic analysis

ABSTRACT

Carbon membrane (CM) separation process for producing oxygen-enriched air (OEA) at a concentration of 50–78 mol% O_2 in a single stage process with no recycle stream has been investigated. This paper (Part II of a two-part study) considers techno-economic analysis for O_2-selective carbon membranes to yield the lowest production cost of "equivalent" pure oxygen (EPO_2) in a single stage separation process based on experimental and predictive membrane performance. Aspen Hysys® interfaced with ChemBrane (in-house developed model) was used to perform the simulations for air separation with CM. Three different approaches with respect to pressure were investigated; (1) feed compression, (2) vacuum on permeate side and (3) combination of (1) and (2). The simulation results and sensitivity analysis showed that with current performance (O_2 permeability: 10 Barrer ($1\ Barrer = 2.736E-09\ m^3(STP)m/(m^2\ bar\ h)$) and O_2/N_2 selectivity: 18), mechanical properties, and cost per m^2 of CM, it is economically most efficient to use the third approach "combination of feed compression and permeate vacuum" to produce EPO_2. A stage cut of 10% was found to be as an average economical optimum when using vacuum pump (approach (2)) to produce OEA. However, the techno-economic analysis for the reported CM showed that a stage cut of 0.15–0.2 was the most cost-effective while using compression approach (1) or (3) to produce EPO_2.

1. Introduction

Cryogenic distillation is the most common technology to produce high purity oxygen (> 99%) at large scale productions (100–300 tons/day). Pressure swing adsorption (PSA) can reach up to 95% oxygen purity and the requirement of sorbents limits the size capacity for small to medium scale plant (20–100 tons/day), mainly due to high capital cost. However, both cryogenic and PSA are considered as energy intensive technologies [1,2]. Therefore, energy efficient methods with low capital investment are required to separate the air into oxygen (as enriched air or pure oxygen) and nitrogen.

Membrane separation is an attractive process alternative due to its simple design, lower energy demand, smaller footprint, good weight efficiency (light weight equipment compared to other technologies), and flexible, modular design. However, compared to conventional technologies commercially available polymeric membranes can not economically produce high purity of O_2. The performance of polymeric membranes is restricted by the trade-off between permeability and selectivity [3]. Polymeric materials may have high permeability for O_2, but rather low O_2/N_2 selectivity (usual range 2–8), and the maximum permeate purity achievable for O_2 with polymeric membranes seems to be 30–60% [4]. Nitrogen of purity up to 99.5% can be produced using polyimide membranes (O_2/N_2 selectivity of 9) [3,5]. Nevertheless, a multi stage separation process with recycle stream is required to achieve high recovery of N_2 which would add more cost and complexity to the system.

High purity oxygen is difficult using membranes because of the high content of nitrogen in the air, (79%) and the relative low selectivity of O_2/N_2 resulting in oxygen enriched air (OEA) in permeate, rather than pure oxygen. Based on the performance of commercially available polymeric membranes, the separation process is competitive only for medium O_2 purity (25–40%) and small-scale plants (10–25 tons/day) [4,6]. OEA is already used for numerous chemical processes (Claus process, the Fluid Catalytic Cracking technology, the oxidation of *p*-xylene to give terephthalic acid) combustion processes (natural gas furnaces, coal gasification), medical purposes, and has more recently also attracted attention for hybrid carbon capture process [7].

Carbon is a class of material that can offer improved performance due to molecular sieving effect. In molecular sieving, the available pore size is below the kinetic diameter of one of the gas components in the feed. This characteristic of the material increases selectivity by reducing the rotational degrees of freedom of nitrogen versus oxygen in the

* Corresponding author.
E-mail address: may-britt.hagg@ntnu.no (M.-B. Hägg).

https://doi.org/10.1016/j.seppur.2018.05.037
Received 23 April 2018; Received in revised form 13 May 2018; Accepted 13 May 2018

Nomenclature

List of symbols and abbreviations

$Q_{f,i}$	molar flow of i in the feed (mol/s)
P_i	permeance for i ($m^3(STP)m/m^2$ bar h)
P_f	feed pressure (bar)
P_p	permeate pressure (bar)
x_{if}	molar fraction of i in the feed side
y_{ip}	molar fraction of i in the permeate side
P	permeance ($m^3(STP)m/m^2$ bar h)
A	membrane area (m^2)
EPO_2	equivalent pure oxygen
OEA	oxygen enriched air
n	molar flow rate (moles/day)
T	mass flow rate (tons/day)
CM	carbon membranes
CMC	carbon membrane cost
CC	compressor cost (installed)
VC	vacuum pump cost (installed)
PC	production cost of EPO_2
MRC	membrane replacement cost
EC	electricity cost
CRC	capital recovery cost
LC	labor cost
TLC	total labor cost
VP	vacuum on permeate side
FC	feed compression approach
FC-VP	combined feed compression and vacuum on permeate side

Greek symbols

θ	stage cut (q_p/q_f)
α	membrane selectivity (O_2/N_2)

diffusion (kinetic) transition state. In addition, carbon membranes (CM) offer superior thermal resistance and chemical stability in corrosive environments [8]. Many prior studies have reported higher selectivity and permeability of CM compared to polymeric membranes for air separation [9–13].

In 1991, Bhide and Stern calculated the membrane performance required to produce OEA at a cost competitive to cryogenically produced oxygen at $ 40–60/ton of equivalent pure oxygen (EPO_2) [4]. They showed that none of the today's polymers can reach the $ 40–60/ton EPO_2 target. To reduce the capital and production cost (PC) of the membrane-based process, both selectivity and permeability must be improved. Higher O_2/N_2 selectivity is required to reach the high purity of O_2 with a lower driving force (partial pressure ratio) hence, the operating cost will be reduced. A higher permeability of O_2 will cut the required membrane area for the separation, therefore, low capital investment is needed. Much academic research is focused on producing highly selective membranes, but if the membranes then have too low permeabilities they are most likely not an optimum choice for the application in focus. The carbon membranes reported here were experimentally documented to have a high selectivity 18 for O_2/N_2 and the permeability of O_2 was increasing exponentially with increase in operating temperature without significant loss in the selectivity [14]. Hence it was found that the separation process with these carbon membranes may be optimized to achieve high purity O_2 with reasonable capital investment and production cost. Predicting the cost of carbon membrane modules is difficult because of the lack of commercial precedent. Based on pilot scale production cost of regenerated cellulose-based CM, this paper focuses on the techno-economical analysis of CM-based air separation process to investigate the viability of CM in OEA market.

In order to obtain OEA economically with polymeric membranes, feed compression is not considered a viable solution due to the high energy cost. Some studies have concluded that applying vacuum on permeate side corresponds to the lowest energy requirement whatever the membrane stage cut is ($\theta = q_p/q_f$, defined as the ratio of permeate flow rate to feed flow rate), because only the permeate stream has to be processed which is a small portion of the feed [4,7]. However, in this study we will compare the three compression approaches; feed compression, permeate vacuum, and a combination of both feed compression and permeate vacuum. The simulation results and sensitivity analysis show that with the present performance, mechanical properties, and cost per m^2 of CM, it is more economical to use a combination of feed compression and permeate vacuum for small scale OEA production.

This study is comprised of two parts. Part I of this study [14] describes laboratory testing of carbon membranes for air separation and regeneration techniques (thermal, chemical and electrical) to achieve a stable performance of the membrane. The CM was shown to exhibit single gas O_2/N_2 selectivity of 18 and O_2 permeability of 10 Barrer *(1 Barrer = 2.736E − 09 $m^3(STP)m/(m^2$ bar h))* at 68 °C. The permeability of O_2 was increasing exponentially with increase in operating temperature without significant loss in the selectivity. Part II of this study (discussed here) examines the economic viability of carbon membranes in the air separation market. Aspen Hysys® interfaced with Chembrane, an in-house built membrane model was used for the simulations. Single stage configuration with CMS membrane was optimized to attain a simple process with minimum cost to produce OEA. The separation properties of the prepared CM were predicted to achieve high O_2 permeability, between100 and 300 Barrer, by keeping the selectivity constant. It has been documented that the assumption on the higher O_2 permeability without sacrificing the O_2/N_2 selectivity, may be achieved by adding the nano particles in the precursor [15,16] or operating the membranes at elevated temperature. The separation process was optimized with respect to installed energy and membrane area to achieve low production cost and total capital investment (TCI). The sensitivity of the process towards membrane area, energy, membrane life time, and membrane cost was investigated in the current study.

Simulation results indicated that these membranes may produce 78% O_2-enriched permeate stream and at the same time obtain 15% O_2 (hypoxic) retentate stream in a single-stage process when using combination of feed compression and vacuum on permeate side. Although retentate stream usage is not considered in the economic calculations, the retentate stream may be used as hypoxic air (Air containing 15 vol% O_2 is named as hypoxic air, and over the last years use of the hypoxic air has increased in venting system to reduce the fire hazards. Further, in multifunctional buildings, electrical appliance rooms and computer rooms use of hypoxic air have been found to be essential to societal important functions [17].

2. Background on membrane model and process simulations

Chembrane, an in-housed membrane model, based on mass transfer equations for co-current, counter current, and a perfectly-mixed flow configuration, was interfaced with Aspen Hysys® V9. The thermodynamic fluid package that uses sour Peng-Robinson equation of state was used to perform all the simulations for air separation with CM. For a shell fed module, based on MemfoACT AS module design [18], the counter-current configuration explains real behavior of gas flow as the best. Therefore, counter-current configuration was also used in the current study. However, other configurations and details of the model can be found elsewhere [19].

A representation of membrane module counter-current

configuration is shown in Fig. 1.

The membrane was divided into m equal area, perfectly mixed stages. Assuming a dense, symmetric membrane, the mole flux for each component, i, on the feed side is given by:

$$dQ_{f,i} = P_i.\ (P_f.\ x_{i,f} - P_p.\ y_{i,p}).dA \quad (1)$$

where $Q_{f,i}$ is the molar flow of i in the feed, P_i is the permeance for i, P_f is the feed side pressure, P_p is the permeate pressure, $x_{i,f}$ is the molar fraction of i in the feed side increment, $y_{i,p}$ is the molar fraction of i in the permeate side increment and A is the membrane area.

The counter-current configuration is complicated to solve, because a concentration profile exists on the permeate side and the permeate exit flows at j = 0 are unknown. An initial estimate for the concentration profile is needed to solve the set of non-linear differential equations. Since the permeate and feed flows are in opposite directions, Eq. (2) may be stated:

$$dQ_{f,i,j} = dQ_{p,i,j} \quad (2)$$

Instead of requiring an initial estimate of the steady state concentration profile, this model solves a total permeate pressure of zero in the first iteration, for which the solution of the mole balance Eq. (1) is insignificant (the value of the second term in parentheses is zero). The permeate pressure is then increased by an increment. The concentration profile generated in the first iteration is used to solve the system in the second iteration. In this manner, the permeate pressure is increased until the actual (steady state) permeate pressure is reached, with small enough increments that the concentration profiles change slightly with each increment. The method is analogous to starting up a membrane module with full vacuum on the permeate side and allowing the pressure to rise by throttling the outflow of permeate. The model uses fourth-order Runge-Kutta method to calculate the flux along membrane length and then uses iterations over permeate values to converge to a solution.

3. Simulation basis and economic parameters

3.1. Experimental data

In this section, gas separation properties of CM, obtained through experiments (Part I [14]), were used to simulate the optimal conditions for production of OEA. The permeability and selectivity data for carbon membranes are experimental data obtained at different temperatures, 5 bar feed pressure and vacuum (10 mbar) on low pressure side, are listed in Table 1.

The driving force is the difference in partial pressures of the components on both sides of the membrane, and this difference is achieved in the simulations by compressing the feed and/or reducing the permeate pressure. The ratio between feed side pressure and permeate side pressure ($\Psi = P_{permeate}/P_{feed}$) is a key operating parameter that effects both separation performance and energy requirement [20].

To achieve required pressure ratio in the simulations, three different compression approaches as shown in Fig. 2(a)–(c) were used to obtain the required energy and membrane area:

- *Feed compression (FC)*; a feed compressor was used to compress the air to 10 bar.
- *Vacuum pump on permeate side (VP);* No compression of the feed air, a vacuum pump was used to create 10 mbar on permeate side of the membrane.
- *Combination of Feed compression and permeate vacuum (FC-VP)*; In this case, feed air was compressed to 10 bar, and vacuum (10 mbar) was used on permeate side of the membrane.

Table 1
Experimental data for simulations.

Temperature (°C)	O_2 Permeability (Barrer)	Selectivity O_2/N_2
20	2.98	18
35	4.58	18
45	5.88	19
50	6.41	19
68	9.93	18

(1 Barrer = 2.736E − 09 m^3(STP)m/(m^2 bar h)).

An ideal gas was considered in the simulations. CMs based on molecular sieving for mixed gases like O_2 and N_2 show separation properties which is equal to or better than single gases [21,22]. Counter-current gas transport without any sweep on low pressure side was modeled. The membrane process was broken down into 150 discrete stages and the mass balance was determined iteratively for each stage. Process simulations and economical assessment were done for a CM unit which would increase O_2 concentration (based on permeation values) in air from 21 mol % to between 50 and 78 mol % in a single stage separation process (no recycle). A single stage membrane system has many advantages; it is simple, compact and passive with no moving parts, except some auxiliary equipments (compressor and vacuum pump). The system is easy to operate when no recycle stream is present. An optimal module design may require only one membrane skid for the whole system and that would significantly reduce the module housing, valves and piping cost. A single stage membrane system is flexible to be linearly scaled up or down, however, scalability of multi stage system with recycle stream is more complex due to involvement of parameters such as inter-stage pressure and recycle ratio.

3.2. Equivalent pure oxygen, EPO_2

The base for the O_2 production was taken to be 1 ton of EPO_2 per day, and EPO_2 is the amount of pure oxygen that would be mixed with air to make a mixture of OEA (n moles) of a specified O_2 concentration. The molar flow rates of EPO_2 and OEA can be related by the simple equation shown as Eq. (3) [4].

$$\frac{n\ EPO_2}{n\ OEA} = \frac{y_{O_2} - 0.21}{0.79} \quad (3)$$

Here "n EPO_2" is the molar flow rate (moles/day) of EPO_2 and "n OEA" is the molar flow rate (moles/day) of OEA, y_{O_2} is the oxygen mole fraction in OEA.

In terms of weight, the flow rates (tons/day) of EPO_2 and of OEA are related as shown in Eq. (4).

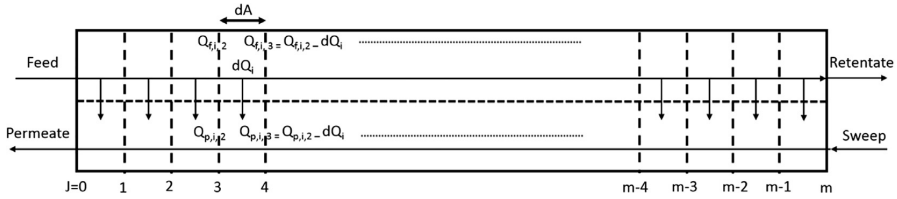

Fig. 1. Counter-current gas flow configuration through a membrane [19].

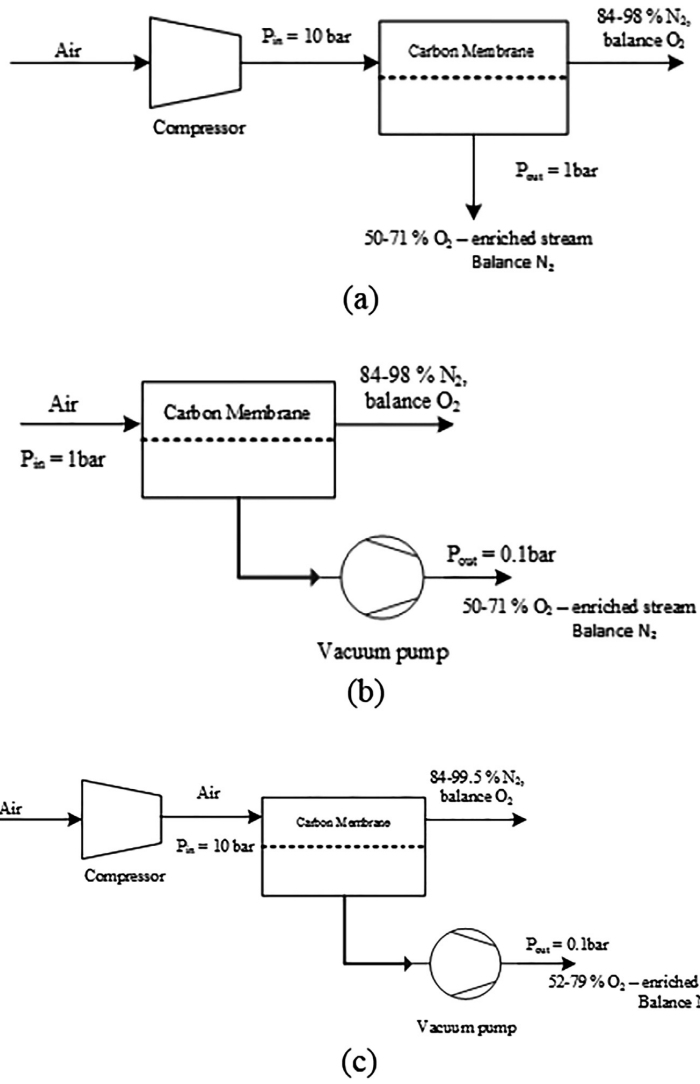

Fig. 2. Single stage process configuration, (a) FC approach, (b) VP approach, (c) FC-VP approach.

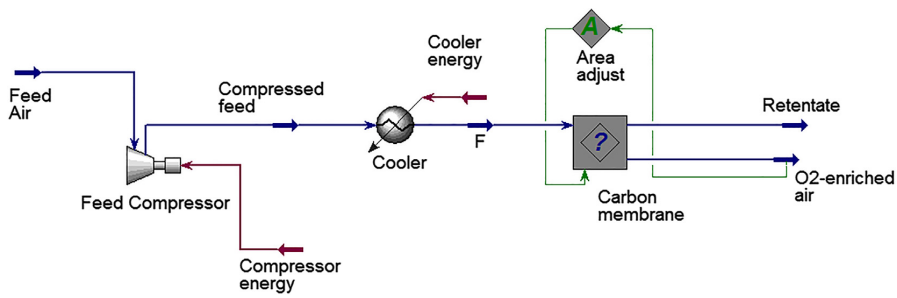

Fig. 3. Single stage separation process in Hysys® simulations.

$$\frac{TEPO_2}{TOEA} = \frac{y_{O_2} - 0.21}{(0.0989 y_{O_2} + 0.692)} \quad (4)$$

Here $TEPO_2$ is the mass flow rate (tons/day) of EPO_2 and TOEA is the mass flow rate (tons/day) of OEA, y_{O_2} is the oxygen mole fraction in OEA.

Fig. 3 presents the single stage process simulation diagram in Hysys®. Pressure and feed flow are adjusted to optimize the trade-off between membrane cost and compression duty cost, and finally to yield the lowest production cost of EPO_2. Permeate stream is an O_2-enriched stream (50–78% O_2) with mass flow adjusted for 1 ton per day of EPO_2. Oxygen molar concentration varies in the retentate stream depending on the stage cut, the area used, and feed pressure.

Considering an economically feasible scenario, O_2 concentration ranges from 3% to 15% balanced with N_2 in the retentate gas stream. Although retentate is not considered in the economic calculations, the retentate stream could be used as hypoxic air (15% O_2) or in another case as 97% N_2 stream as blanketing gas to prevent hazardous conditions [17].

3.3. Predicted values of O_2 permeability

CM have superior thermal resistance compared to polymeric membranes and can be operated at elevated temperatures. The reported membranes showed exponential increase in O_2 permeability with increasing temperature and according to Arrhenius model (extrapolation of experimental data as in Table 1), the separation process at elevated temperature between 190 and 205 °C using reported CM may achieve high permeability of O_2 without sacrificing the selectivity. Another solution may be to achieve high permeability by adding some nano particles to the precursor [16]. Liu et al. [15] prepared a carbon/ZSM-5 nanocomposite membrane incorporating different weight% of nano particles (ZSM-5) in the polyimide precursor and carbonizing it at 600 °C. They have reported experimental results at 25 °C which showed an increase in O_2 permeability from 2.21 Barrer prior adding nano particles to 499 Barrer with 16.7 wt% of the nano particles. The O_2/N_2 selectivity loss was only 9%.

Three permeability values; 100, 200, and 300 Barrer with constant O_2/N_2 selectivity of 18 were considered in the current work to investigate the effect on production cost of EPO_2 and total capital investment of the plant. Parameters and operating conditions used in simulations are shown in Table 2.

3.4. Economic parameters

The cost of an installed membrane separation process is determined by two contributions, the capital cost, and the operating cost. In this cost analysis, capital cost includes membrane modules cost, compressor cost, and vacuum pump cost. Whereas, operational cost involves membrane replacement cost during the expected lifetime of the plant, plus the power requirement for compression and vacuum pump and labor cost. The economic evaluation of a given membrane separation process can significantly vary depending on the method used for analysis, the cost of raw materials, equipment and utility cost, labor cost, depreciation policy, interest rates etc.

The assumptions and parameters used in the present economic assessment are shown in Table 3. CM module cost is considered $ 100 per m^2 based on pilot scale manufacturing of CM [23]. Predicting the cost of CM modules and life of the membranes is challenging due to the lack of commercial precedent. The expected life of the membrane is considered as 5 years. However, based on pilot scale demonstration of CM at biogas plant [24], it was observed that some of the CM modules may experience fiber breakage (due to vibration or handling/shipping of the modules) and therefore, cannot be used until repaired. Again, other modules may perform well for longer time. The first-time installation of membrane modules was included in the TCI. However, membrane replacement cost (MRC) was added in PC as a variable cost which is proportional to plant's operation rate. MRC was calculated based on daily usage (1 ton/day production of EPO_2) via dividing the total membrane area cost by total plant life (10 years) and then multiplied by plant availability (90%). MRC, electricity cost, capital recovery cost, and total labor costs were added to get PC of EPO_2.

The techno-economic calculation is based on a small-scale plant (1 ton/day). The membrane operation does not need continuous labor inspection. Therefore, labor cost (LC) has been estimated as 8 hr/day per 25 tons per day of EPO_2. The total labor was twice the labor cost which includes: maintenance (5% of LC), supervision (15% of LC), benefits (40% of LC), and plant overheads (40% of LC). This cost analysis considers a CM price of $ 100/m^2, a depreciation rate of 10% for the plant which includes compressor, vacuum pump, valves, and piping (except membrane), and a return on investment of 12%/year.

The CM offer a high O_2/N_2 selectivity of 18 to obtain O_2 concentration (50–78%) in a single stage process. However, carbon membrane cost is much higher than polymeric membranes. The retentate stream can be adjusted to obtain a required N_2 concentration in a range between 84 and 99.5%. The assumptions made in this economic analysis involves many adjustable variables, therefore a sensitivity analysis has been performed to determine the cost of EPO_2 which involves variation in CM module cost, membrane life time, and operating temperature which is directly related to membrane permeability.

4. Results and discussions

4.1. Simulations and economic assessment based on experimental data

Fig. 4 shows the effect of stage cut (q_p/q_f) on the O_2 concentration in permeate and retentate stream while using different compression approaches. The O_2 concentration would be similar for FC and VP approach due to the same pressure ratio across the membrane in both approaches. However, the concentration values are slightly different for FC-VP approach. The concentration of 78 mol % O_2 at 0.1 stage cut is obtained on the permeate side while using the FC-VP approach. In addition, 15% O_2 was obtained in the retentate stream which is considered as hypoxic air. Although the retentate stream is not considered here in economic calculations, it is still of importance while estimating the full plant cost. At lowest stage cut value, the O_2 concentration in permeate is highest but the flow rate of the permeate is very low because only a small fraction of the feed permeates through the membrane. It can be seen in Fig. 4 that O_2 concentration is decreasing in both permeate and retentate streams with an increase in stage cut. The stage cut value of 0.4 gives 50 mol % O_2 on the permeate side and almost 99% N_2 in the retentate stream for the membrane with O_2/N_2 selectivity of 18.

Fig. 5 presents the energy requirement while using different compression approaches. As can be seen FC and FC-VP approaches offer maximum energy requirement at lowest stage cut. However, the energy demand reduces up to 50% at stage cut of 0.25. The FC-VP approach offers high energy requirement because a direct feed gas (air)

Table 2
Parameters used to simulate the single-stage air separation process.

Feed composition	21 vol% O_2, 79 vol% N_2
Permeate flow rate	1 ton per day of EPO_2
Permeate composition	50–78 mol% of O_2; balance N_2
Permeate pressure	1 bar (10 mbar in vacuum mode)
Feed flow rate	variable*
Feed pressure	10 bar for FC and FC-VP approach, 1 bar for VP approach
Adiabatic efficiency of compressor and vacuum pump	75%

* Feed flow rate and feed pressure are adjusted to optimize the membrane area and compressor energy consumption.

Table 3
Economic parameters used to calculate TCI and PC per ton of EPO_2 [4,25]

Total capital investment (TCI)	
CM module cost: CMC	\$ 100/m^2
Installed compressor cost: CC	\$ 8700 × ([a]HP)$^{0.82}$
Installed vacuum pump cost: VC	\$ 32,500 × ([a]HP/10)$^{0.5}$
Production cost (PC)	
Membrane replacement cost: MRC	at \$ 100/m^2
Electricity cost: EC	\$ 0.05/kWh
Capital recovery cost: CRC	0.25 × (TCI)
Labor cost: LC	\$ 15/hr
Production cost: PC	MRC + EC + CRC + TLC
Other assumptions	
Membrane life time	5 years
Annual depreciation of the plant except membrane	10% over 10 years
Annual Return on capital investment	12%
Plant availability	90% (329 days/year)
Labor requirement	8 hr/day per 25 tons per day of EPO_2
Total labor cost (TLC)	2 × LC

[a] HP is the installed horse power for the installed compressor.

compression require a higher energy and in this context, using vacuum pump at the same time will need even more power as shown in Fig. 5. At the contrary, lowest energy requirement of vacuum pumping in VP approach results from the fact that the permeate flow only has to be pumped. The VP approach is an energy efficient process compared to FC, FC-VP, and cryogenic distillation. The membrane area required for a plant to produce one ton of EPO_2 per day is presented in Fig. 6. As shown in Fig. 6, the membrane area is minimum at 0.1 stage cut for all three compression approaches. At stage cut of 0.1, the area for the VP approach is 10 times higher than for the FC approach and 15 times larger compared to the FC-VP approach. Here comes the trade-off between membrane cost and energy cost while considering an economically viable process with lowest PC and TCI. Presently, carbon membrane cost is very high, and it is more economical to operate the system at higher pressure instead of using high membrane area which would also result in extra piping, valves, and maintenance cost. In this scenario, VP approach is not viable at even lowest value of membrane area and energy which is at 0.1 stage cut.

Fig. 6 shows that increasing stage cut value from 0.1 to 0.25 would result in almost 65% rise in required membrane area for all three compression approaches. Due to five years of averaged membrane lifetime expectancy, the total membrane area needs to be reinstalled again after five years hence, the cost of membrane is directly related to PC and TCI. On the other hand, the energy cost reduces to half for the FC and FC-VP approaches at stage cut 0.25 and that ultimately would reduce the PC for these approaches. The desired production rate of EPO_2 depends on both the oxygen concentration in the permeate stream and the permeate flow. The trade-off between area and energy is optimized here to get the minimum production cost per ton of EPO_2 at 1 bar in single stage membrane process.

The plots in Fig. 7 present the production (PC) cost per ton of EPO_2 (bar chart) and total capital investment (TCI) which is shown as scatter plot for a carbon membrane based single stage air separation system at 68 °C. Only the optimal stage cut values with respect to the lowest production cost per ton of EPO_2 for different compression approaches are presented here. All three approaches are optimal at stage cut 0.1 when O_2 permeability is 10 Barrer. The cost per ton of produced EPO_2 and the total capital cost is the minimum for FC-VP approach at 0.1 stage cut. This minimum value is the consequence of lowest membrane area. Due to 5 years of expected membrane life, the one-time replacement would increase the PC to very large value for the VP approach. Higher TCI value results in high capital recovery cost which also adds in PC. The TCI and PC for VP approach are more sensitive to the area than energy due to low permeability at 68 °C.

Although the membrane performance is within the commercially attractive region of Robeson plot as shown in Fig. 8, and FC-VP approach has lowest production cost \$ 644/ton of EPO_2, the price is nevertheless very high compared to other technologies. Increase in O_2 permeability would to some extent would scale down the effect of membrane price on FC-VP approach since the membrane area is optimized for the required production rate.

As already shown in Table 1, the permeability of O_2 and selectivity of O_2/N_2 are very much dependent on operating temperature. Thus, higher temperature offers high permeability of O_2 with sufficient O_2/N_2 selectivity to keep the membrane in the commercially attractive region as presented in Fig. 8. Operating membrane at 205 °C gives O_2 permeability of 300 Barrer with O_2/N_2 selectivity of 18 in comparison to operation at 190 °C which offers O_2 permeability of 200 Barrer with O_2/

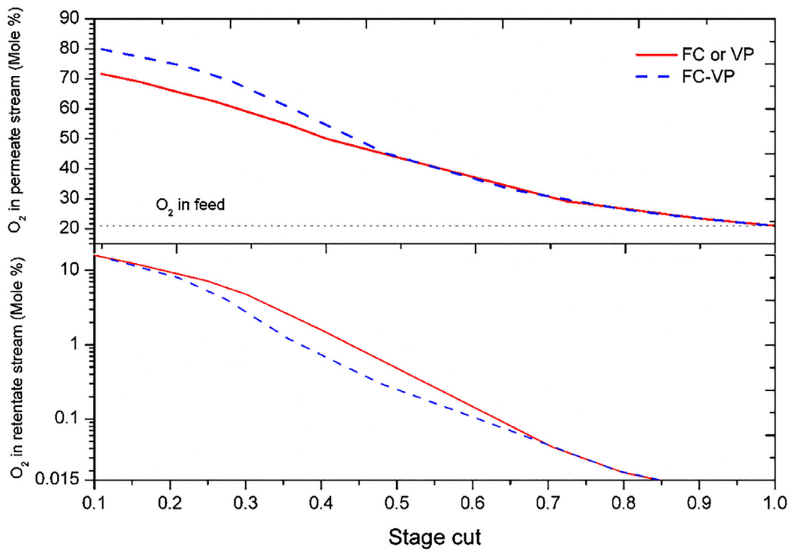

Fig. 4. Mole-fraction of O_2 in permeate and retentate streams as function of stage cut in a single stage separation process (O_2/N_2 selectivity: 18).

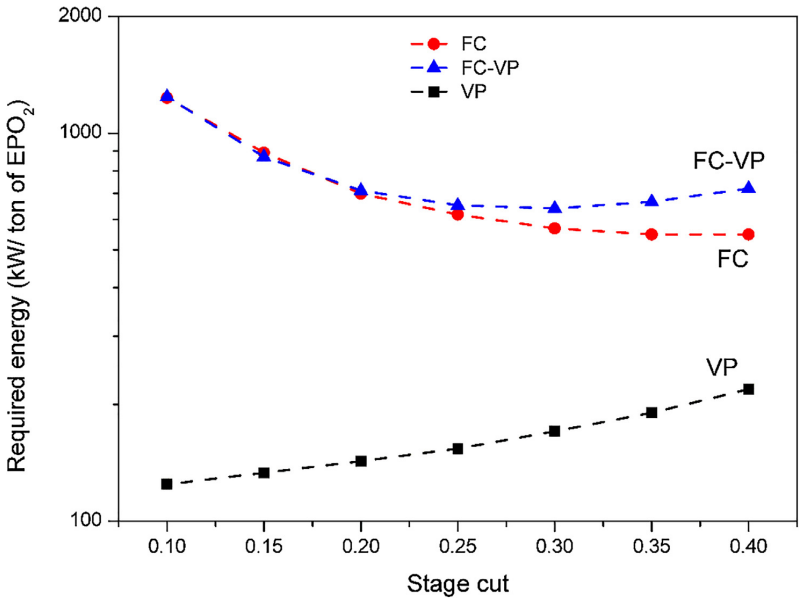

Fig. 5. Required energy to produce 1 ton of EPO_2 as a function of stage cut while using different compression approaches (Energy for cryogenic unit: 285 kW/ton of 99.6% O_2 [7]).

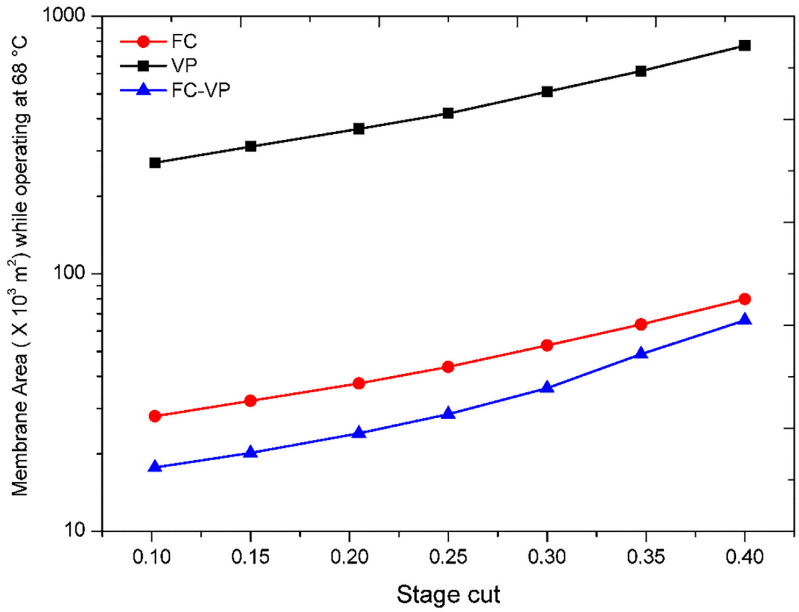

Fig. 6. Required membrane area as a function of stage cut while operating at 68 °C (O_2 Permeability: 10 Barrer).

N_2 selectivity of 18 (according to Arrhenius model extrapolation of experimental data shown in Table 1). Elevated temperature operations are costly, so the extra energy cost adds up to the TCI and PC per ton of EPO_2. The adiabatic heating of the compressor can be utilized to increase the gas temperature for achieving higher flux. Depending on compressor type, the actual compression may heat the gas significantly to increase the temperature to well beyond 100 °C. In addition, the separation operated at elevated temperature may act as regeneration by removing physically adsorbed gases and eliminating the water aging effect on the carbon membranes. However, a good sealing/potting material for module construction is challenging to develop when operating at temperatures higher than 150 °C. Another solution could be to improve O_2 permeability of the membrane without sacrificing O_2/N_2 selectivity; this may be achievable by adding some nano particles to the precursor [15,16].

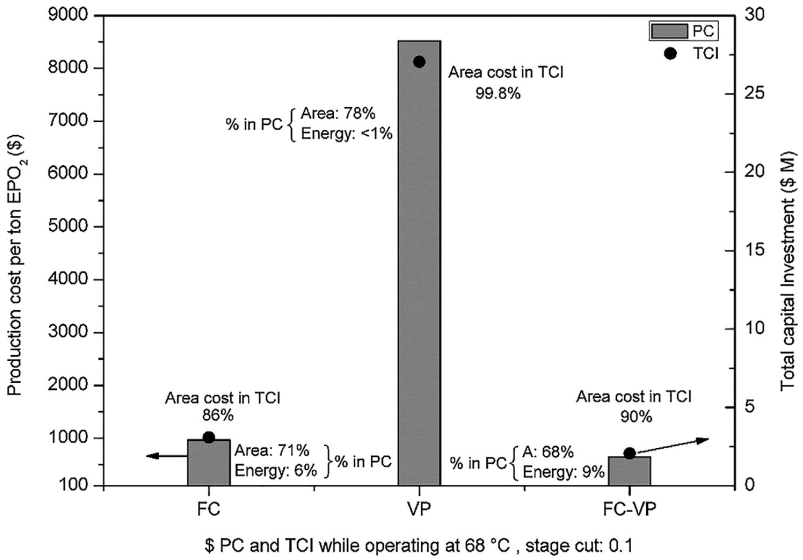

Fig. 7. Lowest PC and TCI for different compression approaches at optimal stage cut value (Operating temperature: 68 °C, Permeability: 10 Barrer).

4.2. Simulations and economic assessment based on predicted data

Fig. 9 is showing the PC and TCI as function of stage cut when O_2 permeability is 100 Barrer and selectivity is 18. The stage cut of 0.1 has been reported as an average economical optimum [4] for VP approach. This study also shows that stage cut of 0.1 is optimal for VP approach however, it is not optimal for FC or FC-VP approaches when O_2 permeability is 100 Barrer as shown in Fig. 9. The reduced membrane area due to high permeability offers maximum benefit to FC-VP approach in dropping the production cost of EPO_2.

Fig. 9 examines the TCI and PC as function of stage cut when EPO_2 is produced using three different compression approaches (O_2 permeability: 100 Barrer, O_2/N_2 selectivity: 18). The lowest production cost $ 127 and $ 130 are achieved by FC-VP approach at stage cut of 0.17 and 0.20 respectively. Hence, the process is optimal at stage cut of ca. 0.17 for minimum PC and TCI. However, the required membrane area is still very high at stage cut 0.17, and the TCI for the FC-VP approach is almost $ 0.4 million for a plant to product one ton of EPO_2 per day.

Figs. 10 and 11 show PC per ton of EPO_2 and TCI of the plant while using three different compression approaches when the O_2 permeability

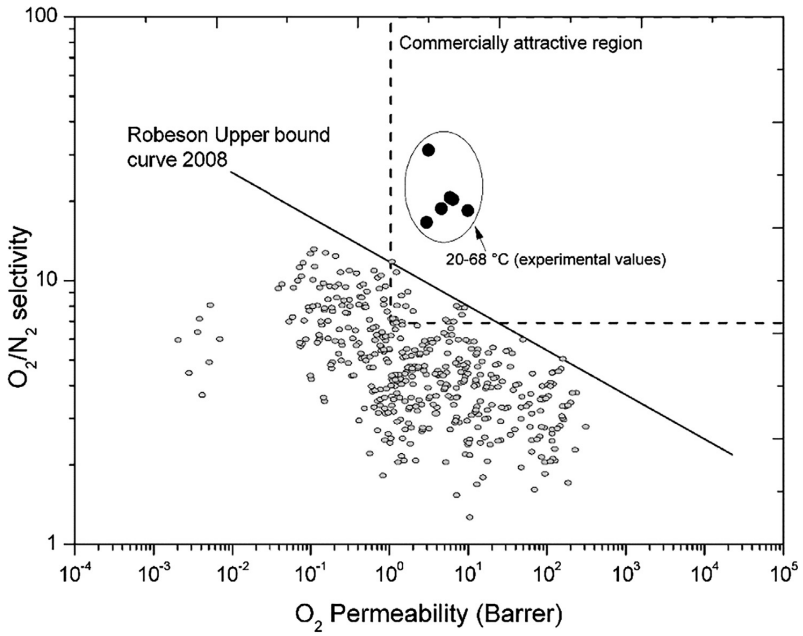

Fig. 8. O_2 permeability and O_2/N_2 selectivity of CM with respect to Robeson upper bound curve (2008) [3].

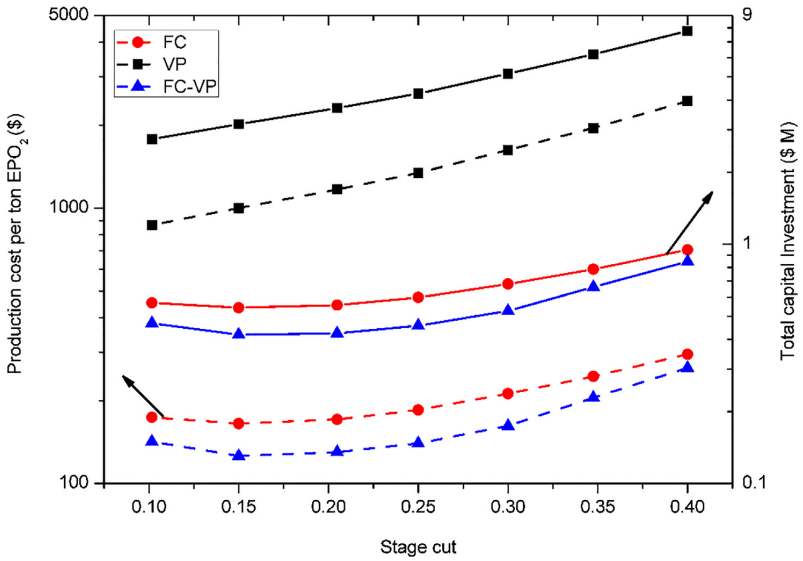

Fig. 9. PC and TCI as function of stage cut, O_2 permeability: 100 Barrer, O_2/N_2 selectivity: 18.

is 200 and 300 Barrer respectively. The energy requirement for all cases remains the same due to constant O_2/N_2 selectivity value of 18. When using FC-VP approach, it reduces the membrane area to a large extent and the TCI and PC are 5 times lower than that of VP approach. As shown in Figs. 10 and 11, the membrane price had great influence on the capital investment and production cost of EPO_2. Increase in operating temperature or O_2 permeability scale down the effect of membrane area because the required area is being more and more optimized towards the required production rate. Almost similar trend is observed while considering the production cost of EPO_2 using different compression approaches. Although very low energy is required in case of vacuum approach, but membrane life time (5 years in this study) is playing a key role to increase the production cost of EPO_2 in this approach. The membrane cost \$ 100 per m^2 and reinstallation of total area (9000–270000 m^2 depending on the different cases) keep the PC higher for all operating permeabilities 10–300 Barrer. Nevertheless, the PC is almost hundred dollars for VP approach when O_2 permeability of CM is higher than 1000 Barrer. Hence, VP approach is not a competent choice when O_2 permeability is below 1000 Barrer while the membrane costs \$ 100/m^2, membrane life 5 years, and O_2/N_2 selectivity is 18.

The lowest production cost with CM process is, \$ 80/ton of EPO_2 for O_2 permeability of 300 and TCI for the corresponding plant is \$ 264,000 while using FC-VP approach as shown in Fig. 11. This production cost is comparable with PSA plant that costs \$ 100/ton of EPO_2 at a plant capacity of 1 ton per day. Nevertheless, the most economical process of producing O_2 on a large scale is by the cryogenic distillation and the

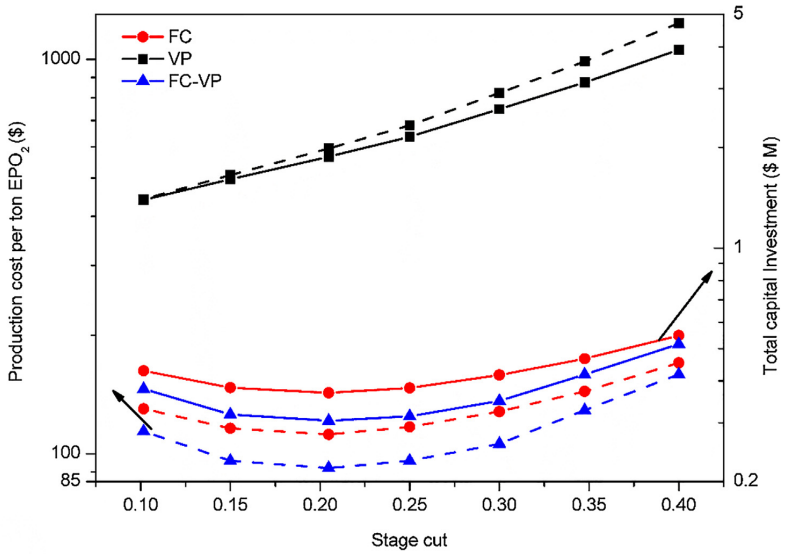

Fig. 10. PC and TCI as function of stage cut, O_2 permeability: 200 Barrer, O_2/N_2 selectivity: 18.

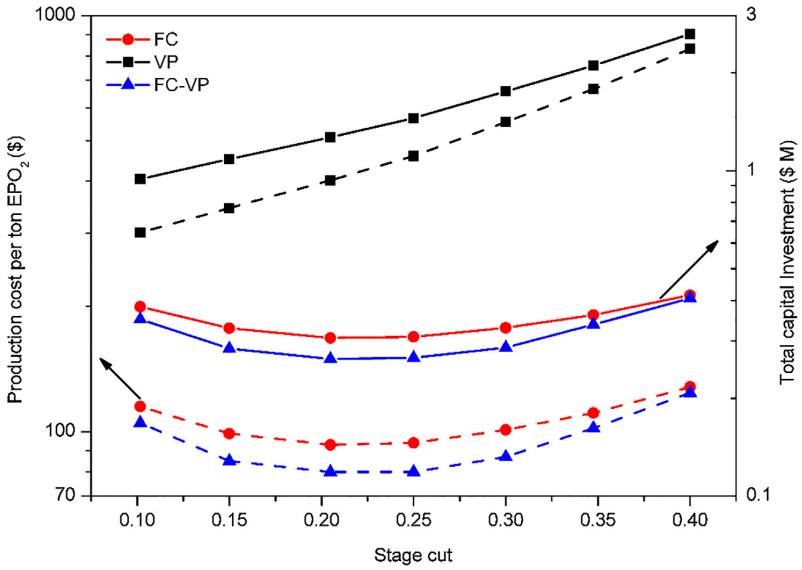

Fig. 11. PC and TCI as function of stage cut, O_2 permeability: 300 Barrer, O_2/N_2 selectivity: 18.

cost can be as low as $ 25/ton at plant capacities above 100 tons/day of EPO_2 [4]. Hence, the TCI and PC of EPO_2 while operating at elevated temperature of 205 °C or permeability up to 300 may compete with PSA plants for small scale plants (1–10 tons/day).

The plots in Fig. 12 demonstrate the lowest PC cost per ton of EPO_2 (bar chart) and TCI (scatter plot) for different compression approaches at optimal stage cut and different permeability values. Results show FC-VP approach is the most efficient approach to produce EPO_2 economically for the CM discussed here. This approach can produce a ton of EPO_2 below $ 100 if the membrane permeability is 200 Barrer and O_2/N_2 selectivity of 18, and this performance can be accomplished either operating the membrane at 190 °C or adding nano particles to the precursor.

4.3. Sensitivity analysis

Sensitivity Analysis was used to identify components that are most sensitive to achieve economically suitable results. This section presents the results of simulation analysis in which impact of different variables on TCI and PC per ton of EPO_2 is investigated and discussed. The parameters investigated here are membrane cost, membrane life time, and operating temperature which directly is related to the permeability of the membrane.

Fig. 13 presents the percent decrease in PC/ton of EPO_2 when CM life time is increased to 10 years. The results show that production cost is significantly affected by the membrane life time while using VP approach. The production cost can be reduced 73–78% by doubling the

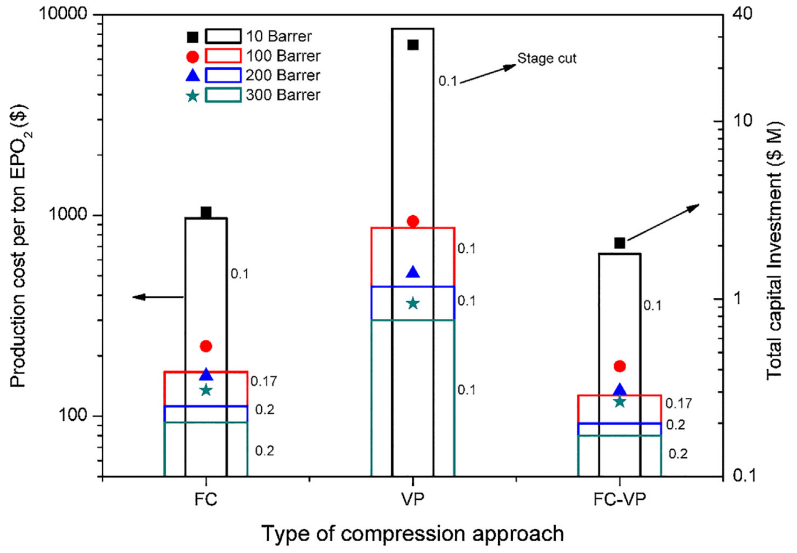

Fig. 12. Lowest PC and TCI for different compression approaches at optimal stage cut value.

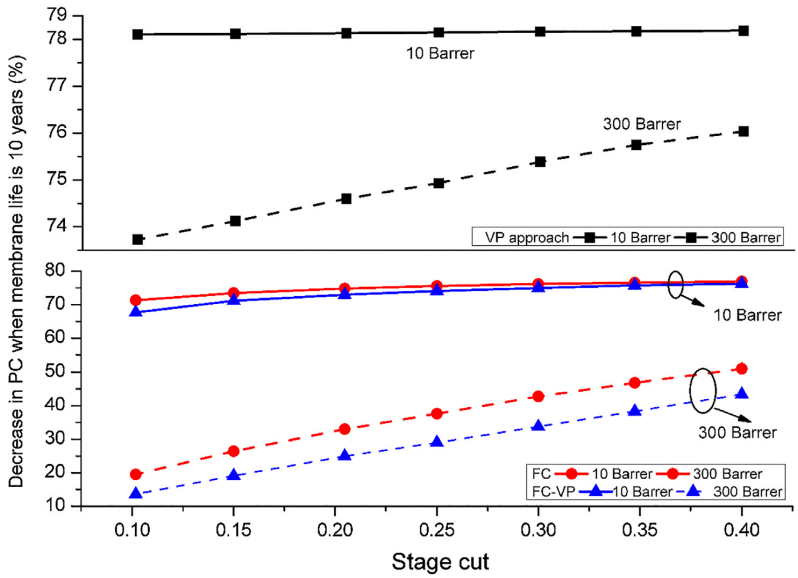

Fig. 13. Effect of CM life time on PC of EPO_2 for different compression approaches (CM cost: \$ 100/m^2.

Table 4
Sensitivity of the process towards membrane life and membrane cost (optimal stage cut for each compression).

Compression approach	Permeability (Barrer)	Membrane life (10 years, cost: \$ 100/m^2)		Membrane cost (\$ 50/m^2)		Stage cut
FC		PC	TCI	PC	TCI	
	10	\$ 270	\$ 3,000,000	\$ 530	\$ 1,600,000	0.1
	100	\$ 87	\$ 540,000	\$ 120	\$ 380,000	0.15
	200	\$ 66	\$ 360,000	\$ 83	\$ 270,000	0.2
	300	\$ 63	\$ 300,000	\$ 73	\$ 240,000	0.2
VP						
	10	\$ 1800	\$ 27,000,000	\$ 4200	\$ 13,000,000	0.1
	100	\$ 200	\$ 2,700,000	\$ 440	\$ 1,300,000	0.1
	200	\$ 110	\$ 1,300,000	\$ 230	\$ 710,000	0.1
	300	\$ 80	\$ 940,000	\$ 160	\$ 490,000	0.1
FC-VP						
	10	\$ 200	\$ 2,000,000	\$ 370	\$ 2,000,000	0.1
	100	\$ 77	\$ 400,000	\$ 95	\$ 310,000	0.15
	200	\$ 62	\$ 300,000	\$ 73	\$ 240,000	0.2
	300	\$ 60	\$ 260,000	\$ 67	\$ 220,000	0.2

Table 5
Lowest values of TCI and PC/ton EPO_2 (CM price: \$ 100/m^2) for different compression approaches.

Compression approach	O_2 permeability	O_2 in permeate	N_2 in retentate	kW/ton of EPO_2	TCI (\$)	\$/ton EPO_2
	Barrer	% mole	% mole			
FC-VP	300	72.71	92.57	741	260,000	80
FC	300	65.68	90.51	727	310,000	93

membrane life and keeping the cost \$ 100 per m^2. The membrane life is considered 5 years in this study due to the challenges with mechanical properties of carbon membranes. FC and FC-VP approaches are also affected by membrane life, but the effect decreases exponentially with increase in permeability up to 300 Barrer. This effect is almost negligible at 400 Barrer as the membrane area seems fully optimized towards the production rate of EPO_2. However, in case of VP approach, the membrane area optimizes towards the production rate of EPO_2 when O_2 permeability is above 1000 Barrer.

Table 4 illustrates the sensitivity of the separation process to the membrane cost, membrane life and operating temperature which is directly related to the permeability of the membrane. VP approach is greatly affected by the membrane cost, for example the PC and TCI for this approach reduces 27 times for permeability of 300 compared to 10 by cutting the membrane cost to half. Similar trend is observed for the PC/ton of EPO_2 when membrane life is 10 years while using VP approach. However, the TCI would remain quite high due to membrane cost of \$ 100/m^2. That is why even the PC is decreased to \$ 80/ton EPO_2, but the TCI is about \$ 0.95 million which is not feasible. The sensitivity of FC and FC-VP approaches towards membrane cost is higher between permeability of 10–100 and beyond that the effect is very small (< 10%). If the carbon membrane production process is fully optimized in future and price is reduced to \$ 50 per m^2 then PC per ton of EPO_2 can be cut to \$ 67 which presently is \$ 80 while operating at 300 Barrer.

5. Conclusions

A single stage membrane process with no recycle stream based on O_2-selective carbon membranes was evaluated for production of OEA. Three compression approaches were simulated to economically produce one ton of EPO_2 per day with low total capital investment. In first section of the study, the experimental data were simulated to evaluate the production of EPO_2. TCI and PC were calculated based on optimal stage cut value. In the second section, the separation properties of the prepared CM were predicted to achieve high O_2 permeability, between100 and 300 Barrer, by keeping the selectivity constant. This improved permeability may be achieved by operating the CM and elevated temperature up to 190–205 °C. The simulation results indicated that CM with O_2 permeability of 200 and a O_2/N_2 selectivity of 18 may produce one ton of EPO_2 in $ 92. The summary of the main conclusions of the study is shown in Table 5.

As shown in Table 5, CM with O_2 permeability of 300 may produce a ton of EPO_2 in $ 80, however, the retentate stream is 92.57% N_2 which is an extra profit and that is not considered in economic analysis. This cost considers a CM price of $ 100/m^2, a depreciation rate of 10% for the plant which includes compressor, vacuum pump, valves, and piping (except membrane), and a return on investment of 12%/year. CM possess weak mechanical properties compared to polymeric membranes. Based on experience from pilot scale production, the membrane life of 5 years and prepared module cost $ 100/m^2 was considered as realistic in this study. Although vacuum pump approach requires less energy compared to cryogenic distillation, it was found that this approach is not economical as the membrane area towards the production rate is not optimal (due to too low permeability of the membrane) which resulted in very high TCI and PC of EPO_2 with current cost of membrane. However, a combined approach, feed compression and vacuum pump, may produce EPO_2 economically for the current price and life of the CM. A sensitivity analysis was performed in which different parameters like membrane cost, membrane life time, and operating temperature which are directly related to the permeability of the membrane, were investigated. The results from sensitivity analysis showed that FC-VP approach may produce a ton of EPO_2 in $ 67 if membrane life time could be increased to 10 years instead of 5.

It can be stated that even though CM is almost five times more expensive than polymeric membranes, the high performance (selectivity) and tolerance to elevated temperatures CM is a potential candidate in production of OEA and or high purity (99.5%) N_2 in a single stage process. The present study indicates that CM process for OEA have the best potential of becoming economically competitive with conventional technologies for small plant capacities (1–10 tons/day) and a high degrees of oxygen enrichment, 50–78 mol % O_2. To be fully competitive with cryogenic distillation and PSA, the membrane cost needs to be reduced and mechanical strength of CM should be increased to maximize the life time of membrane.

Acknowledgement

The authors would like to thank The Department of Chemical Engineering at NTNU for providing the possibility to work with this article.

References

[1] M. Anheden, J. Yan, G. De Smedt, Denitrogenation (or oxyfuel concepts), Oil Gas Sci. Technol. 60 (3) (2005) 485–495, http://dx.doi.org/10.2516/ogst:2005030.
[2] A.R. Smith, J. Klosek, A review of air separation technologies and their integration with energy conversion processes, Fuel Process. Technol. 70 (2) (2001) 115–134, http://dx.doi.org/10.1016/S0378-3820(01)00131-X.
[3] L.M. Robeson, The upper bound revisited, J. Membr. Sci. 320 (1–2) (2008) 390–400, http://dx.doi.org/10.1016/j.memsci.2008.04.030.
[4] B.D. Bhide, S.A. Stern, A new evaluation of membrane processes for the oxygen-enrichment of air. I. Identification of optimum operating conditions and process configuration, J. Membr. Sci. 62 (1) (1991) 13–35, http://dx.doi.org/10.1016/0376-7388(91)85002-M.
[5] R. Prasad, F. Notaro, D.R. Thompson, Evolution of membranes in commercial air separation, J. Membr. Sci. 94 (1) (1994) 225–248, http://dx.doi.org/10.1016/0376-7388(93)E0193-N.
[6] S.L. Matson, W.J. Ward, S.G. Kimura, W.R. Browall, Membrane oxygen enrichment, J. Membr. Sci. 29 (1) (1986) 79–96, http://dx.doi.org/10.1016/S0376-7388(00)82020-7.
[7] B. Belaissaoui, Y. Le Moullec, H. Hagi, E. Favre, Energy efficiency of oxygen enriched air production technologies: cryogeny vs membranes, Energy Procedia 63 (2014) 497–503, http://dx.doi.org/10.1016/j.egypro.2014.11.054.
[8] W.N.W. Salleh, A.F. Ismail, Carbon membranes for gas separation processes: recent progress and future perspective, J. Membr. Sci. Res. 1(Issue 1) (2015) 2–15.
[9] C.W. Jones, W.J. Koros, Carbon molecular sieve gas separation membranes-I. Preparation and characterization based on polyimide precursors, Carbon 32 (8) (1994) 1419–1425, http://dx.doi.org/10.1016/0008-6223(94)90135-X.
[10] W. Shusen, Z. Meiyun, W. Zhizhong, Asymmetric molecular sieve carbon membranes, J. Membr. Sci. 109 (2) (1996) 267–270, http://dx.doi.org/10.1016/0376-7388(95)00205-7.
[11] J.E. Koresh, A. Sofer, Molecular Sieve carbon permselective membrane. Part I. Presentation of a new device for gas mixture separation, Sep. Sci. Technol. 18 (8) (1983) 723–734, http://dx.doi.org/10.1080/01496398308068576.
[12] H. Hatori, Y. Yamada, M. Shiraishi, H. Nakata, S. Yoshitomi, Carbon molecular sieve films from polyimide, Carbon 30 (4) (1992) 719–720, http://dx.doi.org/10.1016/0008-6223(92)90192-Y.
[13] J.A. Lie, M.-B. Hägg, Carbon membranes from cellulose: synthesis, performance and regeneration, J. Membr. Sci. 284 (1–2) (2006) 79–86, http://dx.doi.org/10.1016/j.memsci.2006.07.002.
[14] S. Haider, A. Lindbråthen, J.A. Lie, M.-B. Hägg, Carbon membranes for oxygen enriched air – Part I: synthesis, performance and preventive regeneration, Sep. Purif. Technol. (2018), http://dx.doi.org/10.1016/j.seppur.2018.05.014.
[15] Q. Liu, T. Wang, J. Qiu, Y. Cao, A novel carbon/ZSM-5 nanocomposite membrane with high performance for oxygen/nitrogen separation, Chem. Commun. 11 (2006) 1230–1232, http://dx.doi.org/10.1039/B516519A.
[16] J.A. Lie, M.-B. Hägg, Carbon membranes from cellulose and metal loaded cellulose, Carbon 43 (12) (2005) 2600–2607, http://dx.doi.org/10.1016/j.carbon.2005.05.018.
[17] G. Jensen, J.G. Holmberg, A. Gussiås, Hypoxic air venting for protection of heritage, Riksantikvaren, Directorate for Cultural Heritage and Crown, 2006.
[18] S. Haider, A. Lindbråthen, J.A. Lie, I.C.T. Andersen, M.-B. Hägg, CO_2 separation with carbon membranes in high pressure and elevated temperature applications, Sep. Purif. Technol. 190 (2018) 177–189, http://dx.doi.org/10.1016/j.seppur.2017.08.038.
[19] D. Grainger, PhD. Thesis (ISBN 978-82-471-4302-5), Development of carbon membranes for hydrogen recovery, NTNU, Trondheim, 2007.
[20] M. Mulder, Basic Priciples of Membrane Technology, Kluwer Academic Publishers, Netherlands, 1996.
[21] J.A. Lie, PhD. Thesis (ISBN 82-471-7191-0): synthesis, performance and regeneration of carbon membranes for biogas upgrading – a future energy carrier, NTNU, Trondheim, 2005.
[22] X. He, J.A. Lie, E. Sheridan, M.-B. Hägg, Preparation and characterization of hollow fiber carbon membranes from cellulose acetate precursors, Ind. Eng. Chem. Res. 50 (4) (2011) 2080–2087, http://dx.doi.org/10.1021/ie101978q.
[23] S. Haider, A. Lindbråthen, M.-B. Hägg, Techno-economical evaluation of membrane based biogas upgrading system: a comparison between polymeric membrane and carbon membrane technology, Green Energy Environ. 1 (3) (2016) 222–234, http://dx.doi.org/10.1016/j.gee.2016.10.003.
[24] S. Haider, A. Lindbråthen, J.A. Lie, P.V. Carstensen, T. Johannessen, M.-B. Hägg, Vehicle fuel from biogas with carbon membranes; a comparison between simulation predictions and actual field demonstration, Green Energy Environ. https://doi.org/10.1016/j.gee.2018.03.003.
[25] B.D. Bhide, S.A. Stern, A new evaluation of membrane processes for the oxygen-enrichment of air. II. Effects of economic parameters and membrane properties, J. Membr. Sci. 62 (1) (1991) 37–58, http://dx.doi.org/10.1016/0376-7388(91)85003-N.

ISBN 978-82-326-4188-8 (printed version)
ISBN 978-82-326-4189-5 (electronic version)
ISSN 1503-8181

NTNU
Norwegian University of
Science and Technology

Shamim Haider

Doctoral Thesis

Doctoral theses at NTNU, 2019:296

Shamim Haider

A Semi-Industrial Scale Process To Produce Carbon Membranes For Gas Separation

NTNU
Norwegian University of
Science and Technology
Faculty of Natural Sciences and Technology
Department of Chemical Engineering

NTNU
Norwegian University of
Science and Technology

Doctoral theses at NTNU, 2019:296

NTNU